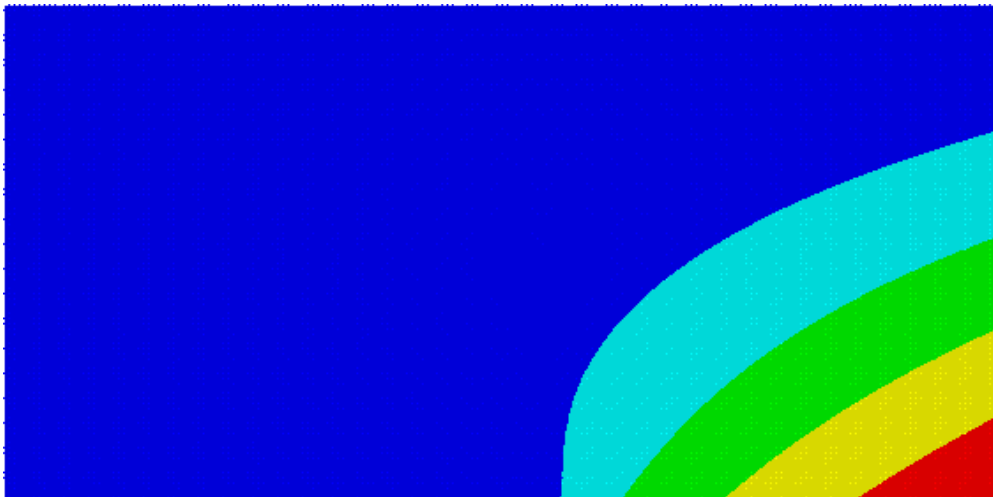




# National Technical University of Athens

**School of Civil Engineering**  
**M.Sc. Analysis and Design of Structures**

## Flexoelectric Materials in Micromechanics



The out-of-plane displacement for the purely hyperbolic region.

**M.Sc. Thesis**  
**Chris Knisovitis**

**Supervisor:** Giannakopoulos A.E., Professor

Athens, ..... 2021





# National Technical University of Athens

**School of Civil Engineering**  
**M.Sc. Analysis and Design of Structures**

## Flexoelectric Materials in Micromechanics

**M.Sc. Thesis**  
**Chris Knisovitis**

**Supervisor:** Giannakopoulos A.E., Professor

Approved by the three-person committee on ... / ..... / 2021

.....  
A.E. Giannakopoulos,  
Professor

.....  
A. Zisis  
Associate Professor

.....  
V. Koumousis,  
Professor Emeritus

Athens, ..... 2021

.....  
Christos Sotirios Knisovitis  
Civil Engineer, Bachelor, M.Sc., NTUA

Copyright © Christos Sotirios Knisovitis

Without prejudice to any right. All rights reserved.

Copy, downloading and distribution of the current thesis, on the whole or partially are forbidden for commercial purposes. For non-profitable educational or research purposes the printing, downloading and distribution are allowed with the condition that the source is mentioned and this message is displayed. Questions about the usage of the thesis for profitable purposes are to be addressed to the author.

Opinions and conclusions that this thesis includes express those of the author, and should not be interpreted to represent the official positions of the National Technical University of Athens.

## Abstract

Flexoelectricity is the phenomenon that allows some materials to convert mechanical strain gradients to electrical polarizations and vice versa. As flexoelectricity is a ferroelectric phenomenon, its applications are of maximum importance and should be studied thoroughly. The polarization magnitude is connected to the strain gradients and so situations that produce large strain gradients are interesting. The cracking seems to be very promising. The mode III crack is an anti-plane problem that can be solved also considering the flexoelectric effect. As known from classic elasticity, the anti-plane problem is a sub-case of 3D-elasticity. The mode III crack, is also a dynamic problem.

By considering the contribution of the flexoelectric phenomenon to the total energy density, a solution of the anti-plane flexoelectric problem can be formed. A direct analogue is presented between the anti-plane flexoelectric problem and the anti-plane couple stress elasticity problem, which allows the distinction of the flexoelectric problem into three regions: the elliptic, the hyperbolic and the intermediate.

The hyperbolic region is studied further. The characteristic lines, a method of solving hyperbolic equations, allows some simplifications of the differential equation and thus a full field analytical solution is presented. Mach cones are visible as the displacement is concerned. For this displacement, the polarization can be calculated. The crack tip and the end of the cohesive zone are the positions of maximum polarization and thus positions of possible electrical yielding (abrupt change of the polarization vector). Also, the polarization of a screw-like dislocation is calculated. In this case, the polarization is described with a “ $\delta$  function” – like distribution.

The anti-plane dynamic problem is responsible for the propagation of waves. Because of the microstructure (for the couple stress elasticity problem, or the flexoelectric properties on the normal anti-plane problem), those waves are dispersive, a fact that signifies the possibilities of a lot more applications. The dispersion is the next thing studied. The dispersion relations show great similarity with viscoelastic materials, as the flexoelectric metamaterials are concerned.

Lastly, through another analogue between the anti-plane problems and the plate problems, numerical calculations are possible for a great number of cases. The analogue is modified in order to be able to solve also hyperbolic problems. This is the first time the Analogue Equation Method is used in a Finite Element Code. Through a standard Finite Element Method (FEM) code ([ABAQUS](#)), the Mach cone - like displacement is proved, in the hyperbolic problem. Also, the angle of the cones, is in agreement with the previous bibliographic suggestions and depends on the microstructure and the velocity of the problem.

## Keywords

Flexoelectricity, direct flexoelectric effect, converse flexoelectric effect, anti-plane, anti-plane polarization, anti-plane flexoelectricity, anti-plane flexoelectric problem, dynamic anti-plane flexoelectric problem, couple stress elasticity, anti-plane couple stress elasticity dynamic problem, elliptic problem, hyperbolic problem, intermediate problem, microstructural length, micro-inertial length, crack mode III, dispersion, phase velocity, group velocity, polarization, anti-plane analogue, FEM – Analogue Equation Method.

## Acknowledgements

For this current project, that happened on the context of the M.Sc. program: Analysis and Design of Structure, I would like to express my gratitude to:

- Professor A.E. Giannakopoulos, who helped me in everything, proposed the majority of the ideas and supervised this work. Without him, there would be no project to present.
- Professor A. Zisis, who helped be with a lot of problems that occurred, specifically using the FEM methods.
- Professor V. Koumouisis, who despite his retirement, stood by my side with his inspiring advice, answering my call with no hesitation and being there for me. Without him, I wouldn't be here.
- Professors G. Tsiatas and P. Tsopelas and Ph.D. candidates S. Papathanasiou and P. Sirimi for their helpful advices.
- My mother and my father for their support. Also, they tried to check this project, despite it being in a foreign language.
- Christina Knisoviti and Giota Sachla for their support and the proofreading of this thesis.
- My sister Evaggelia and her children who allowed me some space, to do this research.
- My friends and co-workers J. Kotzias, A. Kaparellos, A. Zarampoukas who triggered me constantly for better results.

# Table of context

<b>1. INTRODUCTION</b>	<b>12</b>
A. PHYSICAL ASPECT OF FLEXOELECTRICITY - WHAT IS FLEXOELECTRICITY?	12
B. THE MATERIALS	15
C. APPLICATIONS	16
D. PREVIOUS RESEARCH	17
<i>i. Bibliographic references on flexoelectricity</i>	17
<i>ii. Toupin's Variational Principle and the total Energy Density</i>	21
<i>iii. The Couple Elasticity Anti-plane problem</i>	24
<i>iv. The plate problem</i>	27
<i>v. The analogue of the anti-plane problem and a prestressed plate</i>	28
<i>vi. Flexoelectricity and magnetism</i>	29
E. AIM	30
<b>2. THE ANTI-PLANE FLEXOELECTRIC PROBLEM</b>	<b>31</b>
A. THE ANTI-PLANE DISPLACEMENT	31
B. THE ANTI-PLANE POLARIZATION	34
C. THE ANTI-PLANE FLEXOELECTRIC PROBLEM	35
<b>3. THE ANTI-PLANE COUPLE ELASTICITY DYNAMIC PROBLEM</b>	<b>40</b>
A. THE ANALOGUE BETWEEN THE FLEXOELECTRIC AND THE COUPLE STRESS ANTI-PLANE PROBLEM	43
B. THE THREE SUB-CASES OF THE PROBLEM	43
C. THE ELLIPTIC SUBSONIC REGION	47
D. THE INTERMEDIATE (SUPERSONIC ELLIPTIC) REGION	50
E. THE HYPERBOLIC REGION	52
<b>4. THE DIFFERENTIAL EQUATION OF THE ANTI-PLANE HYPERBOLIC FLEXOELECTRIC PROBLEM</b>	<b>56</b>
A. THE PROFILE OF THE CRACK	60
B. THE INTEGRALS WITH THE HEAVISIDE TERMS	61
<i>i. The integral with the negative sign</i>	64
<i>ii. The integral with the positive sign</i>	65
C. THE POLARIZATION WHILE THE JOINTING FUNCTION IN LINEAR	67
D. THE POLARIZATION WHILE THE JOINTING IS A 3 <sup>RD</sup> DEGREE FUNCTION	70
E. THE BOUNDARY CONDITIONS	74
F. THE SCREW DISLOCATION	81
<b>5. DISPERSION RELATION ON PRODUCED WAVES</b>	<b>87</b>
A. THE EXISTENCE OF WAVES	87
B. DISPERSION RELATIONS OF FREQUENCY	92
C. PHASE VELOCITY	100
D. GROUP VELOCITY	105
E. DISPERSION IN METAMATERIALS	110
<b>6. PLATES</b>	<b>113</b>
A. INTRODUCTION	113
B. THE ISOTROPIC PLATE	113
C. THE STATIC ANALOGUE	116

D.	THE PRESTRESSED ORTHOTROPIC PLATE .....	120
E.	THE DYNAMIC ANALOGUE .....	122
<b>7.</b>	<b>FEM APPLICATIONS .....</b>	<b>125</b>
A.	THE TWO-PLATE METHOD .....	126
B.	THE FEM MODEL .....	131
C.	THE CASES .....	132
<i>i.</i>	<i>The purely hyperbolic case.....</i>	<i>134</i>
<i>ii.</i>	<i>The elliptic – hyperbolic case.....</i>	<i>138</i>
<i>iii.</i>	<i>The intermediate - hyperbolic case .....</i>	<i>140</i>
<b>8.</b>	<b>EPILOGUE .....</b>	<b>142</b>
A.	THE RESEARCH .....	142
B.	VISION .....	143
<b>9.</b>	<b>APPENDICES .....</b>	<b>144</b>
A.	THE GOVERNING EQUATIONS OF THE ANTI-PLANE FLEXOELECTRIC PROBLEM .....	144
B.	THE TRANSFORMATION OF THE ANTI-PLANE FLEXOELECTRIC EQUATION (REMOVE THE TIME) .....	161
C.	THE COUPLE STRESS ELASTICITY THEORY .....	163
<i>iv.</i>	<i>The anti-plane formulation in terms of couple stress elasticity.....</i>	<i>168</i>
<i>v.</i>	<i>The anti-plane dynamic couple stress elasticity problem.....</i>	<i>172</i>
D.	THE TRANSFORMATION ON THE HYPERBOLIC PROBLEM BASED ON THE CHARACTERISTICS.....	175
E.	THE INTEGRATION WITH THE DISCONTINUITIES.....	178
<i>i.</i>	<i>The integral <math>gx * Hx - cdx</math>.....</i>	<i>178</i>
<i>ii.</i>	<i>The integral <math>gx * \delta x - cdx</math> .....</i>	<i>178</i>
<i>iii.</i>	<i>The integral <math>gx * \delta'x - cdx</math> .....</i>	<i>180</i>
<i>iv.</i>	<i>The spike .....</i>	<i>181</i>
F.	THE JOINING FUNCTIONS .....	183
<i>i.</i>	<i>The polynomial function of 3<sup>rd</sup> order .....</i>	<i>183</i>
<i>ii.</i>	<i>The polynomial function of 5<sup>th</sup> order .....</i>	<i>184</i>
G.	THE CALCULATIONS THAT DESCRIBE THE INDUCED POLARIZATION.....	186
<i>i.</i>	<i>Linear Function .....</i>	<i>186</i>
<i>ii.</i>	<i>3<sup>rd</sup> degree function .....</i>	<i>190</i>
<b>10.</b>	<b>BIBLIOGRAPHY .....</b>	<b>199</b>



# Table of Figures

FIG. 1.	PIEZOELECTRICITY.....	13
FIG. 2.	THE SCHEMATIC EXPLANATION OF FLEXOELECTRICITY.....	13
FIG. 3.	A FEM REPRESENTATION OF A MODE I CRACK AND THE INDUCED STRAINS.....	14
FIG. 4.	THE EXPERIMENTS. ....	14
FIG. 5.	THE FLEXOELECTRIC CONSTANTS FOR VARIOUS CUBIC SEMICONDUCTORS.....	15
FIG. 6.	THE PIEZOELECTRIC CONSTANT FOR VARIOUS CUBIC SEMICONDUCTORS .....	15
FIG. 7.	THE FLEXOELECTRIC CONSTANTS FOR VARIOUS CUBIC ALKALI HALIDES.....	16
FIG. 8.	THE FLEXOELECTRIC CONSTANTS FOR VARIOUS CUBIC PEROVSKITES.....	16
FIG. 9.	THE D-CONE PROBLEM IS THE BEST WAY TO MODEL A CRUMPLED SHEET. ....	18
FIG. 10.	SCREW DISLOCATION.....	19
FIG. 11.	THE ANTI-PLANE STRAIN CRACK PROBLEM. ....	26
FIG. 12.	SCHEMATIC REPRESENTATION OF THE ANTI-PLANE PROBLEM SOLVED BY PROF. ZISIS (ZISIS (2018)).....	27
FIG. 13.	THE STRAINS IN THE ANTI-PLANE FORMULATION. ....	31
FIG. 14.	THE TWIST OF BEAMS.....	32
FIG. 15.	A THIN PLATE. ....	32
FIG. 16.	THE PULL OUT OF THE REINFORCEMENT ON ONE-DIMENSIONAL CONCRETE ELEMENT LIKE A BEAM OR A COLUMN IS A PURELY ANTI-PLANE PROBLEM.....	32
FIG. 17.	MODE I CRACK.....	33
FIG. 18.	MODE II CRACK.....	33
FIG. 19.	THE MODE III CRACK. ....	34
FIG. 20.	TYPICAL MATERIAL PARAMETERS .....	36
FIG. 21.	THE BOUNDARY CONDITIONS REQUIRED IN THE ANTI-PLANE FLEXOELECTRIC FORMULATION, .....	38
FIG. 22.	THE BOUNDARY CONDITIONS NEEDED FOR THE ANTI-PLANE COUPLE STRESS ELASTICITY PROBLEM, .....	42
FIG. 23.	THE THREE REGIONS THAT DEFINE THE ANTI-PLANE DYNAMIC PROBLEM TO HYPERBOLIC ELLIPTIC OR INTERMEDIATE. ....	45
FIG. 24.	THE REGIONS THAT APPEAR ON A DYNAMIC ANTI-PLANE FLEXOELECTRIC PROBLEM LIKE THE PROPAGATION OF A MODE III CRACK.....	46
FIG. 25.	THE ELLIPTIC SUBSONIC REGION. ....	47
FIG. 26.	THE OPENING OF A CRACK. ....	48
FIG. 27.	THE FEM MODEL THAT WAS USED TO CAPTURE THE RESPOND OF THE PROPAGATION OF THE MODE III CRACK .....	49
FIG. 28.	THE ANTI-PLANE PROBLEM OF THE PROPAGATION OF A MODE III CRACK, AS SOLVED BY THE USE OF THE ANALOGUE .....	49
FIG. 29.	THE INFLUENCE OF THE VELOCITY, IN THE ELLIPTIC SUBSONIC CASE (DISPLACEMENTS),.....	49
FIG. 30.	THE INFLUENCE OF THE MICROSTRUCTURAL LENGTH IN THE ELLIPTIC SUBSONIC CASE (DISPLACEMENTS).....	50
FIG. 31.	THE INTERMEDIATE REGION. ....	51
FIG. 32.	THE HYPERBOLIC REGION.....	52
FIG. 33.	THE OUT OF PLANE DEFORMATION IN THE HYPERBOLIC CASE, AS SUGGESTED BY THEORY.....	55
FIG. 34.	THE TRAPEZOIDAL FUNCTION.....	60
FIG. 35.	ASSUMPTION OF THE HYPERBOLIC CRACK PROFILE. ....	61
FIG. 36.	THE OUT-OF-PLANE DISPLACEMENT AND ITS DERIVATIVES.....	68
FIG. 37.	THE POLARIZATION ASSUMING A LINEAR FUNCTION TO TAKE PART IN THE DISPLACEMENT RELATION. ....	70
FIG. 38.	THE POLARIZATION FOR A DISPLACEMENT DESCRIBED BY A 3 <sup>RD</sup> ORDER FUNCTION. ....	73
FIG. 39.	THE COMPARISON OF THE POLARIZATION BETWEEN THE LINEAR CASE AND THE 3 <sup>RD</sup> ORDER FUNCTION CASE .....	73
FIG. 40.	THE FIRST SET OF THE DIAGRAMS ASSUMING SOME BOUNDARY CONDITIONS. ....	78
FIG. 41.	THE SECOND SET OF THE DIAGRAMS ASSUMING SOME BOUNDARY CONDITIONS. ....	79
FIG. 42.	THE BOUNDARY CONDITION IN A RIBBON PLATE. ....	80
FIG. 43.	THE SCREW DISLOCATION.....	81
FIG. 44.	THE FIRST DERIVATIVE OF THE DISPLACEMENT.....	82
FIG. 45.	THE SECOND DERIVATIVE OF THE DISPLACEMENT.....	82

FIG. 46.	THE POLARIZATION FOR A SCREW DISLOCATION.....	86
FIG. 47.	THE DEVELOPMENT OF ANTI-PLANE SURFACE WAVES.....	87
FIG. 48.	THE DISPERSION RELATION FOR TWO DIFFERENT MATERIALS. ....	89
FIG. 49.	THE FREQUENCY AS A FUNCTION OF THE WAVENUMBER (OR THE INVERSE OF THE ARCLength) IN THE MECHANICAL WAVES. ....	93
FIG. 50.	THE FREQUENCY AS A FUNCTION OF THE WAVENUMBER IN THE OPTICAL WAVES. ....	94
FIG. 51.	THE FREQUENCY AS A FUNCTION OF THE WAVENUMBER FOR <b>ratio</b> = 0.5 AND <b>ratio</b> = 0.25. ....	95
FIG. 52.	THE PERCENTAGE OF DIVERGENCE OF THE ANALYTICAL FROM THE ASYMPTOTIC VALUE, FOR <b>ratio</b> = 0.5. ....	97
FIG. 53.	THE PERCENTAGE OF DIVERGENCE OF THE ANALYTICAL FROM THE ASYMPTOTIC VALUE, FOR <b>ratio</b> = 0.25. ....	97
FIG. 54.	THE FREQUENCY AS A FUNCTION OF WAVENUMBERS FOR <b>ratio</b> = 0. ....	97
FIG. 55.	THE FREQUENCY AS A FUNCTION OF WAVENUMBERS FOR <b>ratio</b> → 0 (0.01) ....	97
FIG. 56.	THE PERCENTAGE OF DIVERGENCE OF THE ANALYTICAL FROM THE ASYMPTOTIC VALUE, FOR <b>ratio</b> = 0.0. ....	98
FIG. 57.	THE PERCENTAGE OF DIVERGENCE OF THE ANALYTICAL FROM THE ASYMPTOTIC VALUE, FOR <b>ratio</b> = 0.01. ....	98
FIG. 58.	DISPERSION CONVERGENCE TO 5% ERROR.....	99
FIG. 59.	MECHANICAL DISPERSION CONVERGENCE.....	99
FIG. 60.	OPTICAL DISPERSION CONVERGENCE. ....	99
FIG. 61.	LEGIT AREA FOR MECHANICAL WAVES.....	99
FIG. 62.	LEGIT AREA FOR OPTICAL WAVES.....	99
FIG. 63.	THE PHASE VELOCITY OF THE MECHANICAL WAVES AS A FUNCTION OF THE WAVENUMBER OF EACH WAVE.....	100
FIG. 64.	THE PHASE VELOCITY OF THE OPTICAL WAVES AS A FUNCTION OF THE WAVENUMBER OF EACH WAVE. ....	101
FIG. 65.	THE PHASE VELOCITY AS A FUNCTION OF THE WAVENUMBER FOR <b>ratio</b> = 0.5.....	102
FIG. 66.	THE PERCENTAGE OF DIVERGENCE OF THE ANALYTICAL FROM THE ASYMPTOTIC VALUE CONCERNING THE PHASE VELOCITY, FOR <b>ratio</b> = 0.5.....	102
FIG. 67.	THE PHASE VELOCITY AS A FUNCTION OF THE WAVENUMBER FOR <b>ratio</b> = 0.25. ....	102
FIG. 68.	THE PERCENTAGE OF DIVERGENCE OF THE ANALYTICAL FROM THE ASYMPTOTIC VALUE CONCERNING THE PHASE VELOCITY, FOR <b>ratio</b> = 0.25.....	102
FIG. 69.	THE PHASE VELOCITY AS A FUNCTION OF THE WAVENUMBER FOR <b>ratio</b> = 0.00.....	103
FIG. 70.	THE PERCENTAGE OF DIVERGENCE OF THE ANALYTICAL FROM THE ASYMPTOTIC VALUE CONCERNING THE PHASE VELOCITY, FOR <b>ratio</b> = 0.00.....	103
FIG. 71.	PHASE VELOCITY CONVERGENCE TO 5% ERROR. ....	103
FIG. 72.	MECHANICAL PHASE VELOCITY CONVERGENCE.....	104
FIG. 73.	OPTICAL PHASE VELOCITY CONVERGENCE.....	104
FIG. 74.	CONVERGENCE RELATION OF FREQUENCY AND PHASE VELOCITY.....	104
FIG. 75.	THE GROUP VELOCITY OF THE MECHANICAL WAVES AS A FUNCTION OF THE WAVENUMBER OF EACH WAVE.....	105
FIG. 76.	THE GROUP VELOCITY OF THE OPTICAL WAVES AS A FUNCTION OF THE WAVENUMBER OF EACH WAVE. ....	106
FIG. 77.	THE GROUP VELOCITY AS A FUNCTION OF THE WAVENUMBER FOR <b>ratio</b> = 0.5.....	107
FIG. 78.	THE PERCENTAGE OF DIVERGENCE OF THE ANALYTICAL FROM THE ASYMPTOTIC VALUE CONCERNING THE GROUP VELOCITY, FOR <b>ratio</b> = 0.5.....	107
FIG. 79.	THE GROUP VELOCITY AS A FUNCTION OF THE WAVENUMBER FOR <b>ratio</b> = 0.25. ....	107
FIG. 80.	THE PERCENTAGE OF DIVERGENCE OF THE ANALYTICAL FROM THE ASYMPTOTIC VALUE CONCERNING THE GROUP VELOCITY, FOR <b>ratio</b> = 0.25.....	107
FIG. 81.	THE GROUP VELOCITY AS A FUNCTION OF THE WAVENUMBER FOR <b>ratio</b> = 0.00. ....	108
FIG. 82.	THE PERCENTAGE OF DIVERGENCE OF THE ANALYTICAL FROM THE ASYMPTOTIC VALUE CONCERNING THE GROUP VELOCITY, FOR <b>ratio</b> = 0.00.....	108
FIG. 83.	MECHANICAL GROUP VELOCITY CONVERGENCE.....	109
FIG. 84.	CONVERGENCE RELATION OF FREQUENCY AND MECHANICAL GROUP VELOCITY FOR ERROR EQUAL TO 5%. ....	109
FIG. 85.	THE DISPERSION RELATIONS FOR META-MATERIAL AND NORMAL DIELECTRICS. ....	110
FIG. 86.	THE PHASE VELOCITY, FOR META-MATERIALS AND NORMAL DIELECTRICS. ....	111

FIG. 87.	THE GROUP VELOCITY, FOR META-MATERIALS AND NORMAL DIELECTRICS.....	112
FIG. 88.	THE TOTAL ACTIONS APPLIED TO A PLATE.....	115
FIG. 89.	THE ANALOGUE.....	118
FIG. 90.	THE COMPLETE ANALOGUE OF THE ANTI-PLANE PROBLEM AND THE PLATE PROBLEM.....	124
FIG. 91.	THE ANALOGUE PLATE TO THE ANTI-PLANE PROBLEM. ....	126
FIG. 92.	THE PLATE-LIKE STRUCTURE THAT CAN BE INSERTED TO THE ANALOGUE. ....	128
FIG. 93.	SKETCHES FROM THE FEM MODEL. ....	132
FIG. 94.	CASES 1, 2 AND 3 AND THEIR POSITION IN THE HYPERBOLIC REGION. ....	133
FIG. 95.	THE ANTI-PLANE PROBLEM AND ITS BOUNDARY CONDITIONS.....	133
FIG. 96.	THE PLATE RESTRAINS.....	134
FIG. 97.	THE BOUNDARY CONDITION OF THE FINAL MODEL. ....	134
FIG. 98.	THE OUT-OF-PLANE DISPLACEMENT FOR THE 1 <sup>ST</sup> CASE, THE FIRST ALTERNATIVE.....	136
FIG. 99.	THE OUT-OF-PLANE DISPLACEMENT FOR THE 1 <sup>ST</sup> CASE, THE SECOND ALTERNATIVE.....	137
FIG. 100.	THE PROFILE OF THE CRACK IN THE PURELY HYPERBOLIC CASE. ....	138
FIG. 101.	THE OUT-OF-PLANE DISPLACEMENT FOR 2 <sup>ND</sup> CASE. ....	139
FIG. 102.	THE OUT-OF-PLANE DISPLACEMENT FOR 3 <sup>RD</sup> CASE. ....	141
FIG. 103.	THE HEAVISIDE FUNCTION.....	179

# 1. Introduction

## A. Physical aspect of flexoelectricity - what is flexoelectricity?

Flexoelectricity is a natural phenomenon that applies to a wide variety of materials. One complete definition of flexoelectricity has been suggested by [Giannakopoulos and Zisis \(2021\)](#).

*“Flexoelectricity is the ability of materials to convert mechanical strain gradients to electric polarization and vice versa”*

All dielectrics and ferroelectrics in paraelectric phase materials are defined as flexoelectric. Those when subjected to non-uniform mechanical strain, can produce electrical polarization.

The direct flexoelectric effect, which converts mechanical strain gradients to electrical polarization, can be described by the following relation:

$$P_i = \mu_{ijkl} \frac{\partial^2 u_j}{\partial x_k \partial x_l}$$

A pretty similar phenomenon, called piezoelectricity, which has been studied extensively, can be added in the above relation, as suggested by [Maranganti et al. \(2006\)](#).

$$P_i = p_{ijk} \varepsilon_{jk} + \mu_{ijkl} \frac{\partial^2 u_j}{\partial x_k \partial x_l}$$

In the above relation  $p_{ijk} \varepsilon_{jk}$  is the piezoelectric term and should be equal to zero when a non-piezoelectric material (a centrosymmetric material), is concerned. If this term is zero, the remaining equation describes the direct flexoelectric effect.

This microscopical effect comes from the atomic crystallin structure. Because of a relative dense crystalline structure, when a strain gradient is applied, some positive cores come closer and thus, this side gets positively charged, while some others, from the opposite side, get further away and thus that side gets negatively charged. This difference in the charges creates a polarization and a respective electric field. The phenomenon of flexoelectricity resembles the condition of a capacitor.

The parameters that affect flexoelectricity, are the strain gradient, which is connected to mechanical characteristics like Lamé's constants, and a module that signifies how dense this crystallin structure is. This module, in the direct flexoelectric effect, is the  $\mu_{ijkl}$  coefficient.

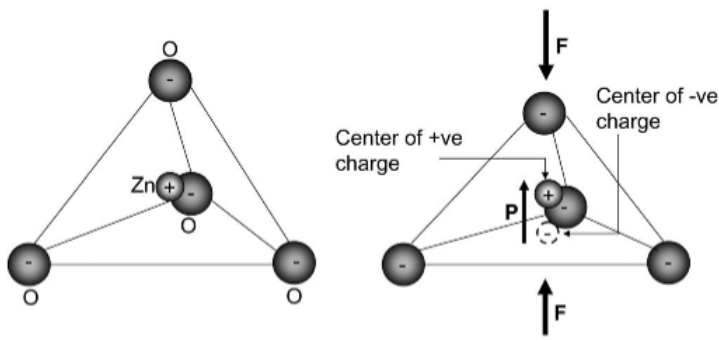
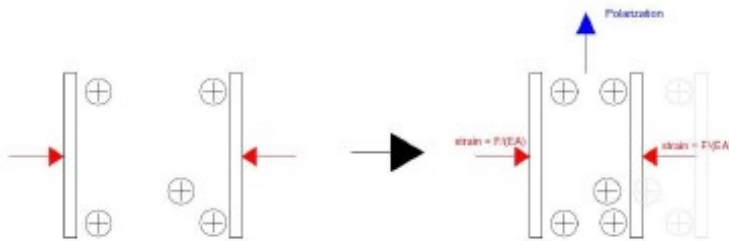


Fig. 1. Piezoelectricity.

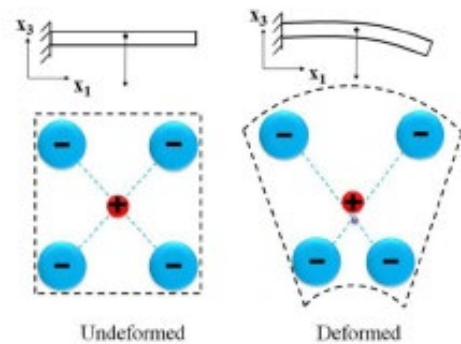
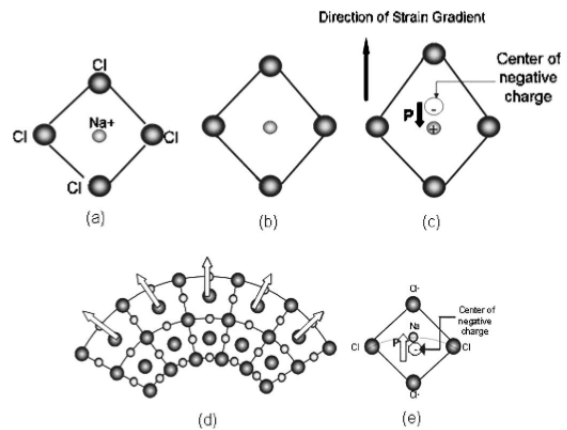
The microscopical explanation of the production of polarization in a non-centrosymmetric crystal through the effect of piezoelectricity, by uniform loading. Maranganti et al. (2006)



And by Knisovitis (2019)

Fig. 2. The schematic explanation of flexoelectricity.

The induced polarization is happening only for a non-uniform deformation that is flex-like. The cell of NaCl is centrosymmetric and thus no polarization can be induced from uniform loading. Maranganti et al. (2006).



A simpler schematic description of the flexoelectric phenomenon is being represented in Seung-Bok Choi and Gi-Woo Kim (2017).

Flexoelectricity is weak in comparison to the stronger piezoelectricity, but in small scales the flexoelectric effect can reach its competitor, as the strain gradients are great. These, also,

have to do with all the parameters that causes this effect. As it has been studied extensively experimentally (Knisovitis (2019) and Giannakopoulos et al. (2020)) near the crack tips the gradients are great and the flexoelectric effect can overtake major role.

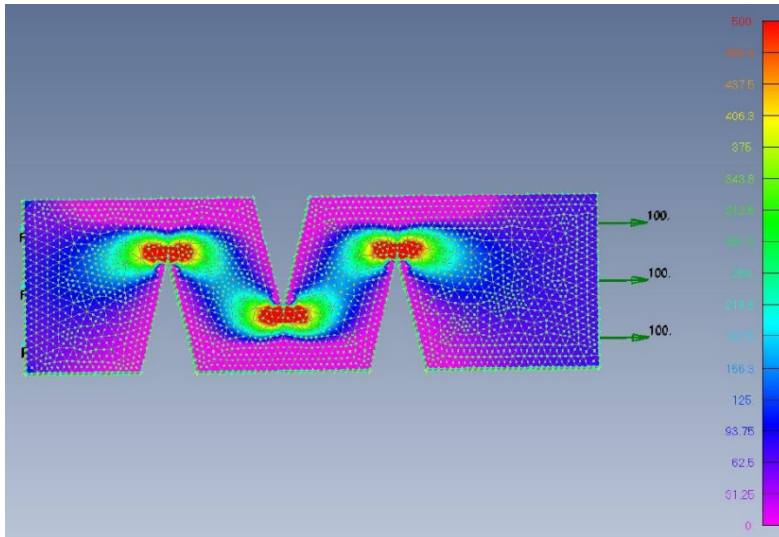


Fig. 3. A FEM representation of a Mode I crack and the induced strains. There is a big concentration of strain gradients near the crack tips. This figure represents the strains  $\varepsilon_{11}$ . Knisovitis (2019)

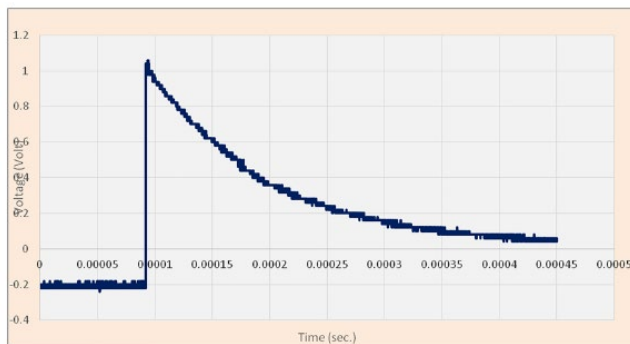
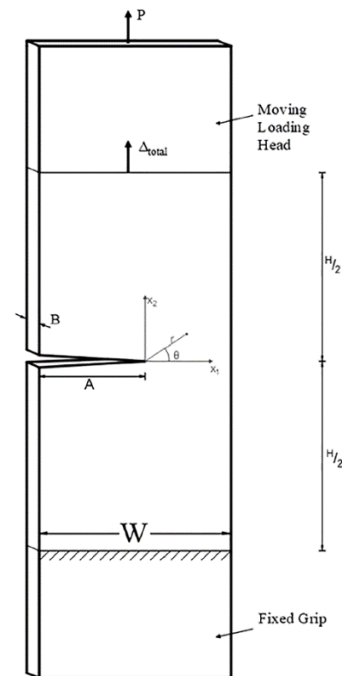


Fig. 4. The experiments.

Described in Knisovitis (2019) and Giannakopoulos et al. (2020). In one-dimensional element, a mode I crack has an effect of a rather large voltage. The oscilloscopes frequency was 1 MHz.



Similar to the direct effect is the converse flexoelectric effect, which uses electrical work and turns it into mechanical. In other words, a polarization applied in a flexoelectric material will result in a strain gradient and thus some deformation.

## B. The materials

Flexoelectric materials can be dielectric or ferroelectrics in a paraelectric phase. [Giannakopoulos and Zisis \(2021 a.\)](#) proposed, that a vast majority of materials are flexoelectric. Some materials that are anisotropic exhibit also piezoelectricity and flexoelectricity combined.

Some rocks including the earth's mantle, are both flexoelectric and piezoelectric. Materials that are characterized as flexoelectric could be ribbons of graphene, carbon or graphene nitride, biological membranes, a lot of polymers (PVDF, plexiglass, paraffin, polystyrene), ceramics (perovskites, magnesium oxide, alkali halides, colloidal crystals) and even crystalline materials like salt. Ice is also flexoelectric. Lastly, many semi-conductors have flexoelectric properties.

The characteristic of a flexoelectric material is the flexoelectric constant  $\mu_{ijkl}$ . Despite the fact that this constant seems like a fourth order tensor, usually it has only three independent components,  $\mu_{11}, \mu_{12}, \mu_{44}$ .

As described in greek literature by [Knisovitis \(2019\)](#) its constant is used for a specific strain gradient. The constant  $\mu_{11}$  is used when the strain is normal to a surface e.g.  $\varepsilon_{11}$  and the gradient is towards the corresponding direction, e.g. direction 1. The constant  $\mu_{12}$  refers to normal strains, but the direction of the gradient is one of the other two and lastly the component  $\mu_{44}$  refers to shear strains.

	$\mu_{11}$ ( $10^{-13}$ C/cm)		$\mu_{12}$ ( $10^{-13}$ C/cm)		$\mu_{44}$ ( $10^{-13}$ C/cm)	
	<i>Ab initio</i>	Shell model	<i>Ab initio</i>	Shell model	<i>Ab initio</i>	Shell model
GaAs	0.5144	0.8512	-0.8376	0.5107	0.2645	0.1702
GaP		0.4653		0.3128		-0.3443
ZnS		-0.311		-1.544		-0.611

Fig. 5. The flexoelectric constants for various cubic semiconductors from [Maraganti and Sharma \(2009\)](#).

	$e_{14}$ (C/m <sup>2</sup> )		
	<i>Ab initio</i>	Shell model	Experiment
GaAs	-0.1464	-0.066	-0.16
GaP		-0.0744	-0.1
ZnS		-0.111	-0.13

Fig. 6. The piezoelectric constant for various cubic semiconductors from [Maraganti and Sharma \(2009\)](#).

	$\mu_{11}$ ( $10^{-13}$ C/cm)		$\mu_{12}$ ( $10^{-13}$ C/cm)		$\mu_{44}$ ( $10^{-13}$ C/cm)	
	Shell model	Askar <i>et al.</i> <sup>a</sup>	Shell model	Askar <i>et al.</i> <sup>a</sup>	Shell model	Askar <i>et al.</i> <sup>a</sup>
NaCl	0.412	0.423	-0.122	-0.119	-0.212	-0.230
KCl	0.403	0.411	-0.122	-0.120	-0.228	-0.231

Fig. 7. The flexoelectric constants for various cubic alkali halides from Maraganti and Sharma (2009). Index “a” is referring to “A. Askar, P. C. Y. Lee, and A. S. Cakmak, Phys. Rev. B 1, 3525 (1970)”.

	$\mu_{11}$ ( $10^{-13}$ C/cm)		$\mu_{12}$ ( $10^{-13}$ C/cm)		$\mu_{44}$ ( $10^{-13}$ C/cm)	
	<i>Ab initio</i>	Experiment	<i>Ab initio</i>	Experiment	<i>Ab initio</i>	Experiment
STO	-26.4	20	-374.7	700	-357.9	300
BTO	15.0		-546.3	$10^6$	-190.4	

Fig. 8. The flexoelectric constants for various cubic perovskites from Maraganti and Sharma (2009). For STO the experimental data was obtained from “P. Zubko, G. Catalan, P. R. L. Welche, A. Buckley, and J. F. Scott, Phys. Rev. Lett. 99, 167601 (2007)”, while for the BTO from “W. Ma and L. E. Cross, Appl. Phys. Lett. 88, 232902 (2006)”.

Similar to those, the reverse flexoelectric constants are symbolized as  $f_{11}, f_{12}, f_{44}$ .

### C. Applications

Flexoelectricity can be used in a great number of applications for energy harvesting, into micro-electro-mechanical systems, for nanotechnology and even for biology, as it has been mentioned by Häusler *et al.* (1984) and Gi-woo Kim *et al.* (2014). In addition to those, which are relevant applications in any ferroelectric problem, flexoelectricity could have major role in situations with great strain gradients. Cracks are cases that exhibits large strain gradients, and thus the application in respect of flexoelectricity is more prominent (Knisovitis (2019), Giannakopoulos *et al.* (2020)).

Ferroelectric phenomena have great applications in conditions of mechanical shock e.g. accidental drop or explosion. Also, flexoelectricity can be used in dynamic cracking while an earthquake is happening. In an earthquake the shear force is similar to cracking, and the earth’s mantle is not only piezoelectric but also flexoelectric. The strains and strain gradients can be significant and thus strong electromagnetic field may be created. It is very interesting, that for non-piezoelectric rocks like marble or limestone an electromagnetic emission occurs and this should be caused by the flexoelectric effect (Giannakopoulos (2019, 2021a, 2021b)).

Last but not least, there is the combination of flexoelectricity with the propagation of waves. Moroni *et al.* (2014), stated that in an anti-plane couple stress elasticity dynamic problem, like the one that is studied in the current research, Rayleigh waves of high frequency may be



produced. Those waves ought to limit the velocity of the crack to a Rayleigh wave speed  $c_R$ . This velocity is relative to the parameter  $\beta$  of the couple stress theory and for  $\beta = 0$ , when the problem is hyperbolic, Rayleigh waves can appear. This comment has been mentioned in [Giannakopoulos and Zisis \(2019\)](#).

In a later study, the same authors, [Giannakopoulos and Zisis \(2021 a\)](#), mentioned the existence of those waves in a flexoelectric anti-plane dynamic problem, that move through the surface. Flexoelectricity should also develop anti-plane surface waves, which would have great applications (e.g., shear-horizontal surface-acoustic-wave (SH-SAW) biosensors). This is something known in piezoelectricity, as it has been established from Bluestein and Gulyavev, but such waves are not supported in the content of classic elastodynamics. Experimental verification in flexoelectricity waves should be performed in the future (in piezoelectricity, experiments have confirmed the existence of such waves however)

Rayleigh waves, lamb waves and love waves too. All those, could get combined with flexoelectricity.

#### D. Previous Research

In a previous research ([Knisovitis \(2019\)](#)) the flexoelectric effect in one-dimensional problems was studied in a great scale. That study was based on the direct effect and proposed a vast majority of applications, that are relevant to the phenomenon. For an initial study of the phenomenon that thesis is recommended.

This study, is about the anti-plane flexoelectric problem, flexoelectricity in other words, when a mode III crack occurs, as this is the most common dynamic anti-plane problem. The formulation of the governing equations of the problem was made with the use of the total energy density and a method called Toupin's Variational Principle. The connection with the couple stress elasticity anti-plane problem is later discussed. An analogue, proposed by Giannakopoulos and his co-workers ([Gavardinias et al. \(2018\)](#)), connects the anti-plane problem, whether it is flexoelectric, or defined through the use of the couple stress elasticity with prestressed plates.

##### i. Bibliographic references on flexoelectricity.

A great portion of research has been done by Maraganti and co-workers. In their research ([Maranganti et al. \(2006\)](#)), they studied flexoelectricity, both in its direct form and its converse. For their calculations, [Maraganti et al. \(2006\)](#) used the internal energy density in order to derive the governing equations. In this relation, both piezoelectric and flexoelectric effects were considered, as they were inserted through the converse effect. For flexoelectricity, the term for energy is  $f_{ijkl}P_iu_{j,kl}$ . The governing equations, which in that project are referred to as "the balance laws" are similar to the ones used later. However, they got extracted via a method proposed by those researchers themselves, in some previous studies.

[Maraganti and Sharma \(2009\)](#) studied the properties of cubic semiconductors, alkali halides and perovskites, in respect of the flexoelectric phenomenon, via atomistic perspective. The

result of the studies was the estimation of the flexoelectric constant  $\mu_{11}, \mu_{12}, \mu_{44}$  by their theory and the comparison with other estimations that could be also experimental.

Yang et al. (2018) published an interesting article about Lamb waves and when those exist in a flexoelectric medium.

An interesting aspect of flexoelectricity has been discussed by Wang et al. (2019), as they suggested that this phenomenon is rather weak, unless it is produced from significant large strain gradients. By describing the phenomenon, the authors related it to piezoelectricity and also, they suggested that with flexoelectricity, piezoelectric applications like energy harvesting (at small scales (nano)), sensors, actuators, in ferroelectric mechanics, or even in biomedicine are easily accessible.

The authors suggested that a way to achieve a great flexoelectric effect is by increasing the strain gradient. This, in other words, is equivalent to reducing the size of the dielectric in which the strain is applied (make the deviator smaller).

One interesting application that the authors studied, which has both large strain gradients and small size (thickness) is the crumpling of a sheet. This crumpling can be studied by using a thin plate with an out-of-plane point load in the center, until folding occurs. The experiment that describes this, is a circular piece of paper above a cup of water, being pressed by a pen.

The picture and figure that are displayed beneath are from Wang et al. (2019) and depict the best way to study the crumpling of a sheet. This model is named d-cone and, from a mechanical perspective, has been solved. In case the sheet is not from paper (paper is still flexoelectric, but not a good one), but from PVDF, (which is one of the best flexoelectric materials) a great amount of polarization should be found.

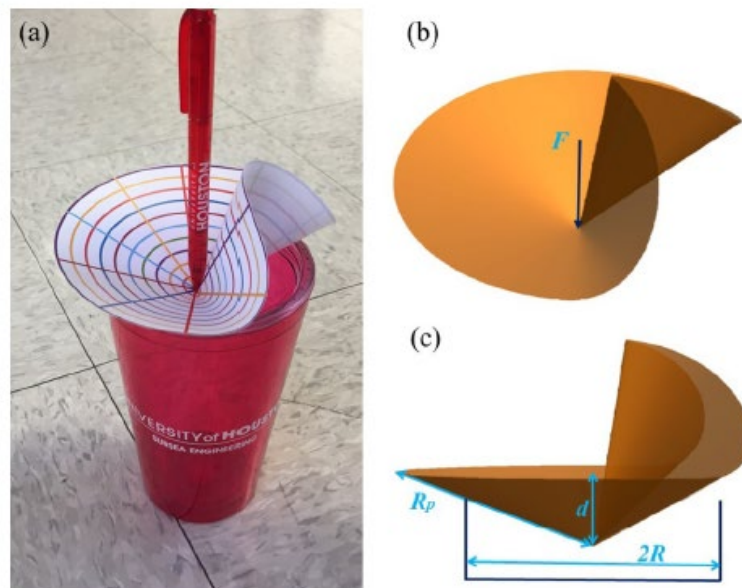


Fig. 9. The d-cone problem is the best way to model a crumpled sheet.

The parameters of the problem are the large radius (of the plate), the small radius (of the restrains), the out-of-plane displacement, and the angle  $\theta$ , between the two radii in which the folding occurred. The picture and sketch were taken from Wang et al. (2019).

The authors used, for the solution of the flexoelectric d-cone problem, the total potential energy. In their research they found a great amount of polarization and found that the smaller the thickness of the sheet, the better the results.

Giannakopoulos and Zisis (2019) suggested that the flexoelectric problem, which is a problem of coupling mechanical with electrical work, can be simplified in a solely mechanical dynamic problem.

Using this suggestion, the authors solved the steady state problem of screw dislocation. A screw dislocation is a Mode III crack in which the cohesive zone has been extremely reduced, and thus there is a discontinuity of the displacement. A screw dislocation can be described by the figure below.

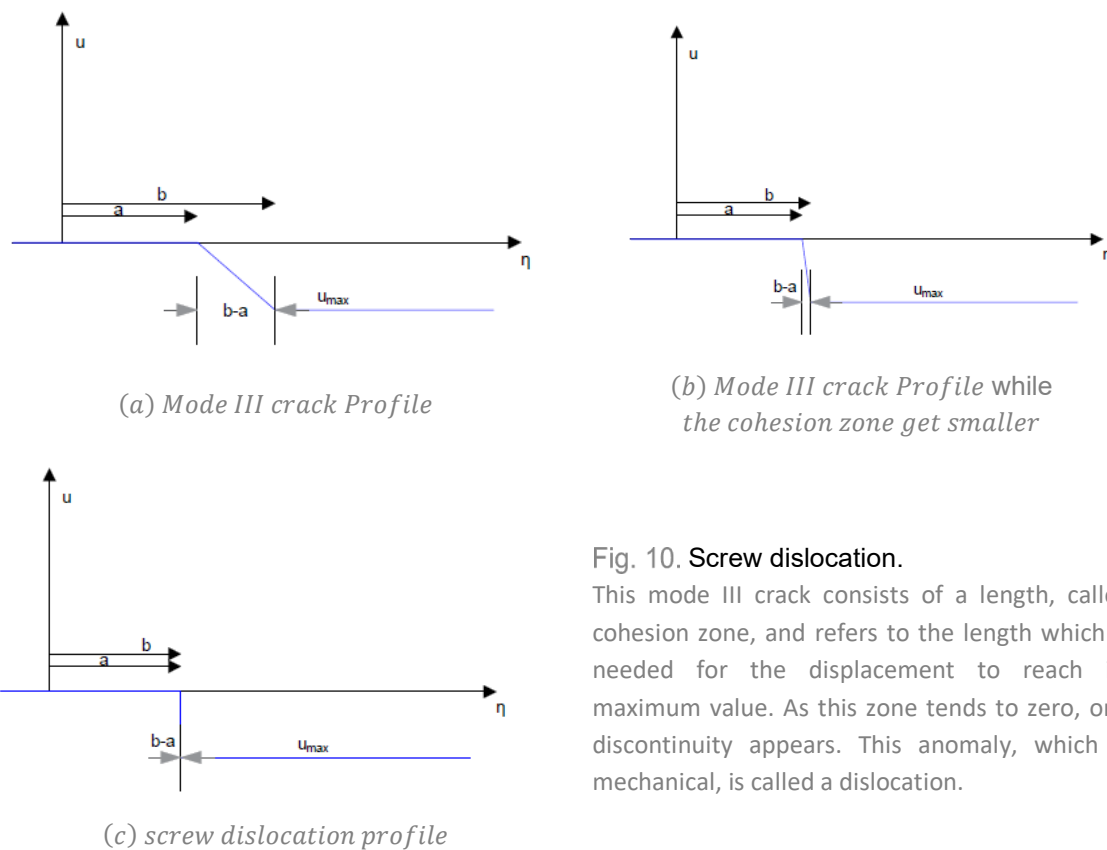


Fig. 10. Screw dislocation.

This mode III crack consists of a length, called cohesion zone, and refers to the length which is needed for the displacement to reach its maximum value. As this zone tends to zero, one discontinuity appears. This anomaly, which is mechanical, is called a dislocation.

The screw dislocation that was taken into consideration by the authors, gives a more accurate perspective of the displacement, as this displacement is known and the mode III crack problem of a screw dislocation is a known anti-plane couple stress elasticity problem. However, the same applies in other anti-plane crack problems. In addition, the authors mentioned the importance of a screw dislocation in subjects such as crystal growth, plasticity, development of thin epitaxial films, micro-component, opto-mechanical devices and the study of seismology.

This study was done by taking into consideration the microstructure, the microstructural length and also the micro-inertia length, for the purely anti-plane problem. For the anti-plane flexoelectric problem however, the solution should be based on classic elasticity.

The dislocation spreads with a constant velocity, that can be subsonic or even supersonic. Also, the displacement in some cases could be like Mach cones and as suggested by the authors, those cones are dependent on the microstructure.

Yang et al. (2020) studied the propagation of Rayleigh waves when flexoelectricity, strain gradient elasticity, surface effects and micro-inertial effects were considered. The authors mentioned that in present days, surface waves are of crucial importance, as they have multiple applications in seismology and geophysics, telecommunications, acoustics and electronics, nondestructive evaluation (monitoring) and microfluidics. In addition to the various applications flexoelectricity enables the propagation of surface waves in flexoelectric materials, which can have an enormous variety of applications with huge impact.

Rayleigh waves are dispersive and have been studied in terms of piezoelectricity, through couple stress effect and through gradient elasticity theory. An acoustic wave (e.g. Rayleigh wave) produces, always, homogeneous strain and electric field in elastic dielectrics. The same applies in flexoelectricity, in which the strain gradients produce electric polarization. Yang et al. (2020) revealed, based on previous researches, that, when waves of small wavenumber are combined with flexoelectricity, the frequencies are enormous. This is something they proved, in their research, as they have shown that with the decrease of the wavelength, the influence of flexoelectricity and the other effects they studied (surface effects, micro-inertial effects, strain gradient elasticity) need to be considered, as their effect is great.

In Giannakopoulos and Zisis (2021 a), the authors once again mentioned the similarity of the flexoelectric anti-plane problem and the couple stress elasticity anti-plane dynamic problem and suggested that the modeling of both can happen via anisotropic plates with biaxial prestressing, different in each direction. They also suggested that the microstructure, the microstructural and the micro-inertial lengths, is crucial for the displacement, which in a steady state anti-plane crack could be like "Mach cone". Lastly, they mentioned the existence of waves, that move through the surface (Rayleigh wave that may spread in the anti-plane dynamic problem).

Rosakis and co-workers (Xia et al. (2004)), suggested that cracks may also spread with supershear velocity. This also was proved experimentally. This suggestion is relevant for both supersonic and subsonic velocities. For high velocities to occur, high stresses should be produced, like the stresses produced in cracks.

Those authors, also, mentioned "electrical yielding" like conditions.

In contrast to their previous work, this time, the authors studied the motion of Mode III crack (instead of a screw dislocation). The material they used had to be flexoelectric. For the analysis, the analogue proposed from their previous studies was used (Giannakopoulos and Zisis (2019), Gavardinas et al. (2018)). This analogue reduces the anti-plane flexoelectric dynamic problem (moving crack) into a dynamic couple stress elasticity problem, and also to a prestressed orthotropic plate. For this problem, two length parameters need to be used.

The microstructural length is connected to the displacement curvature and is used in the couple stress elasticity theory on many occasions.

The micro-inertial length is used for the introduction of a non-classic kinetic energy associated with the micro-rotations. Moroni et al. (2013) suggested that the slope of Mach cones that can occur on the hyperbolic problem are related to this length. Giannakopoulos and Zisis (2021 a)

also suggested that because of this length (and this is obvious via the formula of the differential governing equations of the problem), Mach cones could appear also for subsonic problems, when hyperbolicity is present.

The classic theory of elasticity, which is used in the flexoelectric problem, enables the option to consider the elastic energy only relevant to the strains and not the strain gradient, in contrast to the case of the anti-plane couple stress elasticity problem.

Giannakopoulos and Zisis (2021 b.) studied once again the flexoelectric effect on a uniformly moving anti-plane crack with some additions.

## ii. Toupin's Variational Principle and the total Energy Density.

The most important parts of Toupin's Variational Principle were described by Mindlin. The theory of gradient elasticity can be better understood from the work of Mindlin (1965), in which one addition to the potential energy density was done, as not only the strains took part, but also its gradients. The total potential energy for a homogeneous isotropic and centrosymmetric material can be written in its full form as follows (in that relation the part relative to the polarizations is missing. This addition however is done by the same author in a later research Mindlin (1968)):

$$\begin{aligned}
 w = & \frac{1}{2} \lambda \varepsilon_{ii} \varepsilon_{jj} + \mu \varepsilon_{ij} \varepsilon_{ij} + a_1 \varepsilon_{ijj} \varepsilon_{ikk} + a_2 \varepsilon_{iik} \varepsilon_{kjj} + a_3 \varepsilon_{iik} \varepsilon_{jjk} + a_4 \varepsilon_{ijk} \varepsilon_{ijk} \\
 & + a_5 \varepsilon_{ijj} \varepsilon_{kji} + b_1 \varepsilon_{iij} \varepsilon_{kkll} + b_2 \varepsilon_{ijkk} \varepsilon_{ijll} + b_3 \varepsilon_{iijk} \varepsilon_{jkll} \\
 & + b_4 \varepsilon_{iijk} \varepsilon_{llkj} + b_5 \varepsilon_{iijk} \varepsilon_{lljk} + b_6 \varepsilon_{ijkl} \varepsilon_{ijkl} + b_7 \varepsilon_{ijkl} \varepsilon_{jkli} \\
 & + c_1 \varepsilon_{ii} \varepsilon_{jjkk} + c_2 \varepsilon_{ij} \varepsilon_{ijkk} + c_1 \varepsilon_{ij} \varepsilon_{kkij} + b_0 \varepsilon_{iijj}
 \end{aligned}$$

In the above relation the components  $\varepsilon_{ij}$ ,  $\varepsilon_{ijk}$ ,  $\varepsilon_{ijkl}$  are the components of  $\varepsilon^1 = (\nabla \tilde{u} + \tilde{u} \nabla)/2$ ,  $\varepsilon^2 = \nabla \nabla \tilde{u}$ ,  $\varepsilon^3 = \nabla \nabla \nabla \tilde{u}$ .

The anti-plane problem leads to a reduction of the above relation as described in the researches from Prof. Giannakopoulos and his co-workers (Giannakopoulos and Zisis (2019), (2021a.), (2021b)).

One of the most necessary parts, concerning the treatment of the problem, through the potential energy and Hamilton's principle is done by using the research of Mindlin (1968). Mindlin uses Toupin's Variation Principle, and by an energy method finds the governing equations of a problem. This principle has the following form.

$$-\delta \int_{V^*} H dV + \int_V (f_i \delta u_i + E_i^0 \delta P_i) \delta V + \int_S t_i \delta u_i \delta S = 0$$

The integrals refer to volume  $V$  which is occupied by a body.  $V^*$  is the total volume that is occupied or not by any body, while  $S$  is the surface of the body.  $H$  is the total enthalpy which is equal to  $H = W - \varepsilon_0 \varphi_{,i} \varphi_{,i} / 2 + \varphi_{,i} P_i$ ,  $W$  is the total potential energy density,  $\varepsilon_0$  is the vacuum permittivity and  $\varphi_{,i}$  is the Maxwell self-field. The first point of interest is the total potential energy density and the parameters from which it depends, Firstly, by assuming that the total potential energy density depends on the strains ( $S_{ij} = (u_{j,i} + u_{i,j})/2$ ) and the polarizations ( $P_i$ ) (mechanical and electrical components), the variation of electric enthalpy density is a relation of stresses ( $T_{ij} = \partial W / \partial S_{ij}$ ) and effective local electric forces ( $\bar{E}_i = -\partial W / \partial P_i$ ),

$$\delta H = \delta \left( W - \frac{1}{2} \varepsilon_0 \varphi_{,i} \varphi_{,i} + \varphi_{,i} P_i \right)$$

$$\delta H = \delta W - \varepsilon_0 \varphi_{,i} \delta \varphi_{,i} + \delta \varphi_{,i} P_i + \varphi_{,i} \delta P_i$$

$$\delta H = T_{ij} \delta S_{ij} - \bar{E}_i \delta P_i - \varepsilon_0 \varphi_{,i} \delta \varphi_{,i} + \delta \varphi_{,i} P_i + \varphi_{,i} \delta P_i$$

Note that in this relation, the total energy density includes terms of polarization but not polarization gradients. Also, by the rule of chain and some manipulations by adding and then removing the same terms, Mindlin (1968), stated that the variation of the enthalpy can be written by the beneath formula.

$$\begin{aligned} \delta H = & -T_{ij,i} \delta u_i - (\bar{E}_i - \varphi_{,i}) \delta P_i - (-\varepsilon_0 \varphi_{,ii} + P_{i,i}) \delta \varphi + (T_{ij} \delta u_j)_{,i} \\ & + [(-\varepsilon_0 \varphi_{,i} + P_i) \delta \varphi]_{,i} \end{aligned}$$

The next step is to insert the above relation into Toupin's variational principle. One point that needs special care in the different spaces the integrals refer to.  $V^*$  is the total space, while  $V$  is the space occupied by the body.

The divergence theorem, transforms the space integral of a body to an area integral of the boundary of the body.

$$\int_{V'} \frac{\partial u_i}{\partial x_i} dV = \int_s u_i n_i ds$$

This way the variational principle it transformed to the following.

$$\int_{V^*} \{ (T_{ij,i} + f_i) \delta u_i + (\bar{E}_i - \varphi_{,i} + E_i^0) \delta P_i + (-\varepsilon_0 \varphi_{,ii} + P_{i,i}) \delta \varphi \} dV + \int_s \{ (t_i - n_i T_{ij}) \delta u_i + n_i [(-\varepsilon_0 [\varphi_{,i}] + P_i) \delta \varphi] \} \delta S = 0$$

Where  $[\varphi_{,i}]$  is the jump in  $\varphi_{,i}$ .

As it is obvious, because of the variational that are potential, the equality of the above relation should hold true for any variational. A number of equations is produced, for each variational. Equations that are generated from this kind of procedure are called Euler equations.

Potential Variable	Governing equations	Where
$\delta u_i$	$T_{ij,i} + f_i = 0$	
$\delta P_i$	$\bar{E}_i - \varphi_{,i} + E_i^0 = 0$	
$\delta \varphi$	$-\varepsilon_0 \varphi_{,ii} + P_{i,i} = 0$	in $V$
$\delta \varphi_{,i}$	$\varphi_{,ii} = 0$	in $V'$

Similarly, the boundary conditions can be obtained from this method, by the area integral.

Potential Variable	Boundary Condition
$\delta u_i$	$t_i - n_i T_{ij} = 0$
$\delta \varphi$	$n_i (-\varepsilon_0 [\varphi_{,i}] + P_i) = 0$

Through this procedure some manipulation can be done:

- To import the dynamic problem, the kinetic energy can be added to the total enthalpy density.
- If the total potential energy density depends on more variables, then the chain rule can be more detailed.

Next, [Mindlin \(1968\)](#) studied the dynamic case, in which the polarization gradient was added (but some other terms were missing). The integral that Mindlin proposed, similar to Toupin's variation principle is the following:

$$\delta \int_{t_0}^{t_1} dt \int_{V^*} \left( \frac{1}{2} \rho \dot{u}_i \dot{u}_i - H \right) dV + \int_{t_0}^{t_1} dt \left[ \int_{V^*} (f_i \delta u_i + E_i^0 \delta P_i) \delta V + \int_s t_i \delta u_i \delta S \right] = 0$$

The governing equations, or the Euler conditions produced in this case are the following:

<i>Governing equations</i>	<i>Where</i>
$-\rho\ddot{u}_i + T_{ij,i} + f_i = 0$	
$\bar{E}_i + E_{ij,i} - \varphi_{,j} + E_j^0 = 0$	
$-\varepsilon_0\varphi_{,ii} + P_{i,i} = 0$	<i>in V</i>
$\varphi_{,ii} = 0$	<i>in V'</i>

And the boundary conditions:

<i>Boundary Condition</i>
$n_i T_{ij} - t_j = 0$
$n_i (-\varepsilon_0 [\varphi_{,i}] + P_i) = 0$
$n_i E_{ij} = 0$

In addition to those boundary conditions, some initial conditions are also needed, as the problem in this case is dynamic. This is something that wasn't commented on Mindlin (1968), but later, Giannakopoulos took it into consideration (Giannakopoulos (2019, 2021a, 2021b)).

In those relations, the added terms are the accelerations,  $\ddot{u}_i$  which were imported through the addition of the kinetic energy through Hamilton's principle and the term  $E_{ij} = \partial W / \partial P_{j,i}$ , a term imported through a polarization gradient. The procedure to derive the governing equations follows the above, with some modifications (Appendix A), as the total energy density was considered a bit different.

### iii. The Couple Elasticity Anti-plane problem

A study of the cracks was made by Gourgiotis and Georgiadis (2007). In this research the authors used the couple stress elasticity theory to study the mode II and mode III cracks. The results of the couple stress elasticity seem to be different from the results of classical fracture mechanics.

In their study, the researchers took into account the microstructure of the material. The aim of that project was to provide a full-field solution for mode II and mode III cracks of finite length, by using a method called distributed dislocations, but this is not something to delve into.

Initially, the authors describe the basic concept of couple stress elasticity. They inserted in the potential energy density, in addition to the term referring to strains, also term referring to strain



gradient of the rotations, with some modifiers that are symbolized as  $\eta$  and  $\eta'$ . Those modifiers are the couple-stress moduli and for them the following relation should hold.

$$-1 < \frac{\eta}{\eta'} < 1$$

And also, in any case  $\eta > 0$ .

The terms of the strains are inserted in the potential energy density through the Lamé constants, for which, in any case the below relations should apply.

$$\begin{aligned} 3\lambda + 2\mu &> 0 \\ \mu &> 0 \end{aligned}$$

The potential energy density equation is proposed as the following

$$W \equiv W(\varepsilon_{ij}, \kappa_{ij}) = \frac{1}{2} \lambda \varepsilon_{ii} \varepsilon_{jj} + \mu \varepsilon_{ij} \varepsilon_{ij} + 2\eta \kappa_{ij} \kappa_{ij} + 2\eta' \kappa_{ij} \kappa_{ji}$$

Whereas the terms  $\kappa_{ij} = e_{jkl} \partial_i \partial_j u_l / 2 = e_{jkl} \partial_k \varepsilon_{il}$  are the strain gradient.

The authors then discuss the cases of plane strain (relative to the mode II crack) and the anti-plane strain which will be discussed further in the [Appendix C](#). According to the theory of Anti-plane strain, the deformation should be zero in the in-plane directions ( $x, y$ ) while non-zero in the out-of-plane direction:

$$\begin{aligned} u_x &\equiv 0 \\ u_y &\equiv 0 \\ u_z &\equiv w(x, y) \neq 0 \end{aligned}$$

In the next figure a crack in the frame of anti-plane strain is being presented. This sketch was obtained from [Gourgiotis and Georgiadis \(2007\)](#).

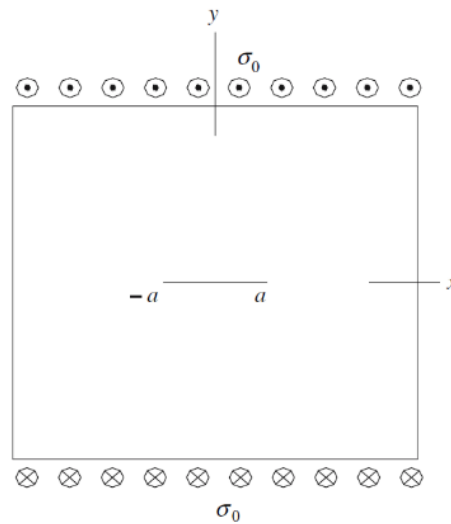


Fig. 11. The Anti-plane strain crack problem.

The loading is in the out-of-plane direction. The crack opens because of the shear contribution of the out-of-plane force (Giorgiotis and Georgiadis (2007)).

The differential equation that describes the anti-plane strain problem is the following:

$$\nabla^2 w - l^2 \nabla^4 w = 0$$

This equation, which is hypersingular with a cubic singularity, describes the anti-plane problem, using the theories of the couple stress elasticity. In that equation the term  $l$  describes the microstructural length. This length is related with the moduli  $\eta$  and  $\eta'$ .

The cracks are usually studied through distributed dislocations. A static mode II crack is usually studied as a glide dislocation distribution, while the static mode III crack as a screw dislocation distribution. Despite the fact that the crack that was used was a screw dislocation, the authors observed a cohesive-like zone near the crack tip in the shear stresses, that had increasing effects while the module  $\beta = \eta/\eta' \rightarrow 1$ . Ahead of that cohesive-like zone the stress gets maximized locally, but that maximum is bounded.

At the work of Zisis (2018) the anti-plane response of half planes and layers of finite thickness bonded on rigid substrates under a point load, in the context of couple stress elasticity, was discussed. This problem, when plain strain theory is used, is also known as Burmister's problem. Also in this paper, solutions near the point in which the load is applied were presented, that were used to be pathological via the classical solutions.

The problem, the author was cast to solve, is not a crack problem but a problem with a shear concentrated force on the surface of the plane and can be represented by the beneath sketch, which is included on the published paper. This problem was solved both analytically and computationally.

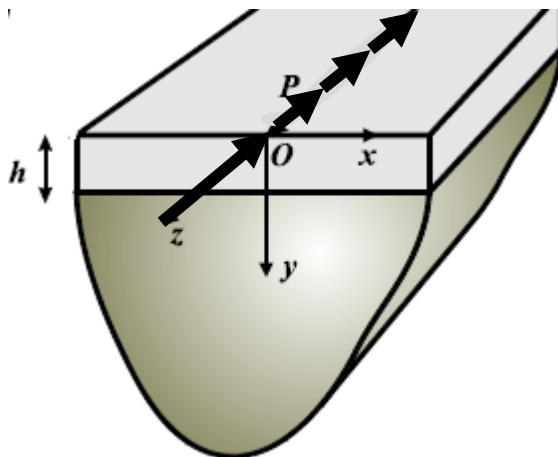


Fig. 12. Schematic representation of the anti-plane problem solved by Prof. Zisis (Zisis (2018)). Note that the direction of the “z” axis was changed from the original, so the system would be orthonormal.

#### iv. The plate problem

The instability of plates was something studied in a sufficient way by Babouskos and Katsikadelis (2009). The authors studied on plates the combined flutter and divergence instability and solved examples through the method of boundary elements. They included both conservative and non-conservative loads (regarding whether the load follows the deformation or not). The conservative force is applied in the undeformed configuration in contrast to the nonconservative load which is applied in the deformed configuration. Both those instabilities refer to axial in-plane force on a plate. The flutter instability describes a vibrational motion, usually happens for smaller loads and by enlarging the load is transformed to a divergence instability, which has smaller frequencies and the amplitude is increased exponential.

The significance of this research is the way the authors extracted the differential equations that describe the problem. They use Hamilton’s principle. According to that, the principle of virtual works, should hold true in any case.

$$\int_{t_1}^{t_2} (\delta T - \delta U + \delta V + \delta W_{nc}) dt = 0$$

In this relation the term  $T$  refers to the total kinetic energy between time  $t_1$  and  $t_2$ .  $U$  is the elastic energy, or as it is mentioned in other points the total potential energy density. The other two terms refer to the conservative and non-conservative forces that may be applied to the configuration.  $V$  is the potential of external forces while  $W$  is the virtual work of the nonconservative or damping loads.

The authors used the analogue equation method, a boundary element method to solve this kind of problems.

The flutter and divergence instability were also studied by [Adali \(1982\)](#). However, the basic theory concerning the plates is the same, as the out-of-plane displacement is concerned. The differential equation that defines the problem is non-other than the one proposed by [Babouskos and Katsikadelis \(2009\)](#). Actually, this research comes first, while the work of [Babouskos and Katsikadelis \(2009\)](#) supplements the theory, as the membrane displacements are studied in addition to the boundary element solution it provides.

Both researches point also the importance of the boundary conditions, which has been further studied in the work of [Shi and Bezzine \(1988\)](#). In this research, the anisotropic plate is being studied, as the authors presented an orthotropic plate in bending problems. The governing differential equation for an anisotropic plate is proposed as the following:

$$D_{11} \frac{\partial^4 w}{\partial x^4} + 4D_{16} \frac{\partial^4 w}{\partial x^3 \partial y} + 2 * (D_{12} + 2D_{66}) \frac{\partial^4 w}{\partial x^2 \partial y^2} + 4D_{26} \frac{\partial^4 w}{\partial x \partial y^3} + D_{22} \frac{\partial^4 w}{\partial y^4} = p(x, y)$$

In this equation  $D_{11}$ ,  $D_{16}$ ,  $D_{12}$ ,  $D_{66}$ ,  $D_{26}$ ,  $D_{22}$  are the flexural rigidities of the anisotropic plate, and  $p(x, y)$  is the bending action.

The boundary conditions that are needed for the solution of this differential equation can be reduced to the following:

Location of the boundary condition	Value of the bounded characteristic	
<i>Clamped edge</i>	$w = 0$	$\frac{\partial w}{\partial n} = 0$
<i>Simply – supported edge</i>	$w = 0$	$M_n = 0$
<i>Free edge</i>	$M_n = 0$	$V_n = 0$

The characteristic values can be defined from the operator  $(\partial(\dots))/\partial n$ ,  $M_n(\dots)$ ,  $V_n(\dots)$ , which can be calculated with a superposition of the gradients. That operator can be defined via the method proposed from of [Shi and Bezzine \(1988\)](#), in any boundary, even if the plate is not rectangular and the boundary is edgy.

#### v. The analogue of the anti-plane problem and a prestressed plate

[Gavardin et al. \(2018\)](#) presented a direct analogue for solving anti-plane problems with theories such as the couple stress elasticity or the dipolar gradient elastic (which are analogue), by solving a plate, prestressed by a biaxial tension and vice versa.

Next, the authors applied this analogue to a problem of crack under anti-plane shear loading. By solving a prestressed plate, the result of the anti-plane crack problem can be obtained via a FEM method.

#### vi. Flexoelectricity and magnetism

For the first time in this research (Giannakopoulos and Zisis (2021 b.)), the authors commented on magnetic effects that may occur. As the polarization has dynamic properties, polarization acceleration that may occur make it unjustifiable to neglect magnetic effects.

For the study of the electromagnetic field Giannakopoulos and Zisis (2021 b.) assumed a Maxwell electric field, which resides in the out-of-plane direction  $E_3(x_1, x_2, t)$  and also a magnetic field in the direction perpendicular to that (the magnetic field is in the other two directions, the in-plane directions),  $B_1(x_1, x_2, t)$  and  $B_2(x_1, x_2, t)$ . The dimension of this magnetic field is  $[Wb/m^2]$ . The authors proceeded by assuming a weak magnetic coupling and so the polarization that was calculated from the anti-plane flexoelectric problem holds. As a result of the polarization, an electric displacement can be induced  $D_3 = \epsilon_0 E_3 + P_3$  and also a current density  $I_3 = \dot{D}_3 [A/m^2]$  (also out-of-plane). As a result, an in-plane flux ( $H$ ) and an in-plane magnetic field ( $B$ ) will be created.

The electromagnetic effect also can be better described on the following table:

<i>Electromagnetic Characteristic</i>	<i>In plane Components</i>		<i>Out of Plane Components</i>
<i>Out of plane Electric Field</i>			$E_3(x_1, x_2, t)$
<i>Electrical Displacement</i>			$D_3 = \epsilon_0 E_3 + P_3$
<i>Current Density <math>[A/m^2]</math></i>			$I_3 = \dot{D}_3$
<i>In plane magnetic flux <math>[Wb/m^2]</math></i>	$B_1(x_1, x_2, t)$	$B_2(x_1, x_2, t)$	
<i>In plane magnetic field <math>[A/m]</math></i>	$H_1(x_1, x_2, t)$	$H_2(x_1, x_2, t)$	

To calculate these magnetic properties, the authors used the research of Mindlin and Toupin (1971). The Maxwell equations that are necessary for this problem are displayed:

$$E_{3,2} + \dot{B}_1 = 0 \quad \text{a}$$

$$-E_{3,1} + \dot{B}_2 = 0 \quad \text{b}$$

$$B_{2,1} - B_{1,2} - \mu_0 \epsilon_0 \dot{E}_3 - \mu_0 \dot{P}_3 \quad \text{c}$$

$$B_{1,1} + B_{2,2} = 0 \quad \text{d}$$

In the above relation  $\mu_0$  is the magnetic permeability of vacuum, when the magnetic susceptibility of dielectrics is being neglected. Its numerical value is  $\mu_0 = 4\pi * 10^{-7} \text{ kgm/C}^2$ . Also, the speed of light in the vacuum is equal to  $c_{light} = (\mu_0 \epsilon_0)^{-1/2} \cong 3 * 10^8 \text{ m/s}$ .

The authors combined **a**, **b** and **c**, to produce the governing differential equation of the electromagnetic problem.

$$\nabla^2 E_3 = \mu_0 \ddot{P}_3 + \mu_0 \epsilon_0 \ddot{E}_3$$

Which can be solved in respect of the out-of-plane electric field  $E_3$  for a known out-of-plane polarization  $P_3$ . The magnetic flux  $B_1, B_2$  is calculated then from **a** and **b** and then the magnetic field can be calculated from the bellow relations:

$$H_1 = \mu_0^{-1} B_1$$

$$H_2 = \mu_0^{-1} B_2$$

### E. Aim

This study will try to analyze the anti-plane flexoelectric problem, while using an analogue with couple stress elasticity. As it will be displayed later, the ferro-electric parameter exposes similar contribution with the microstructural parameters on a normal anti-plane problem through the theory of couple stress elasticity. Those, the microstructural and the micro-inertial length characterize an anti-plane dynamic couple stress elasticity problem as hyperbolic or elliptic, supersonic or subsonic. The same applies to the ferroelectric parameters for the flexoelectric anti-plane problem. In chapter 2 the flexoelectric parameters will get substituted by some other parameters called  $l$  and  $H$ , in order to show similarities with the couple stress problem.

The hyperbolic case will be studied in detail for the anti-plane flexoelectric problem and the polarization will be calculated.

The dispersive nature of this flexoelectric dynamic problem will later be discussed, while last but not least, by using an analogue, the flexoelectric problem will be solved via a FEM method, that will also allow a solution for the hyperbolic case.

## 2. The anti-plane flexoelectric problem

### A. The anti-plane displacement

One special case of three-dimensional elasticity is the anti-plane problem (similar to the plane stress and plane strain problem). The theory of the anti-plane strain demands some limitations to the in-plane displacements:

$$u_x = u_1 \equiv 0$$

$$u_y = u_2 \equiv 0$$

$$u_z = u_3 = w(x, y) = w(x_1, x_2) \neq 0$$

This restriction of displacements allows only the development of the in-plane shear strains, and the cross-section shear strains in the out-of-plane direction. Those are also independent from the out-of-plane direction.

$$\varepsilon_{13} = \varepsilon_{31} = \frac{1}{2} \left( \frac{\partial u_1}{\partial x_3} + \frac{\partial u_3}{\partial x_1} \right) = \frac{1}{2} \frac{\partial w(x_1, x_2)}{\partial x_1}$$

$$\varepsilon_{23} = \varepsilon_{32} = \frac{1}{2} \left( \frac{\partial u_2}{\partial x_3} + \frac{\partial u_3}{\partial x_2} \right) = \frac{1}{2} \frac{\partial w(x_1, x_2)}{\partial x_2}$$

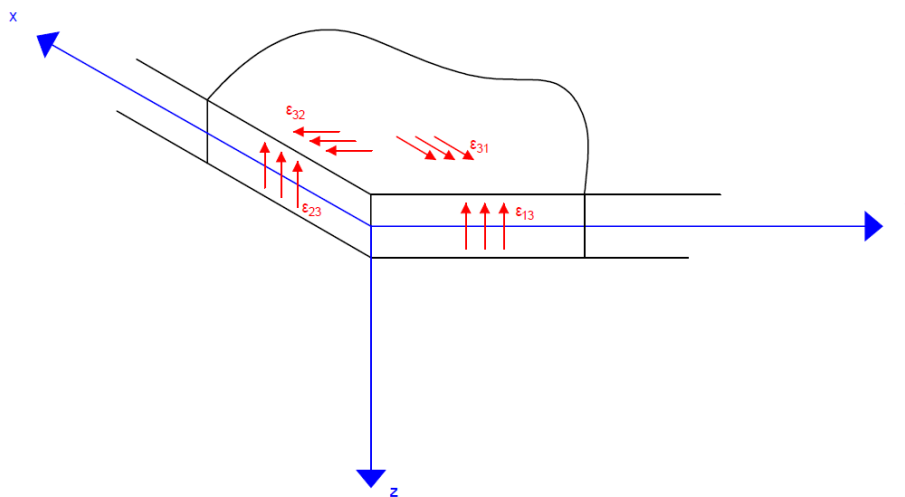


Fig. 13. The strains in the anti-plane formulation.

Only four out of the nine components of the strain tensor are non-zero.

$$\varepsilon_{ij} = \begin{bmatrix} 0 & 0 & \varepsilon_{13} \\ 0 & 0 & \varepsilon_{23} \\ \varepsilon_{13} & \varepsilon_{23} & 0 \end{bmatrix} = \begin{bmatrix} 0 & 0 & \frac{1}{2}u_{3,1} \\ 0 & 0 & \frac{1}{2}u_{3,2} \\ \frac{1}{2}u_{3,1} & \frac{1}{2}u_{3,2} & 0 \end{bmatrix}$$

An example of an anti-plane problem is the pull-out of the reinforcing bar anchored in concrete e.g. columns and beams made by reinforcing concrete. A Mode III crack is also a case of an anti-plane problem. Except the purely anti-plane problems, there are those that have great similarities. The Twist of beams and the out-of-plane loading of a thin plate, are problems that are recognized as “anti-plane-like” problems.

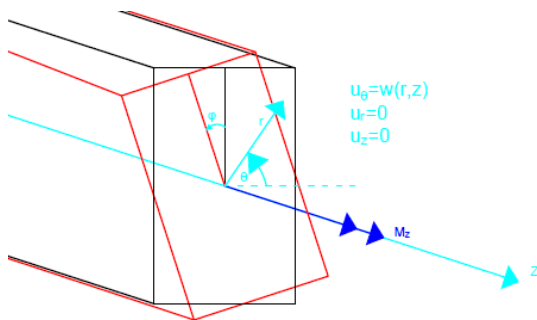


Fig. 14. The Twist of beams.

By using cylindrical coordinates, only the radial displacement is active and thus this problem can bring similarities to an anti-plane problem. However, it is not a purely anti-plane problem.

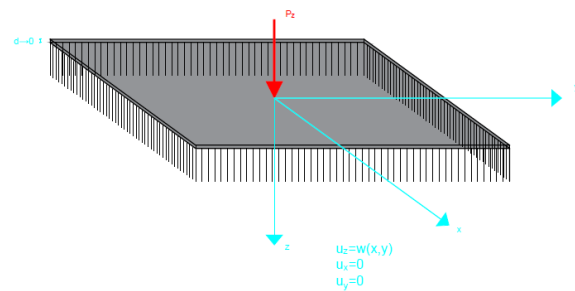


Fig. 15. A thin plate.

By considering a very thin plate, the axial (in-plane) displacements can be neglected (under conditions) and then the problem exhibits anti-plane similarities. However, it is not an anti-plane problem.

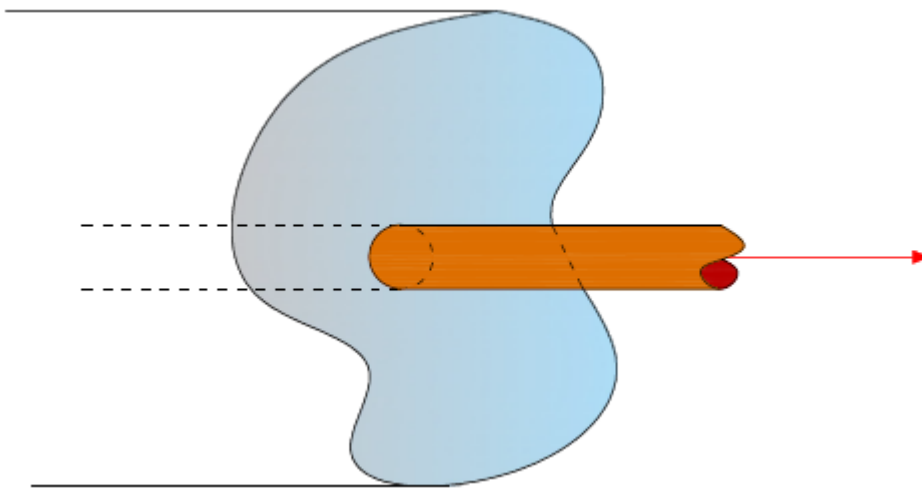


Fig. 16. The pull out of the reinforcement on one-dimensional concrete element like a beam or a column is a purely anti-plane problem.



The cracks that can happen are of three types. The mode I and II cracks are both in-plane problems as the mode I crack is opening in the in-plane direction perpendicular to the discontinuity and the mode II crack is opening along the discontinuity (shear mode). The mode III crack, which is of interest, is a scissor like crack and the displacement occurs perpendicular to the discontinuity and to the surface. The displacement is “out-of-plane displacement” and the problem is anti-plane.

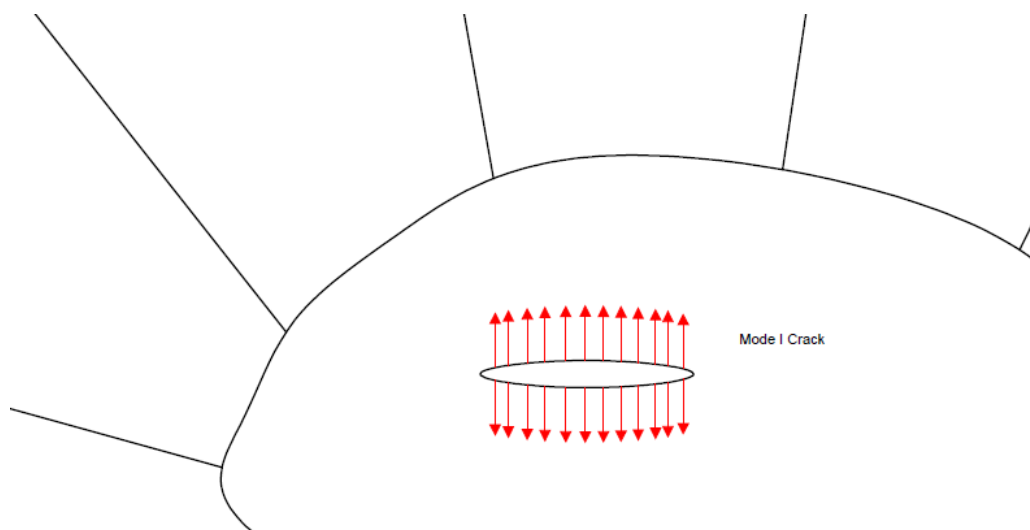


Fig. 17. Mode I crack.

The crack is opening in the in-plane direction perpendicular to the discontinuity of the crack. The problem is an “in-plane” problem

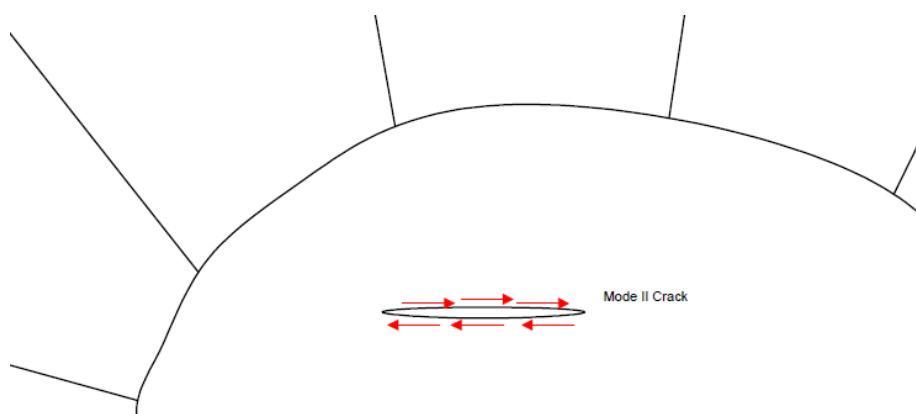


Fig. 18. Mode II crack.

The crack is opening in the in-plane direction, parallel to the discontinuity of the crack. The problem is an “in-plane” problem

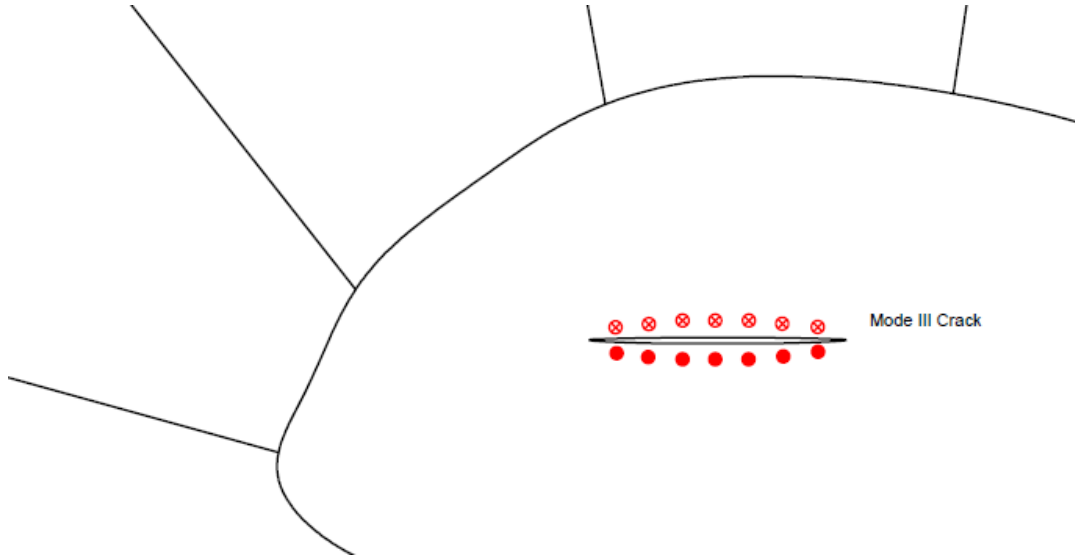


Fig. 19. The mode III crack.

The crack is “scissor-like”. It is opening in the out-of-plane direction and can be considered an anti-plane problem.

All problems have been studied by various researchers such as [Giorgiots and Georgiadis \(2007\)](#), [Giannakopoulos and Zisis \(2021 a, b\)](#), and others.

A significant comment is being addressed by [Giannakopoulos and Zisis \(2021 b.\)](#), who suggested that in order for a problem to be a true anti-plane problem, either the Maxwell surface traction should be very small or the electric field.

$$E_3 \ll \sqrt{2\mu a}$$

Where  $E_3$  is the out-of-plane electric action,  $\mu$  is the shear modulus and  $a$  is the reciprocal dielectric constant. This, however, is usually not violated.

## B. The anti-plane polarization

The flexoelectric anti-plane problem, includes also polarizations. The anti-plane formulation demands the in-plane components of the polarization to be zero and the out-of-plane component to be independent from the out-of-plane coordinate, similarly to displacement.

$$P_x = P_1 \equiv 0$$

$$P_y = P_2 \equiv 0$$

$$P_z = P_z(x, y) = P_3(x_1, x_2) \neq 0$$

### C. The anti-plane flexoelectric problem

The anti-plane flexoelectric problem is a combination of two problems. The first one is the well-known anti-plane problem that is described in general as a displacement (not necessarily a displacement vector as this vector, in the anti-plane problem has only one component, the out-of-plane one), that is caused from an action (that usually is also out-of-plane, like the examples shown previously). The displacement produced however has an additional effect, the flexoelectric phenomenon, which refers to the second one.

This indicates that in an anti-plane formulation, such as the propagation of a mode III crack, an electric field will be produced with an out-of-plane polarization, the  $P_3$ . This polarization will be the effect of flexoelectricity.

The general idea of the anti-plane flexoelectric problem is to solve the anti-plane problem considering the contribution of flexoelectricity by mechanical terms (converse flexoelectric effect). The methodology was described by [Giannakopoulos and Zisis \(2019\)](#). The difference with a normal anti-plane problem is that the converse flexoelectric phenomenon should be considered in the formula of potential energy density.

To make things a bit simpler [Giannakopoulos and Zisis \(2019\)](#) neglect an “a priori” internal length scales as implied in non-local elastic theories and so it is feasible to neglect the elastic strain energy produced by strain gradient effects. By using the formula described by [Mindlin \(1968, 1969\)](#), the authors reduce the energy density to the beneath (they added also some terms):

$$\begin{aligned}
 U = \frac{1}{2} & \left[ aP_3^2 + (b_{44} + b_{77})(P_{3,1}^2 + P_{3,2}^2) \right. \\
 & + 2e_{44} \left( (\varepsilon_{13} + \varepsilon_{31})P_{3,1} + (\varepsilon_{23} + \varepsilon_{32})P_{3,2} \right) \\
 & \left. + 2f_{12} \left( (\varepsilon_{13,1} + \varepsilon_{31,1})P_3 + (\varepsilon_{23,2} + \varepsilon_{32,2})P_3 \right) + 2\mu(\varepsilon_{13}^2 + \varepsilon_{23}^2) \right] \quad 1
 \end{aligned}$$

The components  $\varepsilon_{ij}$  are the anti-plane strains,  $P_3$  is the out-of-plane polarization,  $(\cdot)_{,i}$  symbolizes the gradient. The other components which are constant are the shear modulus  $\mu$  [ $N/m^2$ ], the flexoelectric constant  $f_{12}$  [ $Nm/C$ ], the inverse flexoelectric constant  $e_{44}$  [ $Nm/C$ ], the gradient polarization constant  $(b_{44} + b_{77})$  [ $Nm^4/C^2$ ] and lastly  $a$  [ $Nm^2/C^2$ ] is the reciprocal dielectric constant.

The above parameters should be bounded:

$$\mu > 0$$

$$\alpha > 0$$

$$f_{12} > 0$$

$$f_{44} > 0$$

$$e_{44} > 0$$

$$b_{44} + b_{77} > 0$$

$$\mu(b_{44} + b_{77}) - e_{44}^2 > 0$$

At the work of [Maranganti et al. \(2006\)](#), some characteristic values of the constants can be obtained. In the beneath table, that was also obtained from [Giannakopoulos and Zisis \(2019\)](#), those values are displayed:

Constant Symbol	Numerical Value	Dimension
$c_{44} = \mu$	$0.32500 * 10^{-2}$	[dyn/nm <sup>2</sup> ]
$f_{12}$	$0.01125 * 10^7$	[dyn nm/C]
$b_{44}$	$0.52550 * 10^{32}$	[dyn nm <sup>4</sup> /C <sup>2</sup> ]
$e_{44}$	$0.35600 * 10^{15}$	[dyn nm/C]
$b_{77}$	$1.92100 * 10^{32}$	[dyn nm <sup>4</sup> /C <sup>2</sup> ]
$a$	$8.76700 * 10^{33}$	[dyn nm <sup>2</sup> /C <sup>2</sup> ]
$\varepsilon_0$	$8.85400 * 10^{-35}$	[C <sup>2</sup> /dyn nm <sup>2</sup> ]
$\rho$	5.3176	[g/cm <sup>3</sup> ]

Where 1 dyn = 10<sup>-5</sup> N

Property	Materials									
	SrTiO <sub>3</sub> [100] 90 K	KTaO <sub>3</sub> [100] 39 K	PbTiO <sub>3</sub> [100] 783 K	BaTiO <sub>3</sub> [111] 423 K	Ge [111]	GaAs [111]	InSb [111]	Si [111]	NaCl [100]	KCl [100]
$a_0$ (nm)	0.391	0.399	0.415	0.396	0.566	0.565	0.648	0.543	0.281	0.314
$\rho$ (kg/m <sup>3</sup> )	5174	6970	7520	6020	5360	5340	5790	2330	2160	1980
$c_{44} = \mu$ (GPa)	122	107	110	543	67.1	59.4	30.2	79.1	12.8	6.8
$\alpha$ (10 <sup>9</sup> Nm <sup>2</sup> /C <sup>2</sup> )	2.12	0.355	0.168	0.565	75.3	94.6	70.6	103	174	243
$(b_{44} + b_{77})(10^{-9} \text{ Nm}^4/\text{C}^2)$	2.00	0.435	0.115	0.0700	1.16	2.20	1.65	1.45	0.688	1.20
$(\epsilon_{44} - f_{12})(\text{Nm}/\text{C}=\text{V})$	-10.0	6.00	2.00	-2.70	8.80 sign?	11.0 sign?	6.90 sign?	11.0 sign?	-2.42	-2.15
$\Omega_0$ (THz)	1.46	4.79	4.58	5.00	9.00	6.90	4.80	15.5	4.90	4.50
$P_s$ ( $\mu\text{C}/\text{cm}^2$ )	4.2		57	26						
$c_s$ (m/s)	4856	3910	4583	4558	3538	3335	2276	5827	2469	1853
$H/\sqrt{12}$ (nm)	3.07	3.50	2.62	1.113	0.393	0.483	0.474	0.376	0.199	0.222
$\ell/\sqrt{2}$ (nm)	2.36	1.66	2.17	0.00	0.00	0.00	0.00	0.00	0.113	0.146

Fig. 20. Typical material parameters

obtained from [Giannakopoulos and Zisis \(2021 b\)](#). The number below the chemical formula of the material symbolizes the crystallographic direction.

As it was discussed, the only non-zero polarization is the out-of-plane, similar to the displacement,  $P_3(x, y)$ . This means that also the polarization gradient  $P_{3,3}$  is zero and thus it was rightly neglected in the formula of total energy density (relation 1).

By considering some of the above constants equal to zero, relation 1, describes some known cases, as example, when  $f_{12} = e_{44} = 0$  the classic dielectric formula is obtained. If also  $a = 0$ , then the formula describes the classic elastic case.

The procedure to conclude the governing equation of the problem, is via Toupin's principle of variations, as described by Mindlin (1968).

The full problem is, in every case, the dynamic anti-plane flexoelectric problem like a mode III crack. This can be described with the addition of kinetic energy, which can be written as  $T = \rho \dot{u}_3 \dot{u}_3 / 2$ , while the dielectric enthalpy, without considering the contribution of optical wave modes, is  $\bar{H} = U - \varepsilon_0 (\Phi_{,1}^2 + \Phi_{,2}^2) / 2$ . In the above relations  $\rho$  is the material mass density and  $(\dots)$  is the time derivative,  $-\Phi$  is the Maxwell self-field and the dielectric constant at vacuum is  $\varepsilon_0$ .

The procedure to extract the governing equations of the anti-plane flexoelectric problem is described in detail in Appendix A. By using Toupin's Variational Principle, 3 Euler conditions are extracted from the volume integral.

The first equation is used to calculate the out-of-plane displacements (A.27):

$$\mu \nabla^2 u_3 - \mu \frac{l^2}{2} \nabla^4 u_3 = \rho \ddot{u}_3 - \frac{\rho H^2}{12} \nabla^2 \ddot{u}_3 \quad 2$$

While the second one is used for the calculations of the out polarization (A.29):

$$P_3 - \frac{l^2}{2} \nabla^2 P_3 = \frac{\rho(e_{44} - f_{12})}{a\mu} \dot{u}_3 \quad 3$$

The terms  $l$  and  $H$  represent the "microstructural" and the "micro-inertial length":

$$\frac{l^2}{2} = \frac{b_{44} + b_{77}}{a} - \frac{(e_{44} - f_{12})^2}{\mu a} \geq 0 \quad 4$$

$$\frac{H^2}{12} = \frac{b_{44} + b_{77}}{a} \geq \frac{l^2}{2} \quad 5$$

This way the problem of the displacement decouples from the polarizations. Note that by using Toupin's Variational Principle, one more Euler condition is being produced, the Maxwell equation, which decouples from the problem. Also, via Toupin's Variational Principle, one second integral is produced, that refers not to the volume of the body, but to its boundary. This integral describes the boundary conditions that are needed for the solution of the problem. For more information the reader is suggested to visit Appendix A. Those could be initial conditions at  $t = 0$  for the out-of-plane displacement, the velocity and the polarization, some electric

boundary conditions referring to the polarization gradient or the polarization, jump conditions or even mechanical boundary conditions.

The boundary conditions that are needed for the problem, are presented in a table in [Giannakopoulos and Zisis 2019](#), that can be seen below.

#### Mutually exclusive boundary conditions for the anti-plane flexoelectric problem.

Mutually Exclusive Boundary Conditions	
Essential Boundary Conditions	Dynamic Boundary Conditions
$P_3$	$(b_{44} + b_{77})P_{3,n} + e_{44}u_{3,n} = 0$
$\Phi$	$n_1(-\varepsilon_0[[\Phi_{,1}]] + n_2(-\varepsilon_0[[\Phi_{,2}]])) = 0$
$u_{3,n}$	$r_3 = f_{12}P_3$
$u_3$	$t_3 = \underbrace{\mu u_{3,n}}_{\text{classic couple}} + \underbrace{(e_{44} - f_{12})P_{3,n}}_{\text{stress elasticity}} + \mu \frac{\ell^2}{2} \frac{\partial}{\partial s} \left( \frac{\partial^2 u_3}{\partial x_1 \partial x_2} \right)$
$u_{3,s}$	$\mu \frac{\ell^2}{2} \left( \frac{\partial^2 u_3}{\partial x_1 \partial x_2} \right)$

Fig. 21. The boundary conditions required in the anti-plane flexoelectric formulation, as presented by [Giannakopoulos and Zisis 2019](#).

Both the governing equations are dynamic equations as they contain terms of accelerations. This happened because of the consideration of a velocity. By replacing the global system  $(x, y)$  with a system of characteristic coordinates  $(\xi, \eta)$ , that moves along the crack and obeys the following transformation:

$$\begin{aligned}\xi &= x + Vt \\ \eta &= y\end{aligned}\tag{6}$$

the problem decouples from the accelerations and the two governing equations transform to the following. The first one, which describes the displacement, is derived from relation 2 by using the [transformation 6](#)

$$\left(1 - \frac{V^2}{c_s^2}\right) \frac{\partial^2 u_3}{\partial \xi^2} + \frac{\partial^2 u_3}{\partial \eta^2} - \frac{l^2}{2} \left(1 - \frac{V^2 H^2}{6l^2 c_s^2}\right) \frac{\partial^4 u_3}{\partial \xi^4} - \frac{l^2}{2} \left(2 - \frac{V^2 H^2}{6l^2 c_s^2}\right) \frac{\partial^4 u_3}{\partial \xi^2 \partial \eta^2} - \frac{l^2}{2} \frac{\partial^4 u_3}{\partial \eta^4} = 0\tag{7}$$

and the second one, which describes the polarization, is derived from [relation 3](#).

$$P_3 - \frac{l^2}{2} \left( \frac{\partial^2 P_3}{\partial \xi^2} + \frac{\partial^2 P_3}{\partial \eta^2} \right) = V^2 \frac{\rho(e_{44} - f_{12})}{a\mu} \frac{\partial^2 u}{\partial \xi^2} \quad 8$$

In those two relations the term  $c_s = \sqrt{\mu/\rho}$ , represents the shear wave velocity. Those transformations are described in detail in [Appendix B](#).

The transformation of coordinates that relation 6 describes, assumes constant velocity, e.g. a [steady state mode III crack](#) (as the one studied in [Giannakopoulos and Zisis 2019, 2021 a, b](#)). The transformation that holds for any case has instead of the velocity, the integral of the velocity.

$$\xi = x + \int_{t_0}^t V(x, y, \tau) d\tau$$

$$\eta = y$$

However, a numerical assumption of the solution of the integral, e.g. using Simpson's law, or Gauss' integration of 1<sup>st</sup> order (rule of the middle value), suggest that the above transformation is equivalent to the transformation proposed by relation 6.

Relation 7 gives a nice perspective of the problem. It can be supersonic, or subsonic, elliptic or hyperbolic. This, however, is something that will be discussed further.

### 3. The anti-plane couple elasticity dynamic problem

One alternative theory to classic elasticity is a theory studied from various researchers such as Giourgiotis and Georgiadis (2007) and Zisis (2018), known as couple stress elasticity theory. This theory takes into consideration the second order gradient of strains and more precisely, the strains of the spins (the whole formulation of the theory of couple stress elasticity is being discussed in Appendix C, as proposed by Giourgiotis and Georgiadis (2007)). This way, terms of strain gradients are added to the energy density formulation and thus the governing equations that describe a problem based on the theory of couple stress elasticity, are in agreement with those gradients. Some could say that the theory of couple stress elasticity completes the classic elasticity theory (Zisis (2018) used this theory to find the displacements in a pathological area, in a problem he solved).

As Zisis (2018) proposed, the theory of couple stress elasticity should be used to enrich the theory with microstructural characteristics. This way, the theory could also be used when studying size effects. He pointed out that classical continuum theories cannot explain size effects that occur in many different materials at micron or nanometer scales, because there is no length scale of the material (the microstructure) and this is the reason why higher order theories such as the couple stress theory are needed. Couple stress elasticity usually replaces classic elasticity in terms of problems relevant to dislocations, plasticity and so on, This theory can be used also in in small scales, or when there are size effects.

In the theory of couple stress elasticity, or the Cosserat theory with constrained rotation as it is also known, some special parameters make an appearance. These parameters are the moduli  $\eta$  and  $\eta'$  and have to do with the importance of microstructure. As these parameters tend to zero, the classical theory replaces the couple stress elasticity. For better observation of the problem, two other parameters are usually used instead of those, the microstructural length  $l = \sqrt{2\eta/\mu}$  (where  $\mu$  is the known Lamé's constant), (Zisis (2018) symbolizes the microstructural length  $l_b$ ) and the parameter  $\beta = \eta'/\eta$ .

One anti-plane problem is possible to be solved via the theory of couple stress elasticity, as any other problem. The restrictions of the displacement that are applied in the anti-plane formulation make feasible some simplifications. The anti-plane couple stress elasticity formulation is being discussed in detail in Appendix C.

The total energy density, as described from Giourgiotis and Georgiadis (2007), can be given by the following formula:

$$U \equiv U(\varepsilon_{ij}, \kappa_{ij}) = \frac{1}{2} \lambda \varepsilon_{ii} \varepsilon_{jj} + \mu \varepsilon_{ij} \varepsilon_{ij} + 2\eta \kappa_{ij} \kappa_{ij} + 2\eta' \kappa_{ij} \kappa_{ji} \quad 9$$

Whereas the terms  $\kappa_{ij} = e_{jkl} \partial_i \partial_j u_l / 2 = e_{jkl} \partial_k \varepsilon_{il}$  is the strain gradient.  $\lambda$  is the other Lamé's constant.



The governing equation of a static anti-plane couple stress elasticity problem is the following (relation 10). By substituting to that equation  $l = 0$  the classic solution of anti-plane problem is produced in terms of classic elasticity.

$$\mu \nabla^2 w - \mu \frac{l^2}{2} \nabla^4 w = 0 \quad 10$$

The boundary conditions that are needed for this differential equation, are usually Saint Venant boundary conditions, according to [Giouriotis and Georgiadis \(2007\)](#)

Bibliography can give various values of the microstructural length and one other parameter as well,  $l_t = l\sqrt{2(1+\beta)}$  (The microstructural length is relevant to the bending and thus is symbolized in the research of [Zisis \(2018\)](#) as  $l_b$ , where  $b$  symbolizes bending. The parameter  $l_t$  consistently is a length property connected with the torsion.)

The microstructural length and the parameter $l_t$ as referred by Radi (2008) ( <a href="#">Zisis (2018)</a> )		
A syntactic foam that consists of hollow glass micro-bubbles embedded in an epoxy matrix	$l = 0.032 \text{ mm}$	$l_t = 0.032 \text{ mm}$
A high-density rigid polyurethane closed cell foam	$l = 0.0327 \text{ mm}$	$l_t = 0.62 \text{ mm}$

Some limitations to the parameters of the couple stress elasticity theory, were described in [Giouriotis and Georgiadis \(2007\)](#) and are the following:

$$-1 < \frac{\eta}{\eta'} < 1$$

$$\eta > 0$$

And of course, the Lamé's constants:

$$3\lambda + 2\mu > 0$$

$$\mu > 0$$

Relation 10, however refers to a static problem, while an anti-plane problem can be dynamic, e.g. the mode III crack propagation. It is not difficult to add the extra dynamic terms on relation 10 with the use of Hamilton's principle.

The kinetic energy in terms of couple stress elasticity has the following form:

$$T = \frac{1}{2} \rho \dot{u}_3 \dot{u}_3 + \frac{\rho H^2}{6} (\dot{\omega}_1 \dot{\omega}_1 + \dot{\omega}_2 \dot{\omega}_2) \quad 11$$

In addition to the normal, out-of-plane velocity,  $\dot{u}_3$ , the kinetic energy should also consist of rotational velocities,  $\dot{\omega}_1$  and  $\dot{\omega}_2$ . The reason is that those were considered to play a prominent role, as the spins are present in the constitutive laws, and the energy density (because of the theory of couple stress elasticity). The term  $\rho$  represents the mass density of the body, while the term  $H$  symbolizes the micro-inertial length (it has length dimensions).

Through Hamilton's principle, the kinetic energy produces an extra term and the governing equation can take the following form:

$$\mu \nabla^2 u_3 - \mu \frac{l^2}{2} \nabla^4 u_3 = \rho \ddot{u}_3 - \frac{\rho H^2}{12} \nabla^2 \dot{u}_3 \quad 12$$

The procedure, in which this result is based on, is described also in detail in [Appendix C](#). In addition, one more boundary condition appears. It refers to the acceleration gradient vertical to the surface and is described by the following formula:

$$\ddot{u}_{3,2} n_2 + \ddot{u}_{3,1} n_1 = 0 \quad 13$$

Boundary conditions for the anti-plane dynamic couple-stress problem.

Mutually Exclusive Boundary Conditions	
Essential Boundary Conditions	Dynamic Boundary Conditions
$\omega_n = \frac{\partial u_3}{\partial n}$	$R_n^{(n)} = 0$
$\omega_s = -\frac{\partial u_3}{\partial s}$	$R_s^{(n)} = \mu \ell^2 \begin{pmatrix} (\beta n_2^2 - n_1^2) \frac{\partial^2 u_3}{\partial x_1^2} + (\beta n_1^2 - n_2^2) \frac{\partial^2 u_3}{\partial x_2^2} \\ -2(1 + \beta) n_1 n_2 \frac{\partial^2 u_3}{\partial x_1 \partial x_2} \end{pmatrix}$
$u_3$	$P_3^{(n)} = \mu u_{3,n} + \frac{H^2}{12} \rho \ddot{u}_{3,n} - \mu \frac{\ell^2}{2} (\nabla^2 u_3)_{,n} - \frac{1}{2} \frac{\partial m_{(nn)}}{\partial s}$

Fig. 22. The boundary conditions needed for the anti-plane couple stress elasticity problem, as presented by [Giannakopoulos and Zisis \(2019\)](#).

Relation 12 which refers to the anti-plane couple stress elasticity problem, seems to be the same with relation 2, which refers to the anti-plane flexoelectric problem

### A. The analogue between the flexoelectric and the couple stress anti-plane problem.

As it was mentioned already, relation 12 which refers to the anti-plane couple stress elasticity problem, seems to be the same with relation 2, which refers to the anti-plane flexoelectric problem.

$$\mu \nabla^2 u_3 + \mu \frac{l^2}{2} \nabla^4 u_3 = \rho \ddot{u}_3 - \frac{\rho H^2}{12} \nabla^2 \ddot{u}_3$$

In relation 2, the displacement is the out-of-plane displacement, the microstructural length equal to  $l^2/2 = (b_{44} + b_{77})/a - (e_{44} - f_{12})/\mu a$  and the micro-inertial length  $H^2/12 = (b_{44} + b_{77})/a$ . Also,  $\rho$  is the mass density,  $\mu$  is one of the Lamé's constant, the shear modulus. The other parameters are relative to flexoelectricity and are specified in detail in previous chapters.

The analogue between the case of the anti-plane flexoelectricity and the anti-plane couple stress elasticity can be better described in the beneath table:

Flexoelectric Anti-plane problem	Anti-plane Couple stress elasticity problem
$\frac{b_{44} + b_{77}}{a} - \frac{(e_{44} - f_{12})^2}{\mu a}$	$\frac{l^2}{2}$
$\frac{b_{44} + b_{77}}{a}$	$\frac{H^2}{12}$

Also, there should be an analogue in the boundary conditions.

A conclusion that can easily be drawn, because both problems are based on an anti-plane formulation, is that the anti-plane flexoelectricity problem is basically a couple stress elasticity problem, where the flexoelectric properties define the microstructure of the material.

### B. The three sub-cases of the problem

The governing equation of the anti-plane couple stress elasticity problem, relation 12, which is the same with relation 2, the governing equation of the anti-plane flexoelectricity problem, are both dynamic equations. Considering that the problem is defined by a velocity,  $V$  (e.g. the velocity which the mode III crack propagates) and then also considering a moving system of coordinates, that depends on this velocity and also on the time (e.g. a moving system in which the beginning of the axis is always the crack tip), the transformation of the axis obeys the following relation (transformation 6, this transformation of the system of coordinates is proposed by Giannakopoulos and Zisis (2019, 2020 a, b)).

$$\xi = x + Vt$$

$$\eta = y$$

Because of this transformation, the governing equation (2, 12) can be written in the below form (equation 7):

$$\left(1 - \frac{V^2}{c_s^2}\right) \frac{\partial^2 u_3}{\partial \xi^2} + \frac{\partial^2 u_3}{\partial \eta^2} - \frac{l^2}{2} \left\{ \left(1 - \frac{V^2 H^2}{6l^2 c_s^2}\right) \frac{\partial^4 u_3}{\partial \xi^4} + \left(2 - \frac{V^2 H^2}{6l^2 c_s^2}\right) \frac{\partial^4 u_3}{\partial \xi^2 \partial \eta^2} + \frac{\partial^4 u_3}{\partial \eta^4} \right\} = 0$$

In this equation the following terms are visible:

- The velocity term:

$$1 - \frac{V^2}{c_s^2}$$

The shear wave velocity is equal to  $c_s = \sqrt{\mu/\rho}$ , while  $V$  is the velocity with which the crack propagates, or any other velocity that was chosen to describe the dynamic behavior of the problem.

If this term is greater than zero, this means that the velocity of the crack is smaller than the shear wave velocity and the motion is subsonic. Otherwise, if the shear wave velocity is smaller than the crack velocity and this term is negative, the motion is called supersonic.

- The term that retains ellipticity (the folding limit):

$$1 - \frac{V^2 H^2}{6l^2 c_s^2}$$

Obviously, if this term is positive, then also the term  $2 - (V^2 H^2)/(6l^2 c_s^2)$ , is positive and then the factors that multiply the fourth order derivatives are negative. This condition turns the problem elliptic. So, if this term is negative the differential equation is hyperbolic. Elseways the differential equation is elliptic.

Whether a problem is hyperbolic or elliptic, has to do with the greatest derivative in the differential equation. The usual procedure suggests the calculation of the eigenvalues of the problem and then checking their sign. One easier way to define the hyperbolicity or ellipticity of a differential equation is by a transformation of coordinates. If by suggesting a transformation (e.g., linear  $\xi = ax + y$ ) and demand the factor of the greater derivative to be zero, then that new variable (e.g.  $\xi$ ) could be real or complex (it has also an imaginary part).

Ellipticity is equivalent to a complex solution. This means that the new coordinate that makes this greater order derivative zero, has also the same number of variables.

Hyperbolicity means that this new variable is real. A new variable can be imported and then both the differential equation gets simplified and the number of unknown variables gets reduced. This means that the solution lies in a combination of the original coordinates. This kind of solution, is a solution based on the characteristics (Lax (1956), Courant and Lax (1955)).

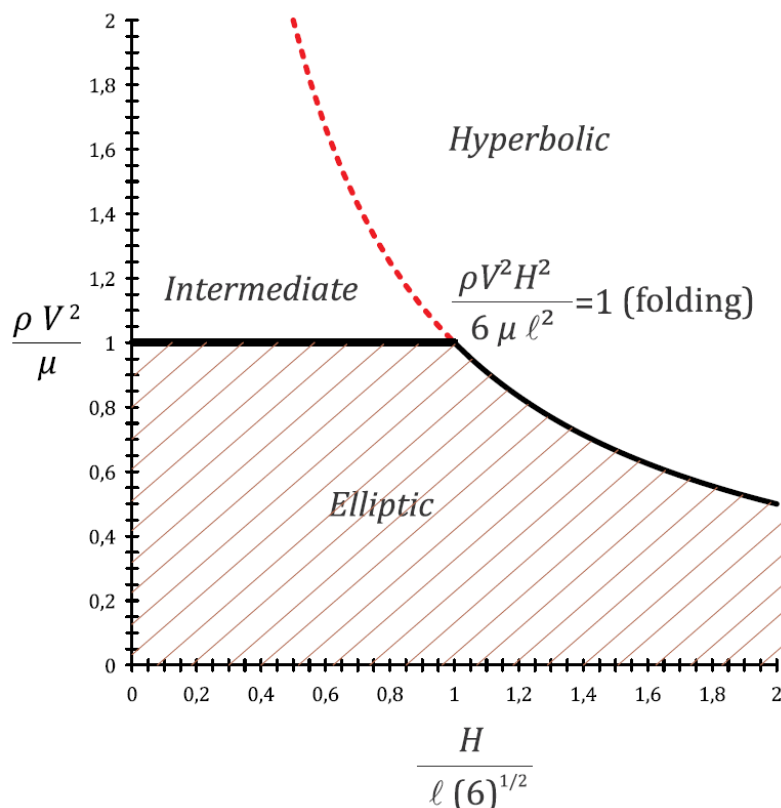


Fig. 23. The three regions that define the anti-plane dynamic problem to hyperbolic elliptic or intermediate.

The same figure holds for both the anti-plane flexoelectric problem and the anti-plane couple stress elasticity problem. This sketch was obtained from Giannakopoulos and Zisis (2019, 2021 a, b).

So, the problem can be hyperbolic or elliptic, subsonic or supersonic. If the problem is subsonic and elliptic, then it will be called elliptic. If the problem is elliptic but supersonic, then it will be called intermediate. Lastly, the problem will be called hyperbolic, whether is hyperbolic subsonic, or hyperbolic concerning only metamaterials.

The elliptic case is free of any pathologies as no radiation stress is needed to maintain the steady state motion of the dislocation.

Typically, however, the intermediate region is inaccessible, (also a great part of the elliptic region) as  $H^2/6\ell^2$  normally cannot be smaller than the unit, considering the flexoelectric problem at least, because according to relation 5 and 6:

$$\frac{l^2}{2} = \frac{b_{44} + b_{77}}{a} - \frac{(e_{44} - f_{12})^2}{\mu a} = \frac{H^2}{12} - \frac{(e_{44} - f_{12})^2}{\mu a} < \frac{H^2}{12} \quad 14$$

Both the shear modulus  $\mu$  and the electric susceptibility of the material  $a$  should be positive. This means that the “microstructural” terms are smaller than the “micro-inertial” term in normal materials. And because both those parameters are positive:

$$\frac{l^2}{2} < \frac{H^2}{12} \rightarrow \frac{6l^2}{H^2} < 1 \rightarrow \frac{H^2}{6l^2} > 1 \rightarrow \frac{H}{\sqrt{6}l} > 1 \quad 15$$

Normal materials cannot exhibit such properties. However, recent studies have shown that a new category of material called “meta-material” can enter this intermediate region (it will be discussed later).

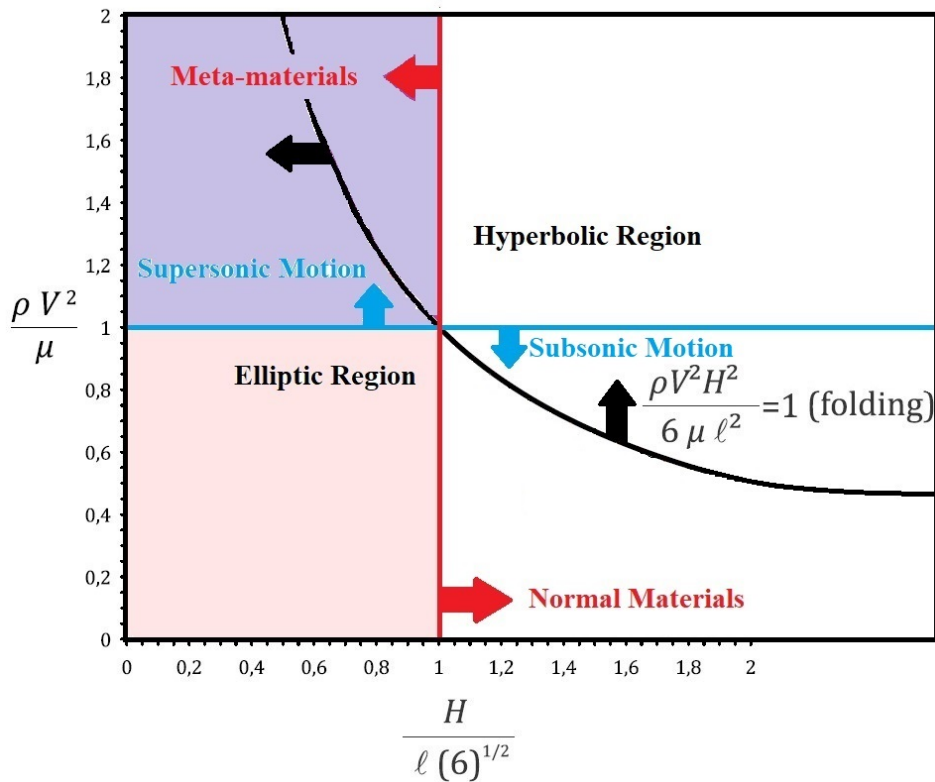


Fig. 24. The regions that appear on a dynamic anti-plane flexoelectric problem like the propagation of a mode III crack.

Note that for a normal material, folding can occur for smaller subsonic velocities. Also, the intermediate region (purple region) is accessible only for meta-material. For meta-material both the elliptic subsonic and the hyperbolic supersonic region are accessible.

So, in an anti-plane dynamic problem, such as the propagation of a mode III crack, in terms of couple-stress elasticity, three regions are visible:

- Elliptic subsonic regions
- Intermediate region (elliptic supersonic)
- Hyperbolic region

These regions, that obviously exist on an anti-plane problem by using the theory of couple stress elasticity, also exist on an anti-plane flexoelectric classic elasticity problem.

### C. The Elliptic subsonic region

The first region, the elliptic region has been studied a lot in the previous years. For this region there are various researches, both analytical and computational. As the analytical solution is concerned, researches exist not only in respect of classic electrodynamics, with no microstructure involved (Giannakopoulos and Zisis (2021 a) demonstrate solutions, pointing at McClintock and Sukhatme (1960)), but also by taking into consideration the microstructure. According to Giannakopoulos and Zisis (2019 a), in respect of classic electrodynamics, the displacement can be calculated from the stresses and the boundary conditions.

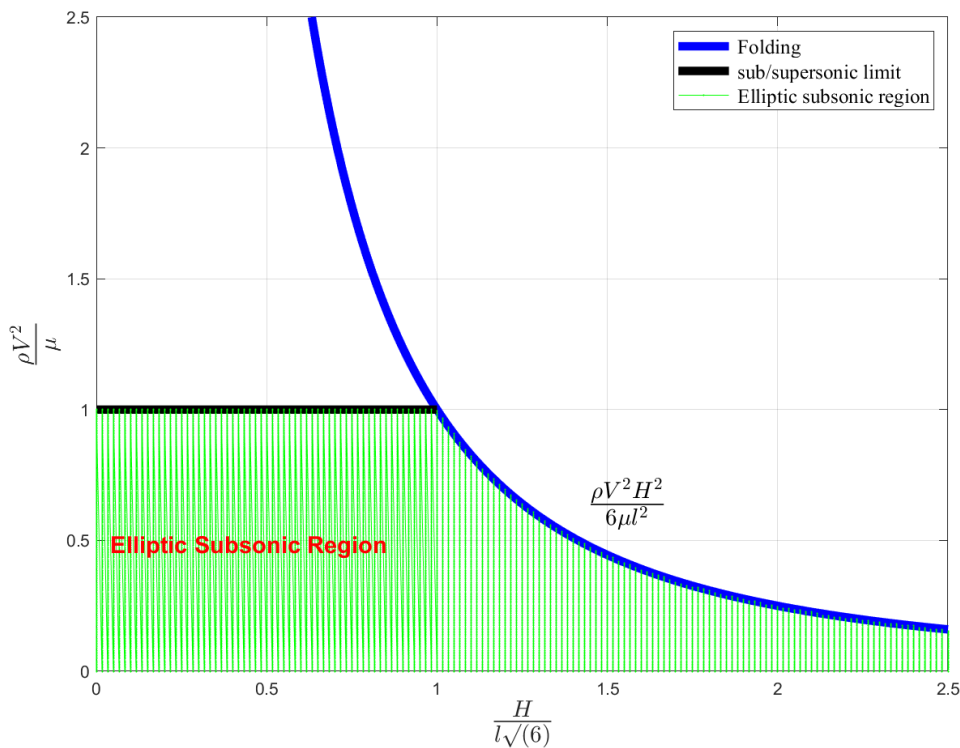


Fig. 25. The elliptic subsonic region.

The elliptic subsonic region is defined by the combination of the velocity of the propagation of the crack tip, the microstructural and the micro-inertial length that gives velocity less than the shear wave velocity and  $1 - (V^2 H^2)/(6l^2 c_s^2) > 0$ . This region includes only elliptic and subsonic cases, but also refers to meta-material in addition to normal dielectrics. This region has no pathologies and can be solved directly, for the static case, while by using the proposed analogue by Giannakopoulos and Zisis (2021 a), for the dynamic case also.

Significant is the contribution of [Gourgiotis and Georgiadis \(2007\)](#) in this subject. Those researchers used a screw dislocation to study the mode III crack problem. They considered the microstructure (by adding the microstructural length), as they used the theory of the couple stress elasticity, but they did not consider the dynamic problem.

The research of [Gavardinas et. al. \(2018\)](#) made a breakthrough in the field of anti-plane problems, by introducing an analogue with a prestress Kirchhoff plate. This analogue enabled the computational methods of analyzing the anti-plane crack to rise. These authors also observed the crack profile, that initially had a “cusp-like” form, for neglectable microstructure (classic solution), but when the microstructure gets large, the profiles transform to a “blunt opening”). This “cusp-like” displacement profile could be connected with the cohesive zone. [Giannakopoulos and Zisis \(2021 a\)](#) suggest that the microstructural length is “essentially equivalent to a cohesive crack model”. The cohesive zone should have a constant length and should be moving along the crack tip.

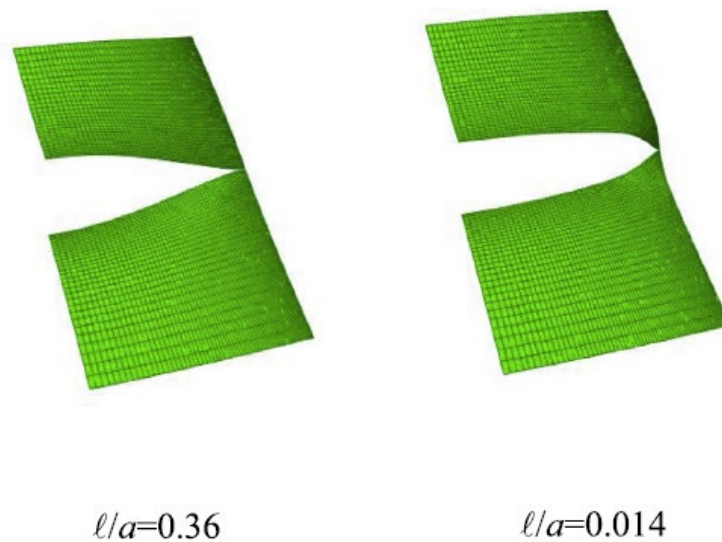


Fig. 26. The opening of a crack.

For small microstructural lengths, the profile is “cusp-like”, but as the length gets larger, the profile gets sharper. This sketch was obtained from [Gavardinas et. al. \(2018\)](#)

However, both [Gourgiotis and Georgiadis \(2007\)](#) and [Gavardinas et. al. \(2018\)](#) studied a static case. The dynamic elliptic subsonic case, was studied from [Giannakopoulos and Zisis \(2021 a, b\)](#). Using a similar analogue to the one proposed by [Gavardinas et. al. \(2018\)](#), in which they added the dynamic part, they studied not only the influence of the microstructural length on the crack profile (for which their results are in agreement with previous researches, e.g. [Gavardinas et. al. \(2018\)](#)), but also the influence of the velocity and the influence of the micro-inertial length.

In this research the authors, Prof. Giannakopoulos and Prof. Zisis, used a steady state crack. This crack propagates with a constant velocity. As it has already been discussed, despite the fact that the velocity doesn't need to be constant, the problem can in any case get simplified through a first order integration rule (Simpson's on Gauss' 1<sup>st</sup> order).





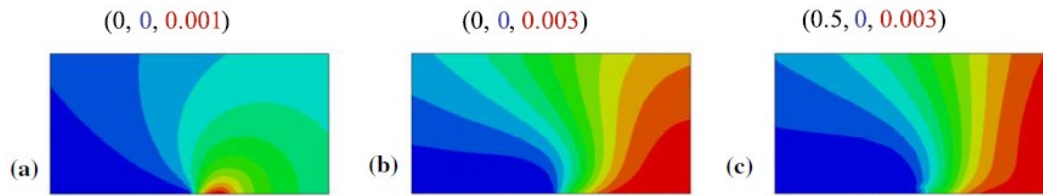
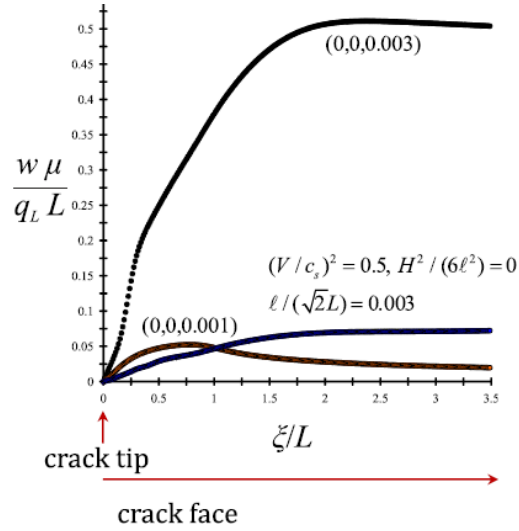


Fig. 30. The influence of the microstructural length in the elliptic subsonic case (displacements). Cases b and c are reaching the folding limit, and Mach cone are visible. In the profiles also the same trapezoidal shape is revealed. The cusp like formation is visible in case a, which is purely elliptic. These results were obtained from [Giannakopoulos and Zisis \(2021 a\)](#).



With the summation of the above contributions, the subsonic elliptic region can be considered fully elaborated.

Studying the elliptic case, [Giannakopoulos and Zisis \(2021 a, b\)](#) reached the hyperbolic case, by making the term:  $(V^2 H^2) / (6l^2 c_s^2) \rightarrow 1$ . The produced deformation creates something similar to folding. The displacement is step like and the Mach cones that are visible are parallel to the tangent axis of the crack ( $\xi/l$ ). The same authors, in a previous study ([Giannakopoulos and Zisis \(2019\)](#)), observed a similar result by using a screw dislocation.

#### D. The Intermediate (supersonic elliptic) region

This region, only briefly studied by [Giannakopoulos and Zisis \(2021 a\)](#), is practically inaccessible from normal materials, as the flexoelectric problem is concerned.

In order for a problem to be in that region, not only it needs to be elliptic, but also supersonic. Because of relation [14](#) and [15](#):

$$\frac{H}{l\sqrt{6}} < 1$$

However, this ratio between the microstructural and the micro-inertial length has a connection with the dielectric properties and more accurately, a positive dielectric susceptibility predicts

this ratio to be greater than one. Thus, the intermediate region is non-accessible for normal dielectric solids.

The introduction of a new category of materials, that has already been studied (Koo (2015)) makes the accessibility to this region possible. These materials can have negative electrical susceptibility. In the literature the term that describes those material is “Dielectric meta-materials” A general description of those meta-materials stated from the authors is: “materials consisted of metal particles in a matrix made of a dielectric”.

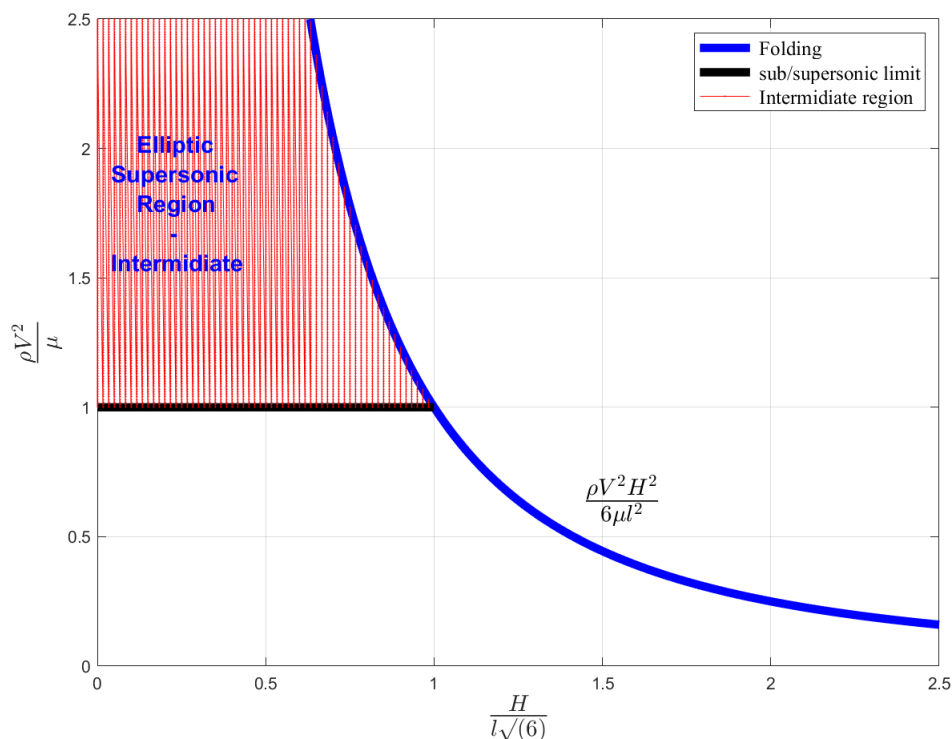


Fig. 31. The Intermediate region.

The intermediate region is defined by the combinations of supersonic velocities (greater than the shear wave velocity), and also combinations of microstructural and microinertia lengths that gets  $1 - (V^2 H^2)/(6l^2 c_s^2) > 0$ , so the problem would be elliptic. As [fig. 24](#) suggests, this region refers only to metamaterials.

[Giannakopoulos and Zisis \(2021 a.\)](#) stated that the study of the cracks in this kind of materials need excessive study in terms of dynamic and nonlinear response, and also a study of the plasticity theory surrounding those materials. Those studies don't exist. However, by using as first approximation the research of [Pham and Ravichandran \(2014\)](#), they suggested that Mach cone would be visible in this region too, however with no connection to the microstructure, as their angle would be  $\sin \theta = c_s/V$ .

### E. The hyperbolic region

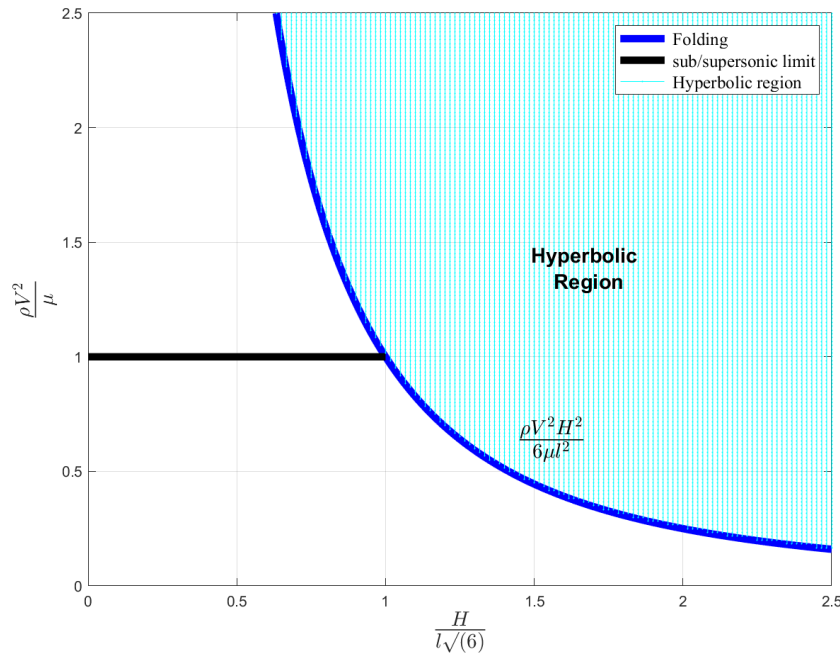


Fig. 32. The hyperbolic region.

The hyperbolic region, cares not about the velocity itself but for the combination of all three parameters, so that the term  $1 - V^2 H^2 / 6l^2 c_s^2 < 0$ . This region contains both subsonic and supersonic problem and concerns both normal dielectric or meta-materials.

As in any hyperbolic differential equation, a new variable can be introduced to define a solution depending on the characteristic lines. [Giannakopoulos and Zisis \(2019\)](#) studied the hyperbolic case. They propose a new coordinate, which can be described by the following formula:

$$\bar{\eta} = \frac{\xi}{l} \pm \frac{\eta}{l} \sqrt{\frac{H^2 V^2}{6l^2 c_s^2} - 1} \quad 16$$

Also, they replace the displacement with a logarithmic term:

$$\bar{h}(\bar{\eta}) = \ln(w)$$

This way, the differential equation that describes the problem, e.g. the anti-plane couple stress elasticity problem (eq. 7) takes the following form. The procedure is described in the [Appendix D](#).

$$\left[ \frac{\partial^2 \bar{h}(\bar{\eta})}{\partial \bar{\eta}^2} + \left( \frac{\partial \bar{h}(\bar{\eta})}{\partial \bar{\eta}} \right)^2 \right] \left[ \frac{H^2 V^2}{6l^2 c_s^2} - \frac{V^2}{c_s^2} \right] = 0 \quad 17$$

The general solution of the above differential equation, was also provided by [Giannakopoulos and Zisis \(2019\)](#), and is as follows, in which the constants  $a_i, b_i$  are calculated with the use of the boundary conditions:

$$\bar{h}(\bar{\eta}) = a_i + \ln(\bar{\eta} + b_i)$$

A Cauchy-type solution can be the following as suggested by [Giannakopoulos and Zisis \(2019\)](#), which describes a trapezoidal profile of displacement (this type of solution will be used).

$$w(\bar{a}\eta + \xi) = -\frac{\tau_0}{\bar{a}\mu} (\langle \bar{a}\eta + \xi \rangle - \langle \bar{a}\eta + \xi - L \rangle) \quad 18$$

The  $\langle \rangle$  symbolize the Macaulay brackets and  $\bar{a}^2 = (V^2 H^2)/(6l^2 c_s^2) - 1 > 0$  because the problem is considered hyperbolic.

This Cauchy-type of solution, relation 18, was created so it could agree with the boundary conditions. At  $\eta = 0$ , and for  $\xi \in (0, L]$  for the first two conditions for  $\xi \in (-\infty, \infty)$  for the last one. Also, it is a solution of equation 17.

<i>condition</i>	$\eta$ <i>coordinate</i>	$\xi$ <i>coordinate</i>
$w' - \frac{l^2}{2} w'''' \left( 1 - \frac{V^2 H^2}{6l^2 c_s^2} \right) = -\frac{\tau_0}{\bar{a}\mu}$	$\eta = 0$	$\xi \in (0, L]$
$w = 0$	$\eta = 0$	$\xi \in (0, L]$
$w'' = 0$	$\eta = 0$	$\xi \in (-\infty, \infty)$

That solution (relation 18) suggests that the displacement forms Mach cones at an angle from the direction of the crack equal to:

$$\sin \theta = \frac{l\sqrt{6} c_s}{H V} \quad 19$$

This displacement, that forms those Mach cones, holds not only in the supersonic hyperbolic region, but also in the subsonic.

As the hyperbolic case is considered [Giannakopoulos and Zisis \(2021 b.\)](#) treated this problem the same way as in [Giannakopoulos and Zisis \(2021 a.\)](#), with the addition of shock wave analysis, by introducing a shock wave with intrinsic velocity  $\bar{U}$ . Their finding was again a slope equal to  $\sin \theta = \bar{U}/V$ , and  $\bar{U} = c_s l\sqrt{6}/H$ . Some crucial comments that [Giannakopoulos and Zisis \(2021 b.\)](#) mentioned about the microstructural length, is that in some material combination this length can be unreal ( $l^2/2 < 0$ ). In this case pure strain gradient effect should be considered as [Maraganti et al. \(2006\)](#) proposed.

The same substitution as the one described by relation 16 can be applied also for the polarization, as the polarization is connected with (controlled by) the displacement. According to [Appendix D](#), the polarization can be described by the following equation:

$$P_3 - A \frac{\partial^2 P_3}{\partial \bar{\eta}^2} = B \frac{\partial^2 u_3}{\partial \bar{\eta}^2} \quad 20$$

Where:

$$A = \frac{V^2 H^2}{12 l^2 c_s^2} \quad 21$$

$$B = \frac{V^2 \rho (e_{44} - f_{12})}{l^2 a \mu}$$

The displacement  $u_3$ , should be described like a function with the below form, as a trapezoidal distribution (note that for simplification reasons the variable " $\bar{\eta}$ " was replaced with the symbol " $x$ ").

$$u_3(x) = \frac{u_{max}}{b-a} * \langle x-a \rangle * \langle b-x \rangle^0 + u_{max} * \langle x-b \rangle^0 \quad 22$$

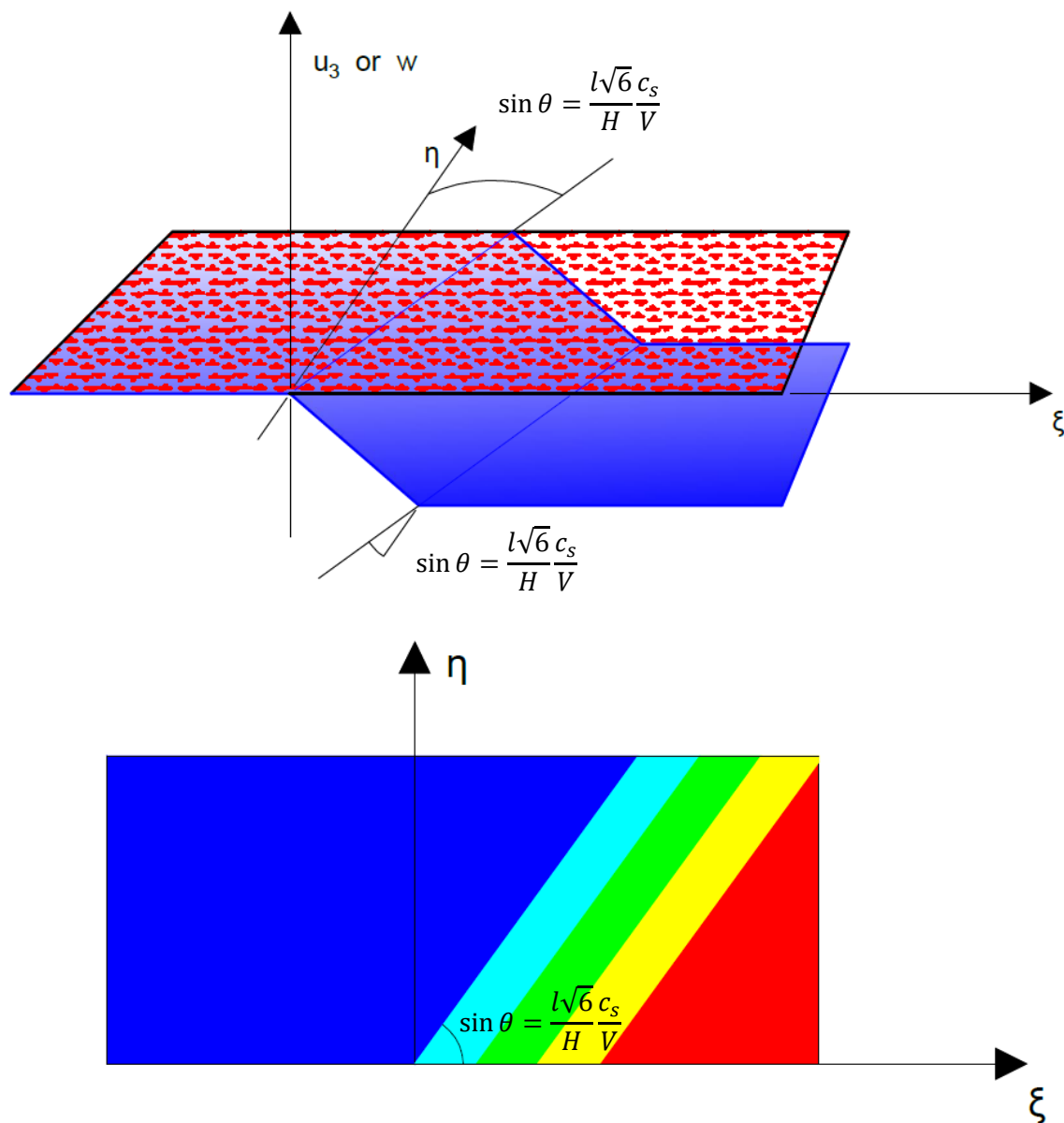


Fig. 33. The out of plane deformation in the hyperbolic case, as suggested by theory.

Relation 22 suggests a trapezoidal displacement. This displacement should propagate in vertical direction to the profile of the crack, with a gradient as proposed by relation 19. This angle is smaller than the corresponding angle suggested by the classic theory ( $\sin \theta_{classic} = c_s/V$ ), because of the ratio of lengths, and the assumption that only normal dielectrics are concerned (no meta-materials,  $(l\sqrt{6})/H < 1$ ).

## 4. The differential equation of the anti-plane hyperbolic flexoelectric problem.

Chapter 3 ended while proposing a differential equation of the variable  $P_3$  (relation 20), with  $A, B$  (relation 21) constants ( $A > 0$ ), while the function  $u_3(\bar{\eta})$  is considered known (e.g. relation 22).

Relation 20 is a second order ordinary differential equation of the following form (Boyce and Diprima, 1997):

$$y'' + f(\eta) * y' + q(\eta) * y = g(\eta) \quad \text{i}$$

For the sake of simplicity, the variable  $\bar{\eta}$ , from now on, will be displayed as  $\eta$ . Note that the crack propagates along the coordinate  $\bar{\eta} = \xi$ .

Obviously, the quantity of  $f(\eta) = 0$ , while the quantity of  $q(\eta) = -1/A$  and  $g(\eta) = -(B/A) * d^2u_3/d\eta^2$ . The method of the integrations by fractions can be used. As the homogeneous differential equation is concerned:

$$y'' - \frac{1}{A} * y = 0$$

The characteristic equation is:

$$\lambda^2 - \frac{1}{A} = 0$$

which gives two possible values of  $\lambda$ :

$$\lambda = +\frac{1}{\sqrt{A}} \qquad \lambda = -\frac{1}{\sqrt{A}}$$

As a result, the homogeneous differential equation has as a general solution the following relation:

$$y = c_1 * e^{+\frac{\eta}{\sqrt{A}}} + c_2 * e^{-\frac{\eta}{\sqrt{A}}} \quad \text{ii}$$



Note that  $y_1(\eta) = \exp(+\eta/\sqrt{A})$ ,  $y_2(\eta) = \exp(-\eta/\sqrt{A})$ . By following the method of integrating by fractions (Boyce and Dpirima, 1997) the solution of the non-homogeneous equation can be written as:

$$y = c_1(\eta) * y_1(\eta) + c_2(\eta) * y_2(\eta) = c_1(\eta) * e^{+\frac{\eta}{\sqrt{A}}} + c_2(\eta) * e^{-\frac{\eta}{\sqrt{A}}} \quad \text{iii}$$

The first derivative of this is the following:

$$y' = c_1'(\eta) * y_1(\eta) + c_1(\eta) * y_1'(\eta) + c_2'(\eta) * y_2(\eta) + c_2(\eta) * y_2'(\eta)$$

Then, the below can be demanded:

$$c_1'(\eta) * y_1(\eta) + c_2'(\eta) * y_2(\eta) = 0 \quad \text{iv}$$

And the derivative becomes the following:

$$y' = c_1(\eta) * y_1'(\eta) + c_2(\eta) * y_2'(\eta)$$

The second derivative of the non-homogeneous is the following:

$$y'' = c_1'(\eta) * y_1'(\eta) + c_1(\eta) * y_1''(\eta) + c_2'(\eta) * y_2'(\eta) + c_2(\eta) * y_2''(\eta) \quad \text{v}$$

By substituting the above expressions (iii, v) to the non-homogeneous differential equation (relation 20), the following is produced:

$$\begin{aligned} c_1'(\eta) * y_1'(\eta) + c_1(\eta) * y_1''(\eta) + c_2'(\eta) * y_2'(\eta) + c_2(\eta) * y_2''(\eta) \\ - \frac{1}{A} * [c_1(\eta) * y_1(\eta) + c_2(\eta) * y_2(\eta)] = -\frac{B}{A} * \frac{d^2 u_3}{d\eta^2} \end{aligned}$$

Which is equivalent to the following:

$$\begin{aligned} c_1(\eta) * \left[ y_1''(\eta) - \frac{1}{A} * y_1(\eta) \right] + c_2(\eta) * \left[ y_2''(\eta) - \frac{1}{A} * y_2(\eta) \right] \\ + c_1'(\eta) * y_1'(\eta) + c_2'(\eta) * y_2'(\eta) = -\frac{B}{A} * \frac{d^2 u_3}{d\eta^2} \end{aligned}$$

Or, because  $y_1, y_2$  are the solutions of the homogeneous ( $y_2''(\eta) - y_2(\eta)/A = 0$ ), the above relation is limited to the below:

$$c_1'(\eta) * y_1'(\eta) + c_2'(\eta) * y_2'(\eta) = -\frac{B}{A} * \frac{d^2u_3}{d\eta^2} \quad \text{vi}$$

This relation (vi) is one equation of a system of differentials equations of the variables  $y_1'(\eta)$ , and  $y_2'(\eta)$ . The first one was the equation iv.

The system of simple differential equations that needs to be solved is:

$$\begin{cases} c_1'(\eta) * y_1(\eta) + c_2'(\eta) * y_2(\eta) = 0 \\ c_1'(\eta) * y_1'(\eta) + c_2'(\eta) * y_2'(\eta) = -\frac{B}{A} * \frac{d^2u_3}{d\eta^2} \end{cases}$$

By using the Wronski determinant, the solution can be given as:

$$c_1'(\eta) = \frac{y_2(\eta) * \frac{B}{A} * \frac{d^2u_3}{d\eta^2}}{W(y_1(\eta), y_2(\eta))} \quad c_2'(\eta) = -\frac{y_1(\eta) * \frac{B}{A} * \frac{d^2u_3}{d\eta^2}}{W(y_1(\eta), y_2(\eta))}$$

And by integrating:

$$c_1(\eta) = \int \frac{y_2(\eta) * \frac{B}{A} * \frac{d^2u_3}{d\eta^2}}{W(y_1(\eta), y_2(\eta))} d\eta + C_3 \quad c_2(\eta) = -\int \frac{y_1(\eta) * \frac{B}{A} * \frac{d^2u_3}{d\eta^2}}{W(y_1(\eta), y_2(\eta))} d\eta + C_4$$

This way, the partial solution of the non-homogeneous differential equation is:

$$Y = y_1(\eta) * \int \frac{y_2(\eta) * \frac{B}{A} * \frac{d^2u_3}{d\eta^2}}{W(y_1(\eta), y_2(\eta))} d\eta + y_2(\eta) * \int -\frac{y_1(\eta) * \frac{B}{A} * \frac{d^2u_3}{d\eta^2}}{W(y_1(\eta), y_2(\eta))} d\eta \quad \text{vii}$$

And the general solution of the non-homogeneous is:

$$y = c_1 * y_1(\eta) + c_2 * y_2(\eta) + Y$$

viii

The Wronski determinant is:

$$\begin{vmatrix} e^{+\frac{\eta}{\sqrt{A}}} & e^{-\frac{\eta}{\sqrt{A}}} \\ \frac{1}{\sqrt{A}} * e^{+\frac{\eta}{\sqrt{A}}} & -\frac{1}{\sqrt{A}} * e^{-\frac{\eta}{\sqrt{A}}} \end{vmatrix}$$

And equal to:

$$W = e^{+\frac{\eta}{\sqrt{A}}} * \frac{-1}{\sqrt{A}} e^{-\frac{\eta}{\sqrt{A}}} - e^{-\frac{\eta}{\sqrt{A}}} * \frac{1}{\sqrt{A}} * e^{+\frac{\eta}{\sqrt{A}}}$$

$$W = \frac{-2}{\sqrt{A}} e^{+\frac{\eta}{\sqrt{A}}} - \frac{\eta}{\sqrt{A}} = -\frac{2}{\sqrt{A}}$$

Then follows the substitution to the partial solution. This way relation vii transforms to the following:

$$Y = e^{+\frac{\eta}{\sqrt{A}}} * \int \frac{e^{-\frac{\eta}{\sqrt{A}}} * \frac{B}{\sqrt{A}} * \frac{d^2 u_3}{d\eta^2}}{-2} d\eta - e^{-\frac{\eta}{\sqrt{A}}} * \int \frac{e^{+\frac{\eta}{\sqrt{A}}} * \frac{B}{\sqrt{A}} * \frac{d^2 u_3}{d\eta^2}}{-2} d\eta \quad \text{ix}$$

Yet, the substitution of equation ix to equation viii, reveals the general solution, relation x:

$$y = c_1 * e^{+\frac{\eta}{\sqrt{A}}} + c_2 * e^{-\frac{\eta}{\sqrt{A}}} - e^{+\frac{\eta}{\sqrt{A}}} * \int \frac{e^{-\frac{\eta}{\sqrt{A}}}}{2} * \frac{B}{\sqrt{A}} * \frac{d^2 u_3}{d\eta^2} d\eta + e^{-\frac{\eta}{\sqrt{A}}} * \int \frac{e^{+\frac{\eta}{\sqrt{A}}}}{2} * \frac{B}{\sqrt{A}} * \frac{d^2 u_3}{d\eta^2} d\eta$$

↔

$$y = c_1 * e^{+\frac{\eta}{\sqrt{A}}} + c_2 * e^{-\frac{\eta}{\sqrt{A}}} + \frac{B}{2 * \sqrt{A}} * \left[ -e^{+\frac{\eta}{\sqrt{A}}} * \int e^{-\frac{\eta}{\sqrt{A}}} * \frac{d^2 u_3}{d\eta^2} d\eta + e^{-\frac{\eta}{\sqrt{A}}} * \int e^{+\frac{\eta}{\sqrt{A}}} * \frac{d^2 u_3}{d\eta^2} d\eta \right]$$

For a more accurate and specific calculation of the polarization, the out-of-plane displacement  $u_3(\eta)$  is needed.

### A. The profile of the crack

As it was mentioned previously, the profile of the crack seems to spread linearly, with an instantly trapezoidal effect. This trapezoidal shape is being made by two parallels, the  $u_3 = 0$  and the  $u_3 = u_{max}$  (the first up to the point  $a$  and the second from point  $b$  and so on). Between those two points, a specific joining function should be inserted, that according to the hyperbolic theory, is linear (the displacement this way will have a trapezoidal shape).

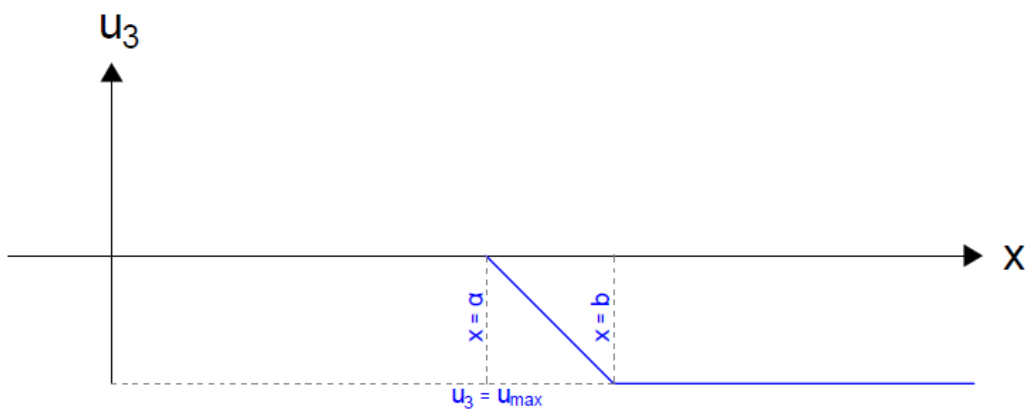


Fig. 34. The trapezoidal function.

Considering that the joining function occupies the distance between "a" and "b", this possible function is described by the above figure. In its general form, the start of the "axis x" is not the point "a" ("a" is different than zero). Also, there could be a continuity of the function to infinite.

The linear function however, despite it agrees with the hyperbolic problem in the best way, is a function with discontinue gradient. A polynomial function could seem promising nonetheless. This joining function can be anything with two major criteria. At points  $a$  and  $b$ , a continuity should be present and secondly, a continuity in its gradients should exist. The linear joining function that was used before, can be described by the following relation:

$$f(x) = \frac{u_{max}}{b - a} * (x - a) \quad \text{xi}$$

In addition to the linear function, a polynomial function of 3<sup>rd</sup> order and one of 5<sup>th</sup> order have been defined in [Appendix F](#) with similar purpose. The modification with the parallels can be made for any joining function, via the Heaviside function.

$$u(\eta) = f(\eta)\langle\eta - a\rangle^0 - f(\eta)\langle\eta - b\rangle^0 + u_{max}\langle\eta - b\rangle^0 \quad \text{xii}$$

By replacing in the above form (relation [xii](#)), the function [xi](#), relation [22](#) will be produced.

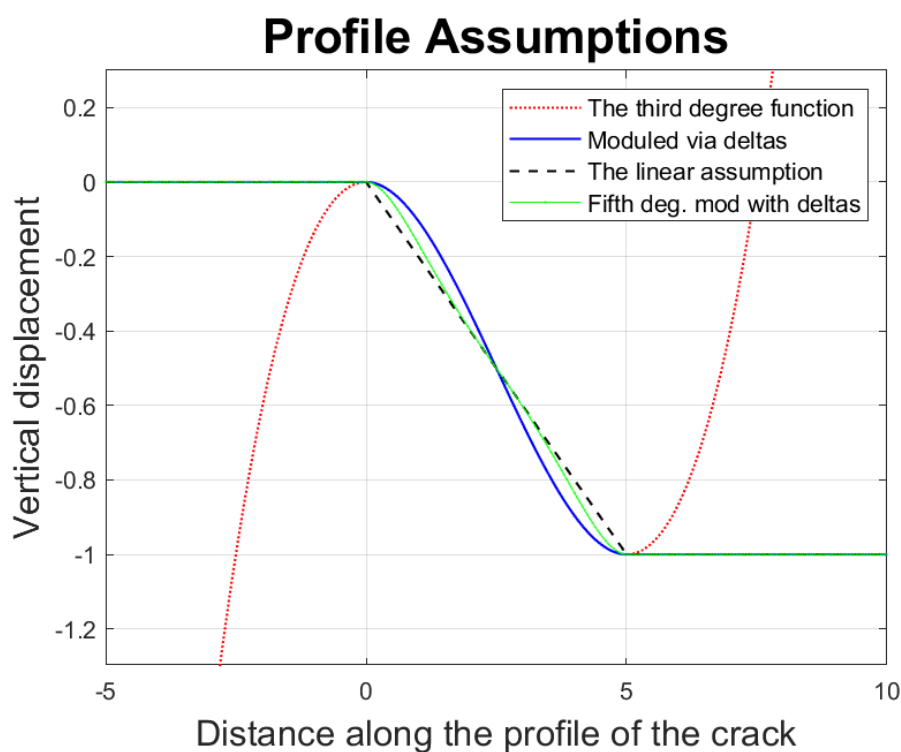


Fig. 35. Assumption of the hyperbolic crack profile.

A linear function suits the theory of the hyperbolic problem. However, polynomial function could also be used. For this purpose, a 3<sup>rd</sup> order and a 5<sup>th</sup> order function were defined ([Appendix F](#)).

## B. The integrals with the Heaviside terms

As it was mentioned above, the relation that describes the displacement can be given by relation [xii](#). In this, those Heaviside terms should also take part in the solution. The polarization is given in the general solution from relation [x](#). That relation includes the second derivative of the displacement and thus the derivatives of the Heaviside term also. The second derivative of the relation that describes the displacement can be calculated as beneath:

$$u_3 = f(\eta)H(\eta - \alpha) - f(\eta)H(\eta - b) + u_{max}H(\eta - b)$$

$$\begin{aligned} \frac{\partial u_3(\eta)}{\partial \eta} &= \frac{\partial f(\eta)}{\partial \eta} * [H(\eta - \alpha) - H(\eta - b)] + f(\eta) * [\delta(\eta - \alpha) - \delta(\eta - b)] \\ &+ u_{max} * \delta(\eta - b) \end{aligned}$$

xiii

$$\begin{aligned} \frac{\partial^2 u_3(\eta)}{\partial \eta^2} &= \frac{\partial^2 f(\eta)}{\partial \eta^2} * [H(\eta - \alpha) - H(\eta - b)] \\ &+ 2 * \frac{\partial f(\eta)}{\partial \eta} * [\delta(\eta - \alpha) - \delta(\eta - b)] \\ &+ f(\eta) * [\delta(\eta - \alpha) - \delta(\eta - b)] + u_{max} * \delta'(\eta - b) \end{aligned}$$

The last expression in relation [xiii](#), which should be added to the integrals described by relation [x](#) contains the Heaviside term, the Dirac's delta function and its derivative. Before the integration proceeds, some rules about those terms should first be implied.

*The integral of a function multiplied with the delta function from minus infinite to infinite is equal to the value of the function to the point where the delta function gets the value of infinite.*

*The same integral with the derivative of delta instead, is the negative integral of the same function, divided by the variable multiplied by the delta.*

*However, those integrals are generalized. The integral used to calculate the differential equation has the meaning of the antiderivative, in this case the area in the integral should be reduced from infinite to the value of the variable of the function. In this case the Heaviside term should be inserted.*

The above suggestions can be seen beneath. The reader, at this point is suggested to visit [Appendix E](#).

$$\int_{-\infty}^{\infty} f(x) * \delta(x - c) dx = f(c)$$

$$\int f(x) * \delta(x - c) dx = \int_{-\infty}^x f(x) * \delta(x - c) dx = f(c) * H(x - c) \quad \text{xiv}$$

$$\int_{-\infty}^{\infty} f(x) * \delta'(x - c) dx = f(x) * \delta(x - c) - \int_{-\infty}^{\infty} \frac{\partial f(x)}{\partial x} * \delta(x - c) dx$$

$$\int f(x) * \delta'(x - c) dx = f(x) * \delta(x - c) - \left. \frac{\partial f(x)}{\partial x} \right|_{x=c} * H(x - c) \quad \text{xv}$$

$$\text{If } \frac{\partial g(x)}{\partial x} = \theta(x)$$

$$\int \theta(x) * H(x - c) = \int \frac{\partial g(x)}{\partial x} * H(x - c)$$

$$= g(x) * H(x - c) - \int g(x) * \delta(x - c)$$

$$= g(x) * H(x - c) - g(c) * H(x - c) \quad \text{xvi}$$

In order to calculate the polarization, the two integrals that are in relation x must be calculated. Those integrals are the beneath:

$$\int e^{\frac{-\eta}{\sqrt{A}}} * \frac{\partial^2 u(\eta)}{\partial \eta^2} d\eta$$

$$\int e^{\frac{\eta}{\sqrt{A}}} * \frac{\partial^2 u(\eta)}{\partial \eta^2} d\eta$$

### i. The integral with the negative sign

By substituting the second derivative of the displacement:

$$\begin{aligned}
 \int e^{\frac{-\eta}{\sqrt{A}}} * \frac{\partial^2 u(\eta)}{\partial \eta^2} d\eta &= \int e^{\frac{-\eta}{\sqrt{A}}} * \frac{\partial^2 f(\eta)}{\partial \eta^2} * [H(\eta - \alpha) - H(\eta - b)] d\eta \\
 &+ \int e^{\frac{-\eta}{\sqrt{A}}} * 2 * \frac{\partial f(\eta)}{\partial \eta} * [\delta(\eta - \alpha) - \delta(\eta - b)] d\eta \\
 &+ \int e^{\frac{-\eta}{\sqrt{A}}} * f(\eta) * [\delta'(\eta - \alpha) - \delta'(\eta - b)] d\eta \\
 &+ \int e^{\frac{-\eta}{\sqrt{A}}} * u_{max} * \delta'(\eta - b) d\eta
 \end{aligned}$$

The **first term** takes the beneath form, by using relation 35:

$$\begin{aligned}
 \int e^{\frac{-\eta}{\sqrt{A}}} * \frac{\partial^2 f(\eta)}{\partial \eta^2} * [H(\eta - a)] d\eta &= g(\eta) * H(\eta - a) - g(a) * H(\eta - a) \\
 \int e^{\frac{-\eta}{\sqrt{A}}} * \frac{\partial^2 f(\eta)}{\partial \eta^2} * [H(\eta - b)] d\eta &= g(\eta) * H(\eta - b) - g(b) * H(\eta - b)
 \end{aligned}$$

Where  $g(\eta)$  in an antiderivative of the expression  $e^{\frac{-\eta}{\sqrt{A}}} * \frac{\partial^2 f(\eta)}{\partial \eta^2}$ .

Because of relation 33 the **second term** of the above integral is equal to:

$$\begin{aligned}
 \int e^{\frac{-\eta}{\sqrt{A}}} * 2 * \frac{\partial f(\eta)}{\partial \eta} * \delta[(\eta - \alpha)] d\eta &= 2 * \frac{\partial f(\eta)}{\partial \eta} * e^{\frac{-\eta}{\sqrt{A}}} \Big|_{\eta=\alpha} * H(\eta - a) \\
 \int e^{\frac{-\eta}{\sqrt{A}}} * 2 * \frac{\partial f(\eta)}{\partial \eta} * \delta[(\eta - b)] d\eta &= 2 * \frac{\partial f(\eta)}{\partial \eta} * e^{\frac{-\eta}{\sqrt{A}}} \Big|_{\eta=b} * H(\eta - b)
 \end{aligned}$$

The **third term** is as follows:



$$\int e^{\frac{-\eta}{\sqrt{A}}} * f(\eta) * \delta'[(\eta - \alpha)] d\eta = e^{\frac{-\eta}{\sqrt{A}}} * f(\eta) * \delta(\eta - \alpha) + \left. \frac{e^{\frac{-\eta}{\sqrt{A}}} * f(\eta)}{\sqrt{A}} \right|_{\eta=\alpha} * H(\eta - \alpha)$$

$$- e^{\frac{-\eta}{\sqrt{A}}} * \left. \frac{\partial f(\eta)}{\partial \eta} \right|_{\eta=\alpha} * H(\eta - \alpha)$$

$$\int e^{\frac{-\eta}{\sqrt{A}}} * f(\eta) * \delta'[(\eta - b)] d\eta = e^{\frac{-\eta}{\sqrt{A}}} * f(\eta) * \delta(\eta - b) + \left. \frac{e^{\frac{-\eta}{\sqrt{A}}} * f(\eta)}{\sqrt{A}} \right|_{\eta=b} * H(\eta - b)$$

$$- e^{\frac{-\eta}{\sqrt{A}}} * \left. \frac{\partial f(\eta)}{\partial \eta} \right|_{\eta=b} * H(\eta - b)$$

While the fourth term is the following:

$$\int e^{\frac{-\eta}{\sqrt{A}}} * u_{max} * \delta'(\eta - b) d\eta = e^{\frac{-\eta}{\sqrt{A}}} * u_{max} * \delta(\eta - b) + \left. \frac{e^{\frac{-\eta}{\sqrt{A}}} * u_{max}}{\sqrt{A}} \right|_{\eta=b} * H(\eta - b)$$

## ii. The integral with the positive sign

Similar formulas can also be produced from the second integral by replacing just the exponential term:

$$\int e^{\frac{\eta}{\sqrt{A}}} * \frac{\partial^2 u(\eta)}{\partial \eta^2} d\eta = \int e^{\frac{\eta}{\sqrt{A}}} * \frac{\partial^2 f(\eta)}{\partial \eta^2} * [H(\eta - \alpha) - H(\eta - b)] d\eta$$

$$+ \int e^{\frac{\eta}{\sqrt{A}}} * 2 * \frac{\partial f(\eta)}{\partial \eta} * [\delta(\eta - \alpha) - \delta(\eta - b)] d\eta$$

$$+ \int e^{\frac{\eta}{\sqrt{A}}} * f(\eta) * [\delta'(\eta - \alpha) - \delta'(\eta - b)] d\eta$$

$$+ \int e^{\frac{\eta}{\sqrt{A}}} * u_{max} * \delta'(\eta - b) d\eta$$

The first term:

$$\int e^{\frac{\eta}{\sqrt{A}}} * \frac{\partial^2 f(\eta)}{\partial \eta^2} * [H(\eta - a)] d\eta = \zeta(\eta) * H(\eta - a) - \zeta(a) * H(\eta - a)$$

$$\int e^{\frac{\eta}{\sqrt{A}}} * \frac{\partial^2 f(\eta)}{\partial \eta^2} * [H(\eta - b)] d\eta = \zeta(x) * H(\eta - b) - \zeta(b) * H(\eta - b)$$

Where  $\zeta(\eta)$  in an antiderivative of the expression  $e^{\frac{\eta}{\sqrt{A}}} * \frac{\partial^2 f(\eta)}{\partial \eta^2}$ .

The second term:

$$\int e^{\frac{\eta}{\sqrt{A}}} * 2 * \frac{\partial f(\eta)}{\partial \eta} * \delta[(\eta - \alpha)] d\eta = 2 * \frac{\partial f(\eta)}{\partial \eta} * e^{\frac{\eta}{\sqrt{A}}} \Big|_{\eta=\alpha} * H(\eta - a)$$

$$\int e^{\frac{\eta}{\sqrt{A}}} * 2 * \frac{\partial f(\eta)}{\partial \eta} * \delta[(\eta - b)] d\eta = 2 * \frac{\partial f(\eta)}{\partial \eta} * e^{\frac{\eta}{\sqrt{A}}} \Big|_{\eta=b} * H(\eta - b)$$

The third term:

$$\int e^{\frac{\eta}{\sqrt{A}}} * f(\eta) * \delta'[(\eta - \alpha)] d\eta = e^{\frac{\eta}{\sqrt{A}}} * f(\eta) * \delta(\eta - a) - \frac{e^{\frac{\eta}{\sqrt{A}}} * f(\eta)}{\sqrt{A}} \Big|_{\eta=a} * H(\eta - a)$$

$$- e^{\frac{\eta}{\sqrt{A}}} * \frac{\partial f(\eta)}{\partial \eta} \Big|_{\eta=a} * H(\eta - a)$$

$$\int e^{\frac{\eta}{\sqrt{A}}} * f(\eta) * \delta'[(\eta - b)] d\eta = e^{\frac{\eta}{\sqrt{A}}} * f(\eta) * \delta(\eta - b) - \frac{e^{\frac{\eta}{\sqrt{A}}} * f(\eta)}{\sqrt{A}} \Big|_{\eta=b} * H(\eta - b)$$

$$- e^{\frac{\eta}{\sqrt{A}}} * \frac{\partial f(\eta)}{\partial \eta} \Big|_{\eta=b} * H(\eta - b)$$

And lastly, the fourth term:

$$\int e^{\frac{\eta}{\sqrt{A}}} * u_{max} * \delta'(\eta - b) d\eta = e^{\frac{\eta}{\sqrt{A}}} * u_{max} * \delta(\eta - b) + \left. \frac{e^{\frac{\eta}{\sqrt{A}}} * u_{max}}{\sqrt{A}} \right|_{\eta=b} * H(\eta - b)$$

By knowing the function which allows the connection between the minimum and the maximum displacement which are zero or  $u_{max}$ . By simple substitution, the terms, from the second one till the fourth of each integral, can be calculated. The first term however needs this antiderivative which is an extra integration.

### C. The polarization while the jointing function in linear

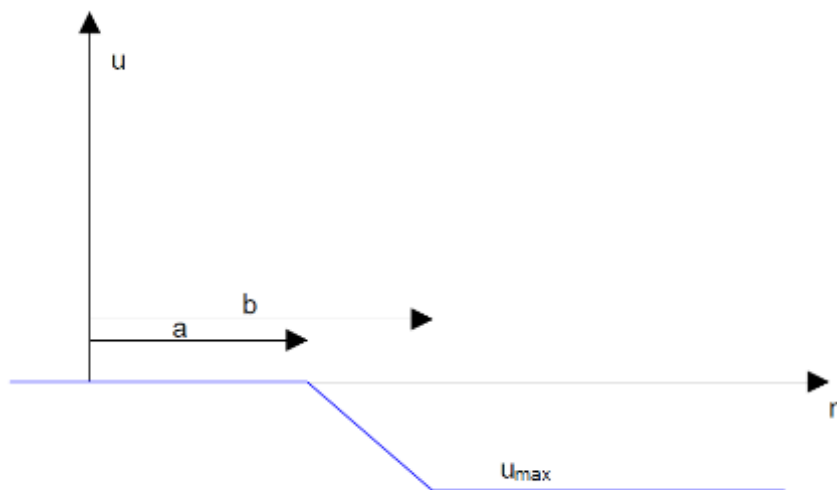
A Polynomial function that can describe the displacement, is a linear function and as it was calculated above, the right formula is the following:

$$f(\eta) = \frac{u_{max}}{b - a} * (\eta - a)$$

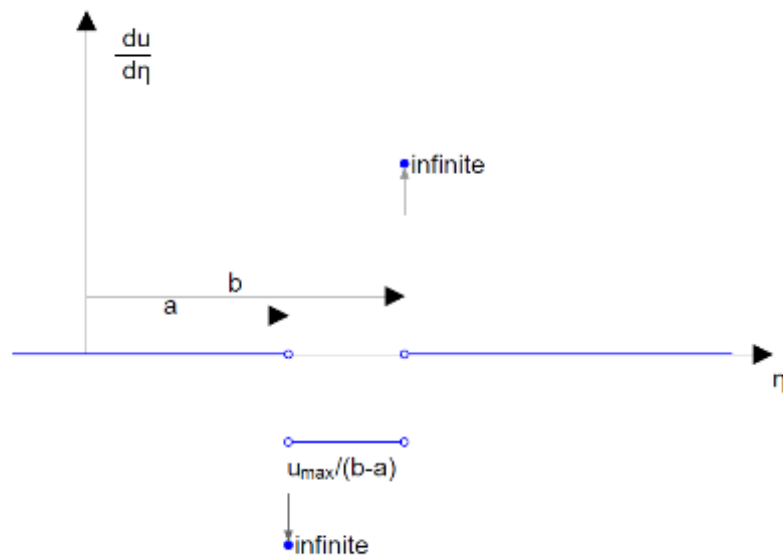
$$\frac{\partial f(\eta)}{\partial \eta} = \frac{u_{max}}{b - a}$$

$$\frac{\partial^2 f(\eta)}{\partial \eta^2} = 0$$

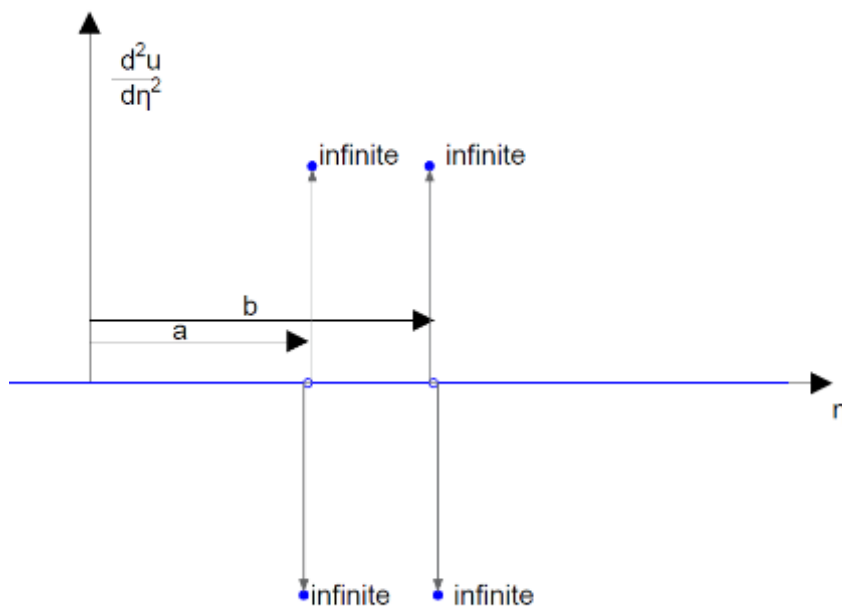
This function is none other than the function that describes the displacement between point  $a$  and  $b$  in relation 22.



(a) the out - of - plane displacement



(b) the first derivative



(c) the second derivative

Fig. 36. The out-of-plane displacement and its derivatives.

In figure (a) there are two points,  $a$  and  $b$  in which the gradient of the displacement changes. The gradient in that point of the function cannot be normally calculated. However in figure (b) the gradient was chosen to be infinite, as mathematics imply. This happens once more, as figure (c) depicts a function which some discontinuities.

Through a substitution of those to the general solution relation  $x$  and a lot of calculation, that are presented in detail in [Appendix G](#), the below result can be extracted:

$$P_3(\eta) = c_1 * e^{+\frac{\eta}{\sqrt{A}}} + c_2 * e^{-\frac{\eta}{\sqrt{A}}}$$

$$+ \frac{B}{2 * \sqrt{A}} * \frac{u_{max}}{b - a} * \left[ \left( -e^{+\frac{\eta-a}{\sqrt{A}}} + e^{-\frac{\eta-a}{\sqrt{A}}} \right) * H(\eta - a) + \left( e^{+\frac{\eta-b}{\sqrt{A}}} - e^{-\frac{\eta-b}{\sqrt{A}}} \right) * H(\eta - b) \right]$$

23

The boundary condition in the limit of the crack which is infinite and minus infinite can give the values of the constants  $c_1$  and  $c_2$ . More specifically, if the polarization on those limits is equal to zero, the boundary condition at minus infinite, gives the values of  $c_2 = 0$ , while the other boundary at infinite can give the value of the constant  $c_1$  equal to:

$$c_1 = -\frac{B}{2 * \sqrt{A}} * \frac{u_{max}}{b - a} * \left[ \left( -e^{-\frac{a}{\sqrt{A}}} \right) + \left( e^{-\frac{b}{\sqrt{A}}} \right) \right]$$

24

$$c_2 = 0$$

Lastly, by considering that the axis of the characteristic coordinate moves along the crack, so that  $a \equiv 0$  always,

$$P_3(\eta) = c_1 * e^{+\frac{\eta}{\sqrt{A}}} + c_2 * e^{-\frac{\eta}{\sqrt{A}}}$$

$$+ \frac{B * u_{max}}{2 * b * \sqrt{A}} * \left[ \left( -e^{+\frac{\eta}{\sqrt{A}}} + e^{-\frac{\eta}{\sqrt{A}}} \right) * H(\eta) + \left( e^{+\frac{\eta-b}{\sqrt{A}}} - e^{-\frac{\eta-b}{\sqrt{A}}} \right) * H(\eta - b) \right]$$

And also:

$$c_1 = -\frac{B * u_{max}}{2 * b * \sqrt{A}} * \left[ 1 + \left( e^{-\frac{b}{\sqrt{A}}} \right) \right]$$

$$c_2 = 0$$

By plotting the above relations for some specific values of  $a, b, u_{max}$ , the following diagram can be produced:

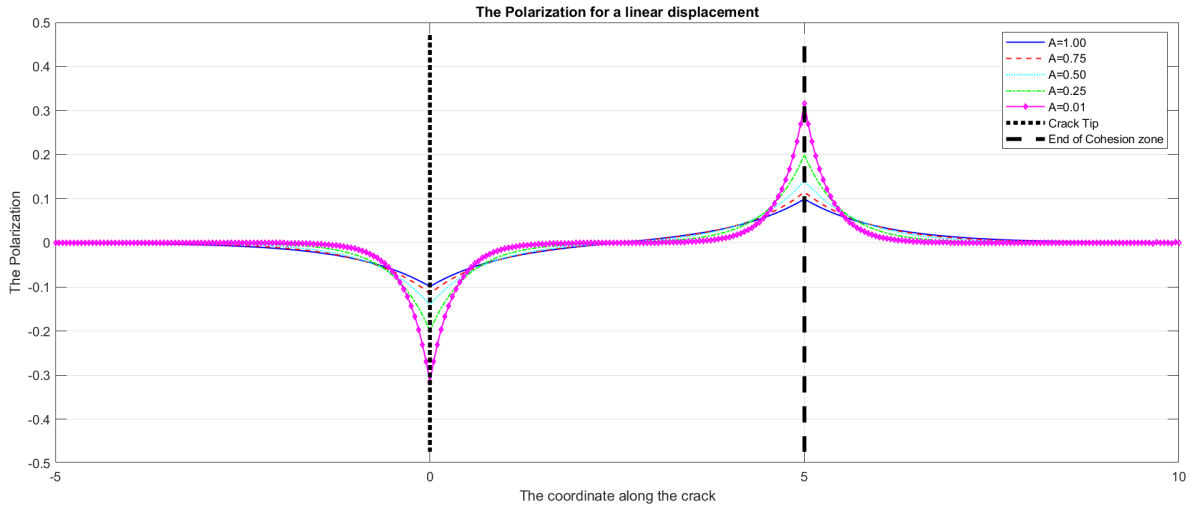


Fig. 37. The Polarization assuming a linear function to take part in the displacement relation.

The value of the constant  $A$ , which should be positive, causes great exponential effects. As it gets larger, the exponent tends to zero and great linearities take place. As it gets smaller, the exponential behavior is significantly magnified to a point that the behavior of the function is treated like a Dirac's delta function. This constant is something like an internal length square. Lastly the constant  $A$  must be subjected to some constrains. Those constrains are:  $\sqrt{A} \ll b - a$  and  $\sqrt{A} \ll b$  in case  $a = 0$ .

The constant  $B$ , which can be positive or negative, seems to have a direct relation with the magnitude of the maximum displacement and seems to have a more mechanical meaning. More specifically, the constant  $B$  increases as the shear modulus of material gets smaller, the density of the material gets bigger and when the dielectric constant gets bigger too. This constant is greatly connected, monotonously with the flexoelectric constant and that's why polymers and ceramics are good flexoelectric materials.

The positions of the spikes are, nonetheless, possible location for electrical yielding. This means that in those locations, the polarization could change direction (this would turn the problem non-anti-plane) or create an electrical bridge (in fig. 33 those positions are visible in a 3D sketch).

#### D. The polarization while the jointing is a 3<sup>rd</sup> Degree function

Another case of a function that can fit in the cohesive zone between the maximum and the minimum values is a polynomial function of third order. That function, that was determined above, has an analogue procedure with the linear function:

$$f(\eta) = \frac{u_{max}}{a^3 - 3ab^2 + 3ab^2 - b^3} \{2\eta^3 - 3(a+b)\eta^2\} + 6ab\eta + (a-3b)a^2$$

$$\frac{\partial^2 f(\eta)}{\partial \eta^2} = \frac{u_{max}}{a^3 - 3ab^2 + 3ab^2 - b^3} * \{12\eta - 6(a+b)\}$$

And the polarization formula, which results from the corresponding substitution, is the following (for information about the calculation the reader is suggested to visit once again [Appendix G](#)):

$$P_3(\eta) = c_1 e^{+\frac{\eta}{\sqrt{A}}} + c_2 e^{-\frac{\eta}{\sqrt{A}}} + \frac{B}{2 * \sqrt{A}} * \frac{u_{max}}{\dots} * \left[ \{ +24\eta\sqrt{A} - 12\sqrt{A}(a+b) \} \{ H(\eta-a) - H(\eta-b) \} \right. \\ \left. + H(\eta-a) \left\{ e^{\frac{\eta-a}{\sqrt{A}}} \{ -12a\sqrt{A} - 12A + 6\sqrt{A}(a+b) \} - e^{-\frac{\eta-a}{\sqrt{A}}} \{ 12a\sqrt{A} - 12A - 6\sqrt{A}(a+b) \} \right\} \right. \\ \left. - H(\eta-b) \left\{ e^{\frac{\eta-b}{\sqrt{A}}} \{ -12b\sqrt{A} - 12A + 6\sqrt{A}(a+b) \} - e^{-\frac{\eta-b}{\sqrt{A}}} \{ 12b\sqrt{A} - 12A - 6\sqrt{A}(a+b) \} \right\} \right]$$

At this point it is possible to calculate the constant  $c_1$  and  $c_2$ , by solving the limit towards infinite to be equal to the wanted polarization e.g., zero. For this case, by considering that for very small numbers near minus infinite both  $H(\eta-a)$  and  $H(\eta-b)$  are equal to zero and also the exponential, which has an exponent that tends to minus infinite, tends to zero, the polarization is given by the formula:

$$\lim_{\eta \rightarrow -\infty} P_3(\eta) = \lim_{\eta \rightarrow -\infty} c_2 e^{-\frac{\eta}{\sqrt{A}}}$$

which gives that  $c_2$  should be zero.

From the opposite direction, as the coordinate tends to infinite, both Heaviside terms are equal to one, and also the exponential that has an exponent that tends to minus infinite is also zero. Those reduce the calculation to the following:

$$\lim_{\eta \rightarrow -\infty} P_3(\eta) = \lim_{\eta \rightarrow \infty} \left\{ c_1 e^{+\frac{\eta}{\sqrt{A}}} + \frac{B}{2\sqrt{A}} \frac{u_{max}}{\dots} \left[ e^{\frac{\eta-a}{\sqrt{A}}} \{ -12a\sqrt{A} - 12A + 6\sqrt{A}(a+b) \} - e^{-\frac{\eta-b}{\sqrt{A}}} \{ -12b\sqrt{A} - 12A + 6\sqrt{A}(a+b) \} \right] \right\}$$

Which gives the value of the constant  $c_1$  equal to the one presented beneath.

$$c_2 = -\frac{B}{2\sqrt{A}} \frac{u_{max}}{\dots} \left[ e^{\frac{a}{\sqrt{A}}} \{-12a\sqrt{A} - 12A + 6\sqrt{A}(a+b)\} - e^{\frac{b}{\sqrt{A}}} \{-12b\sqrt{A} - 12A + 6\sqrt{A}(a+b)\} \right]$$

$$c_2 = 0$$

This equation can easily be plotted, for various values of the constant A.

Also, by considering once again that  $a \equiv 0$ ,

$$P_3(\eta) = c_1 e^{+\frac{\eta}{\sqrt{A}}} + c_2 e^{-\frac{\eta}{\sqrt{A}}}$$

$$\begin{aligned} & -\frac{B * u_{max}}{2 * b^3 * \sqrt{A}} * \left[ \{+24\eta\sqrt{A} - 12b\sqrt{A}\} \{H(\eta) - H(\eta - b)\} \right. \\ & \quad \left. + H(\eta) \left\{ e^{\frac{\eta}{\sqrt{A}}} \{-12A + 6b\sqrt{A}\} - e^{-\frac{\eta}{\sqrt{A}}} \{-12A - 6b\sqrt{A}\} \right\} \right. \\ & \quad \left. - H(\eta - b) \left\{ e^{\frac{\eta-b}{\sqrt{A}}} \{-12b\sqrt{A} - 12A + 6b\sqrt{A}\} - e^{\frac{\eta-b}{\sqrt{A}}} \{12b\sqrt{A} - 12A - 6b\sqrt{A}\} \right\} \right] \end{aligned}$$

25

While the boundary conditions are turned to:

$$c_2 = -\frac{B}{2\sqrt{A}} \frac{u_{max}}{b^3} \left[ \{-12A + 6b\sqrt{A}\} - e^{\frac{b}{\sqrt{A}}} \{-12b\sqrt{A} - 12A + 6b\sqrt{A}\} \right]$$

$$c_2 = 0$$

26



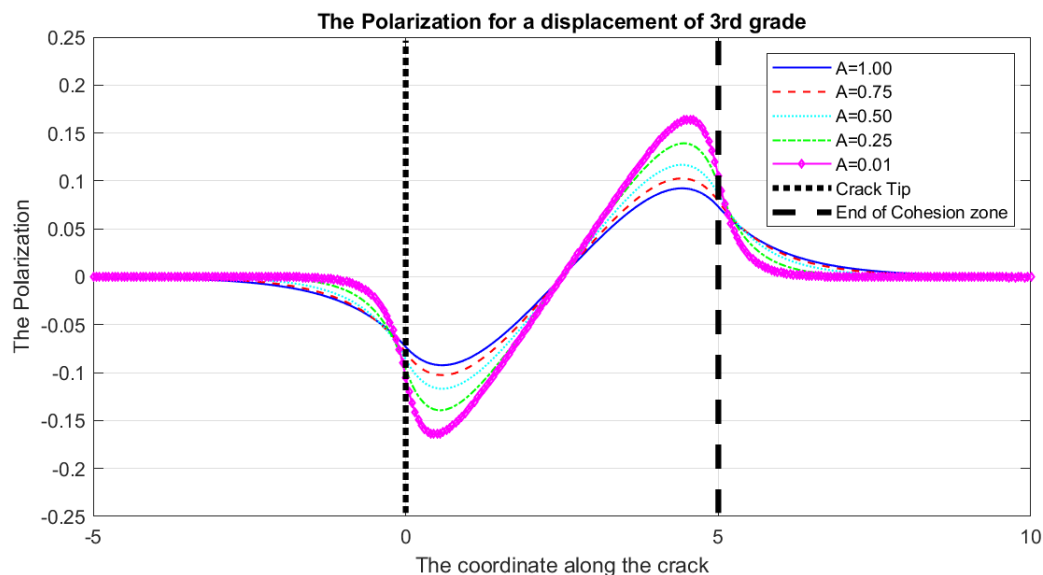


Fig. 38. The polarization for a displacement described by a 3<sup>rd</sup> order function.

The polarization is relatively close to the previous case, however smaller. The spikes in this case don't occur to the start and end of the cohesive zone (point a and b). Lastly, the effect of the constants A and B seems to be the same.

Interesting is to compare the cases with a linear function and a polynomial of 3<sup>rd</sup> order. This comparison seems to be independent from the selection of the value of the constant A.

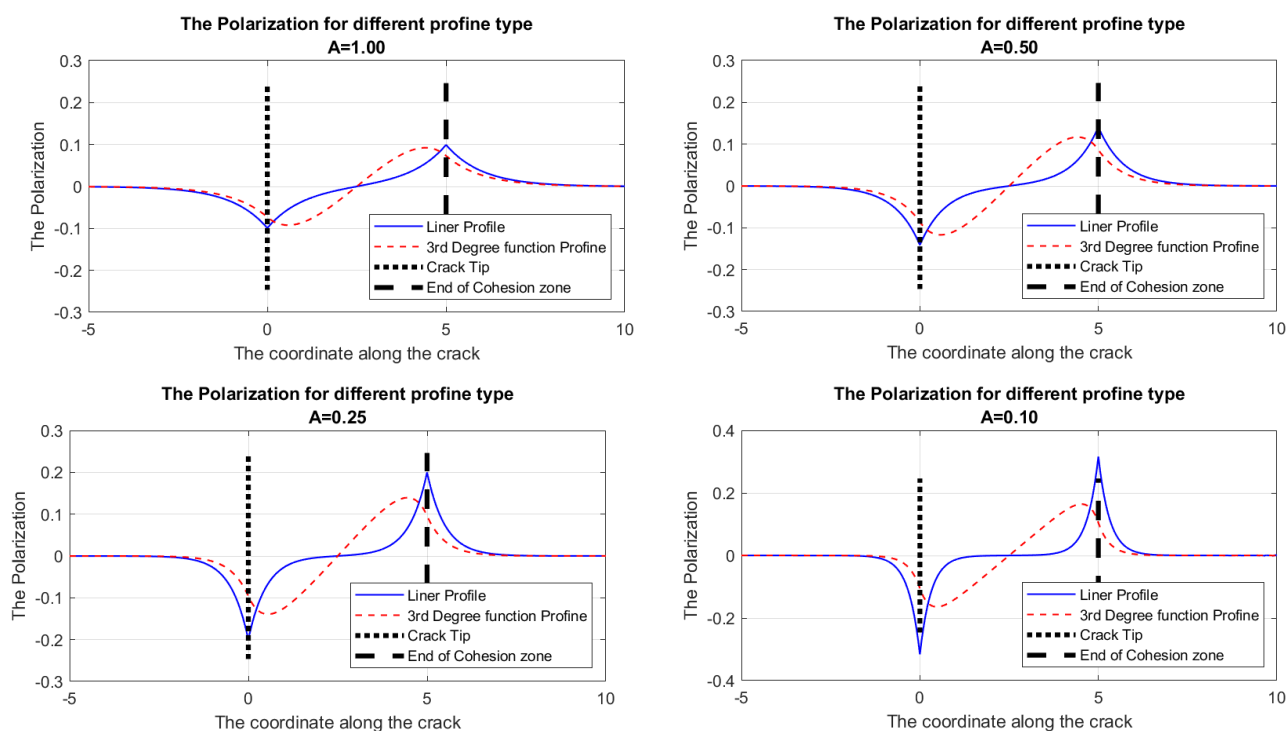


Fig. 39. The comparison of the polarization between the linear case and the 3<sup>rd</sup> order function case. Macroscopically the integral (area) of the polarization is always zero, as one spike cancels out the other. The observer must be close to the cohesive area to see the spike of the electromagnetic field.

### E. The boundary conditions.

The linear case as theory demands is more fitting and thus, will be the main solution. The relation of the polarization can be given by the beneath formula:

$$P_3(\eta) = c_1 * e^{+\frac{\eta}{\sqrt{A}}} + c_2 * e^{-\frac{\eta}{\sqrt{A}}} + \frac{B}{2 * \sqrt{A}} * \frac{u_{max}}{b-a} * \left[ -e^{+\frac{\eta-a}{\sqrt{A}}} * H(\eta-a) + e^{-\frac{\eta-a}{\sqrt{A}}} * H(\eta-a) \right. \\ \left. + e^{+\frac{\eta-b}{\sqrt{A}}} * H(\eta-b) - e^{-\frac{\eta-b}{\sqrt{A}}} * H(\eta-b) \right]$$

The boundary condition can be given via a formula as:

$$P_3(\eta_1) = Pol_1$$

That point, “ $\eta_1$ ” can be anything. If this point tends to some infinite (e.g.,  $\pm\infty$ ), the boundary relations is by considering its limit to the respective infinite. However, because the function of the polarization is made by some parts, to make things simpler, when

$$\eta \rightarrow -\infty \quad e^{+\frac{\eta}{\sqrt{A}}} \rightarrow 0$$

$$\eta \rightarrow +\infty \quad e^{-\frac{\eta}{\sqrt{A}}} \rightarrow 0$$

Also, as “ $\eta \rightarrow -\infty$ ”, “ $H(\eta-a) = H(\eta-b) = 0$ ”, because “ $\eta < a < b$ ” and respectively, as “ $\eta \rightarrow +\infty$ ”, “ $H(\eta-a) = H(\eta-b) = 1$ ”, because “ $\eta > b > a$ ”

Because of those:

$$\lim_{\eta \rightarrow -\infty} P_3(\eta) = \lim_{\eta \rightarrow -\infty} \left[ c_2 * e^{-\frac{\eta}{\sqrt{A}}} \right]$$

$$\lim_{\eta \rightarrow +\infty} P_3(\eta) = \lim_{\eta \rightarrow +\infty} \left[ c_1 * e^{+\frac{\eta}{\sqrt{A}}} + \frac{B}{2 * \sqrt{A}} * \frac{u_{max}}{b-a} * \left\{ -e^{+\frac{\eta-a}{\sqrt{A}}} + e^{+\frac{\eta-b}{\sqrt{A}}} \right\} \right]$$

If the boundary condition to some infinities is zero, then the constants  $c_1, c_2$  can be easily given by demanding the relation that multiplies the terms that tend to infinite to be zero. This way,

If:

$$\lim_{\eta \rightarrow -\infty} P_3(\eta) = 0$$

$$\lim_{\eta \rightarrow -\infty} \left[ c_2 * e^{-\frac{\eta}{\sqrt{A}}} \right] = 0$$

$$c_2 = 0$$

$$\lim_{\eta \rightarrow +\infty} P_3(\eta) = 0$$

$$\lim_{\eta \rightarrow +\infty} \left[ c_1 * e^{+\frac{\eta}{\sqrt{A}}} + \frac{B}{2 * \sqrt{A}} * \frac{u_{max}}{b-a} * \left\{ -e^{+\frac{\eta-a}{\sqrt{A}}} + e^{+\frac{\eta-b}{\sqrt{A}}} \right\} \right] = 0$$

$$\lim_{\eta \rightarrow +\infty} \left[ e^{+\frac{\eta}{\sqrt{A}}} * \left\{ c_1 + \frac{B}{2 * \sqrt{A}} * \frac{u_{max}}{b-a} * \left\{ -e^{-\frac{a}{\sqrt{A}}} + e^{-\frac{b}{\sqrt{A}}} \right\} \right\} \right] = 0$$

$$c_1 = -\frac{B}{2 * \sqrt{A}} * \frac{u_{max}}{b-a} * \left\{ -e^{-\frac{a}{\sqrt{A}}} + e^{-\frac{b}{\sqrt{A}}} \right\}$$

However, if:

$$\lim_{\eta \rightarrow -\infty} P_3(\eta) = P \neq 0$$

$$\lim_{\eta \rightarrow -\infty} \left[ c_2 * e^{-\frac{\eta}{\sqrt{A}}} \right] = P$$

Which means that if  $P$  is negative or positive, this is also the constant  $c_2$ . Also, as these limits tends to some infinite, despite the value of  $c_2$ ,  $P$  should be only some infinite.

The same stands for the other limit to  $+\infty$

For any scenario considered, whether

$$\lim_{\eta \rightarrow \pm\infty} P_3(\eta) = 0$$

or

$$\lim_{\eta \rightarrow \pm\infty} P_3(\eta) = \pm\infty$$

As there is no other legit option.

In case the boundary condition is given at some point e.g.,  $\eta_1 \in (-\infty, +\infty)$ , then the constant  $c_1$  and  $c_2$  should be calculated from a two-by-two system of equations. However, each equation has a different form, whether the point  $\eta_1 \in (-\infty, a]$ ,  $\eta_1 \in [b, a]$  or  $\eta_1 \in [b, \infty)$ . The brackets are meant to be this way, as in case the point  $\eta_1 = a$  or  $\eta_1 = b$ , the equation would be the same either way as the polarization is continued. Those spaces, are related to the value of the Heaviside term. In the first space, both Heaviside terms are zero, in the second,  $H(\eta - a) = 1$  but  $H(\eta - b) = 0$  and in the third both are equal to one.

Also, by manipulating the equation of the polarization, someone can rewrite it as follows:

$$c_1 * e^{+\frac{\eta}{\sqrt{A}}} + c_2 * e^{-\frac{\eta}{\sqrt{A}}} = P_3(\eta) - \frac{B}{2 * \sqrt{A}} * \frac{u_{max}}{b - a} * \left[ -e^{+\frac{\eta-a}{\sqrt{A}}} * H(\eta - a) + e^{-\frac{\eta-a}{\sqrt{A}}} * H(\eta - a) \right. \\ \left. + e^{+\frac{\eta-b}{\sqrt{A}}} * H(\eta - b) - e^{-\frac{\eta-b}{\sqrt{A}}} * H(\eta - b) \right]$$

And by this, someone can substitute the term:  $P_3(\eta) - \frac{B}{2 * \sqrt{A}} * \frac{u_{max}}{b - a} * \left[ -e^{+\frac{\eta-a}{\sqrt{A}}} * H(\eta - a) + e^{-\frac{\eta-a}{\sqrt{A}}} * H(\eta - a) + e^{+\frac{\eta-b}{\sqrt{A}}} * H(\eta - b) - e^{-\frac{\eta-b}{\sqrt{A}}} * H(\eta - b) \right]$  with  $V$ . This way, for  $\eta_1$  this term is  $V_1$ .

Also this term is the one manipulated by the value of  $\eta_1$  by the Heaviside. Because continuity is in place it is possible to split the cases.

$$\eta_1 \in (-\infty, a]$$

$$V_1 = P_3(\eta_1)$$

$$\eta_1 \in [b, a]$$

$$V_1 = P_3(\eta_1) - \frac{u_{max}}{b - a} * \left[ -e^{+\frac{\eta_1-a}{\sqrt{A}}} + e^{-\frac{\eta_1-a}{\sqrt{A}}} \right]$$

$$\eta_1 \in [b, +\infty)$$

$$V_1 = P_3(\eta_1) - \frac{u_{max}}{b - a} * \left[ -e^{+\frac{\eta_1-a}{\sqrt{A}}} + e^{-\frac{\eta_1-a}{\sqrt{A}}} + e^{+\frac{\eta_1-b}{\sqrt{A}}} - e^{-\frac{\eta_1-b}{\sqrt{A}}} \right]$$

And so, the equation of the boundary condition can be written in matrix form as beneath:

$$\begin{bmatrix} e^{+\frac{\eta_1}{\sqrt{A}}} & e^{-\frac{\eta_1}{\sqrt{A}}} \end{bmatrix} * \begin{bmatrix} c_1 \\ c_2 \end{bmatrix} = \begin{bmatrix} V_1 \end{bmatrix}$$

In order to find both constants, two equations are needed, one second equation in a second point e.g.,  $\eta_2$  for which the value of the polarization is  $V_2$ . The system that is produced can be written in matrix form and easily be solved.

$$\begin{bmatrix} e^{+\frac{\eta_1}{\sqrt{A}}} & e^{-\frac{\eta_1}{\sqrt{A}}} \\ e^{+\frac{\eta_2}{\sqrt{A}}} & e^{-\frac{\eta_2}{\sqrt{A}}} \end{bmatrix} * \begin{bmatrix} c_1 \\ c_2 \end{bmatrix} = \begin{bmatrix} V_1 \\ V_2 \end{bmatrix}$$

For some more tangible results, some cases where plot. The points  $\eta_i$  could be smaller than  $a$ , bigger than  $b$ , or something in between. Because the order of  $\eta_1$  and  $\eta_2$  doesn't matter, there is a total of six combinations of the locations of the point included in the equation (instead of nine). The value of the boundary condition could be positive, negative, or zero. This gives a total of four (the boundary values can be negative (-0.1) or positive (0.1)) plus other four (where the boundary values can be positive or negative and zero) and plus one (The case where both boundary values are zero).

The combinations of the location of the point can be plotted in the same diagram and the combination of the values of the boundary conditions can be plotted in separate diagrams.

Considering $a = 0$ & $b = 5$					
1.	$\eta_1 = -5$	$\eta < a$		$a < \eta < b$	$b < \eta$
	$\eta_2 = -2$	$\eta < a$		$\eta < a$	$\eta < a$
2.	$\eta_1 = -2$	$\eta < a$	3.	$\eta_1 = +1$	$a < \eta < b$
	$\eta_2 = +2$	$a < \eta < b$		$\eta_2 = +4$	$a < \eta < b$
					$a < \eta < b$
4.	$\eta_1 = -2$	$\eta < a$	5.	$\eta_1 = +2$	$a < \eta < b$
	$\eta_2 = +7$	$b < \eta$		$\eta_2 = +7$	$b < \eta$
			6.	$\eta_1 = +6$	$b < \eta$
				$\eta_2 = +9$	$b < \eta$

For the first set of the boundary values, the polarizations diagrams are the beneath:

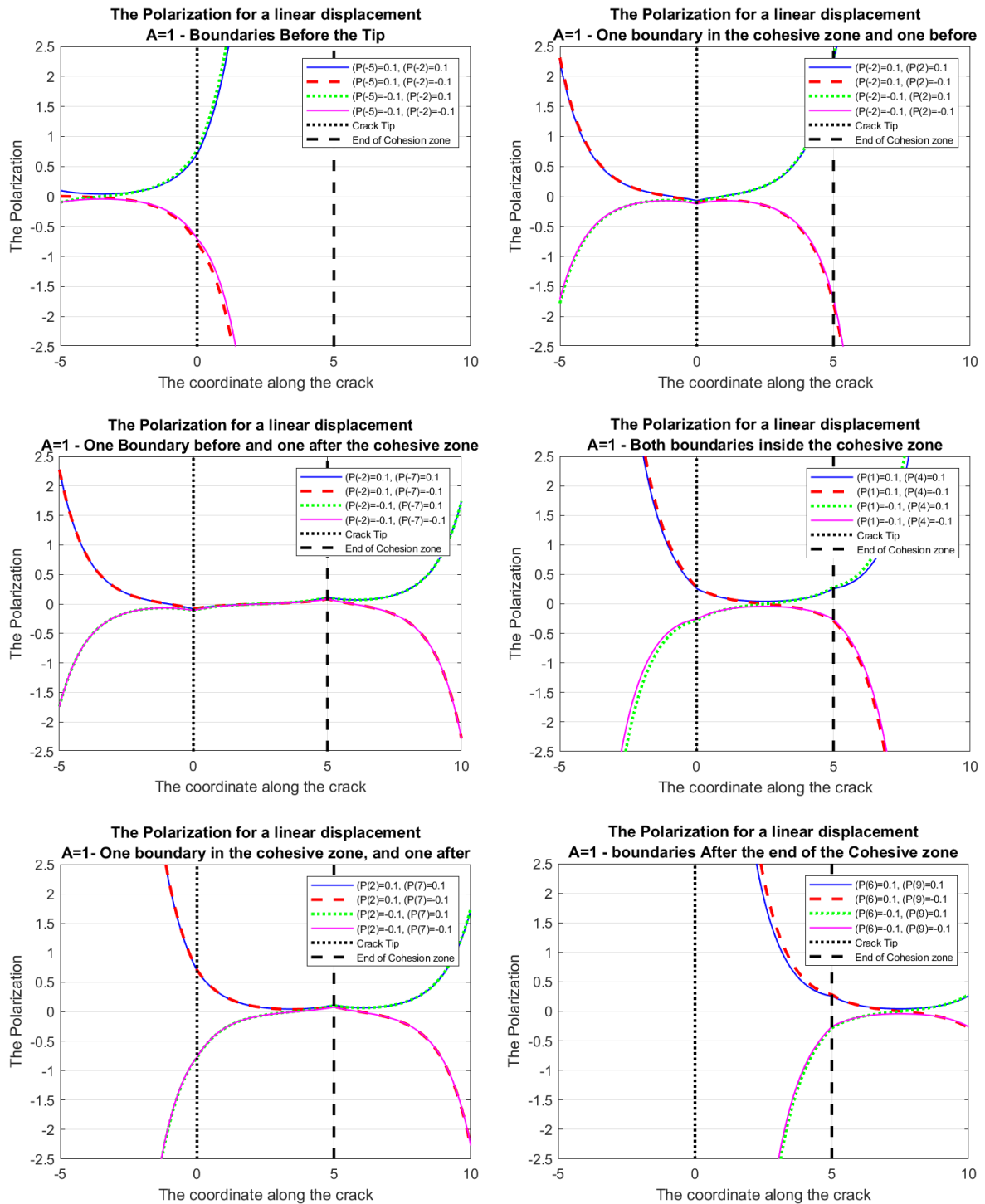


Fig. 40. The first set of the diagrams assuming some boundary conditions.

In each diagram, there is a total of four lines. Those lines are referring to the value of the boundary condition. In this set of diagrams, the value of the boundary conditions can be either positive, negative or both.

As it can be seen, neither case could exist as the polarization tends to infinite, exponentially, which obviously can't happen. The polarization should vanish as the coordinate tends to the open edge, or the edge in which the crack hasn't yet reached.

While for the second set are the following:

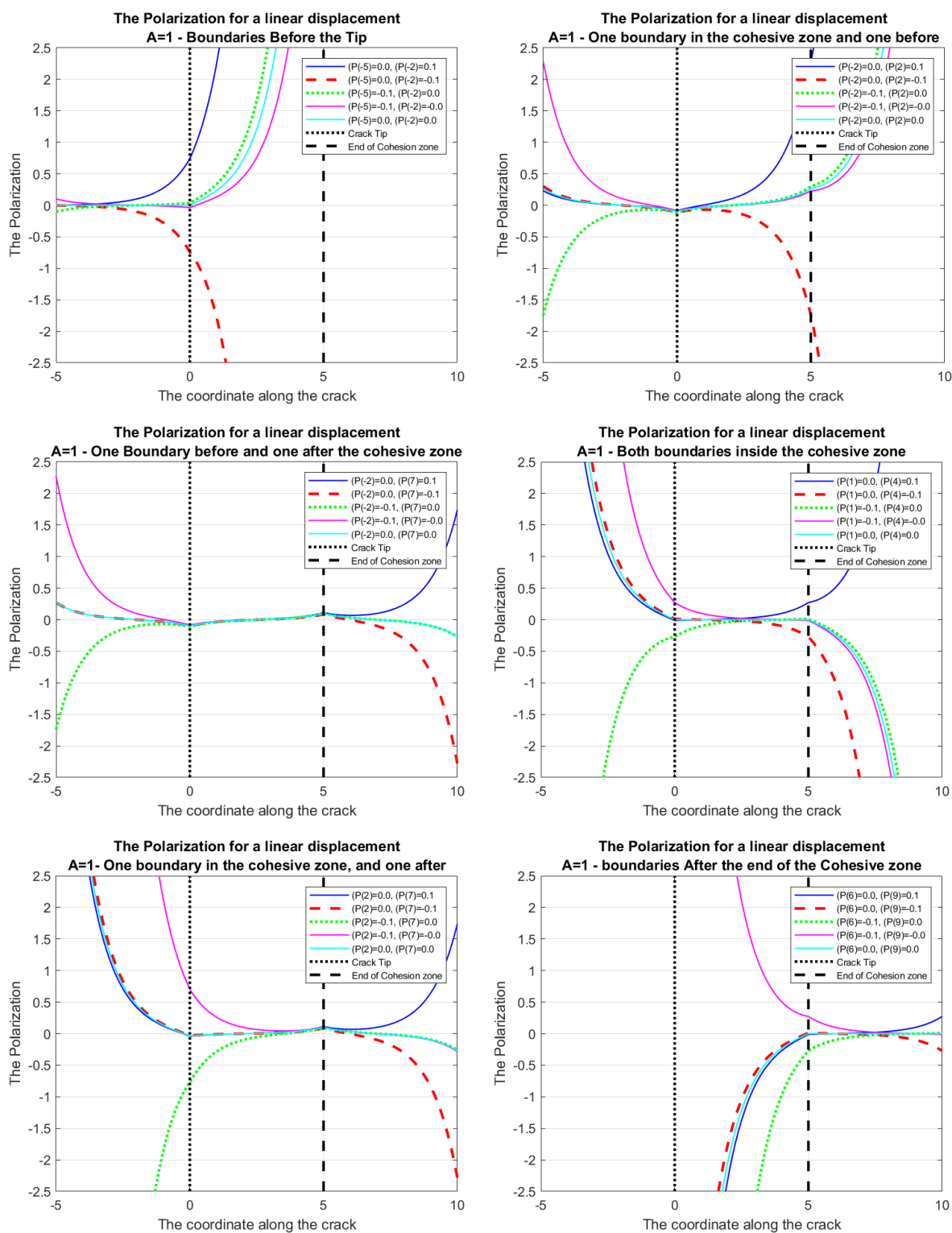


Fig. 41. The second set of the diagrams assuming some boundary conditions.

In each diagram, there is a total of five lines. Those lines are referring to the value of the boundary condition. In this set of diagrams, the value of the boundary conditions can be either positive or negative or zero, but at least one should be zero.

As it can be seen neither case could exist as the polarization tends also to infinite, exponentially, which obviously can't happen. The polarization should vanish as the coordinate tends to the open edge, or the edge in which the crack hasn't yet reached.

Interesting is to see also the case when both the boundary values before the crack tip and after the end of the cohesion zone are zero (fig. 41, middle left diagram). This diagram is different than the one made with the boundary condition referring to the infinities, while also is unnatural.

To conclude, concerning this boundary condition analysis, it is obvious, that the only reasonable boundary conditions that should be considered are the conditions that demand the polarization to be zero to each infinite.

In this case, however, the plate that was considered was infinite. In a ribbon plate, with  $\eta_{max} \neq +\infty$ ,  $\eta_{min} \neq -\infty$ , this analysis is helpful as a solution from the second set should be used (or even the first), as the polarization in the edges of the ribbon should be zero.

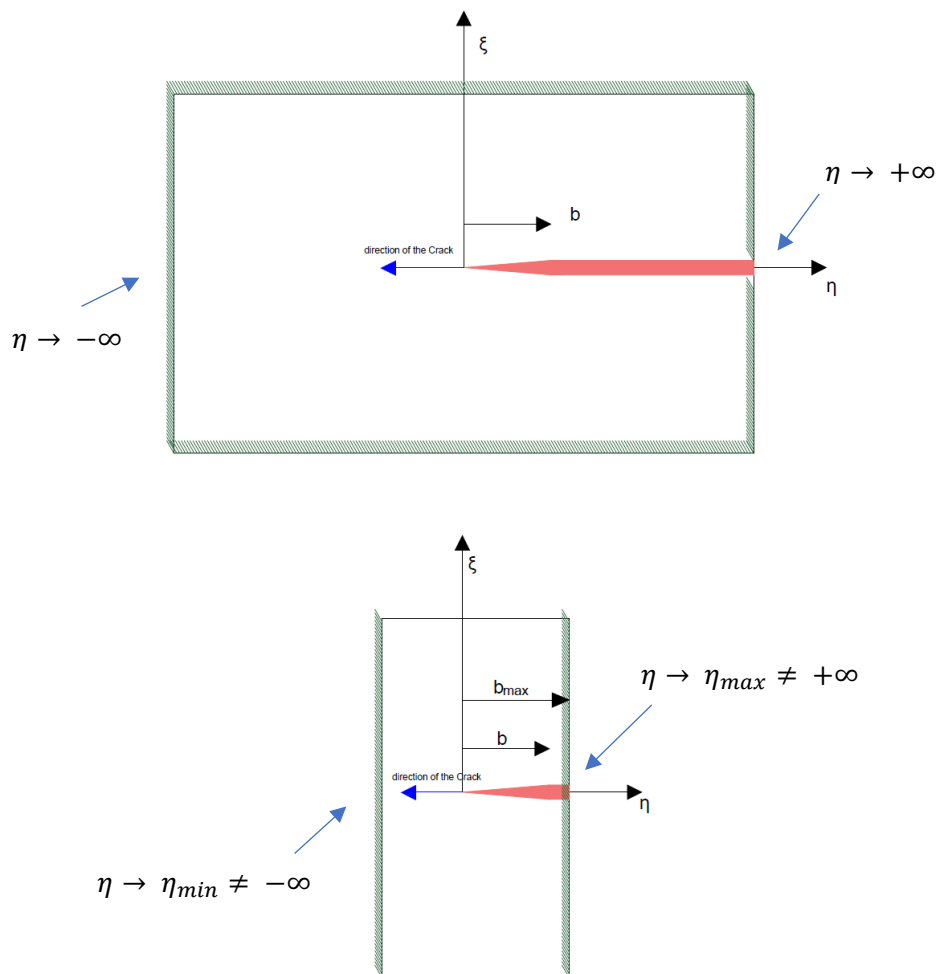


Fig. 42. The boundary condition in a ribbon plate.

The coordinate cannot reach to great values that can be considered infinite, this way a boundary condition in a point e.g.,  $\eta_1$  should be considered.



### F. The screw dislocation

The term  $b - a$  which describes the cohesive zone, could get smaller and smaller. When this term reaches zero, the crack will become a screw dislocation.

$$(b - a) \rightarrow 0$$

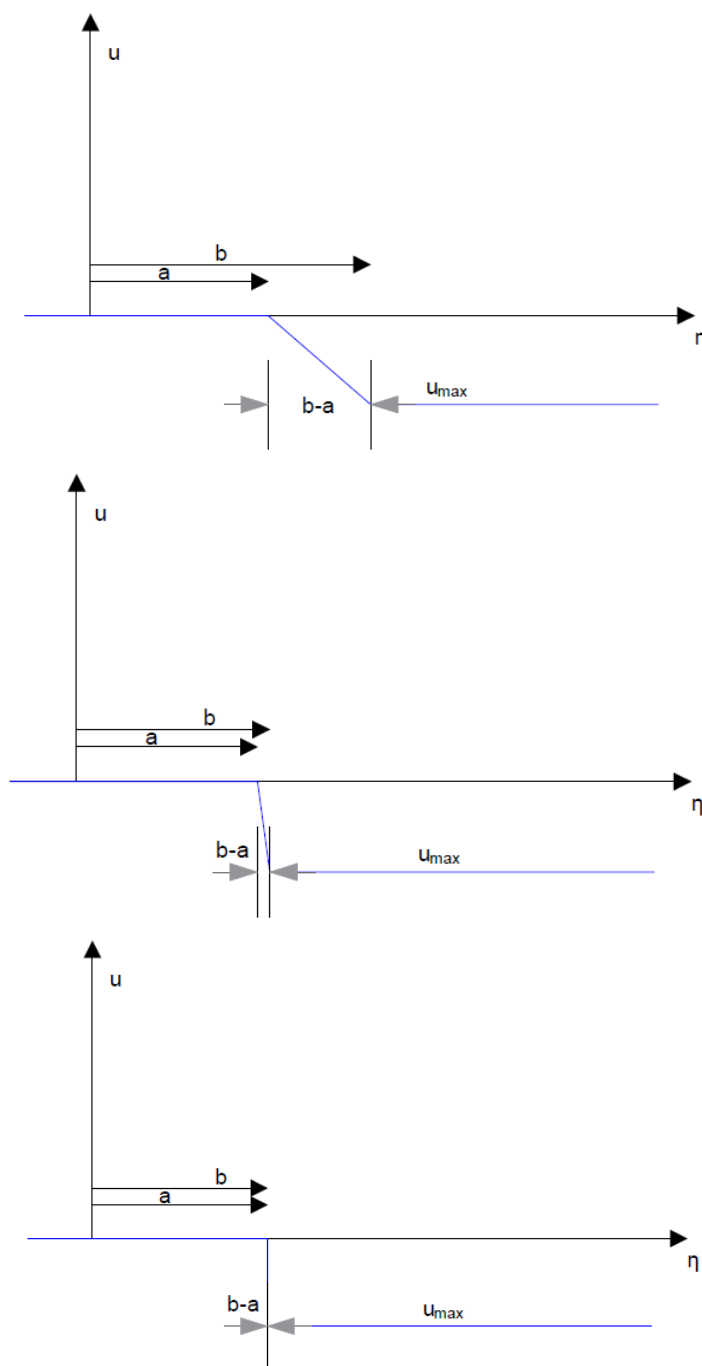


Fig. 43. The screw Dislocation.

As the cohesive zone tends to zero, a mechanical dislocation is created. This dislocation is also called screw dislocation.

The relation of the polarization for the linear case can be given by 23:

$$P_3(\eta) = c_1 * e^{+\frac{\eta}{\sqrt{A}}} + c_2 * e^{-\frac{\eta}{\sqrt{A}}} + \frac{B}{2 * \sqrt{A}} * \frac{u_{max}}{b-a} * \left[ -e^{+\frac{\eta-a}{\sqrt{A}}} * H(\eta-a) + e^{-\frac{\eta-a}{\sqrt{A}}} * H(\eta-a) + e^{+\frac{\eta-b}{\sqrt{A}}} * H(\eta-b) - e^{-\frac{\eta-b}{\sqrt{A}}} * H(\eta-b) \right]$$

The term  $b - a$  is in the numerator of the relations, however when  $b$  is close to  $a$ , also the numerator gets equal to zero. There are two ways to calculate the polarization in a screw dislocation. The first one is by considering the new function that describes this displacement, while the second one is by calculating the limit of the polarization when  $b \rightarrow a$ .

The new function that describes the displacements is the following:

$$u_3(\eta) = u_{max} * H(\eta - a)$$

The value of the displacement for  $a = \eta$  is either zero or  $u_{max}$  or something in between, however in no case there is a continuity of the displacement. The derivatives of the displacements are the following:

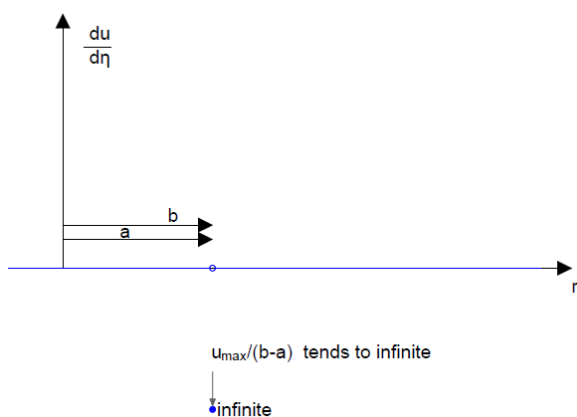


Fig. 44. The first derivative of the displacement. The gradient of the displacement can be given via the below formula that is described the sketch.

$$\frac{\partial u_3(\eta)}{\partial \eta} = u_{max} * \delta(\eta - a)$$

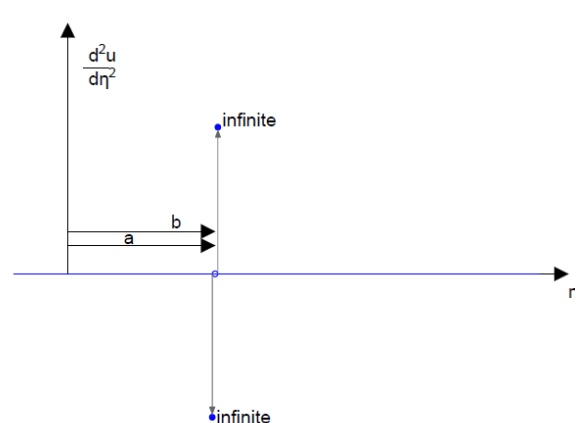


Fig. 45. The second derivative of the displacement.

The second derivative is described by the following relation.

$$\frac{\partial^2 u_3(\eta)}{\partial \eta^2} = u_{max} * \delta'(\eta - a)$$

This is also the relation that will be inserted to the solution of the differential equation.

By substituting the second derivative of the displacement in relation 29 the polarization takes the following form:

$$P_3(\eta) = c_1 * e^{+\frac{\eta}{\sqrt{A}}} + c_2 * e^{-\frac{\eta}{\sqrt{A}}} + \frac{B}{2 * \sqrt{A}} * \left[ -e^{+\frac{\eta}{\sqrt{A}}} * \int e^{-\frac{\eta}{\sqrt{A}}} * \frac{d^2 u_3}{d\eta^2} d\eta \right. \\ \left. + e^{-\frac{\eta}{\sqrt{A}}} * \int e^{+\frac{\eta}{\sqrt{A}}} * \frac{d^2 u_3}{d\eta^2} d\eta \right]$$

$$P_3(\eta) = c_1 * e^{+\frac{\eta}{\sqrt{A}}} + c_2 * e^{-\frac{\eta}{\sqrt{A}}} + \frac{B}{2 * \sqrt{A}} * \left[ -e^{+\frac{\eta}{\sqrt{A}}} * \int e^{-\frac{\eta}{\sqrt{A}}} * u_{max} * \delta'(\eta - a) d\eta \right. \\ \left. + e^{-\frac{\eta}{\sqrt{A}}} * \int e^{+\frac{\eta}{\sqrt{A}}} * u_{max} * \delta'(\eta - a) d\eta \right]$$

However:

$$\int e^{-\frac{\eta}{\sqrt{A}}} * u_{max} * \delta'(\eta - a) d\eta = e^{-\frac{\eta}{\sqrt{A}}} * u_{max} * \delta(\eta - a) + \frac{e^{-\frac{\eta}{\sqrt{A}}} * u_{max}}{\sqrt{A}} \Big|_{\eta=a} * H(\eta - a) \\ = e^{-\frac{\eta}{\sqrt{A}}} * u_{max} * \delta(\eta - a) + \frac{e^{-\frac{a}{\sqrt{A}}} * u_{max}}{\sqrt{A}} * H(\eta - a)$$

And the other integral:

$$\int e^{+\frac{\eta}{\sqrt{A}}} * u_{max} * \delta'(\eta - a) d\eta = e^{+\frac{\eta}{\sqrt{A}}} * u_{max} * \delta(\eta - a) - \left. \frac{e^{\frac{\eta}{\sqrt{A}}} * u_{max}}{\sqrt{A}} \right|_{\eta=a} * H(\eta - a)$$

$$= e^{+\frac{\eta}{\sqrt{A}}} * u_{max} * \delta(\eta - a) - \frac{e^{\frac{a}{\sqrt{A}}} * u_{max}}{\sqrt{A}} * H(\eta - a)$$

By substituting those:

$$P_3(\eta) = c_1 * e^{+\frac{\eta}{\sqrt{A}}} + c_2 * e^{-\frac{\eta}{\sqrt{A}}} + \frac{B}{2 * \sqrt{A}} * \left[ -u_{max} * \delta(\eta - a) - \frac{e^{+\frac{\eta-a}{\sqrt{A}}} * u_{max}}{\sqrt{A}} * H(\eta - a) \right. \\ \left. + u_{max} * \delta(\eta - a) - \frac{e^{-\frac{\eta-a}{\sqrt{A}}} * u_{max}}{\sqrt{A}} * H(\eta - a) \right]$$

$$P_3(\eta) = c_1 * e^{+\frac{\eta}{\sqrt{A}}} + c_2 * e^{-\frac{\eta}{\sqrt{A}}} - \frac{B * u_{max}}{2 * A} * \left\{ e^{+\frac{\eta-a}{\sqrt{A}}} + e^{-\frac{\eta-a}{\sqrt{A}}} \right\} * H(\eta - a) \quad 27$$

The second way to calculate the relation of the polarization for the screw dislocation is by calculating the limit:

$$\lim_{b \rightarrow a} P_3(\eta) = \lim_{b \rightarrow a} P_{3, \text{homogeneous}} + \lim_{b \rightarrow a} P_{3, \text{partial}}$$

$$\lim_{b \rightarrow a} P_3(\eta) = c_1 * e^{+\frac{\eta}{\sqrt{A}}} + c_2 * e^{-\frac{\eta}{\sqrt{A}}} + \frac{B * u_{max}}{2 * \sqrt{A}} * \lim_{b \rightarrow a} R \quad \text{xvii}$$

Where  $R = \left[ \left\{ -e^{+\frac{\eta-a}{\sqrt{A}}} + e^{-\frac{\eta-a}{\sqrt{A}}} \right\} * H(\eta - a) + \left\{ +e^{+\frac{\eta-b}{\sqrt{A}}} - e^{-\frac{\eta-b}{\sqrt{A}}} \right\} * H(\eta - b) \right] / [b - a]$ . This limit has the form 0/0 and thus, the theorem of D' L' Hospital can be applied.

$$\lim_{b \rightarrow a} R = \lim_{b \rightarrow a} \frac{\partial \left[ \left\{ -e^{+\frac{\eta-a}{\sqrt{A}}} + e^{-\frac{\eta-a}{\sqrt{A}}} \right\} * H(\eta - a) + \left\{ +e^{+\frac{\eta-b}{\sqrt{A}}} - e^{-\frac{\eta-b}{\sqrt{A}}} \right\} * H(\eta - b) \right]}{\partial b}$$

$$= \lim_{b \rightarrow a} \left[ \left\{ \frac{-e^{+\frac{\eta-b}{\sqrt{A}}} - e^{-\frac{\eta-b}{\sqrt{A}}}}{\sqrt{A}} \right\} * H(\eta - b) + \left\{ +e^{+\frac{\eta-b}{\sqrt{A}}} - e^{-\frac{\eta-b}{\sqrt{A}}} \right\} * \delta(\eta - b) \right]$$

And by substituting into relation xvii:

$$\lim_{b \rightarrow a} P_3(\eta) = c_1 * e^{+\frac{\eta}{\sqrt{A}}} + c_2 * e^{-\frac{\eta}{\sqrt{A}}} - \frac{B * u_{max}}{2 * A} * \left\{ e^{+\frac{\eta-\alpha}{\sqrt{A}}} + e^{-\frac{\eta-\alpha}{\sqrt{A}}} \right\} * H(\eta - \alpha)$$

$$+ \frac{B * u_{max}}{2 * \sqrt{A}} * \left\{ e^{+\frac{\eta-\alpha}{\sqrt{A}}} - e^{-\frac{\eta-\alpha}{\sqrt{A}}} \right\} * \delta(\eta - \alpha)$$

28

The second term of this relation is a spike term and if for any reason (e.g. [Appendix E](#)), we can erase it, then the polarization can be expressed in both ways the same. However, by ignoring this spike, there is a step in the diagram of the polarization, as it was also in the displacement.

As for the constants  $c_1$  and  $c_2$ , the boundary condition that should be used are referring to the infinities, where the polarization should be zero.

This way:

$$c_1 = \frac{B * u_{max}}{2 * A} * e^{-\frac{\alpha}{\sqrt{A}}}$$

29

$$c_2 = 0$$

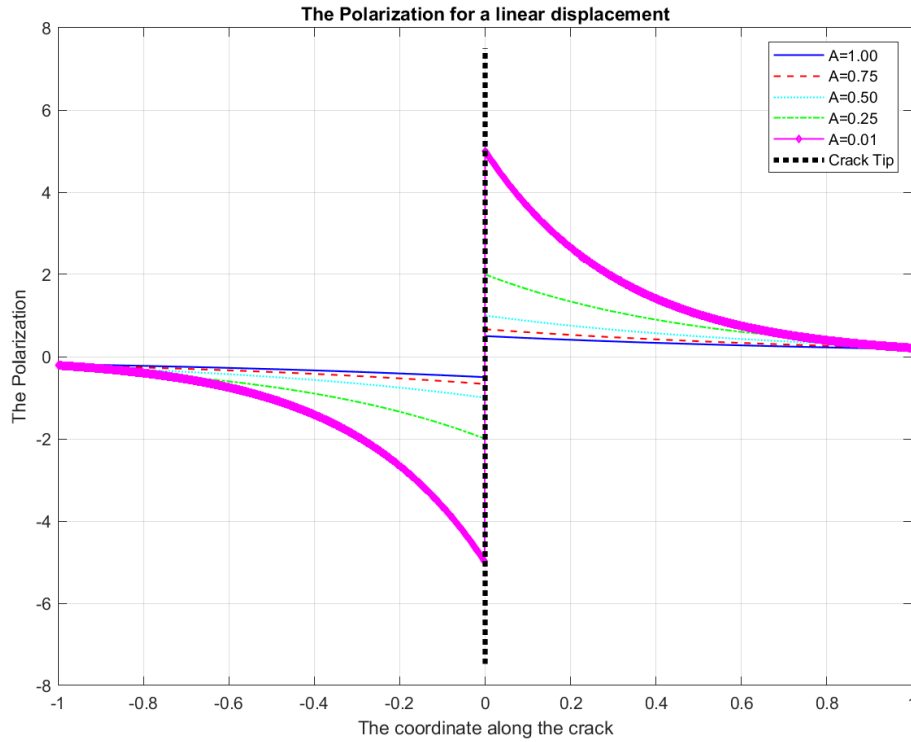


Fig. 46. The polarization for a screw dislocation.

There is an obvious discontinuity of the polarization on the crack tip, which is also the end of the cohesion zone. Comparing this with the case when  $a - b \neq 0$ , the diagram looks the same, with the difference that there is no curve fitting between maximum and minimum polarization. This procedure happens in contradiction with the step, instead of a continuous smooth way. As it seems a spike could also occur at this point.

By considering that the point  $a$  is the characteristic coordinate of the crack tip, while the characteristic axis is defined by the crack, we can substitute  $a$  with zero, as the crack tip is the beginning of the characteristic axis. Then relation 28 transforms to the following:

$$P_3(\eta) = c_1 * e^{+\frac{\eta}{\sqrt{A}}} + c_2 * e^{-\frac{\eta}{\sqrt{A}}} - \frac{B * u_{max}}{2 * A} * \left[ \left\{ e^{+\frac{\eta}{\sqrt{A}}} + e^{-\frac{\eta}{\sqrt{A}}} \right\} * H(\eta) - \left\{ e^{+\frac{\eta}{\sqrt{A}}} - e^{-\frac{\eta}{\sqrt{A}}} \right\} * \sqrt{A} * \delta(\eta) \right]$$

Actually, this relation is the one plotted in the figure above, as it has been considered that the value of point  $a$  is zero.

## 5. Dispersion relation on produced waves

### A. The existence of waves

The flexoelectric problem that is currently being studied is an anti-plane dynamic problem. The previous chapters reveal, that the anti-plane problem with flexoelectricity is the same with the anti-plane problem when the theory of couple stress elasticity is used. However, as the problem of the propagation of cracks is a dynamic problem, waves can be emitted from the crack toward the free surface.

Moroni et al. (2014) as revealed in [Giannakopoulos and Zisis \(2019\)](#) commented on those theories by revealing that Rayleigh waves of high frequency may be produced. Those waves ought to limit the velocity of the crack to a Rayleigh wave speed  $c_R$ . This velocity is relative to the parameter  $\beta$  of the couple stress theory and for  $\beta = 0$ , when the problem is hyperbolic, Rayleigh waves can appear. Similar to the couple stress elasticity, flexoelectricity can exist simultaneously with those waves.

Any material with discrete atomic structure of crystals, as flexoelectric materials are, is not only a medium in which the waves can propagate, but also a medium in which they can disperse. The addition of the phenomenon of the dispersion, to a ferroelectric phenomenon like flexoelectric, seems to be extremely beneficial. Through the phenomenon of dispersion a lot of applications are accessible, the most common is the total recognition of the material through the use of various devices (spectrometers).

The dynamic nature of the problem is responsible for a vibration, which produces waves that move through the material. The frequency and the arc length (wavenumber) of the wave can be calculated by the differential equation that describes the problem.

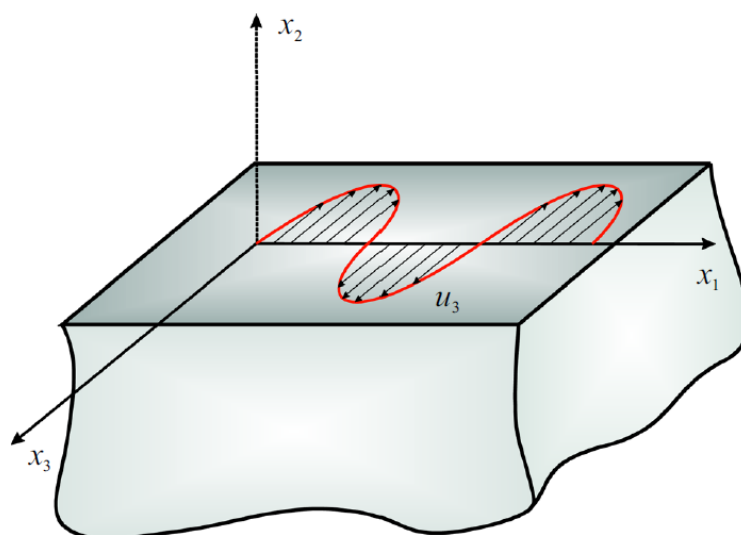


Fig. 47. The development of anti-plane surface waves.

This figure was obtained from [Giannakopoulos and Zisis \(2021 a\)](#).

Giannakopoulos and Zisis (2019) proposed as a displacement for the differential equation 2 (the governing equation in respect of displacement) a solution of the below form:

$$u_3 = \bar{u}_3 e^{-i\omega t} e^{ik(n_1 x_1 + n_2 x_2)}$$

The quantities  $n_1$  and  $n_2$  are the coordinates of an in-plane unit vector with the direction of the travelling wave, that was assumed.

By importing this into relation 2, the dispersion relation, which is displayed beneath, can be extracted. Relative to the wave's dispersion, there are also the phase velocity and the group velocity, all of which are going to be studied later.

$$\omega^2 = k^2 c_s^2 \left(1 + \frac{l^2}{2} k^2\right) \left(1 + \frac{H^2}{12} k^2\right)^{-1} \quad 30$$

In the above relation,  $\omega$  [ $s^{-1}$ ] is the frequency  $k$  [ $ms^{-1}$ ] is the wavenumber  $c_s$  is the shear wave velocity,  $l$  the microstructural length and  $H$  the micro-inertial.

The microstructural and the micro-inertial terms concern the couple elasticity problem. However, some variables appear in the flexoelectric problem also and by reverting the substitution, proposed by relations 4 and 5, the dispersion relation for the anti-plane flexoelectric problem can have the following form:

$$\omega^2 = \frac{k^2}{\rho} \left( \frac{a\mu + ((b_{44} + b_{77})\mu - (e_{44} - f_{12})^2 k^2)}{a + (b_{44} + b_{77})k^2} \right) \quad 31$$

The dispersion occurs because of the microstructure, the ratio between the microstructural and the microinertia length. For no dispersion, the ratio  $l/H$  should be equal to  $1/\sqrt{6}$ . For greater flexoelectric effect, the ratio between the microstructural and the micro-inertial length should be less than  $1/\sqrt{6}$ . Concerning flexoelectricity, this is the limit of the normal dielectrics while  $l/H > 1/\sqrt{6}$  is equivalent to metamaterials. This case will be studied later too.

For such a low ratio ( $< 1/\sqrt{6}$ ) the phase velocity decreases with the wavenumber and a lattice type of dispersion is produced (Giannakopoulos and Zisis (2019)).

Dispersion can also be considered through the equation of the polarization, (relation 3). That wave would not transfer mass but energy. For this type of dispersion, the optical dispersion, the polarization should be considered of the below form:



$$P_3 = S_p \bar{u}_3 e^{-i\omega t} e^{ik(n_1 x_1 + n_2 x_2)}$$

The equation that relates the wavenumber and the frequency, produced from the above consideration, is the following:

$$\omega^2 = c_s^2 \frac{-a}{e_{44} - f_{12}} S_p \left( 1 + \frac{l^2}{2} k^2 \right) \quad 32$$

Giannakopoulos and Zisis (2019) named this equation “dispersion-like” relation and consider it acceptable for a soft mode optical dispersion. In order for the frequencies to be real, the term  $-a(e_{44} - f_{12})S_p$  should be positive. This relation can also be written as follows, considering  $c_s^2 S_p (-a/\{e_{44} - f_{12}\}) = \Omega_0^2$  and  $c_s^2 (-a/\{e_{44} - f_{12}\}) S_p (l^2/2) = \Lambda$ .

$$\omega^2 = \Omega_0^2 + \Lambda k^2$$

The dispersion relation is not fully analogue as it makes a shifting because of the constant term  $\Omega_0^2$ , which in many cases can be enormous (terahertz).

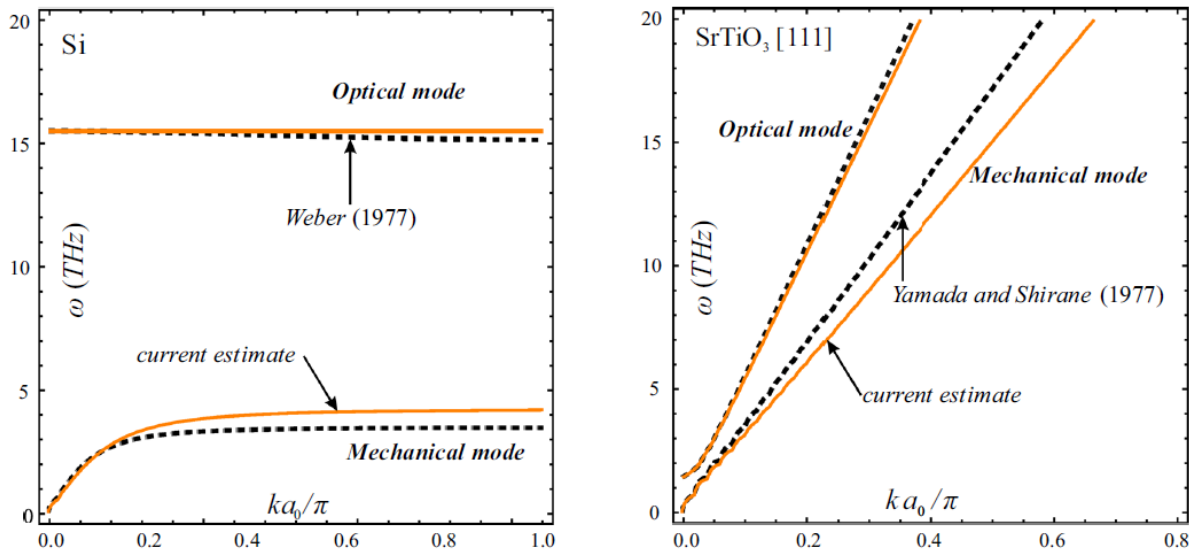


Fig. 48. The Dispersion relation for two different materials.

The “current estimate” represents the estimate of Giannakopoulos and Zisis (2021 a). Note that for some materials like the silicone, the constant term  $\Omega_0^2$  is extremely large. This figure was obtained from the research of Giannakopoulos and Zisis (2021 a).

This second dispersion, the optical dispersion, is connected with flexoelectricity in contradiction to the first one which is more acoustic like. [Giannakopoulos and Zisis \(2019\)](#) also suggested, that in the crack faces, Bluestein-Gulyaev waves may appear. Those waves have been found both experimentally and theoretically concerning the piezoelectric effect.

In a later research, the same authors, [Giannakopoulos and Zisis \(2021 a.\)](#) showed that Rayleigh waves can appear in any hyperbolic case and they are dispersive. They assumed a Rayleigh type of surface wave with velocity equal to  $c_R = \omega / k$ , that spreads from the crack tip, with a possible displacement:

$$u_3(x_1, x_2, t) = (Ae^{-ax_2/l} + Ae^{-\beta x_2/l})e^{i(kx_1 - \omega t)}$$

The parameters  $a$  and  $\beta$  should be only positive ( $a > 0$ ,  $\beta > 0$ ).

By replacing this displacement to the equation 2, the governing equation for the out-of-plane displacement in the anti-plane flexoelectric problem is reduced to the following:

$$\mu \nabla^2 u_3 - \mu \frac{l^2}{2} \nabla^4 u_3 = \rho \ddot{u} - \frac{\rho H^2}{12} \nabla^2 \ddot{u}_3$$

$$a^4 + A_1 a^2 + A_2 = 0$$

$$\beta^4 + A_1 \beta^2 + A_2 = 0$$

As it seems, the equations are similar for the parameter  $a$  and  $\beta$ . The calculation of those, which are the same, depends on the parameters  $A_1$ ,  $A_2$ , which are the following:

$$A_1 = -\frac{2}{l^2} \left[ a + \left( \frac{1}{m_R^2} - \frac{H^2}{12l^2} \right) \frac{\omega^2 l^2}{c_s^2} \right]$$

$$A_2 = \frac{2}{l^4} \left[ \left( \frac{1}{m_R^2} - \frac{H^2}{6l^2} \right) \frac{\omega^4 l^4}{m_R^2 c_s^2} - 2 \left( 1 - \frac{1}{m_R^2} \right) \frac{\omega^2 l^2}{c_s^2} \right]$$

while  $m_R = c_R / c_s$ .

Moroni et al. (2014) suggested a region called “sub-Rayleigh zone” in which  $(H^2 m_R^2) / (12l^2) < 1$  and  $m_R < 1$ . For those two conditions as it seems the parameters  $a$  and  $\beta$  are real. The same authors also named the region in which  $(H^2 m_R^2) / (12l^2) \geq 1$  and  $m_R \geq 1$  “super-Rayleigh zone”.

Giannakopoulos and Zisis (2021 a.) considered as boundary conditions the traction of the dipolar force condition at the surface of the crack.

$$\left\{ \begin{array}{l} t_3(x_1, 0) = 0 \\ u_{3,22}(x_1, 0) = 0 \end{array} \right.$$

$$\left\{ \begin{array}{l} u_{3,2}(x_1, 0) - \frac{l^2}{2} \left[ \left( 2 - \frac{H^2 V^2}{6l^2 c_s^2} \right) u_{3,112} + u_{3,222} \right] = 0 \\ u_{3,22}(x_1, 0) = 0 \end{array} \right.$$

From these boundary conditions the authors extracted the dispersion relation for this case. By assuming a boundary condition in infinity, e.g.  $\omega \rightarrow \infty$  ( $k^2 l^2 \rightarrow \infty$ ) a solution of the displacement occurs.

$$u_3(x_1, x_2, t) = B \left[ e^{-\sqrt{\left(1 - \frac{H^2}{6l^2} m_R^2\right) x_2 k^2 l} - \left(1 - \frac{H^2}{6l^2} m_R^2\right) e^{-x_2 k^2 l}} \right] e^{i(kx_1 - \omega t)}$$

In contrast, if the boundary condition near zero is assumed,  $\omega \rightarrow 0$  ( $k^2 l^2 \rightarrow 0$ ), the displacement is then described by the beneath expression:

$$u_3(x_1, x_2, t) = B \left[ \frac{1}{3} e^{-\frac{\sqrt{2} x_2}{l}} + 1 \right] e^{i(kx_1 - \omega t)}$$

Further details can be found in [Giannakopoulos and Zisis \(2021 a.\)](#)

In addition to [Giannakopoulos and Zisis \(2019, 2021 a, b\)](#), a lot of other researchers studied the dispersion of waves. [Yang et al. \(2018\)](#) studied the case of gradient elasticity, which has been shown multiple times that it is analogue to the flexoelectric anti-plane problem as the Lamb waves are concerned.

They mention for both those cases, the case of the flexoelectric material and the case of the gradient elasticity, that a special study should be made, while for large wavenumbers, both the dispersion relations and the phase velocity are significantly depended. They concluded that both flexoelectricity and strain gradient elasticity depend on the wave number (they prove that both piezoelectricity and flexoelectricity are important in the propagations of Lamb waves when the wavenumber is large, in contradiction to a small wavenumber in which those effects are unimportant), the material properties and the thickness of the plate.

The authors suggested that it is only natural one wave that transfers mass (acoustic wave) to produce strains and strain gradients and thus polarization, in the direction of the propagation and in the out-of-plane direction. Between the polarization and the strain gradient there is a coupling: The converse flexoelectric effect transforms the polarization to strain gradient, while the direct transforms the strain gradient to polarization. As the strain gradients are increased with the increase of the wavenumber, phenomena related to those increase as well (the polarization through the effect of flexoelectricity).

Studies have been made involving different types of waves. Most recently, Shengping Shen and his co-workers studied love waves, and the dispersion of Rayleigh waves, by also combining them with flexoelectricity (Qian Deng et al. (2020), Yang et al. (2020))

## B. Dispersion Relations of frequency

Starting from a waveform of various waves, while each wave has its own wavenumber, some waves will go faster and some slower. The dispersion in any case seems to be greatly influenced by the ratio of two lengths, the microstructural and the micro-inertial length as it can be seen from relation 30, 32. For various possibilities of this ratio from zero, which is a lower bound, to  $1/\sqrt{6}$ , which is the upper bound (for normal dielectrics at least), some relations considering the wavenumber and the frequency or velocity were plotted. It is necessary to mention that there is a little difference in the mechanical wave relation and the optical, which is like the polarization.

The mechanical frequency is described by relation 30. This relation can be simplified by considering the microstructural length  $l_b = l/\sqrt{2}$  (the same Zisis (2018) proposed) and the micro-inertial length  $h = H/\sqrt{12}$ .

Obviously as it was mentioned in the third chapter, a positive electrical susceptibility, (normal materials) suggest that  $l_b/h < 1$ . Also, this ratio should be positive, as both constants are positive. This way relation 30 transforms to the following:

$$\omega^2 = k^2 c_s^2 (1 + l_b^2 k^2) (1 + h^2 k^2)^{-1}$$

From this point on and until the end of this chapter, the microstructural length  $l_b$  will be symbolized for simplicity purposes as  $l$ . Considering  $\bar{k} = k * h$  and  $\bar{\omega} = \bar{\omega}_{mechanical} = \omega * h/c_s$  the above relation transforms to the following:

$$\frac{\bar{\omega}^2 c_s^2}{h^2} = \frac{\bar{k}^2}{h^2} c_s^2 \left( 1 + \frac{l^2}{h^2} \bar{k}^2 \right) \left( 1 + \frac{h^2}{h^2} \bar{k}^2 \right)^{-1}$$

And through simplifications the following dispersion relation is produced:

$$\bar{\omega} = \bar{k} \sqrt{\frac{1 + \bar{k}^2 (l/h)^2}{1 + \bar{k}^2}}$$

33

For various values of the ratio  $l/h$  the above relation can be plotted.

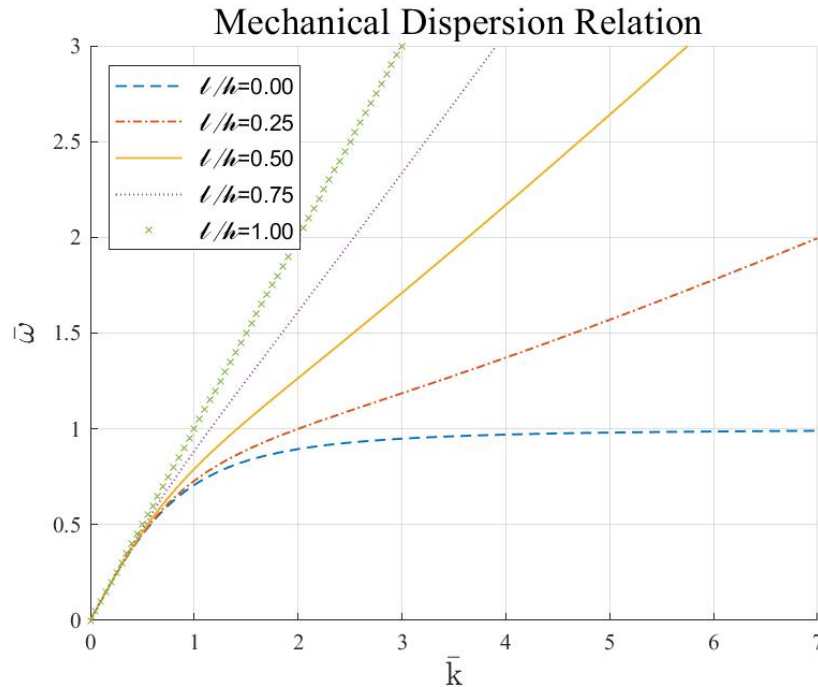


Fig. 49. The frequency as a function of the wavenumber (or the inverse of the arclength) in the mechanical waves.

The dispersion occurs for wavenumbers greater than half. As the microstructure gets more intense, the ratio of the two lengths, the microstructural and the micro-inertial, tends to zero, the dispersion gets bigger. Note that the two axes represent  $\bar{k} = k * h$  and  $\bar{\omega} = \omega * h/c_s$ .

From this figure the below conclusions can be extracted:

- For small wavenumbers there is no dispersion (lower than 0.5).
- The dispersion increases as the wavenumber increases too.
- The curve seems to tend asymptotically to the linear  $y = (l/h) * x$ . This conclusion can be seen efficiently in some of the next figures.

In all these conclusions someone should keep in mind that the wavenumber is equal to the reverse of the arclength of a wave and the dispersion of those relations is nothing else than the difference of frequency for a specific wavenumber between the cases.

Similar to the mechanical dispersion, the optical dispersion, which is described by relation 32, transforms to the following, when the microstructural and the micro-inertial terms are replaced as described above.

$$\omega^2 = c_s^2 \frac{-a}{e_{44} - f_{12}} S_p (1 + l^2 k^2)$$

Also, by considering  $\bar{k} = k * h$ , and differently from the mechanical case,  $\bar{\omega} = \bar{\omega}_{optical} = (-\omega * \{e_{44} - f_{12}\}^{0.5}) / (c_s * a^{0.5} * S_p^{0.5})$ .

$$\bar{\omega}^2 c_s^2 \frac{-a}{e_{44} - f_{12}} S_p = c_s^2 \frac{-a}{e_{44} - f_{12}} S_p (1 + \bar{k}^2 (l/h)^2)$$

This way, the relation of the optical frequency can be described from the below relation, while the graphic representation is the following:

$$\bar{\omega} = \sqrt{1 + \bar{k}^2 (l/h)^2}$$

34

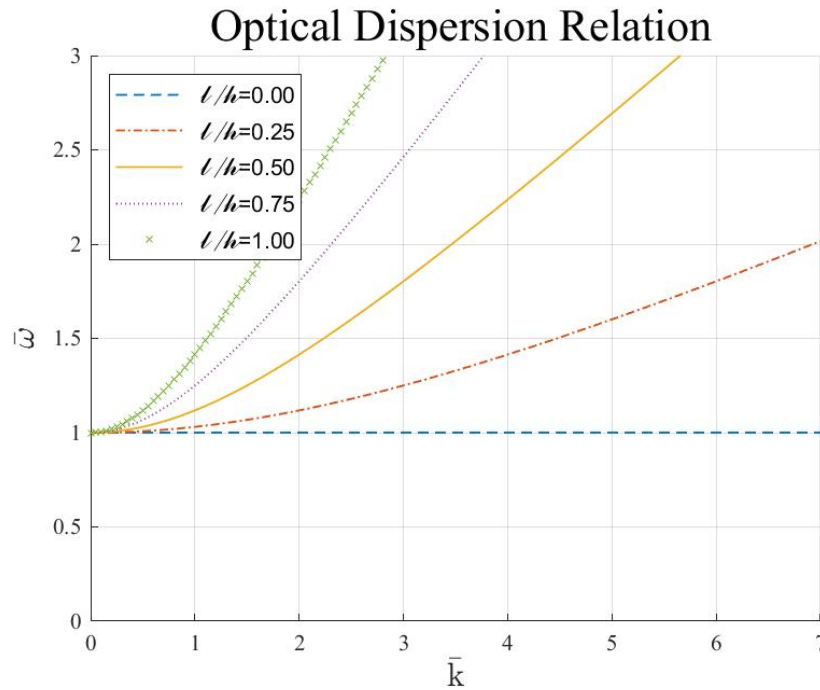


Fig. 50. The frequency as a function of the wavenumber in the optical waves.

There is a cut-off, which means that frequencies lower than the unit cannot occur. The dispersion also in those waves occurs for wavenumber larger than half and gets bigger as the microstructure gets important. Note that the two axes represent  $\bar{k} = k * h$  and  $\bar{\omega} = (-\omega * \{e_{44} - f_{12}\}^{0.5}) / (c_s * a^{0.5} * S_p^{0.5})$ .

In the above figure the conclusions that can be extracted are similar to the ones from the mechanical waves. However, some questions that may occur are about the asymptomatic line, whether it is the same for mechanical and optical waves.

To summarize, initially, it is very important to point out that the mechanical and the optical waves describe entirely different problems. The polarization is a problem that is described by the optical waves. **In the anti-plane flexoelectric problem both waves exist, mechanical and optical.**

As the length of the wave decreases the frequency increases. When the wavenumber is small and so the length of the wave is large, there is a linearity in the curves. It seems that the microstructure is not very important to long waves, as the dispersion typically does not exist. When the wavenumber is big, which means the length of the wave is small, the microstructure plays a significant role because the ratio of the length  $l/h$  becomes as a parameter more important. This ratio is equivalent to the electrical structure and those curves describe the material electrically.

The questions that arise, considering both mechanical and optical waves, concerning the asymptomatic lines, as mentioned, can be answered by isolating the curves for a specific ratio of length e.g. 0.5, 0.25 (fig. 51).

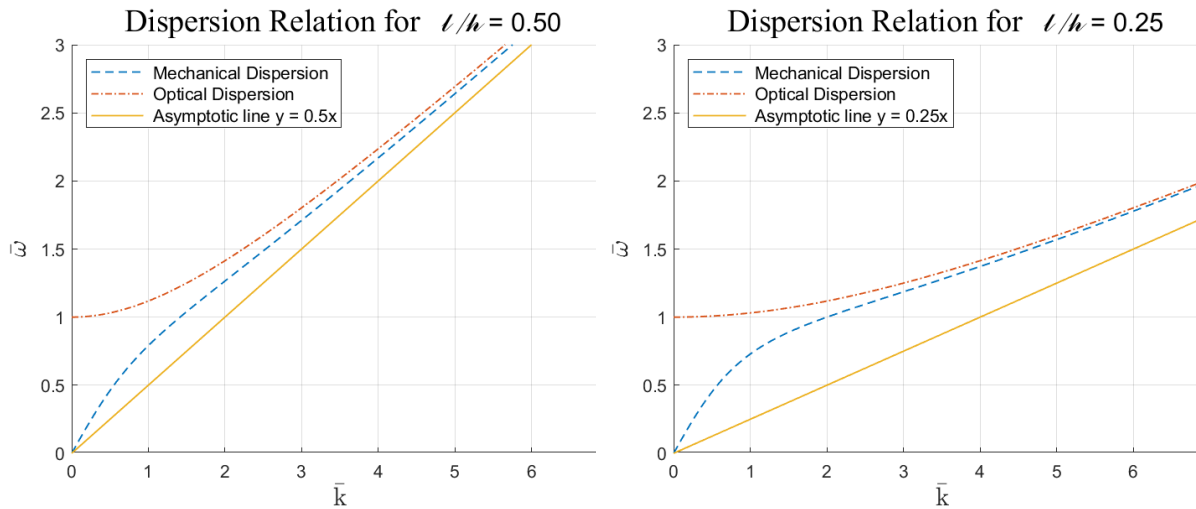


Fig. 51. The frequency as a function of the wavenumber for **ratio = 0.5** and **ratio = 0.25**.

For a specific ratio of lengths equal to half, the frequency of both optical and mechanical waves tends to the asymptotic line  $y = 0.5 * x$  and  $y = 0.25 * x$  respectively. The convergence is being achieved for bigger wavenumbers.

Note that there is a difference in the vertical axis (the frequency in the mechanical dispersion is different than the frequency in the optical):

$$\bar{\omega}_{mechanical} = \omega * \frac{h}{c_s}$$

$$\bar{\omega}_{optical} = \frac{-\omega * \{e_{44} - f_{12}\}^{0.5}}{c_s * a^{0.5} * S_p^{0.5}}$$

In the above diagrams, it is visible that the convergence to the asymptotic actually happens. However, a comment that the mechanical frequency is always smaller than the optical is not

necessarily true, as the two frequencies, the mechanical and the optical are normalized differently.

Interesting is also to see where the convergence happens. But what means “the convergence to happen” is something that in order to be answered, the magnitude of error must be introduced. Usually, the error is a magnitude that shows how much in a percentage the value that was calculated differs from the true value. In our case however, it is not simple to define the calculated and the true value.

Three types of error can be defined:

- The first one is being described by the difference of the two values in absolute, divided by the value of the analytical expression.

$$Error = \frac{|analytical\ value - asymptotic\ value|}{|analytical\ value|} \quad 35$$

- The second is by changing the deviator of the above relation. This time the difference will be divided by the asymptotic value.

$$Error = \frac{|analytical\ value - asymptotic\ value|}{|asymptotic\ value|}$$

Those two values of error are close, considering that the nominator is considerably small and the deviator is almost the same.

- In some cases, where these values, which are more or less the same, tend to zero, there is a problem in the deviator, which is almost equal to the nominator. This problem can easily be bypassed by moving the axis to some other value, e.g. 1. This means that, from that point on the error will be calculated not from how close the difference is to zero, but how close to one is the difference from one. The expression of this kind of error can be written as beneath:

$$Error = \frac{|(analytical\ value + 1) - (asymptotic\ value + 1)|}{|asymptotic\ value + 1|} \quad 36$$

Here, again, there is a dilemma about the deviator. Should it be the the asymptotic value, or the numerical value. However, the result in any case should be almost the same.

In the current project, the first definition of error was used. In cases that one of those numbers was very small, the third definition was used, with the asymptotic value as deviator.

By using these definitions of error, the following diagrams are possible.

Those diagrams show the speed of the convergence to the asymptotic line. As it seems, for smaller ratios of lengths, greater wavenumber are necessary for convergence to the asymptotic line.

Interesting is the behavior near zero, which can be seen considering a value that tends to zero and the value of zero. In this case also, the first type of error was used.



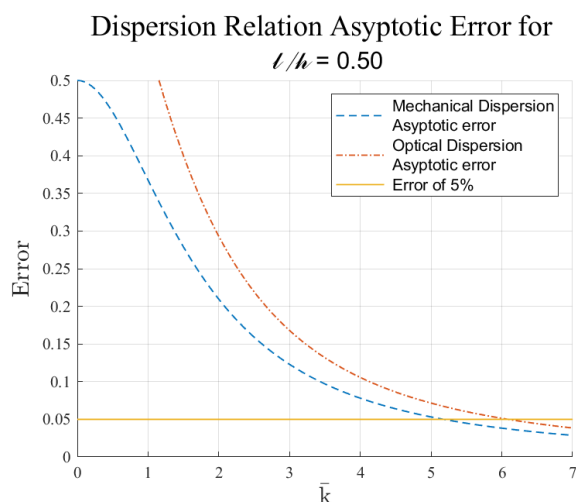


Fig. 52. The percentage of divergence of the analytical from the asymptotic value, for **ratio = 0.5**.

The asymptotic line is described by the relation  $y = 0.5 * x$ . The convergence occurs for a wavenumber between 5 and 6, for an eligible error equal to 5%. Also, it seems that the mechanical wave converges “faster” (for lower wavenumber) than the optical.

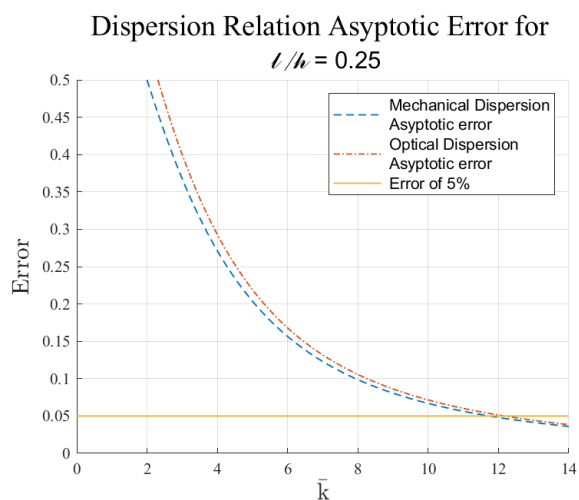


Fig. 53. The percentage of divergence of the analytical from the asymptotic value, for **ratio = 0.25**.

The asymptotic line is described by the relation  $y = 0.25 * x$ . The convergence occurs for a wavenumber between 11 and 12, for an eligible error equal to 5%. The ratio of the lengths is crucial for the convergence. The smaller the ratio, the larger the wavenumber in which the convergence occurs.

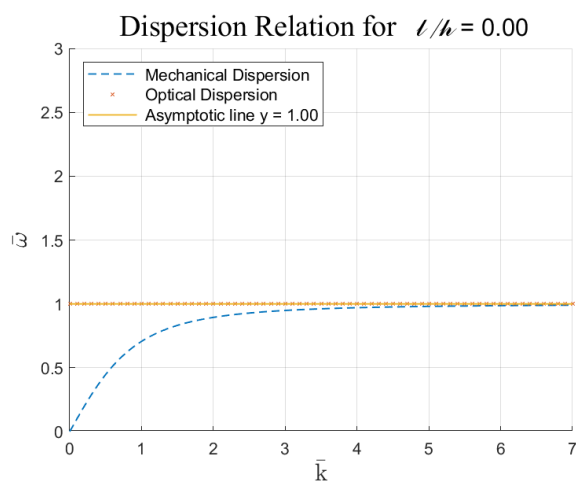


Fig. 54. The frequency as a function of wavenumbers for **ratio = 0**.

The asymptotic line seems to be the line  $y = 1$  and the convergence happens considerably “faster” than a case with a ratio that tends to zero

However, the asymptotic line should be  $y = 0$ . Those two lines theoretically intersect to infinity, where the actual convergence should occur.

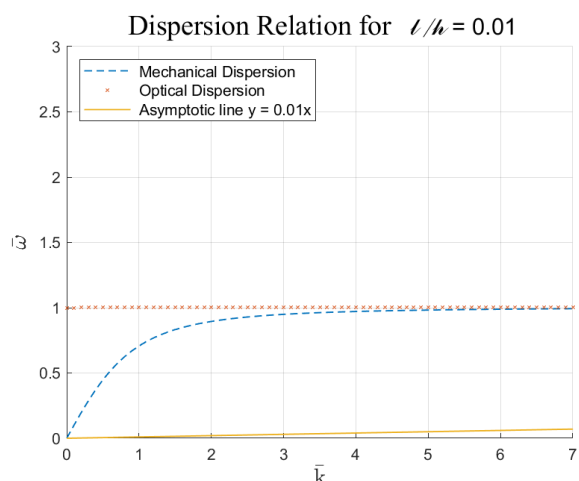


Fig. 55. The frequency as a function of wavenumbers for **ratio  $\rightarrow 0$  (0.01)**

The asymptotic line seems to be the line  $y = 0.01 * x$  and the convergence doesn't seem to happen for usual wavenumbers.

The case, when the ratio tends to zero is a theoretical case and should be treated with special care.

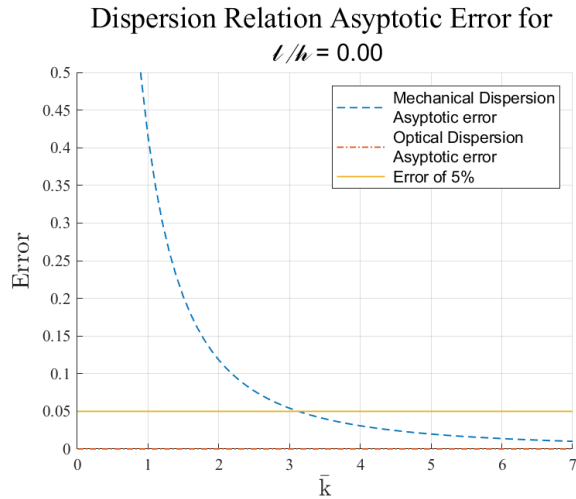


Fig. 56. The percentage of divergence of the analytical from the asymptotic value, for **ratio = 0.0**.

The asymptotic line was considered  $y = 1$ . The mechanical frequency convergences for a considerably small wavenumber, while the optical frequency converges immediately.

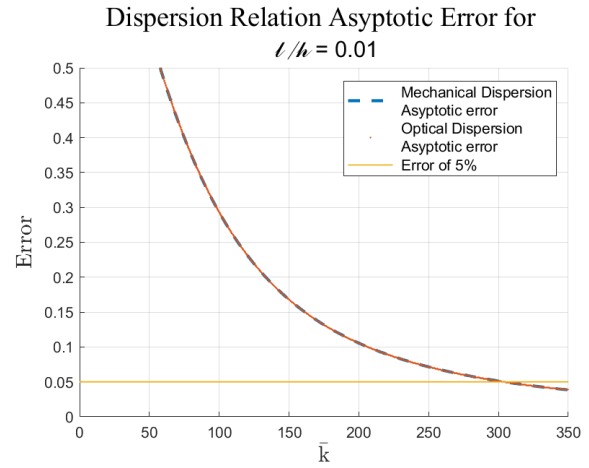


Fig. 57. The percentage of divergence of the analytical from the asymptotic value, for **ratio = 0.01**.

The asymptotic line was considered  $y = 0.01 * x$ . The convergence happens for a considerably big wavenumber, that could tend to infinity both for the mechanical and the optical frequency.

The asymptotic line is normally the line  $y = 0$ . However, the line  $y = 1$  is just a parallel of that. Typically, the interception of two parallels will happen to infinity, as the last figure (fig. 57) tends to reveal. However, by using a different definition of the asymptotic line (fig. 56), the convergence will happen for a very small wavenumber. The case when the ratio becomes zero is a limit case and should be treated with special care.

In addition to those diagrams, a combination can be considered, of the ratio of lengths and the wavenumber, in which the asymptotic line and the analytic values have just converged. With an  $\bar{\omega} = f(\bar{k}, l/h)$ , where  $\bar{\omega}$  is the frequency, a relation in which the error is equal to a specific value e.g. 5% can be calculated. This explicit function, that is shown beneath can be plotted.

$$g(\bar{k}, l/h) = \frac{\bar{\omega}_{numerical} - \bar{\omega}_{asymptotic}}{\bar{\omega}_{numerical}} - Error = 0 \quad 37$$

and by assuming a legit area of error less than e.g. 5%, it is possible to choose whether the result can be obtained by the asymptotic line, instead of the analytical relation, for an error less or equal to 5%. That area can be seen in the beneath diagram:

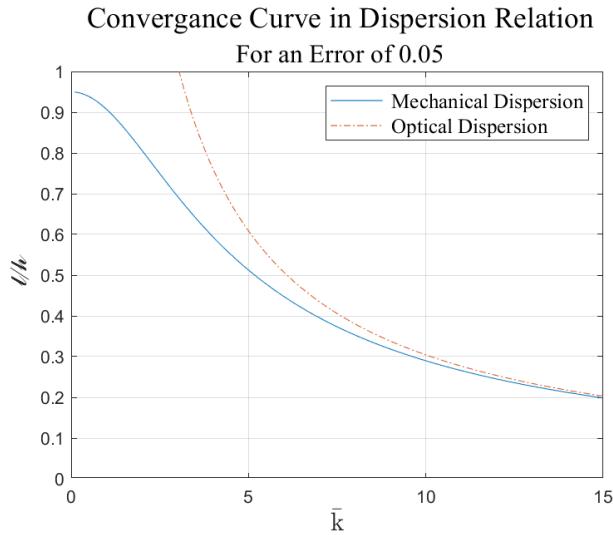


Fig. 58. Dispersion convergence to 5% error. The curve that describes the combination of the wavenumber and the ratio of length, so the divergence from the asymptotic line gives an error equal to 5%, for the mechanical and the optical frequency.

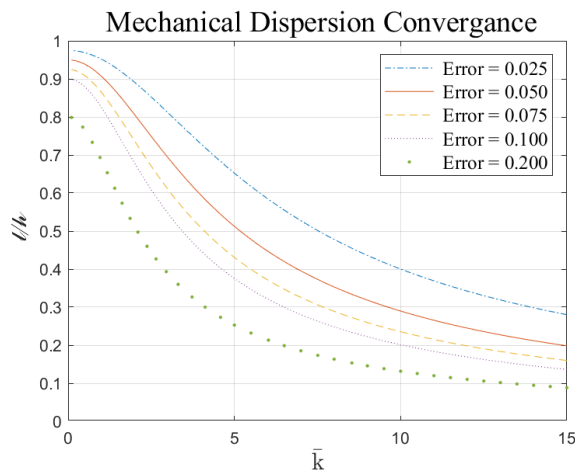


Fig. 59. Mechanical dispersion convergence. The curves that describe the combination of the wavenumber and the ratio of lengths, so the divergence could be legit, for the mechanical dispersion.

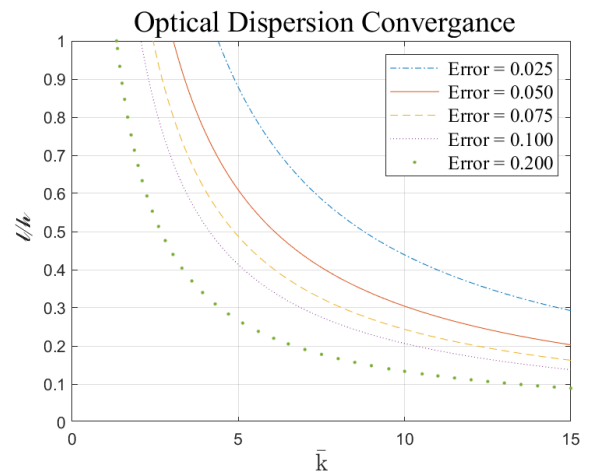


Fig. 60. Optical dispersion convergence. The curves that describe the combination of the wavenumber and the ratio of lengths, so the divergence could be legit, for the optical dispersion.

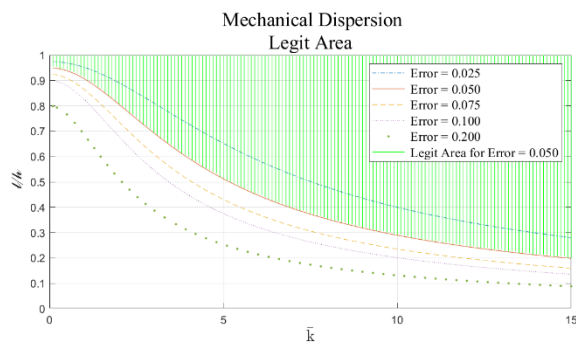


Fig. 61. Legit area for mechanical waves

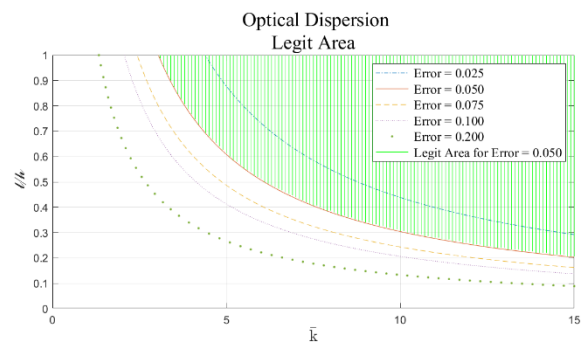


Fig. 62. Legit Area for optical waves.

The area in which the relation of dispersion and the relation of the asymptotic line are the same (error 5%) in the mechanical waves.

Combination of wavenumber and microstructure that reside in this “legit area” will give almost the same frequency by using either the analytical expression or the asymptotic line.

The area in which the relation of dispersion and the relation of the asymptotic line are the same (error 5%) in the optical waves.

### C. Phase Velocity

By multiplying the frequency with the arc length, something that has the dimension of the velocity is produced. This way it is possible to extract from the above relations the velocity of the mechanical and optical waves in relation with the wavenumber for various microstructural cases.

The relation that describes the mechanical phase velocity, symbolized by the term  $\bar{\omega}/\bar{k}$ , is the below:

$$\bar{\omega}/\bar{k} = \sqrt{\frac{1 + \bar{k}^2 * (l/h)^2}{1 + \bar{k}^2}}$$

38

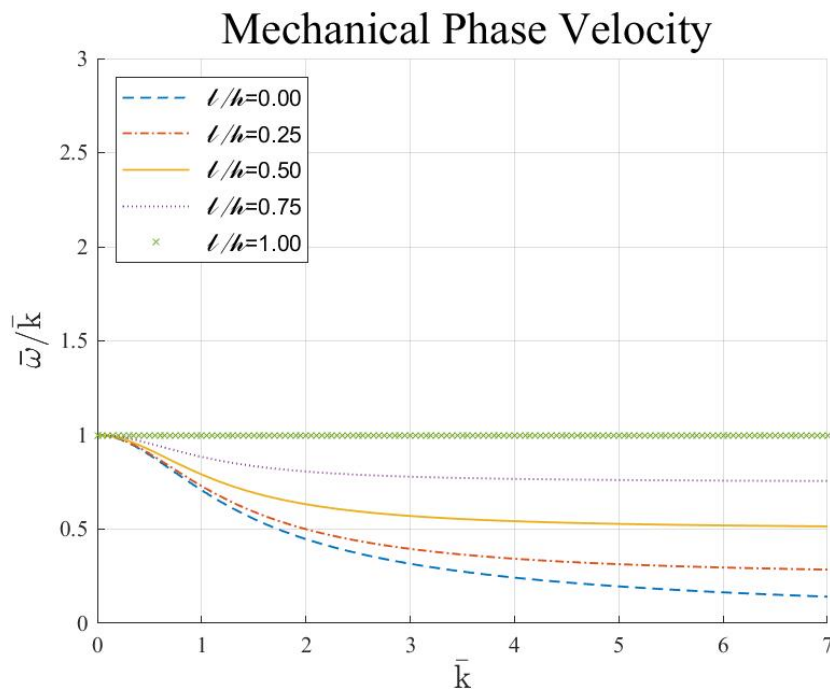


Fig. 63. The phase velocity of the mechanical waves as a function of the wavenumber of each wave.

The dispersion is being transferred in the phase velocity.

As the microstructure gets more important the velocity of the wave itself decreases.

Keeping in mind that the velocity is the gradient of the displacement, someone can come to the conclusion, that for small wavenumbers, or long waves, the velocity keeps constant a value. As the arclength of the wave gets smaller, then the waves in which the microstructure is more significant, the velocity will get smaller and smaller, until the wave does not move.

One thing that someone should notice in this figure, is that in this case the asymptotic line, in which the curve tends in non-other than the line with an equation of:  $y = l/h$  (the convergence points the same with the velocities and the frequencies, as it will be displayed later). Interesting is to observe the case, when this ratio becomes zero.

The optical phase velocity is described by the following function:

$$\bar{\omega}/\bar{k} = \frac{1}{\bar{k}} * \sqrt{1 + \bar{k}^2 * (l/h)^2}$$

39

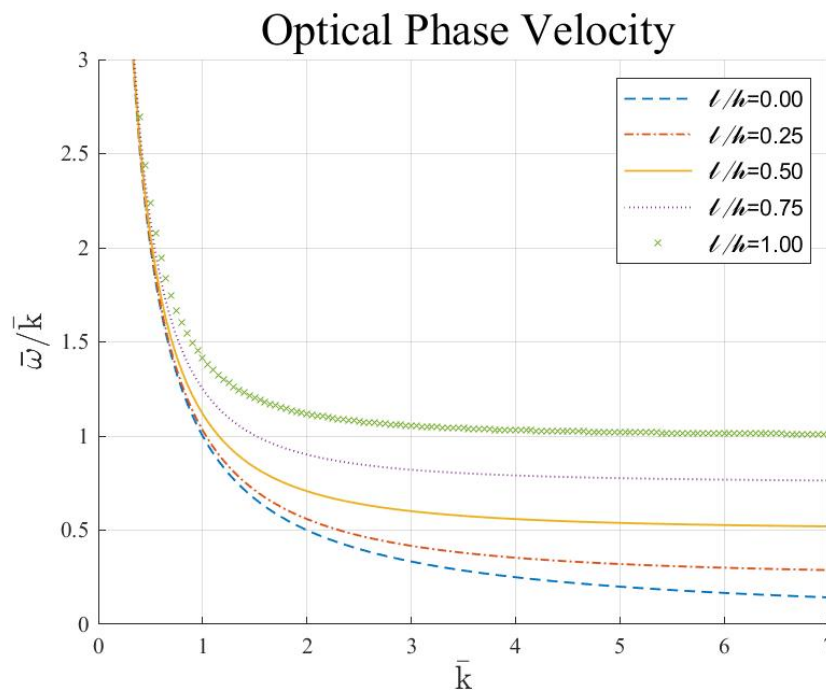


Fig. 64. The phase velocity of the optical waves as a function of the wavenumber of each wave. The dispersion is being transferred to the phase velocity. As the microstructure gets more important, the velocity of the wave decreases. For minimum wavenumbers, the velocity tends to infinite independently from the microstructure.

For a small wavenumber, this velocity tends to infinite, because the frequency is constant on those values. The phase velocity, which has a geometrical difference of  $1/\bar{k}$  should behave this way.

For materials, that have the ratio of lengths near to zero and are called semiconductors, the velocity yet again tends to zero. The semiconductors are nonetheless flexoelectric.

Those conclusions can be better understood while isolating the diagrams for a specific ratio of lengths. Yet, it is also possible to create the previous diagrams of convergence, to study about how the curve converges to the asymptotic line.

Fig. 65-70 show that the convergence to the asymptotic line happens simultaneously, both in the frequency and the velocity. However, in the phase velocity, in contrast to the frequency, the case when the ratio of the length is zero is smoother and follows the flow of the greater ratios (in this case the error was calculated with the third method).

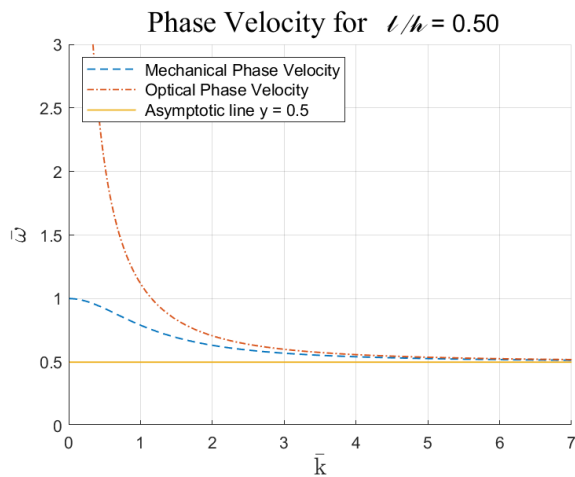


Fig. 65. The phase velocity as a function of the wavenumber for **ratio** = 0.5. Both the mechanical and the optical velocity tend asymptotically to the line  $y = 0.5$ .

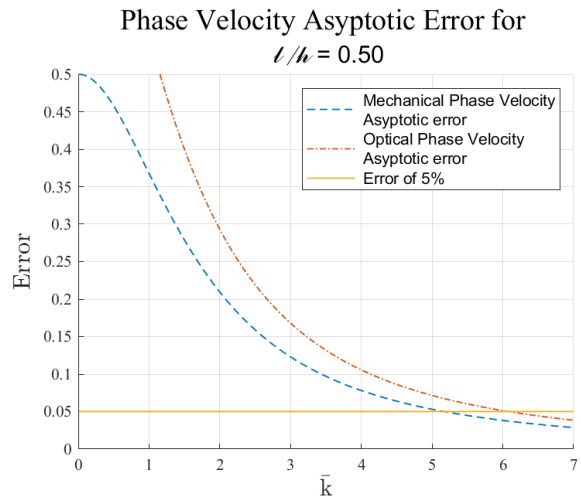


Fig. 66. The percentage of divergence of the analytical from the asymptotic value concerning the phase velocity, for **ratio** = 0.5. This diagram is similar to the one of frequency.

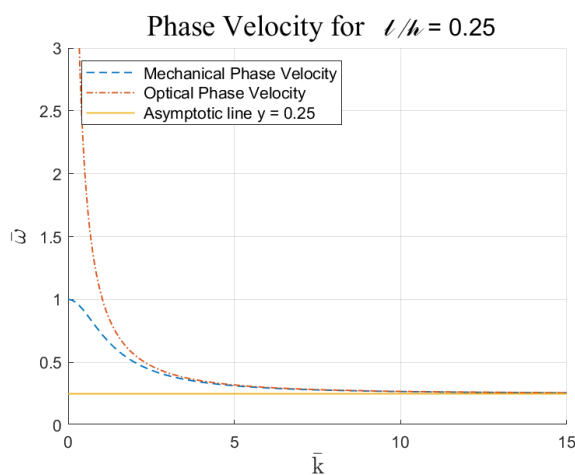


Fig. 67. The phase velocity as a function of the wavenumber for **ratio** = 0.25. Both the mechanical and the optical velocity tend asymptotically to the line  $y = 0.25$ .

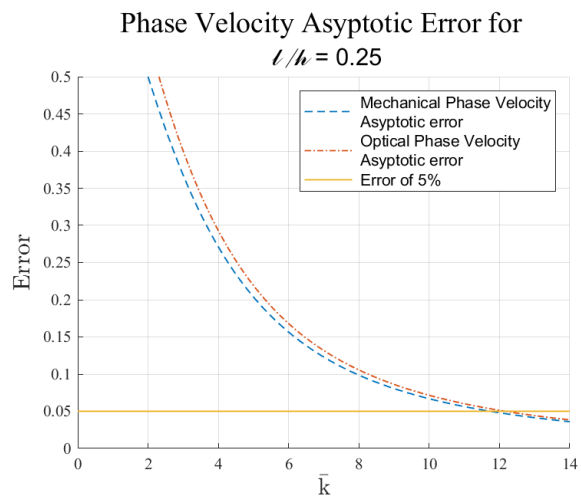


Fig. 68. The percentage of divergence of the analytical from the asymptotic value concerning the phase velocity, for **ratio** = 0.25. This diagram is similar to the one of frequency.

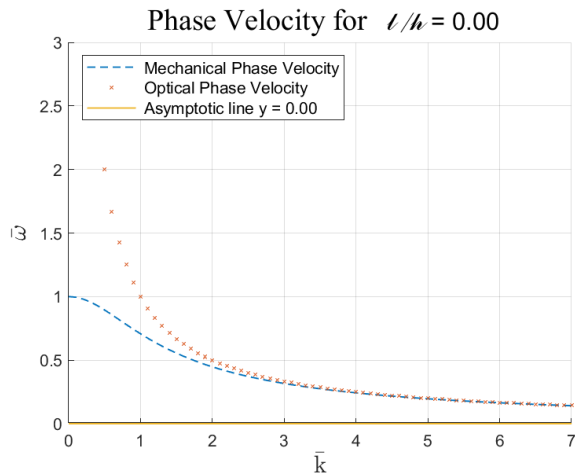


Fig. 69. The phase velocity as a function of the wavenumber for **ratio = 0.00**. Both the mechanical and the optical velocity tend asymptotically to the line  $y = 0.00$ . However, the convergence seems to happen for large wavenumbers.

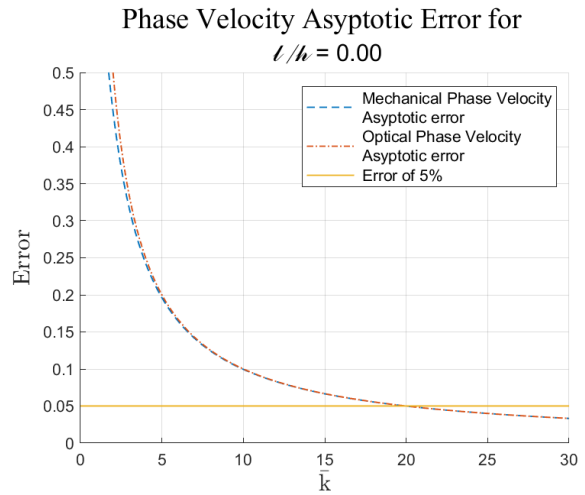


Fig. 70. The percentage of divergence of the analytical from the asymptotic value concerning the phase velocity, for **ratio = 0.00**. The convergence to the asymptotic line seems to happen for wavenumbers near 20. This diagram is different from the one produced from the frequency (fig. 57). However, in this situation the error was calculated using the third method.

Considering the point when the convergence with an allowed error occurs, the beneath diagrams are presented:

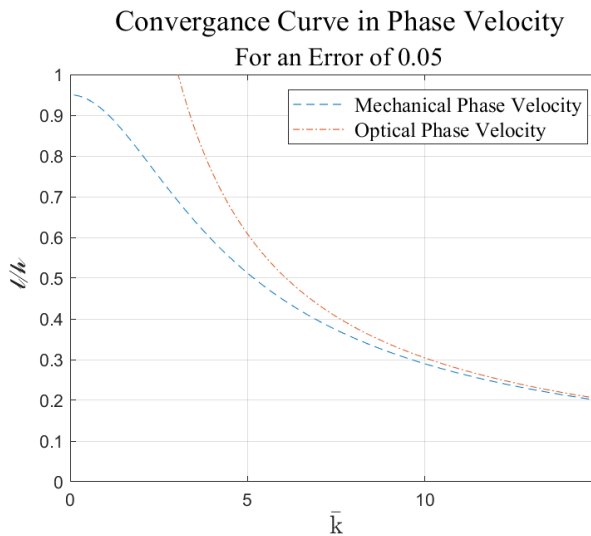


Fig. 71. Phase velocity convergence to 5% error. The curve that describes the combination of the wavenumber and the ratio of length, so the divergence from the asymptotic line gives an error equal to 5%, for the mechanical and the optical frequency.

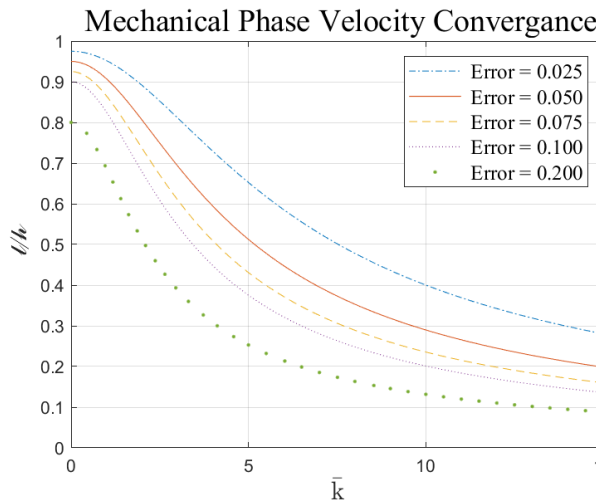


Fig. 72. Mechanical phase velocity convergence  
The curves that describe the combination of the wavenumber and the ratio of lengths, so mechanical phase velocity could be legit, from the asymptotic, with the corresponding error.

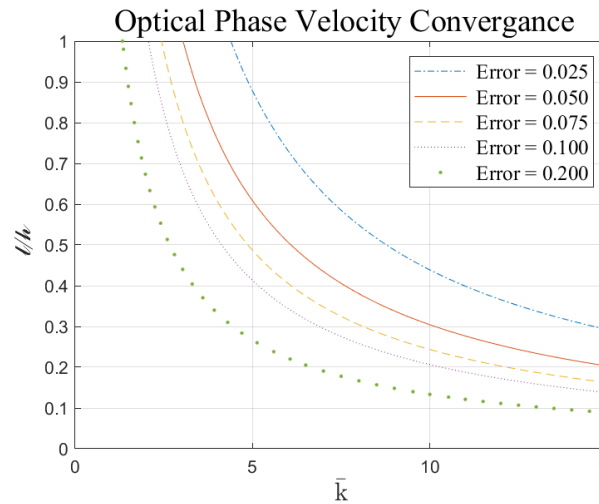


Fig. 73. Optical phase velocity convergence  
The curves that describe the combination of the wavenumber and the ratio of lengths, so the optical phase velocity can be legit, from the asymptotic, with the corresponding error.

Those diagrams are actually the same with the ones produced by the frequency. This means that the convergence both in the frequency and in the phase velocity happens at the same time (for the same wavenumber for a give ratio of lengths) (fig. 74). As a result of this similarity, the legit area in this situation is the same (fig. 61,62).

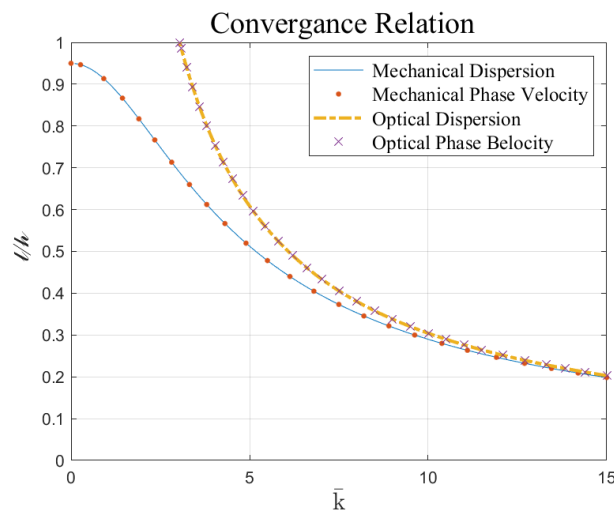


Fig. 74. Convergence Relation of frequency and phase velocity.  
The convergence both in the frequency and the phase velocity is the same.



### D. Group Velocity

One more important velocity that has not yet been discussed is the group velocity. Unlike the previous velocity, this one is not considered as something like an overall velocity, but like an instant velocity. In order to form this, a differentiation of the relation was made. The velocity then can be described by the term  $\partial\bar{\omega}/\partial\bar{k}$ . The relation, which is calculated by differentiating, is the following:

$$\frac{\partial\bar{\omega}}{\partial\bar{k}} = \sqrt{\frac{1 + \bar{k}^2 * \left(\frac{l}{h}\right)^2}{1 + \bar{k}^2}} + \frac{\bar{k}^2 * \left(\left(\frac{l}{h}\right)^2 - 1\right)}{\left(1 + \left(\frac{l}{h}\right)^2 * \bar{k}^2\right)^{1/2} * (1 + \bar{k}^2)^{3/2}} \quad 40$$

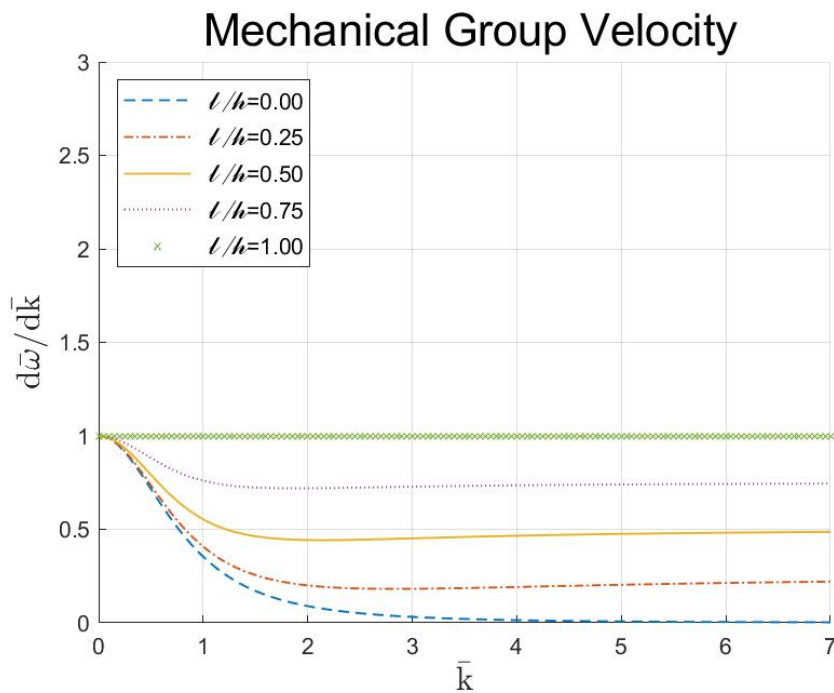


Fig. 75. The group velocity of the mechanical waves as a function of the wavenumber of each wave.

As the microstructure gets more important the velocity of the wave itself decreases.

The velocity is the gradient of the frequency, as it was derived from it. Initially, for low wavenumbers the frequency is linear and so the gradient should be constant and equal to one. When the microstructure of the materials starts to take part in the motion of the waves, the frequency deviates and the materials with the smaller length ratio get a reduction in the increase of the frequency. That means that the curves gradient has decreased (the smaller the ratio, the more it has). When the frequency stabilizes in the asymptotic line, the gradient gets once again steady, equal to to asymptotic gradient.

One very interesting observation is that in the above diagram, the curves seem to intersect with the asymptotic line before the stabilization to them. This phenomenon is more visible in the case where the ratio of the length is equal to half (solid line). This will be described more in the following figures (fig. 77 - 81)

The last quantity that should be studied is the group velocity in optical waves. The relation of the optical group velocity is the beneath and can be plotted as follows:

$$\frac{\partial \bar{\omega}}{\partial \bar{k}} = \frac{\bar{k} * \left(\frac{l}{h}\right)^2}{\sqrt{1 + \bar{k}^2 * \left(\frac{l}{h}\right)^2}} \quad 41$$

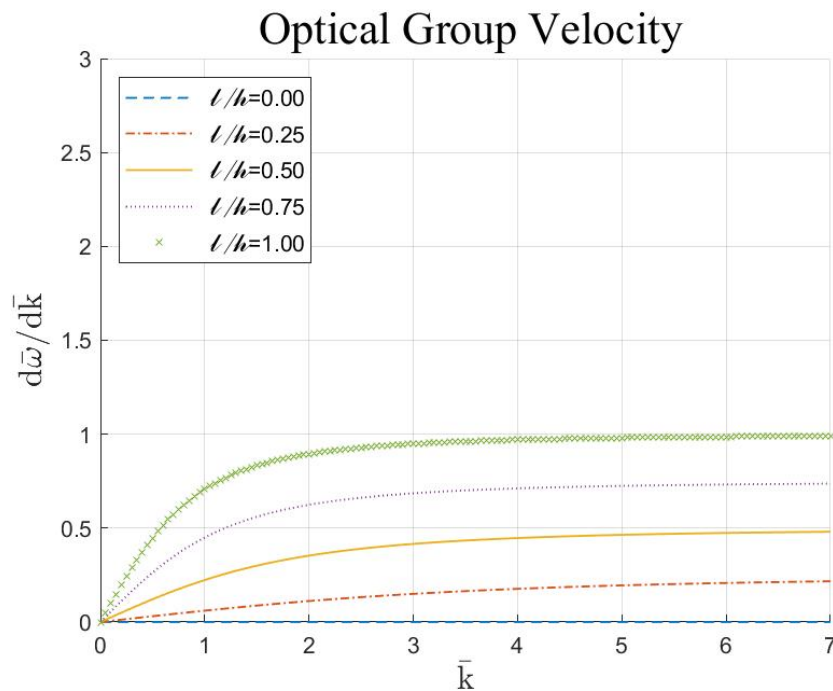


Fig. 76. The group velocity of the optical waves as a function of the wavenumber of each wave. As the microstructure gets more important, the velocity of the wave itself decreases.

The meaning of this diagram is equivalent to the energy an optical wave can transfer. As it can be seen, long waves cannot transfer much energy. There is also an optimization possibility by choosing a big enough wavenumber and choosing a material with smooth enough microstructure ( $3G \rightarrow 4G \rightarrow 5G$ ).

In the anti-plane flexoelectric problem, someone must choose whether the need is to optimize the phase velocity or the group velocity. The first transfers the wave, while the second transfers the energy. It's up to the application what should be optimized.

A comparison of the convergence of the mechanical and the optical velocity for some specific ratios of lengths is possible.

Dispersion relation on produced waves

In the mechanical group velocity, as it can be seen for a ratio of length equal to  $l/h = 0.5$ , initially the analytical relation converges to the asymptotic, but then diverges to converge once again.

In the next diagrams, the right figures (fig. 78, 80, 82) depict the convergence for some different values of ratios of the lengths. The phenomenon mentioned above can be seen more visibly.

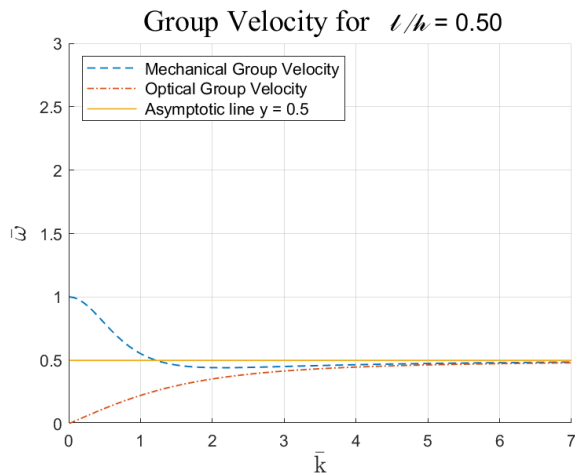


Fig. 77. The group velocity as a function of the wavenumber for **ratio = 0.5**. Both the mechanical and the optical velocity tend asymptotically to the line  $y = 0.5$ . Also, the mechanical velocity intersects the asymptotic line and then tends to her from the other side.

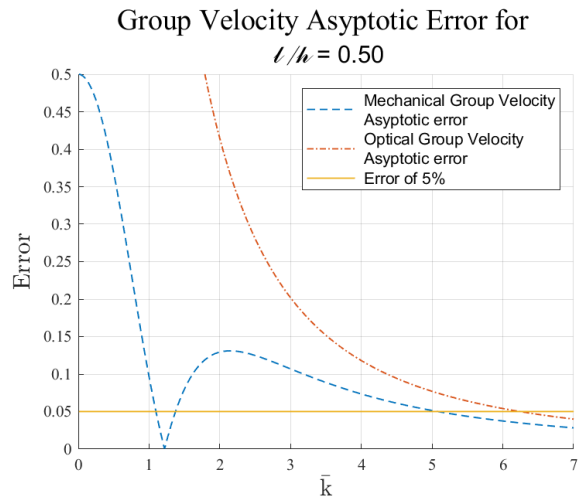


Fig. 78. The percentage of divergence of the analytical from the asymptotic value concerning the group velocity, for **ratio = 0.5**. This diagram was made by using the absolutes. The convergence of the mechanical velocity forms and oscillation. As the wavenumber increases, the oscillation tends to find the stabilization point.

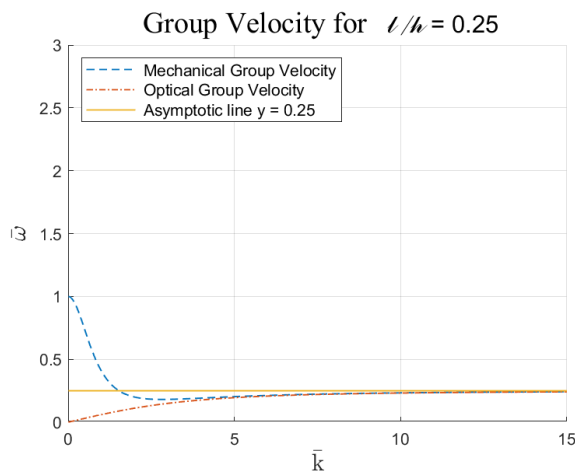


Fig. 79. The group velocity as a function of the wavenumber for **ratio = 0.25**. Both the mechanical and the optical velocity tend asymptotically to the line  $y = 0.25$ . In this case

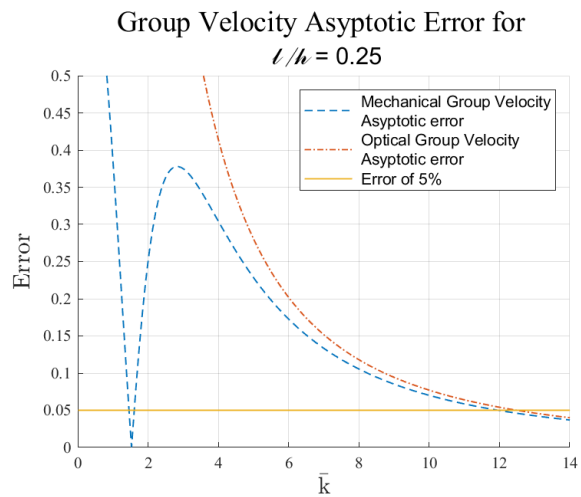


Fig. 80. The percentage of divergence of the analytical from the asymptotic value concerning the group velocity, for **ratio = 0.25**. The convergence, divergence and then again convergence phenomenon is one again visible.

also the mechanical group velocity intersects with the asymptotic line and then converges.

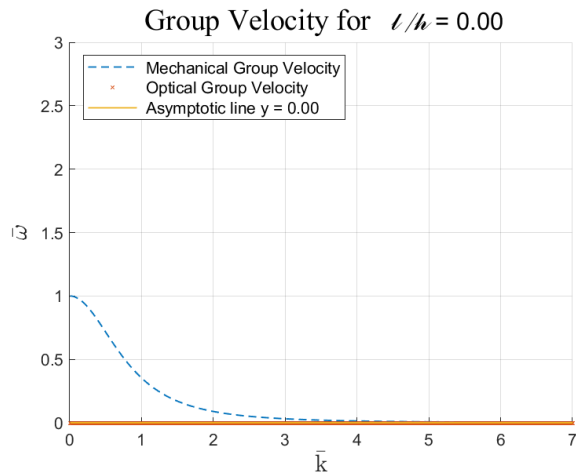


Fig. 81. The group velocity as a function of the wavenumber for *ratio* = 0.00.

The mechanical group velocity tends asymptotically to the line  $y = 0.00$ , while the optical velocity is constant and always equal to zero. In this case there is no intersection prior to the convergence.

Comparing these results with the previous case, the divergence magnitude increases, and the maximum divergence happens for smaller wavenumber. The convergence too.

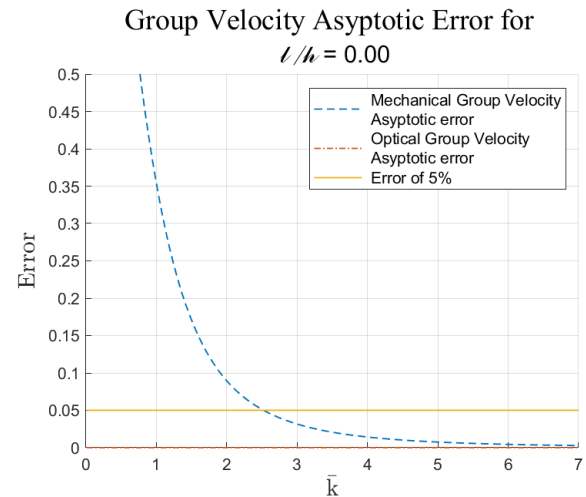


Fig. 82. The percentage of divergence of the analytical from the asymptotic value concerning the group velocity, for *ratio* = 0.00.

In this diagram there is only a convergence, in contrast with the previous cases. the mechanical group velocity tends asymptotically to the right line, for a generally small wavenumber. However, in this case the third type of error was used.

Next, it is possible to define the combinations of a wavenumber and a ratio of lengths that give an eligible amount of error between the analytical and the asymptotic relations.

The mechanical group velocity has a peculiarity. For a specific ratio of lengths there are two wavenumbers that give a legit error, one before the divergence and one after. It can be imagined that the same happens for a specific wavenumber. This assumption can be proven by the beneath diagram (fig. 83). Also, it is interesting that this peculiarity can be best fitted by the same diagram of the frequency (and the phase velocity), as it can be seen beneath.

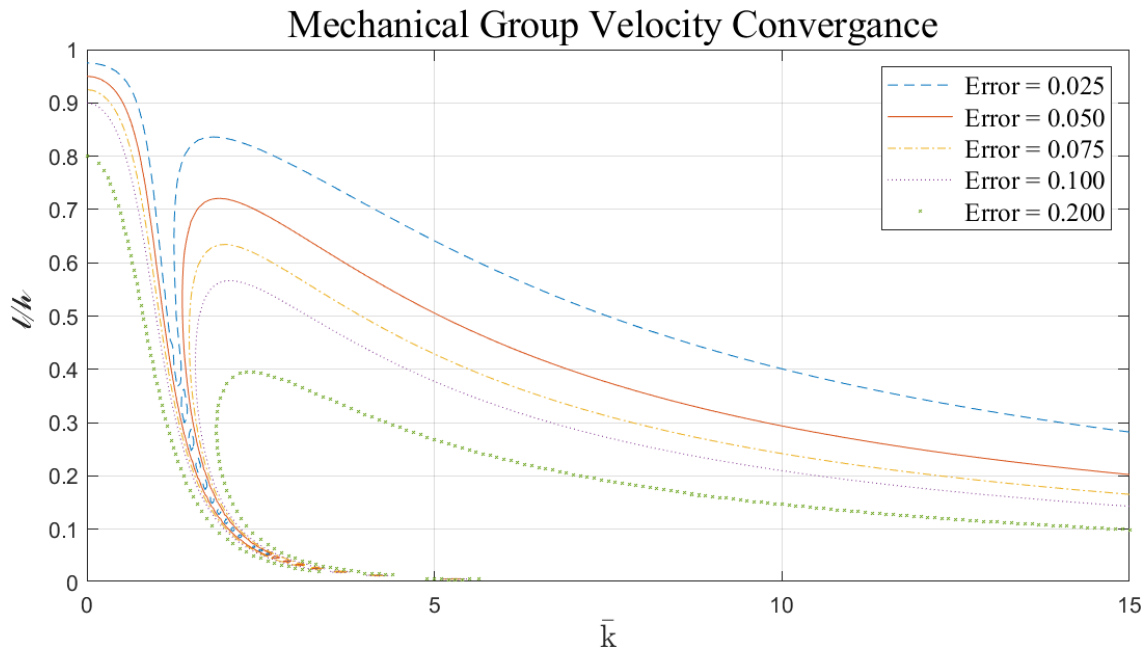


Fig. 83. Mechanical group velocity convergence.

The curve that describes the combination of the wavenumber and the ratio of length, so the divergence from the asymptotic line gives an eligible error. This oscillation is being presented as a spike. In a specific curve e.g., the one that describes the convergence for an error equal to 5%, for big enough ratio of the lengths, (when the microstructure is irrelevant) there is no intersection (for  $l/h > 0.7$ ). As the ratio decreases there is a spiking as the horizontal line intersects twice with the curve. The distance (difference of the wavenumber) of those two intersections decreases as the ratio of length decreases, as the microstructure gets more relevant.

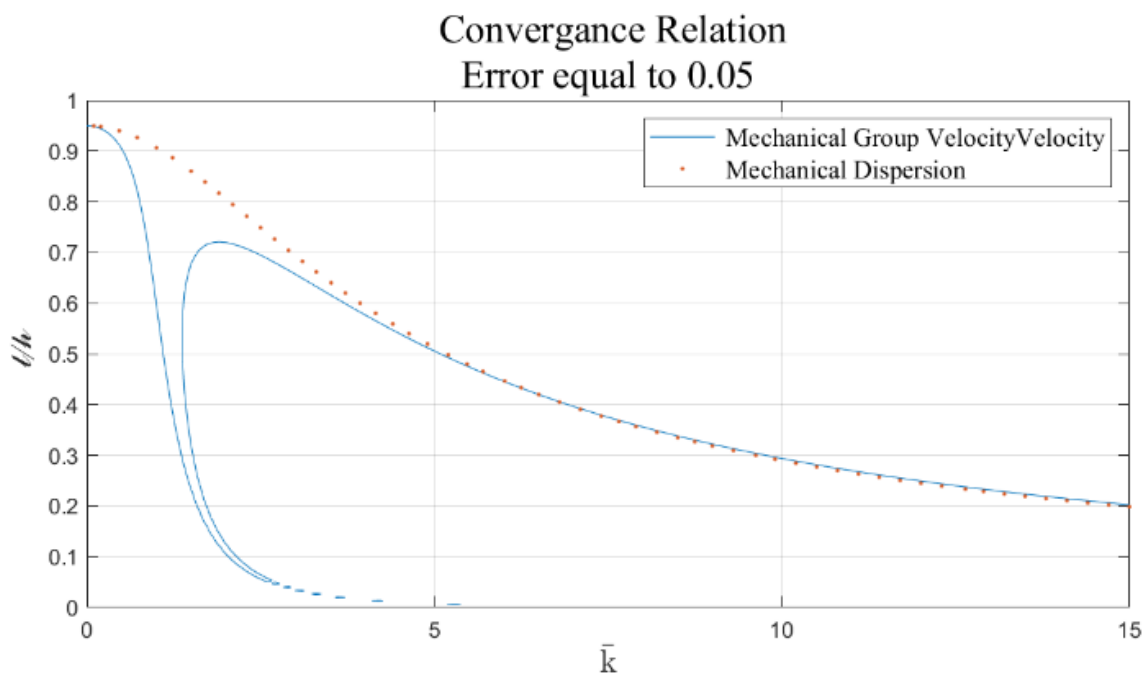


Fig. 84. Convergence relation of frequency and mechanical group velocity for error equal to 5%.

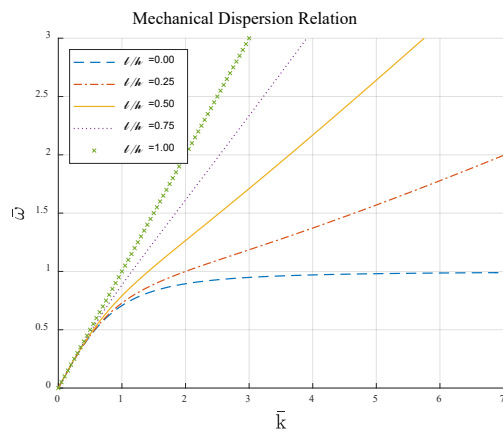
Those two curves are not the same, the group velocity convergence is different from the convergence in the frequency or the phase velocity. The main difference is this oscillation. However, the frequency convergence curve and the mechanical group velocity curve are the same for larger wavenumbers.

The optical velocity should not have such a singularity.

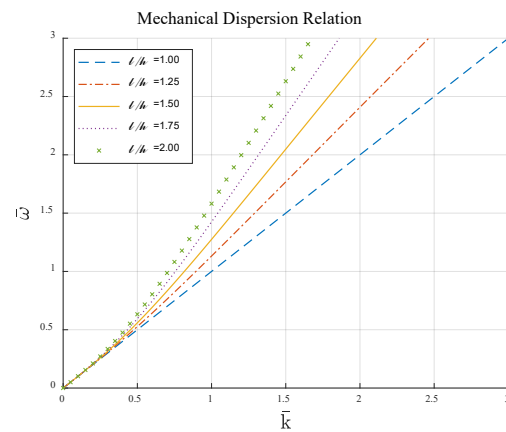
### E. Dispersion in metamaterials

The previous analysis, was considering a normal dielectric and thus the ratio of the lengths was bounded. This bound suggests that the materials have positive electrical susceptibility, as all normal dielectrics. However, the existence of materials with negative susceptibility has been proven. For more information about those metamaterials the reader is suggested to visit chapter 3 – Intermediate region.

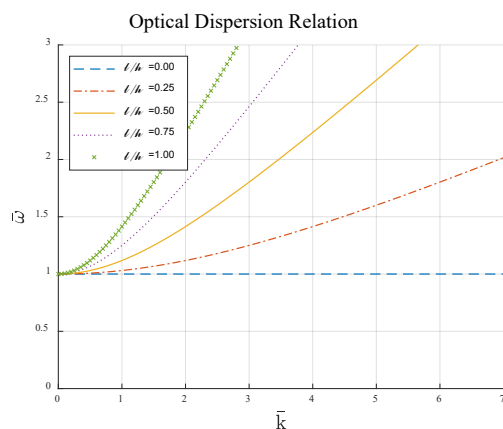
Accepting a negative electrical susceptibility, the upper bound of the ratio  $l/h$  is canceled. Relations 33, 34, 38, 39, 40, 41 however, can be used for these ratios, nonetheless.



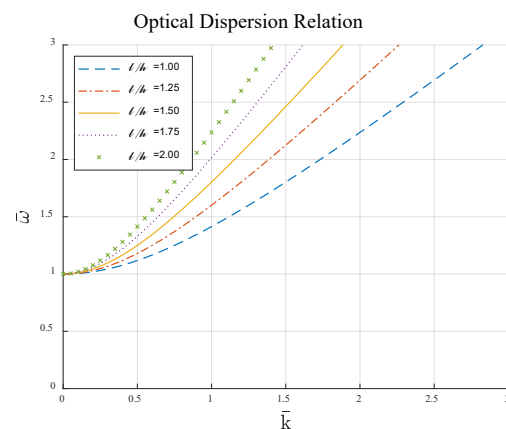
(a) Mechanical Dispersion for normal dielectrics



(b) Mechanical Dispersion for meta – materials



(c) Optical Dispersion for normal dielectrics



(d) Optical Dispersion for meta – materials

Fig. 85. The Dispersion relations for meta-material and normal dielectrics.

The figures in the right side are the new figures. The dispersion curves, both on the mechanical and the optical waves, seem to disperse from the other side of the non-dispersive case.

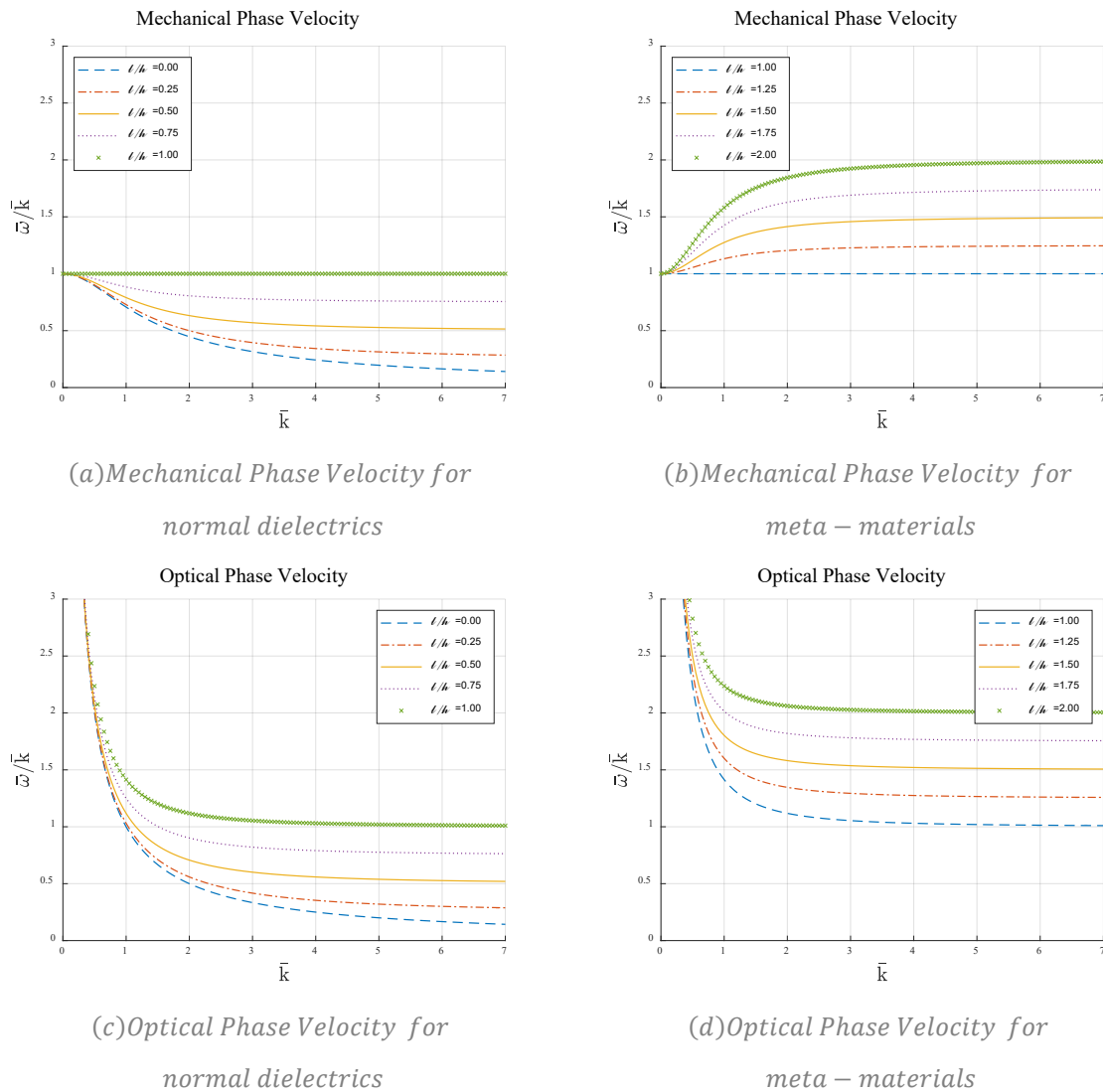
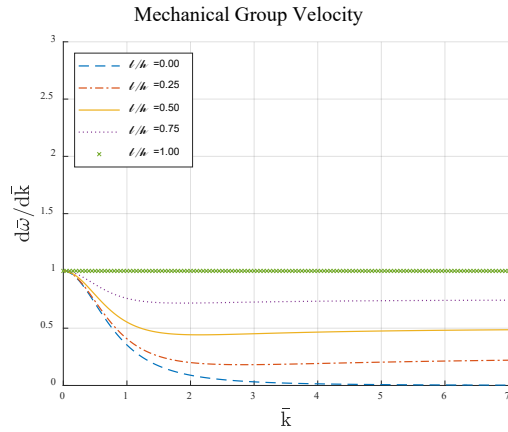


Fig. 86. The phase velocity, for meta-materials and normal dielectrics.

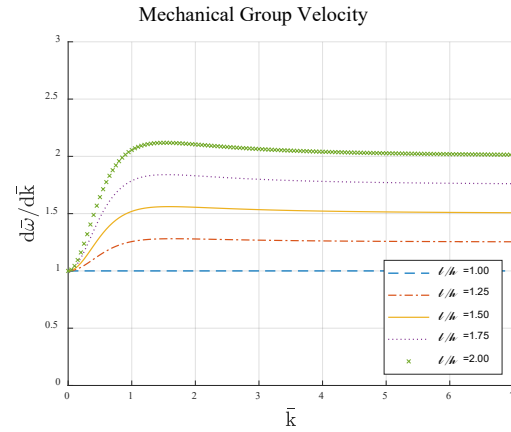
The figures in the right side are the new figures. The mechanical phase velocity makes a shifting, as the mechanical phase velocity for the metamaterials is reversed (mirror) from the other side of the line  $y = 1$ . Those forms remind dispersions of viscoelastic materials.

The optical velocity however for meta-materials is usual, as the form of the curves remains the same, but the asymptotic line rises (rises the value of the coordinate which characterizes it).

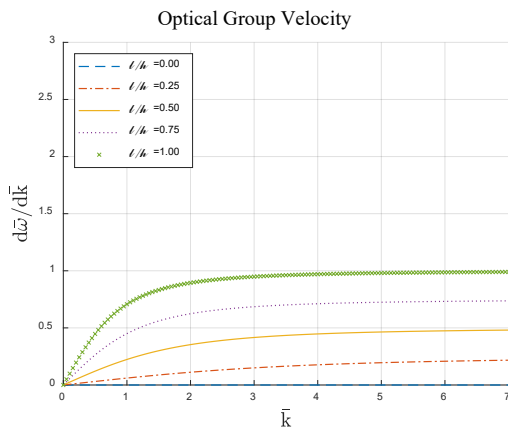
There is an obvious shifting in the mechanical phase velocity, which is also visible in the group velocity. The curves in the meta-materials tends from the other direction of the critical non-dispersive value. Similar dispersion has been observed also in viscoelastic materials.



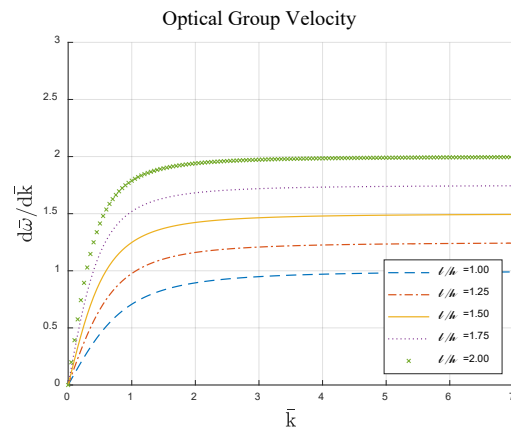
(a) Mechanical Group Velocity for normal dielectrics



(b) Mechanical Group Velocity for meta-materials



(c) Optical Group Velocity for normal dielectrics



(d) Optical Group Velocity for meta-materials

Fig. 87. The group velocity, for meta-materials and normal dielectrics.

The figures in the right side are the new figures. The mechanical group velocity similarly to the mechanical phase velocity makes a shifting (mirror) from the other direction of the non-dispersive case. Also, the phenomenon of the oscillation-like (converges  $\rightarrow$  diverges  $\rightarrow$  converges) can be observed.

The optical velocity however for meta-materials is usual, as the form of the curves remains the same, but the asymptotic line rises (rises the value of the coordinate which characterizes it).



## 6. Plates

### A. Introduction

The last part of the study is based on an analogue suggested by [Gavardinas et al. \(2018\)](#) and [Giannakopoulos and Zisis \(2019\)](#) between the case of the anti-plane couple elasticity problem and a plate problem. As they have suggested, those two problems are analogues and the solution of the one is equivalent to the solution of the other. In chapter 3, it was mentioned, that [Giannakopoulos and Zisis \(2019\)](#) solved computationally a plate problem that was similar with a mode III crack problem with the theory of couple stress elasticity ([fig. 27, 28](#)).

In those two last chapters this analogue will be studied. Initially the basic concepts of plates will be mentioned, then the analogues will be displayed and finally on chapter 7, with the use of these analogue a FEM application will be suggested.

### B. The isotropic plate

The plate problem has been studied in a great scale, as it is common, not only for micro-mechanical purposes but also for structural. The plate is something found in almost every structure. Plates exist in every house. A plate is where someone stands now and the weight of this person, is a load that the plate has to cope with.

The plates are shell elements, that react in the out-of-plane load with bend, in difference to membranes, which are stressed only axially. This, the out-of-plane load, is the most common load that can be applied in a plate. However, in civil engineering structures, large plates made of concrete could be profitable when prestressed.

The plates are characterized with a fourth order differential equation and they were studied at a large scale by [Timoshenko and Woinowsky-Krieger \(1964\)](#).

However, the prestressed plate, which is of interest, has not been studied that much. An axial stressing on the plate can cause instabilities (flutter and divergence instability). [Babouskos and Katsikadelis \(2009\)](#) studied those instabilities on plates, one each time and also by combining them.

In their study, they included both conservative and non-conservative loads, which have to do with whether the load follows the deformation or not. The conservative force is applied in the undeformed configuration in contrast to the non-conservative load which is applied in the deformed configuration. The flutter instability describes a vibrational motion and usually happens for smaller loads. By enlarging the load, the instability becomes divergence instability, which has smaller frequencies and the amplitude increases exponential.

The instability of plates, in addition to the axial prestress, could also be a dynamic problem. [Babouskos and Katsikadelis \(2009\)](#) used Hamilton's principle to calculate the governing equation of motion. According to that, the following equation should hold true in any case.

$$\int_{t_1}^{t_2} (\delta T - \delta U + \delta V + \delta W_{nc}) dt = 0$$

In this relation the term  $\delta T$  refers to the total kinetic energy between time  $t_1$  and  $t_2$ .  $U$  is the elastic energy, or the total potential energy density. The other two terms refer to the conservative and non-conservative forces that may be applied to the configuration.  $V$  is the potential of external actions while  $W$  is the virtual work of the non-conservative or damping loads.

By substituting the kinetic energy (produced from an out-of-plane velocity), the elastic energy (with calculation of the rigidities of the plate) and the other mechanical actions, the authors extracted two differential equations, one referring to the in-plane deformation and one referring to the out-of-plane.

The one referring to the out-of-plane deformation, which is also the one of interest for this study, includes the biharmonic term, harmonic terms because of the axial, in-plane stress, terms of first order because of surface traction (in-plane), or tangent tension to the plane (out-of-plane) and also terms of inertia (dynamic terms).

$$D\nabla^4 w - (N_x + P_x)w_{,xx} - 2(N_{xy} + P_{xy})w_{,xy} - (N_y + P_y)w_{,yy} + (n_x + q_x)w_{,x} + (n_y + q_y)w_{,y} + \rho h\ddot{w} + c\dot{w} = 0 \quad 42$$

$D$  is the plate's bending rigidity  $D = (Eh^3)/(12(1 - \nu^2))$ :  $E$  is the modulus of elasticity,  $\nu$  is the Poisson's ratio,  $h$  is the height of the plate's section.  $\rho h$  is the mass per area and lastly  $c$  is the dumping constant of possible dumpers. The actions that are present in the above equation can be seen in a sketch from that study (fig. 88).

From that equation it is possible to eliminate:

- the boundary shear action, both conservative and non,  $(N_{xy}, P_{xy})$ ,
- the in-plane surface action  $(n_x, n_y)$ ,
- the out-of-plane aerodynamic pressure,  $(q_x, q_y)$
- the dumping force  $(c)$ .

Also, the differentiation between the conservative and non-conservative action can be considered the same  $(N_x + P_x) = (N_x)$ .

$$D\nabla^4 w - N_x w_{,xx} - N_y w_{,yy} + \rho h\ddot{w} = 0 \quad i$$

And then if the problem is static:

$$D\nabla^4 w - N_x w_{,xx} - N_y w_{,yy} = 0$$

ii

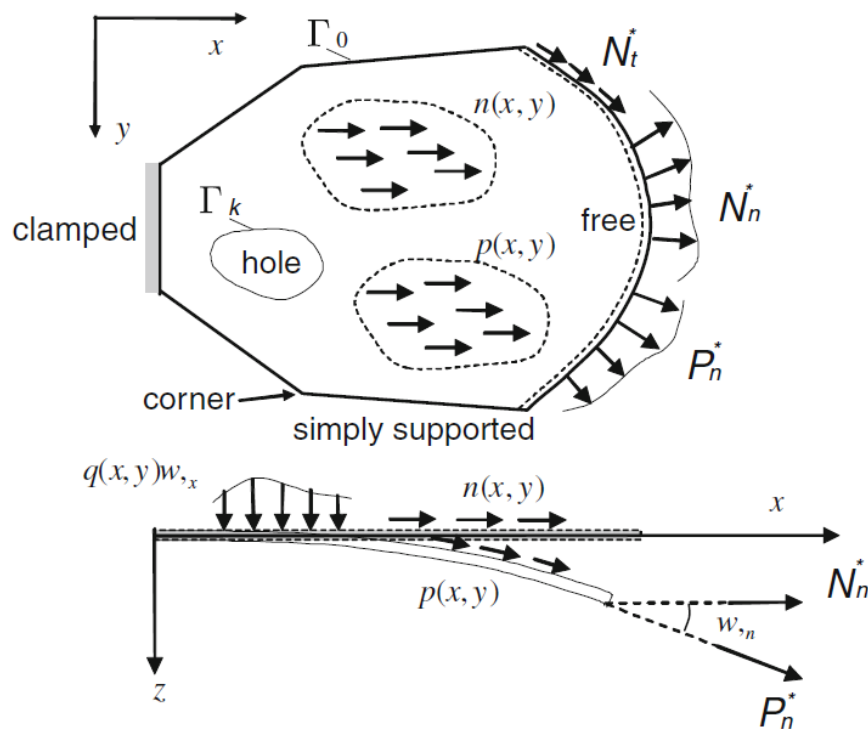


Fig. 88. The total actions applied to a plate.

Except from the boundary conditions, there could be in-plane actions, axial or shear. Out-of-plane actions tangent to the surface of the plane and singular geometry of the surface. This figure was obtained from Babouskos and Katsikadelis (2009).

For equal biaxial tension,  $N_x = N_y = N$ , relation i becomes relation iii.

$$D\nabla^4 w - N\nabla^2 w + \rho h \ddot{w} = 0$$

iii

For the static case of the problem, the differential equation that governs the problem of the equally biaxial prestress plate is described by the following relation:

$$D\nabla^4 w - N\nabla^2 w = 0$$

iv

Relations i, ii, iii, iv are referring to a configuration in which there are no external out-of-plane loads, in the direction of displacement, e.g. the load of a human above the plate. To add this kind of load, the work produced from it should be added in the principle. This work can be written as follows:

$$W_{ext} = P(x, y) * w(x, y) \rightarrow \delta W_{ext} = P(x, y) \delta w \quad \mathbf{v}$$

The governing equation 42, was produced by the demand that the factor that multiplies the potential out-of-plane displacement is zero. The term described by relation **v** takes also part in this factor and so the external load  $P(x, y)$  should be added in the left hand-side of the equation **i**, **ii**, **iii**, **iv**.

$$D\nabla^4 w - N_x w_{,xx} - N_y w_{,yy} + \rho h \ddot{w} = P(x, y) \quad 43$$

$$D\nabla^4 w - N_x w_{,xx} - N_y w_{,yy} = P(x, y) \quad 44$$

$$D\nabla^4 w - N\nabla^2 w + \rho h \ddot{w} = P(x, y) \quad 45$$

$$D\nabla^4 w - N\nabla^2 w = P(x, y) \quad 46$$

The boundary conditions of the problem are extremely necessary for those differential equations. Some possible boundary conditions could be the following:

- the displacements or the forces on the boundary
- the rotations of the displacement or the moments on the boundary
- The initial conditions (this condition is necessary, if the problem is dynamic)

Gavardinas et al. (2018) observed that relation **iv** looked a lot similar with relation 10 the one from couple stress elasticity.

### C. The static analogue

The comparison of those cases, the prestressed plate and the anti-plane couple stress elasticity resides in the differential equations of each case. Relation 10, when also considering an external out-of-plane load ( $B_z$ ) has the below form:

$$\nabla^2 w - \frac{l^2}{2} \nabla^4 w = \frac{B_z}{\mu}$$

While relation 46 can be written also as follows:

$$\nabla^2 w - \frac{D}{N} \nabla^4 w = -\frac{P}{N} \quad 46$$

The analogue is obvious.

<i>Prestressed Plate problem</i>	<i>Anti – plane couple stress elasticity problem</i>
$\frac{D}{N}$	$\frac{l^2}{2}$
$-\frac{P}{N}$	$\frac{B_z}{\mu}$

In the above relation  $l$  is the microstructural length,  $B_z$  is the vertical load and  $\mu$  is the shear modulus. Fig. 89 displays this analogue with great efficiency.

The governing equations are analogue and by modifying the parameters ( $\mu, \eta, l$  for the anti-plane problem and  $D, h, v, N$  for the plate problem), the solution of the one suggests the solution of the other.

Some notes that need to be written down:

- The static analogue demands equally biaxial prestress
- The material in both cases should be isotropic
- The Poisson's ratio, as it exists in the relation of the plate, is bounded from  $-1$  to  $0.5$ . However, as the analogue, could be used only theoretically for computational reasons, this bound could be ignored.

All the above were concluded by the research of [Gavardinas et al. \(2018\)](#).

The main purpose of this analogue, is an easy way to solve the anti-plane couple elasticity problem. The analogue demands the problem to be static. This limits many anti-plane problems that could be solved. However, there are ways to bypass this. For example, one easy way to study the mode III crack is by using a screw dislocation distribution.

The differential equations are the same and thus an analytical solution has exactly the same difficulty to be calculated. This analogue brights up numerically, where the plate problem can very easily be solved numerically with FEM. The same solution however, would apply to the analogue anti-plane problem (the displacements and rotations would be exactly the same).

The boundary conditions also need to be characterized as analogues. The plate problem demands the displacement in the boundary and the rotations. The same also could apply in the anti-plane problem. The boundary condition could also be Saint Venant boundary conditions.

In the next table, that was created based on the theory of [Gavardinas et al. \(2018\)](#) the analogies that are created are displaced.

The actions, and how they are symbolized, are displayed in the next figure.

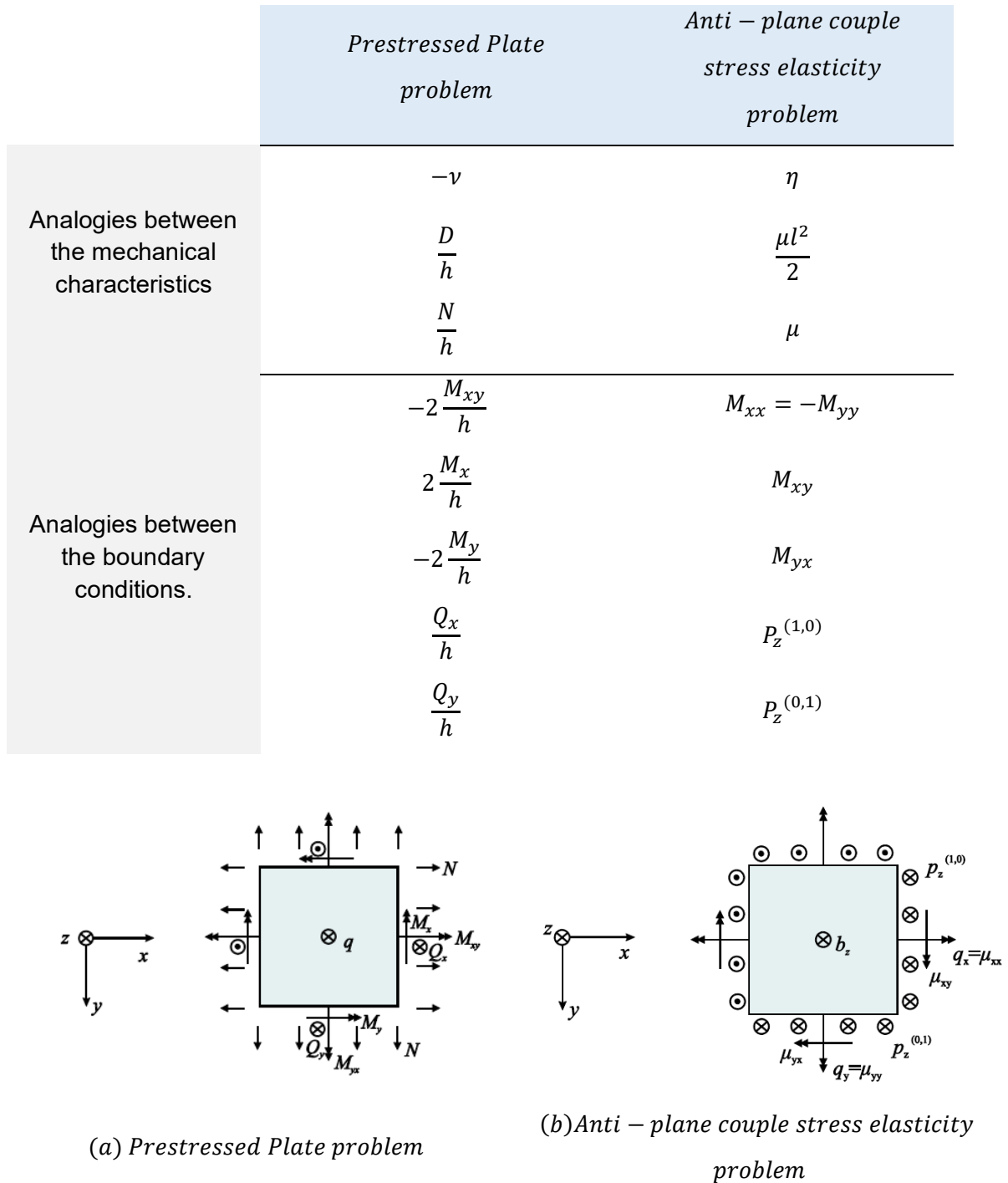


Fig. 89. The analogue.  
Schematic comparison between the anti-plane couple stress elasticity problem and the prestress plate, By [Gavardinas et al. \(2018\)](#).

The analogies between the boundary conditions include also the rotations and the displacements. When the displacement in the direction e.g.  $x$  is zero in the plate problem, the

shear action  $Q_x \neq 0$  and according to the above analogies,  $P_z^{(1,0)} \neq 0$ , which is equivalent with zero out-of-plane displacement for the anti-plane problem.

The anti-plane flexoelectric problem as it is also an anti-plane problem, solved via the method of couple stress elasticity theory, has the same analogies with the anti-plane couple elasticity problem. For the static anti-plane flexoelectric problem, for which the governing equation is the following (relation 2 by considering no acceleration in the out-of-plane direction, with an external action).

$$\nabla^2 u_3 - \left\{ \frac{b_{44} + b_{77}}{a} - \frac{(e_{44} - f_{12})^2}{\mu a} \right\} \nabla^4 u_3 = \frac{B_z}{\mu}$$

This problem obeys the following analogies:

<i>Prestressed Plate problem</i>	<i>Anti – plane flexoelectric problem</i>
$\frac{D}{N}$	$\left\{ \frac{b_{44} + b_{77}}{a} - \frac{(e_{44} - f_{12})^2}{\mu a} \right\}$
$-\frac{P}{N}$	$\frac{B_z}{\mu}$

And more detailed:

	<i>Prestressed Plate problem</i>	<i>Anti – plane flexoelectric problem</i>
<i>Analogies between the mechanical characteristics</i>	$-v = 0$	0
	$\frac{D}{h}$	$\mu \left\{ \frac{b_{44} + b_{77}}{a} - \frac{(e_{44} - f_{12})^2}{\mu a} \right\}$
	$\frac{N}{h}$	$\mu$

Analogies between  
the boundary  
conditions.

$$\begin{array}{ll}
 -2 \frac{M_{xy}}{h} & M_{xx} = -M_{yy} \\
 2 \frac{M_x}{h} & M_{xy} \\
 -2 \frac{M_y}{h} & M_{yx} \\
 \frac{Q_x}{h} & P_z^{(1,0)} \\
 \frac{Q_y}{h} & P_z^{(0,1)}
 \end{array}$$

#### D. The prestressed orthotropic Plate

The anisotropic plate, is something not well studied, as the structural engineering bypasses this by considering that the plate is supported in only one direction (e.g. mixed plates of concrete and steel). However, plates can be made by materials which are not isotropic, e.g. wood, and thus some studies exist.

In one project, by [Shi and Bezzine \(1988\)](#), the anisotropic plate was studied (in bending). They proposed as the governing equation of the problem the following relation:

$$D_{11} \frac{\partial^4 w}{\partial x^4} + 4D_{16} \frac{\partial^4 w}{\partial x^3 \partial y} + 2 * (D_{12} + 2D_{66}) \frac{\partial^4 w}{\partial x^2 \partial y^2} + 4D_{26} \frac{\partial^4 w}{\partial x \partial y^3} + D_{22} \frac{\partial^4 w}{\partial y^4} = p(x, y) \quad \text{vi}$$

In this equation  $D_{11}$ ,  $D_{16}$ ,  $D_{12}$ ,  $D_{66}$ ,  $D_{26}$ ,  $D_{22}$  are the flexural rigidities of the anisotropic plate, and  $p(x, y)$  is the out of plane action that causes the bending.

In an orthotropic plate those bending rigidities can be defined as follows.

$$D_{11} = \frac{E_x h^3}{12(1 - \nu_x \nu_y)}$$

$$D_{22} = \frac{E_y h^3}{12(1 - \nu_x \nu_y)}$$

$$D_{12} = D_{11} \nu_y = D_{22} \nu_x$$

$$D_{66} = \frac{G_{xy} h^3}{12}$$

$$D_{16} = D_{26} = 0$$



Also, the Poisson's ratios in each direction depends on the one of the other directions.

$$v_y = \frac{v_x E_y}{E_x}$$

The governing equation is reduced to the following:

$$\frac{E_x h^3}{12(1 - v_x v_y)} \frac{\partial^4 w}{\partial x^4} + \left( \frac{v_y E_x h^3}{12(1 - v_x v_y)} + \frac{v_x E_y h^3}{12(1 - v_x v_y)} + \frac{4G_{xy} h^3}{12} \right) \frac{\partial^4 w}{\partial x^2 \partial y^2} + \frac{E_y h^3}{12(1 - v_x v_y)} \frac{\partial^4 w}{\partial y^4} = p(x, y) \quad 46$$

This relation represents the modified fourth order derivative in relation 42. By substituting 46 in that fourth order term, the full solution of the orthotropic plate shall be extracted. The orthotropy influences only the material characteristics. In relation 42 the only material characteristic are the bending rigidities of the plate and concerns only the fourth order derivative. Thus, the below can be considered.

When in relation 43 the left hand-side of relation 46 substitutes the fourth order term, the following relation is produced:

$$\begin{aligned} \frac{E_x h^3}{12(1 - v_x v_y)} w_{xxxx} + \left( \frac{v_y E_x h^3}{12(1 - v_x v_y)} + \frac{v_x E_y h^3}{12(1 - v_x v_y)} + \frac{4G_{xy} h^3}{12} \right) w_{xxyy} \\ + \frac{E_y h^3}{12(1 - v_x v_y)} w_{yyyy} - N_x w_{,xx} - N_y w_{,yy} + \rho h \ddot{w} = p(x, y) \end{aligned} \quad 47$$

Relation 47 is the governing equation of a prestressed orthotropic plate. Considering  $v_x = v_y = 0$ , a theoretical plate is being described, that allows the analogue. This assumption is necessary as it not only simplifies the relations but also settles some boundary conditions. This way, an anti-plane problem either it is considered couple stress or flexoelectric can be solved through a plate solution. Relation 47, transforms to the following expression (also for non-zero out-of-plane external load, but zero acceleration  $\ddot{w}$ ):

$$\frac{E_x h^3}{12} w_{xxxx} + \frac{G_{xy} h^3}{3} w_{xxyy} + \frac{E_y h^3}{12} w_{yyyy} - N_x w_{,xx} - N_y w_{,yy} = p(x, y) \quad 48$$

### E. The dynamic analogue

Giannakopoulos and Zisis (2019), noticed a similarity between the relation 48 and relation 2, 12. and by changing the order of the derivatives, this equation (vii) can also be written as beneath, to follow the formula of relation 7:

$$\frac{N_x}{N_y} \frac{\partial^2 w}{\partial x^2} + \frac{\partial^2 w}{\partial y^2} - \frac{E_x h^3}{12N_y} \frac{\partial^4 w}{\partial x^4} - \frac{G_{xy} h^3}{3N_y} \frac{\partial^4 w}{\partial x^2 \partial y^2} - \frac{E_y h^3}{12N_y} \frac{\partial^4 w}{\partial y^4} = -\frac{p(x, y)}{N_y} \quad \text{vii}$$

For convenient reasons here, once again relation 7 is displayed (also with an external load).

$$\left(1 - \frac{V^2}{c_s^2}\right) \frac{\partial^2 u_3}{\partial \xi^2} + \frac{\partial^2 u_3}{\partial \eta^2} - \frac{l^2}{2} \left(1 - \frac{V^2 H^2}{6l^2 c_s^2}\right) \frac{\partial^4 u_3}{\partial \xi^4} - \frac{l^2}{2} \left(2 - \frac{V^2 H^2}{6l^2 c_s^2}\right) \frac{\partial^4 u_3}{\partial \xi^2 \partial \eta^2} - \frac{l^2}{2} \frac{\partial^4 u_3}{\partial \eta^4} = \frac{B_z}{\mu}$$

A direct analogue is visible. The main analogies which also define the problem as intermediate, elliptic or hyperbolic are the following:

<i>Prestressed Plate problem</i>		<i>Anti – plane flexoelectric problem</i>	
$\frac{N_x}{N_y}$	=	$1 - \frac{V^2}{c_s^2}$	viii
$\frac{E_x h^3}{12N_y}$	=	$\frac{l^2}{2} \left(1 - \frac{V^2 H^2}{6l^2 c_s^2}\right)$	ix
$\frac{G_{xy} h^3}{3N_y}$	=	$\frac{l^2}{2} \left(2 - \frac{V^2 H^2}{6l^2 c_s^2}\right)$	x
$\frac{E_y h^3}{12N_y}$	=	$\frac{l^2}{2}$	xi
$-\frac{p(x, y)}{N_y}$	=	$\frac{B_z}{\mu}$	

Relation xi suggests an equivalence concerning the microstructural length. Substituting the equivalent in relations ix, x, the above table gets as follows:

<i>Prestressed Plate problem</i>	<i>Anti – plane flexoelectric problem</i>
$\frac{N_x}{N_y}$	$= 1 - \frac{V^2}{c_s^2}$
$\frac{E_x}{E_y}$	$= \left(1 - \frac{V^2 H^2}{6l^2 c_s^2}\right)$
$4 \frac{G_{xy}}{E_y}$	$= \left(2 - \frac{V^2 H^2}{6l^2 c_s^2}\right)$
$\frac{E_y h^3}{12N_y}$	$= \frac{l^2}{2}$
$-\frac{p(x,y)}{N_y}$	$= \frac{B_z}{\mu}$

49

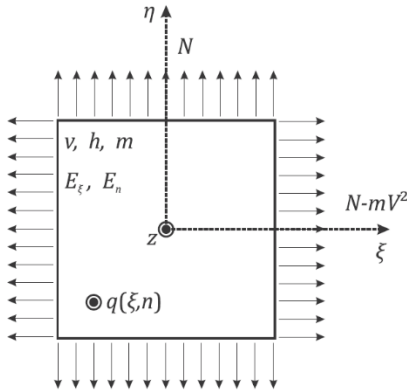
The analogue continues to the boundary conditions. Those are similar to the ones proposed in the static case, with the addition of some dynamic boundary condition (including initial conditions).

Giannakopoulos and Zisis (2019) studied this analogue. In this research the authors present the full analogy in a sketch in the following page.:

Obviously from the last relation 49, if  $N_\xi > N_\eta$  then the problem is subsonic, while if  $N_\xi < N_\eta$  the problem is supersonic.

One note that should be mentioned is that this manipulation of the plate equation from relation 47 to relation vii, helped the solution of the anti-plane problem. The opposite, solving an anti-plane couple stress elasticity problem, or a flexoelectric anti-plane problem and then obtain the solution for the analogue plate problem is possible, but unnecessary as the plate problem is usually the easy one to solve. There are a lot of tables in bibliography and also the plates are common to FEM codes.

Next in the last chapter, this theory will be used to solve the anti-plane flexoelectric dynamic problem of mode III crack, with the use of FEM.



Anti-plane Couple-Stress Elasticity	Pre-Stressed Plate
$w(\xi, \eta)$	$w(\xi, \eta)$
$\partial w / \partial \xi, \partial w / \partial \eta, \text{ etc}$	$\partial w / \partial \xi, \partial w / \partial \eta, \text{ etc}$
$\mu > 0$	$N_\eta / h, (N_\eta > 0)$
$-\beta, (-1 < \beta < 1)$	$\nu_\xi = \nu_\eta = \nu, (-1 < \nu < 1)$
$\frac{\ell^2}{2}, (\ell > 0)$	$D_\eta / N_\eta$
$1 - \rho V^2 / \mu$	$N_\xi / N_\eta$
$1 - \rho V^2 H^2 / (6\mu\ell^2)$	$D_\xi / D_\eta = E_\xi / E_\eta$
$2\rho / (\mu\ell^2)$	$m / D_\eta$
$2X_z / (\mu\ell^2)$	$q_{plate} / D_n$
$1 - \rho V^2 H^2 / (12\mu\ell^2)$	$(D_\xi \nu + D_\eta \nu + 4D_{\xi\eta}) / D_\eta$
$F_3$	$Z / h$
$m_{12}$	$M_\eta / h$
$m_{21}$	$-M_\xi E_\eta / (h E_\xi)$
$m_{22} = -m_{11}$	$-M_{\xi\eta} E_\eta / (2h G (1 + \nu))$ with $G = (E_\eta + E_\xi (1 - 2\nu)) / (4(1 - \nu^2))$
$m_{(xx)}$	$M^{(sn)} / h$
$\sigma_{13}$	$Q_\xi / h$
$\sigma_{23}$	$Q_\eta / h$
$P_3^{(n)}$	$V^{(n)} / h$
$R_\xi^{(n)}$	$M^{(n)} / h$

The prestressed plate. The Axial pre – tension depends on the velocity of the crack for  $\nu = 0$ . The Complete Analogue between the orthotropic prestressed plate and the anti – plane couple stress elasticity problem of a mode III crack.

Fig. 90. The complete analogue of the anti-plane problem and the plate problem. This scetch was obtained from [Giannakopoulos and Zisis \(2019\)](#).

## 7. FEM applications

As the previous chapter suggested, analogue 49 allows the solution of the couple elasticity problem, or the anti-plane flexoelectric problem, via a solution of plates. This analogue, for the elliptic problems is viable and computational solutions have already been made. The elliptic problem suggests that all the quantities of analogue 49 are positive, in respect of the anti-plane problem and thus the plate problem can be defined properly.

The three regions however, suggest the possibility, some of those constants to be negative. The intermediate problem suggests  $1 - V^2/c_s^2 < 0$ , while the hyperbolic problem also suggests  $1 - (V^2H^2)/(6l^2c_s^2) < 0$ . The second one is equivalent to  $E_x/E_y < 0$  in the plate problem. According to classic elasticity, however, the moduli of elasticity in an orthotropic material should be positive and thus the analogue seems like it cannot be used.

From the mathematical point of view, the problem is described by a linear partial differential equation, that should be solved with respect of  $w(\xi, \eta)$ :

$$A_1 \frac{\partial^4 w}{\partial \xi^4} + 2A_2 \frac{\partial^4 w}{\partial \xi^2 \partial \eta^2} + A_3 \frac{\partial^4 w}{\partial \eta^4} - \left( B_1 \frac{\partial^2 w}{\partial \xi^2} + B_2 \frac{\partial^2 w}{\partial \eta^2} \right) = P(\xi, \eta)$$

Where  $A_3 > 0$ ,  $B_2 > 0$ ,  $B_2 \geq B_1$  and  $A_2 > A_1$ . If  $A_1 > 0$  the problem is elliptic. If  $A_1 = 0$  the problem is parabolic. Both those cases have already been addresses by [Giannakopoulos and Zisis \(2019\)](#).

However, if  $A_1 < 0$  the problem is hyperbolic. To overcome this difficulty, a method inspired by the so called "Analogue Equation Method" that was originated in the context of Boundary Elements by [Katsikadelis \(1994\)](#) is suggested. The idea is to obtain some appropriate "body force"  $q(\xi, \eta)$  that will be common between the actual and the analogue equations (the analogue equation could be also parabolic). Two cases are distinguished.

- a.  $A_1 < 0$  and  $A_2 > 0$ .

Then the original equation splits into two analogue equations according to:

$$(0) * \frac{\partial^4 w}{\partial \xi^4} + 2A_2 \frac{\partial^4 w}{\partial \xi^2 \partial \eta^2} + A_3 \frac{\partial^4 w}{\partial \eta^4} - \left( (0) * \frac{\partial^2 w}{\partial \xi^2} + B_2 \frac{\partial^2 w}{\partial \eta^2} \right) - P(\xi, \eta) = q(\xi, \eta)$$

*and*

$$q(\xi, \eta) = -A_1 \frac{\partial^4 w}{\partial \xi^4} - 2 * (0) * \frac{\partial^4 w}{\partial \xi^2 \partial \eta^2} - (0) * \frac{\partial^4 w}{\partial \eta^4} + \left( B_1 \frac{\partial^2 w}{\partial \xi^2} + (0) * \frac{\partial^2 w}{\partial \eta^2} \right)$$

- b.  $A_1 < 0$  and  $A_2 < 0$ .

Then the original equation splits into two analogue equations according to:

$$(0) * \frac{\partial^4 w}{\partial \xi^4} + 2 * (0) * \frac{\partial^4 w}{\partial \xi^2 \partial \eta^2} + A_3 \frac{\partial^4 w}{\partial \eta^4} - \left( (0) * \frac{\partial^2 w}{\partial \xi^2} + B_2 \frac{\partial^2 w}{\partial \eta^2} \right) - P(\xi, \eta) = q(\xi, \eta)$$

and

$$q(\xi, \eta) = -A_1 \frac{\partial^4 w}{\partial \xi^4} - 2A_2 \frac{\partial^4 w}{\partial \xi^2 \partial \eta^2} - (0) * \frac{\partial^4 w}{\partial \eta^4} + \left( B_1 \frac{\partial^2 w}{\partial \xi^2} + (0) * \frac{\partial^2 w}{\partial \eta^2} \right)$$

Next, the materialization of the above analogue equations to prestressed Kirchhoff plate problem, takes place. This is the first applications of the “Analogue Equation Method” in the context of Finite Element.

### A. The two-plate method

The main idea is to use the equation 48 and in the term of the external loading, in addition to the analogue load produced from the anti-plane problem, an extra term should be added, the area load  $q(x, y)$ , from another plate that reinforces this original one. The governing equation of this original plate will be relation i.

$$\frac{E_x^{orig} \cdot h_{orig}^3}{12} w_{,xxxx}^{orig} + \frac{G_{xy}^{orig} \cdot h_{orig}^3}{3} w_{,xxyy}^{orig} + \frac{E_y^{orig} \cdot h_{orig}^3}{12} w_{,yyyy}^{orig}$$

$$- N_x^{orig} w_{,xx}^{orig} - N_y^{orig} w_{,yy}^{orig} \quad i$$

$$= p(x, y) + q(x, y)$$

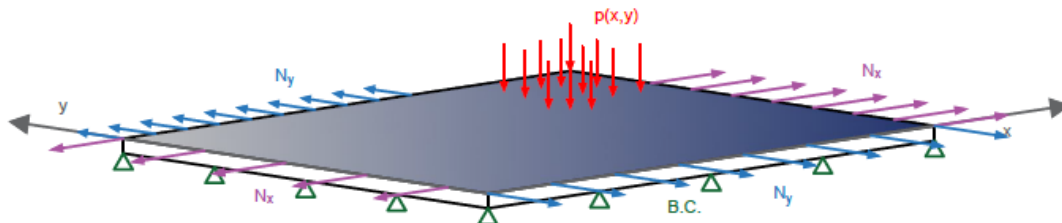


Fig. 91. The analogue plate to the anti-plane problem.

The plate should in any case be prestressed, biaxially and the prestress should be different between the directions. The plate should be constrained with the analogue's boundary conditions, that could be something else than hinges. The load  $p(x, y)$  should be also the analogue load of the anti-plane problem. The load should be applied in the necessary surface (e.g., for a mode III crack, it will be a line load)

The second plate, has also a governing equation that defines it.

$$\begin{aligned} & \frac{E_x^{rein} \cdot h_{rein}^3}{12} w_{,xxxx}^{rein} + \frac{G_{xy}^{rein} \cdot h_{rein}^3}{3} w_{,xxyy}^{rein} + \frac{E_y^{rein} \cdot h_{orig}^3}{12} w_{,yyyy}^{rein} \\ & - N_x^{rein} \cdot w_{,xx}^{rein} - N_y^{rein} \cdot w_{,yy}^{rein} \quad \text{ii} \\ & = q(x, y) \end{aligned}$$

The actions between them are action-reaction forces and thus the left hand-side of relation ii can be inserted into relation i, substituting the term of the action  $q(x, y)$ . Also, by considering the same plate thickness and the same out-of-plane displacement, the below relation is produced:

Original Plate		Reinforcing Plate		New Problem
$h_{og}$	=	$h_{rf}$	=	$h$
$w^{og}$	=	$w^{rf}$	=	$w$

$$\begin{aligned} & \frac{E_x^{og} h^3}{12} w_{,xxxx}^{og} + \frac{G_{xy}^{og} h^3}{3} w_{,xxyy}^{og} + \frac{E_y^{og} h^3}{12} w_{,yyyy}^{og} - N_x^{og} w_{,xx}^{og} - N_y^{og} w_{,yy}^{og} \\ & - \frac{E_x^{rf} h^3}{12} w_{,xxxx}^{rf} - \frac{G_{xy}^{rf} h^3}{3} w_{,xxyy}^{rf} - \frac{E_y^{rf} h^3}{12} w_{,yyyy}^{rf} + N_x^{rf} w_{,xx}^{rf} + N_y^{rf} w_{,yy}^{rf} \quad \text{iii} \\ & = p(x, y) \end{aligned}$$

The index  $rg$  represents the original plate, while the index  $rf$  represents the reinforcing plate. The suggestion that the out-of-plane displacement is common for the two plates, demands the connection between them to be rigid enough.

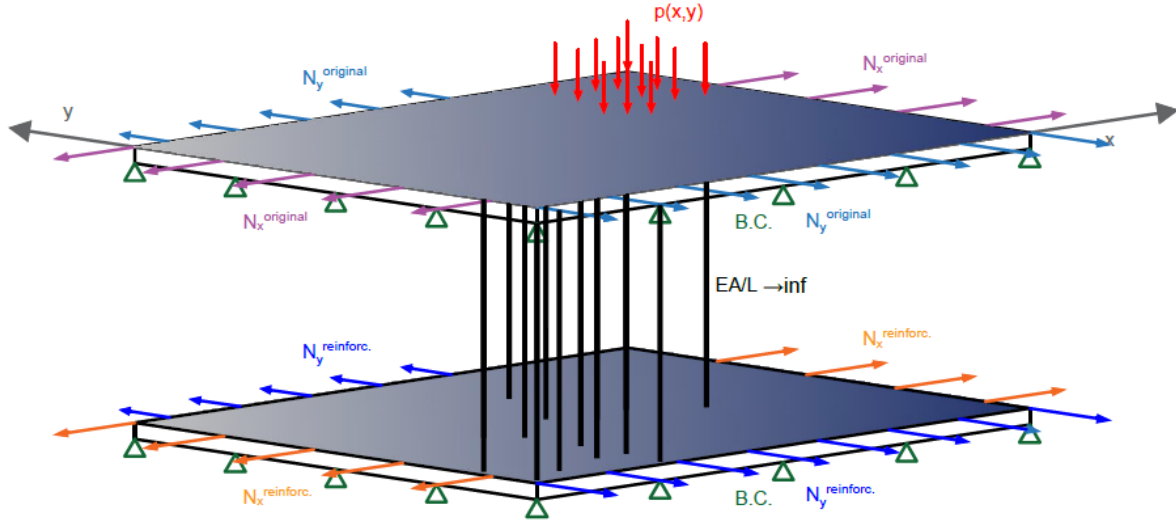


Fig. 92. The plate-like structure that can be inserted to the analogue.

The above plate, that is called original plate is the plate in which the analogue load is being applied. That can be seen in relation i. One second plate, similar to the first, but without the analogue load, is connected with a rigid manor, to the original plate.

The reinforcing (below plate) could be prestressed or not, orthotropic or isotropic (the calculations will provide these information).

The limitation: "rigid" should demand the out-of-plane displacement in both plates to be zero. As only the out-of-plane displacement is demanded to be constrained, those connectors can be short truss elements with great modulus of elasticity and cross-section area. Those connectors should be placed close enough, so their reaction can be considered the common surface load  $q(x, y)$ .

By applying some calculation in relation iii, the following relation is produced:

$$\begin{aligned} & \frac{(E_x^{og} - E_x^{rf})h^3}{12} w_{,xxxx} + \frac{(G_{xy}^{og} - G_{xy}^{rf})h^3}{3} w_{,xxyy} + \frac{(E_y^{og} - E_y^{rf})h^3}{12} w_{,yyyy} \\ & - (N_x^{og} - N_x^{rf})w_{,xx} - (N_y^{og} - N_y^{rf})w_{,yy} \\ & = p(x, y) \end{aligned} \quad \text{iv}$$



And by reordering, with the purpose that relation iv will look like relation vii (chapter 6), the following is produced:

$$\begin{aligned} & \frac{(N_x^{og} - N_x^{rf})}{(N_y^{og} - N_y^{rf})} \frac{\partial^2 w}{\partial x^2} + \frac{\partial^2 w}{\partial y^2} \\ & - \frac{(E_x^{og} - E_x^{rf})h^3}{(N_y^{og} - N_y^{rf})12} \frac{\partial^4 w}{\partial x^4} - \frac{(G_{xy}^{og} - G_{xy}^{rf})h^3}{(N_y^{og} - N_y^{rf})3} \frac{\partial^4 w}{\partial x^4} - \frac{(E_y^{og} - E_y^{rf})h^3}{(N_y^{og} - N_y^{rf})12} \frac{\partial^4 w}{\partial x^2 \partial y^2} \quad \text{v} \\ & = - \frac{p(x,y)}{(N_y^{og} - N_y^{rf})} \end{aligned}$$

The analogue, according to relation v can be modified as follows:

<i>Prestressed Plate problem</i>		<i>Anti – plane flexoelectric problem</i>	
$\frac{(N_x^{og} - N_x^{rf})}{(N_y^{og} - N_y^{rf})}$	=	$1 - \frac{V^2}{c_s^2}$	vi
$\frac{(E_x^{og} - E_x^{rf})h^3}{(N_y^{og} - N_y^{rf})12}$	=	$\frac{l^2}{2} \left( 1 - \frac{V^2 H^2}{6l^2 c_s^2} \right)$	vii
$\frac{(G_{xy}^{og} - G_{xy}^{rf})h^3}{(N_y^{og} - N_y^{rf})3}$	=	$\frac{l^2}{2} \left( 2 - \frac{V^2 H^2}{6l^2 c_s^2} \right)$	viii
$\frac{(E_y^{og} - E_y^{rf})h^3}{(N_y^{og} - N_y^{rf})12}$	=	$\frac{l^2}{2}$	ix
$= - \frac{p(x,y)}{(N_y^{og} - N_y^{rf})}$	=	$\frac{B_z}{\mu}$	

And with the use of relation ix, relation vii and viii can be simplified a bit. The following analogue can replace analogue 49. The advantage of this new analogue is that it is not bounded by signs as the modified moduli that are analogue with the anti-plane flexoelectric parameters can be also negative and so the intermediate and the hyperbolic region are accessible. The new, modified analogues can be described by the following relations:

<i>Prestressed Plate problem</i>	<i>Anti – plane flexoelectric problem</i>
$\frac{(N_x^{og} - N_x^{rf})}{(N_y^{og} - N_y^{rf})}$	$= 1 - \frac{V^2}{c_s^2}$
$\frac{(E_x^{og} - E_x^{rf})(N_y^{og} - N_y^{rf})}{(N_y^{og} - N_y^{rf})(E_y^{og} - E_y^{rf})}$	$= \left(1 - \frac{V^2 H^2}{6l^2 c_s^2}\right)$
$4 \frac{(G_{xy}^{og} - G_{xy}^{rf})(N_y^{og} - N_y^{rf})}{(N_y^{og} - N_y^{rf})(E_y^{og} - E_y^{rf})}$	$= \left(2 - \frac{V^2 H^2}{6l^2 c_s^2}\right)$
$\frac{(E_y^{og} - E_y^{rf})h^3}{(N_y^{og} - N_y^{rf})12}$	$= \frac{l^2}{2}$
$-\frac{p(x, y)}{(N_y^{og} - N_y^{rf})}$	$= \frac{B_z}{\mu}$

50

By considering that the reinforcing plate, is not prestressed, analogue 50 is modified as follows (analogue 51):

<i>Prestressed Plate problem</i>	<i>Anti – plane flexoelectric problem</i>
$\frac{N_x^{og}}{N_y^{og}}$	$= 1 - \frac{V^2}{c_s^2}$
$\frac{(E_x^{og} - E_x^{rf})}{(E_y^{og} - E_y^{rf})}$	$= \left(1 - \frac{V^2 H^2}{6l^2 c_s^2}\right)$
$4 \frac{(G_{xy}^{og} - G_{xy}^{rf})}{(E_y^{og} - E_y^{rf})}$	$= \left(2 - \frac{V^2 H^2}{6l^2 c_s^2}\right)$
$\frac{(E_y^{og} - E_y^{rf})h^3}{(N_y^{og} - N_y^{rf})12}$	$= \frac{l^2}{2}$
$-\frac{p(x, y)}{N_y^{og}}$	$= \frac{B_z}{\mu}$

51

These simplifications, allows for a better finding of the right parameters but may limit the cases as well. From analogue 51 it seems that the problem resided with the following methodology:

- Find the prestress of the plate that calibrates the velocity of the anti-plane dynamic problem.
- Find the combination of the Elasticity moduli that calibrate the hyperbolicity.
- Modify the shear moduli to conclude the analogue.

### B. The FEM model

Using the FEM program **ABAQUS**, some numerical calculations were possible. In this program the plate structures were made, both, from orthotropic materials and connected with truss elements of great stiffness (short and with an enormous modulus of elasticity). The plate thickness and the cross-section of the truss elements were considered small enough. The connection of the two plates, with the truss elements, was done in every finite element (on the nodes of it).

More specifically, about the FEM model:

- The original and the reinforcing plate was made from a 3D (deformable) homogeneous shell (planar) element of thickness  $h = 0.001$ . The other dimensions were set to  $0.2 \times 0.1$ .
- The materials of both plates, were defined as orthotropic, with each constant defined according to the analogue.
- The element type for the two plates, was a shell element, cubic, with four nodes.
- The integration points were defined to be five, using the Simpson's method.
- The connectors were defined as truss elements, with a cross-section of  $A = 10^{-6}$ .
- The material of the connectors was set as isotropic, with a modulus of elasticity orders greater than the material of the plate (the biggest) and zero Poisson's ratio. In the next analysis the material constant was set by "try an error". For bigger moduli than the desired, mathematical instabilities messed with the results and for smaller, the connectors were deformed greatly.
- The FEM model was using square elements with side equal to 0.001.
- The joining of the elements should be done only as geometrical.
- The boundary conditions and the applied load to the plate were left to be chosen via the analogue.

Sketches about the FEM model can be seen in [fig. 93](#).

The analysis would be set as non-linear, with one step. The load would be applied in two phases. Firstly, the pre-stress would be applied first and would affect the element (this is not demanded by the theory, however, if not, the program would not understand the prestress) and then the out-of-plane loading would be applied, for the out-of-plane deformation to be produced.

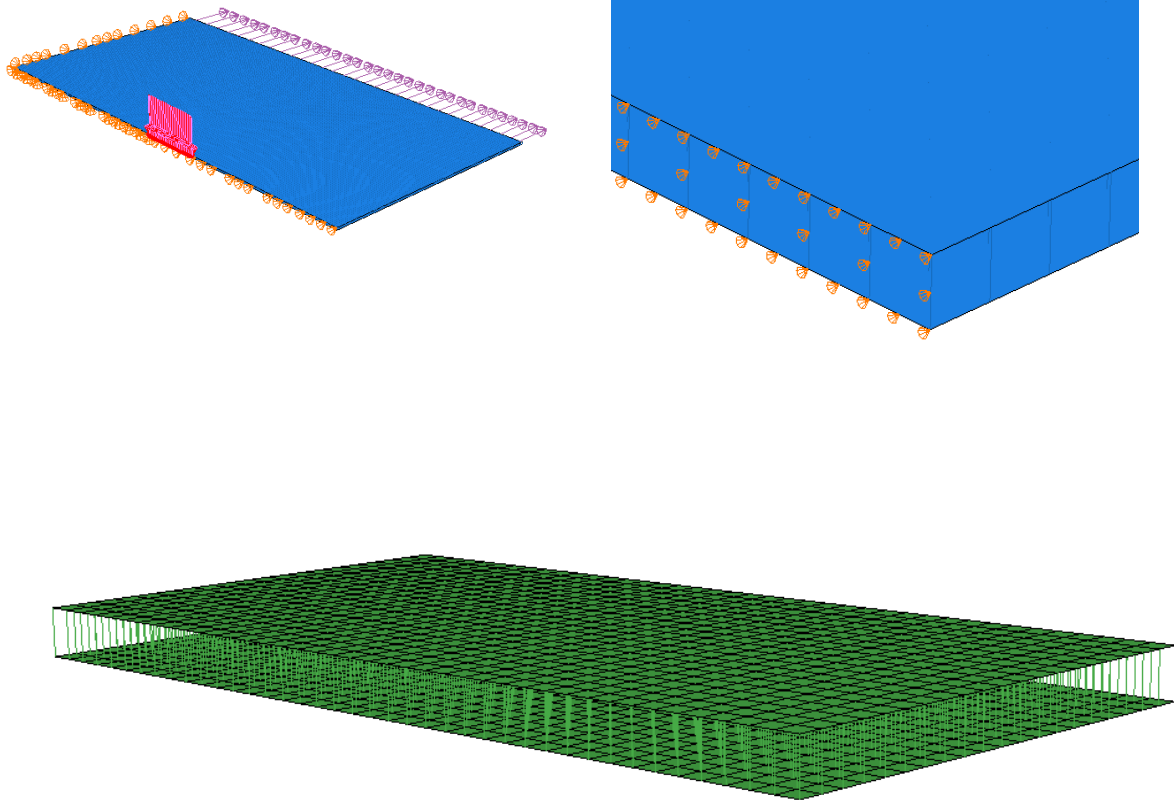


Fig. 93. Sketches from the FEM model.

### C. The cases

As it was mentioned already before, the elliptic region (the region for which analogue 49 applies) is a region well studied (chapter 3). The purpose of this chapter is to study cases where the anti-plane problem is hyperbolic, or even intermediate.

The main study of this chapter will focus on the hyperbolic problem, analyzing some cases. The hyperbolic problem, is defined for combinations of velocity and microstructure, that has a result  $1 - (V^2 H^2)/(6l^2 c_s^2) < 0$ . Three cases will be studied:

- Case 1: A purely hyperbolic case, for which  $V^2/c_s^2 = 1$ ,  $H/(l\sqrt{6}) = 2$
- Case 2: An elliptic – hyperbolic case, for which  $V^2/c_s^2 = 0.25$ ,  $H/(l\sqrt{6}) = 2$
- Case 3: An Intermediate – hyperbolic case, for which  $V^2/c_s^2 = 1$ ,  $H/(l\sqrt{6}) = 2$

These scenarios of combinations, all exist in the hyperbolic region, as it can be seen in figure 94 and thus the FEM model that was proposed on chapter 7.A, that uses the analogue 51 will be used.

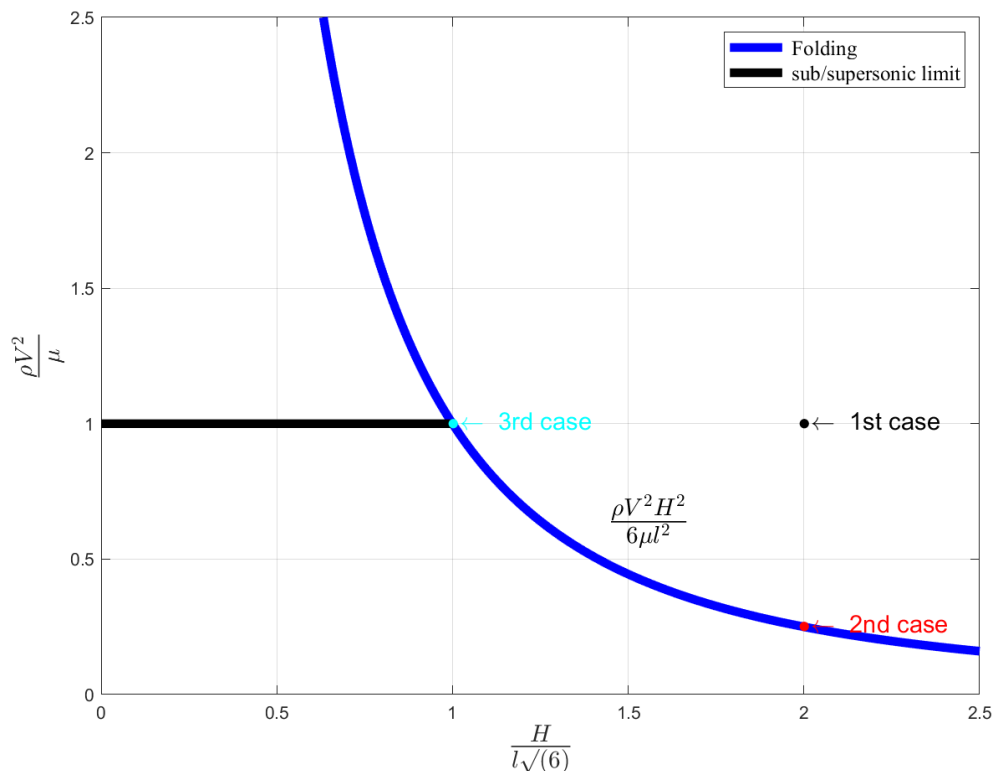


Fig. 94. Cases 1, 2 and 3 and their position in the hyperbolic region.

Case 1 is a purely hyperbolic case, while case 2 and 3 shows some ellipticity. Case 2 is in the boundary of the hyperbolic and the elliptic region and should prohibit behavior elliptic like (figure 27 and figure 28), while case 3 is in the boundary of all three regions, as its velocity is also sonic.

For those problems, one thing is left to be decided, the boundary conditions. A mode III crack, which is an anti-plane 3D problem, is defined by some boundary conditions. Those conditions should be moved to the analogue plate problem, so some restrains can be inserted in the FEM applications. (Those restrains are better to be imported for both plates, however, the rigid connector will correct it). In the following figures (figure 95, 96, 97) those restrains are being discussed.

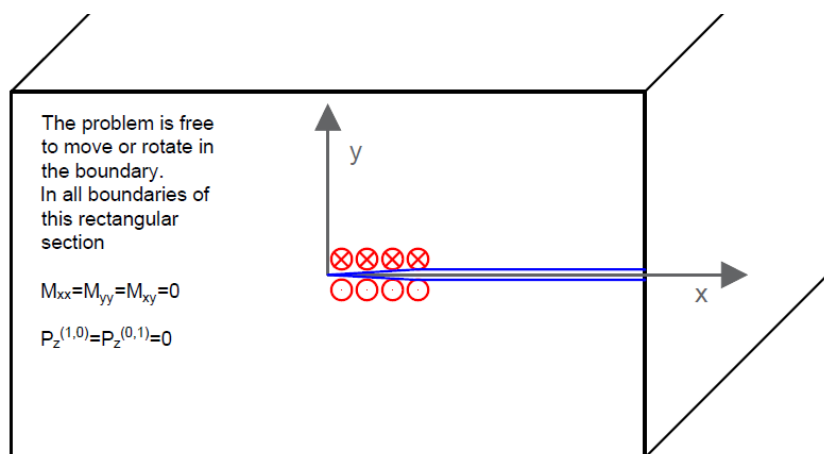


Fig. 95. The anti-plane problem and its boundary conditions.

The edges in a mode III problem, could be free to move, or rotate. The anti-plane load is applied in the crack, for a specific length.

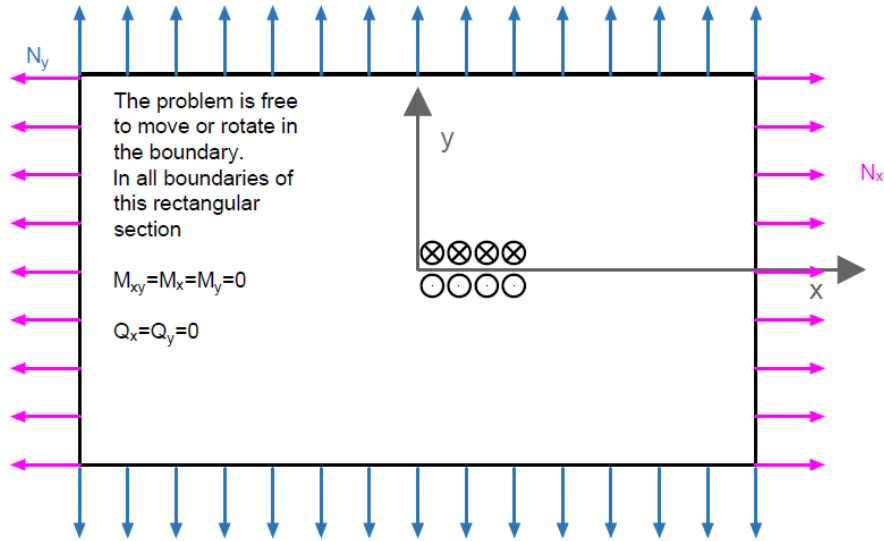


Fig. 96. The plate restrains.

Because of the analogue suggested, no boundary conditions are needed. This, however suggests a stability issues and must be treated.

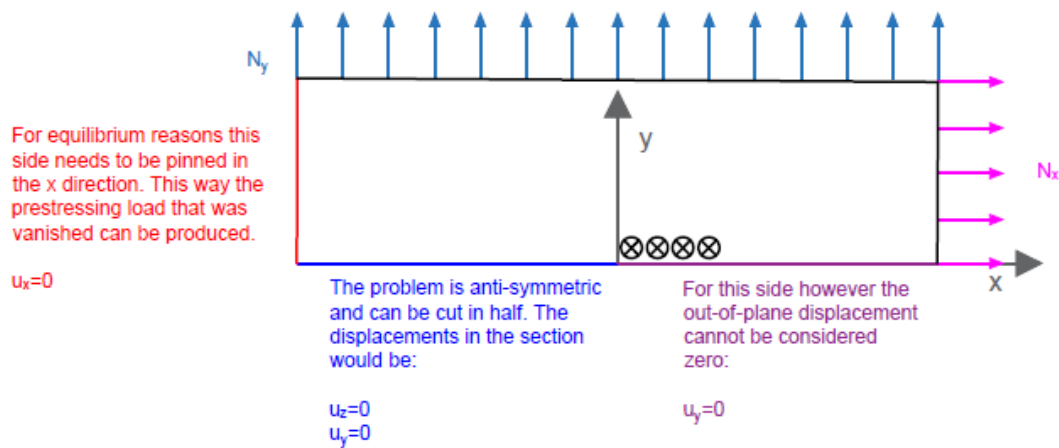


Fig. 97. The boundary condition of the final model.

Using the obvious anti-symmetry, some boundary conditions that make the plate stable, can be extruded. Also, the prestress from the one direction can be replaced with analogue restrains. This way the plate is stable and can be solved.

**i. The purely hyperbolic case.**

Using the analogue 51, a system of some unknown variables is produced:

$$\frac{N_x^{og}}{N_y^{og}} = 1 - \frac{V^2}{c_s^2} = 0 \quad \text{x}$$

$$\frac{(E_x^{og} - E_x^{rf})}{(E_y^{og} - E_y^{rf})} = \left(1 - \frac{V^2 H^2}{6l^2 c_s^2}\right) = -3 \quad \text{xi}$$

$$4 \frac{(G_{xy}^{og} - G_{xy}^{rf})}{(E_y^{og} - E_y^{rf})} = \left(2 - \frac{V^2 H^2}{6l^2 c_s^2}\right) = -2 \quad \text{xii}$$

An obvious solution of relation **x** suggests that  $N_x^{og} = 0$ ,

As for relation **xi**, choosing  $E_x^{og} = E_y^{og} = 10000$  and  $E_y^{rf} = 0$  demands  $E_x^{rf} = 40000$ .

Lastly by considering  $G_{xy}^{og} = 0$ , in order relation **xii** to hold true  $G_{xy}^{rf} = 5000$ .

According to the above, the purely hyperbolic problem can be described from the beneath moduli.

<i>Prestress</i>	$N_x^{og} = 0$	$N_y^{og} \neq 0$	
<i>Original Mat.</i>	$E_x^{og} = 10000$	$E_y^{og} = 10010$	$G_{xy}^{og} = 10$ <span style="float: right;">52</span>
<i>Reinforc. Mat.</i>	$E_x^{rf} = 40000$	$E_y^{rf} = 10$	$G_{xy}^{rf} = 5010$

The same system however, can be solved for a different combination of moduli.

<i>Prestress</i>	$N_x^{og} = 0$	$N_y^{og} \neq 0$	
<i>Original Mat.</i>	$E_x^{og} = 10000$	$E_y^{og} = 1010$	$G_{xy}^{og} = 10$ <span style="float: right;">53</span>
<i>Reinforc. Mat.</i>	$E_x^{og} = 13000$	$E_y^{rf} = 10$	$G_{xy}^{rf} = 510$

By applying those moduli, to the model created for this scope, the beneath results are visible:

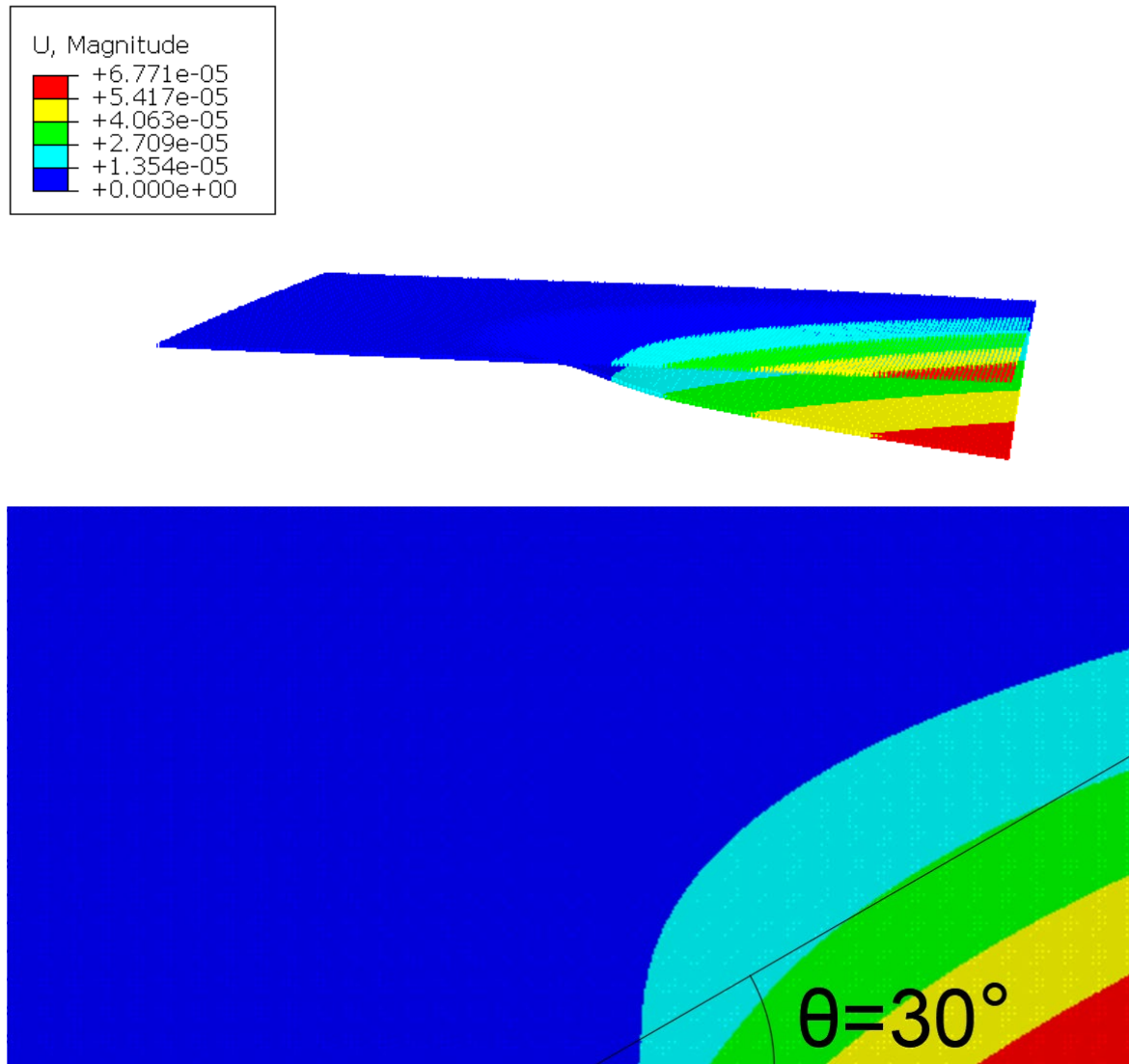


Fig. 98. The out-of-plane displacement for the 1<sup>st</sup> case, the first alternative.

For the combination of moduli 52 the out-of-plane displacement form Mach cones. The angle of those cones can be measured as 30 degrees, the same that can be calculated from relation 19. The modulus of elasticity of the connectors for this scenario was set to  $8 * 10^9$ . For greater moduli, mathematical instabilities occurred, while for smaller, the connectors were not as effective as desired.



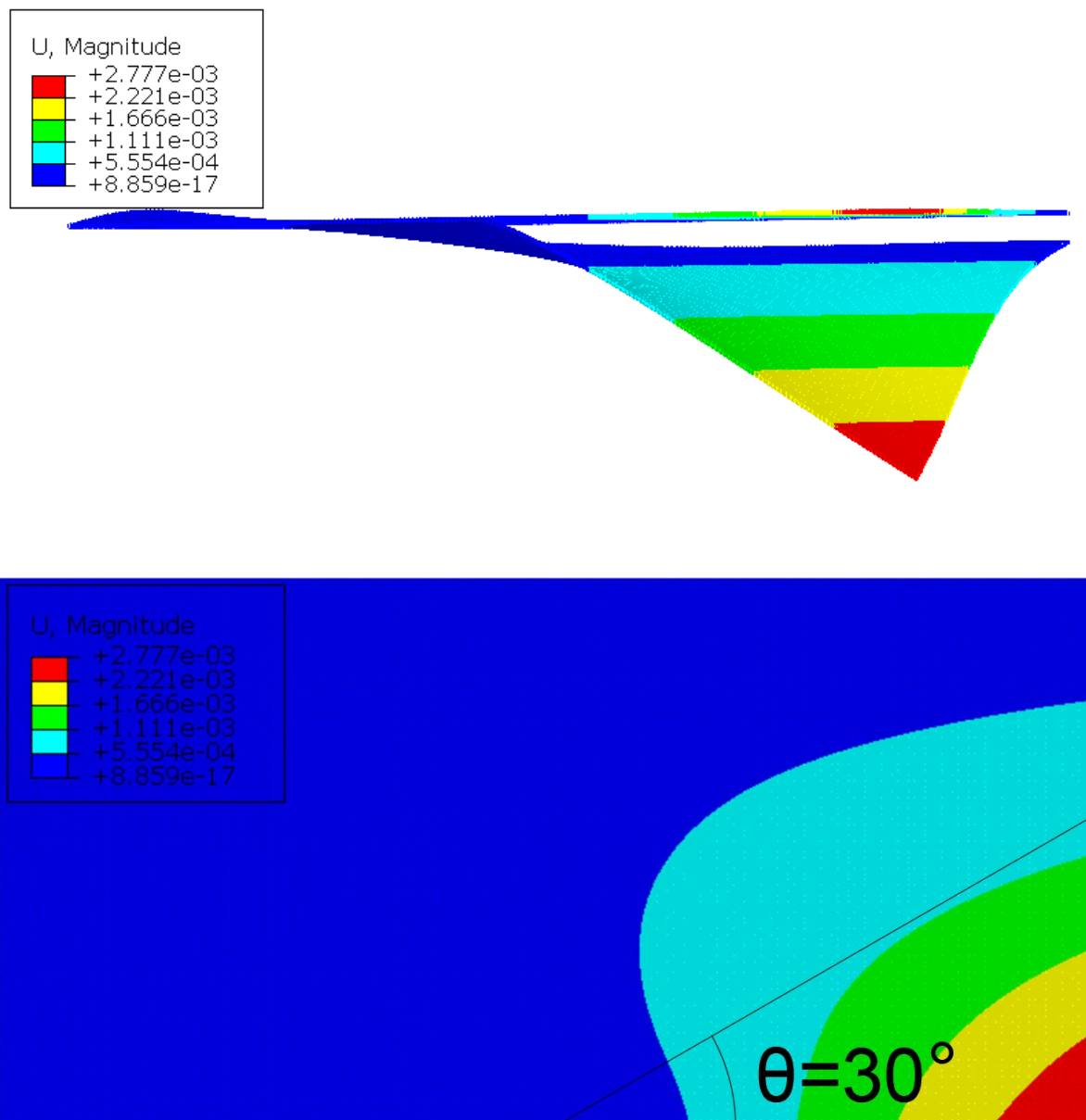


Fig. 99. The out-of-plane displacement for the 1<sup>st</sup> case, the second alternative.

For the combination of moduli 53, the displacement formed similar Mach cones (the angle is briefly bigger), while the moduli were greatly different. The modulus of elasticity of the connectors was set to  $2 \cdot 10^9$ . Further studies about the angle of the Mach cones are suggested. Some difference between the theoretical angle and the calculated angle could be due to the finite plate, and connections. Were the model infinite, then the angles should be more accurate.

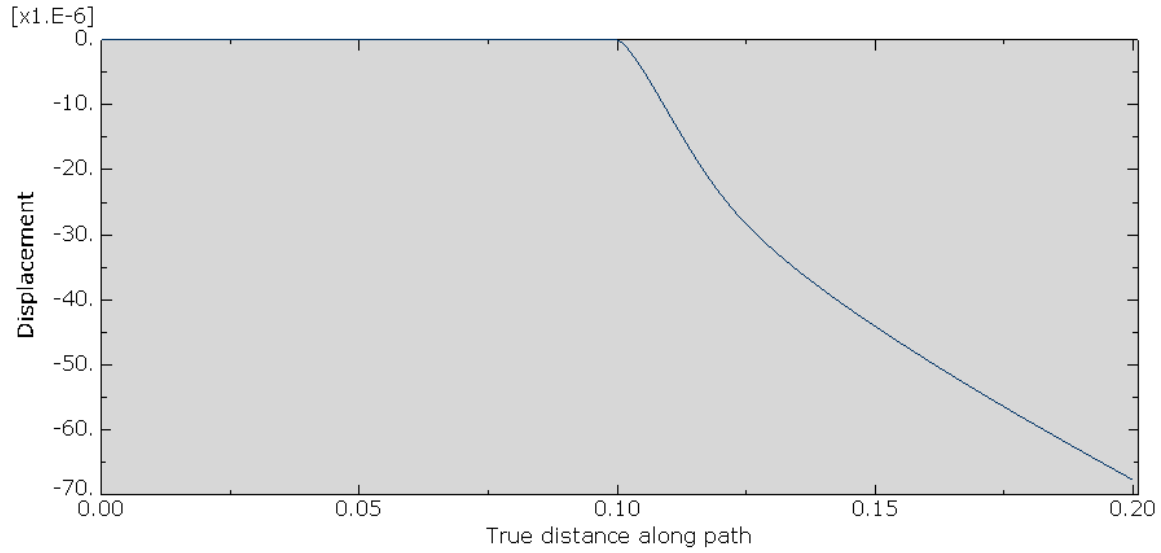


Fig. 100. The profile of the crack in the purely hyperbolic case. Under no circumstances the displacement is going to fade for greater lengths (as the hyperbolicity suggests).

## ii. The elliptic – hyperbolic case

For this case, the system that needs to be solved is the following:

$$\frac{N_x^{og}}{N_y^{og}} = 1 - \frac{V^2}{c_s^2} = 0.75$$

$$\frac{(E_x^{og} - E_x^{rf})}{(E_y^{og} - E_y^{rf})} = \left(1 - \frac{V^2 H^2}{6l^2 c_s^2}\right) = 0$$

$$4 \frac{(G_{xy}^{og} - G_{xy}^{rf})}{(E_y^{og} - E_y^{rf})} = \left(2 - \frac{V^2 H^2}{6l^2 c_s^2}\right) = 1$$

One of the combinations for which the above system holds true, is the following:

<i>Prestress</i>	$N_x^{og} = 7.5 * 10^{-8}$	$N_y^{og} = 10^{-7}$	
<i>Original Mat.</i>	$E_x^{og} = 10000$	$E_y^{og} = 10010$	$G_{xy}^{og} = 2510$
<i>Reinforc. Mat.</i>	$E_x^{rf} = 10000$	$E_y^{rf} = 10$	$G_{xy}^{rf} = 10$

The results are the following:

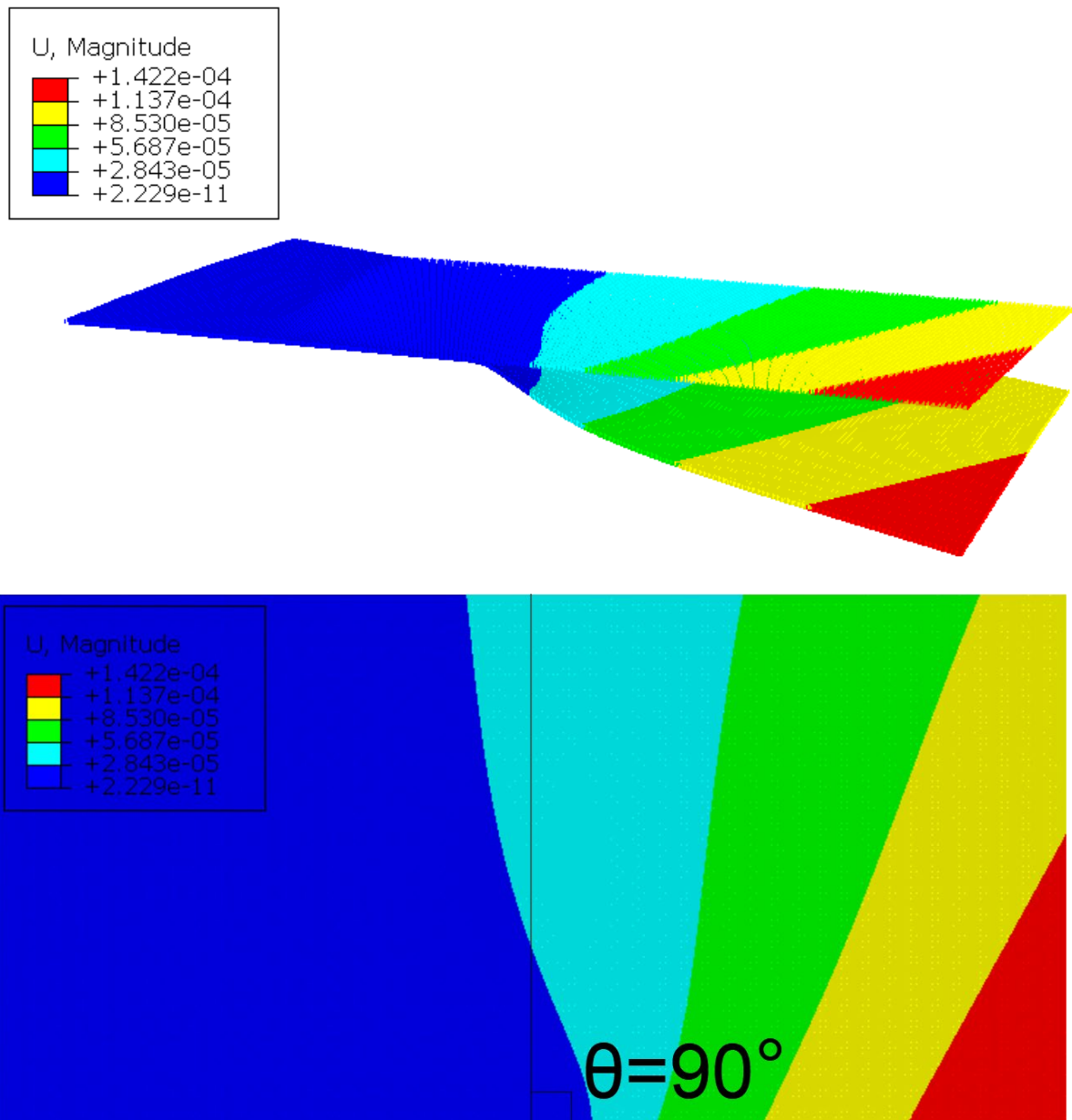


Fig. 101. The out-of-plane displacement for 2<sup>nd</sup> case.

For the combination of moduli (54), the modulus of elasticity of the connectors was set to  $0.5 \cdot 10^9$ . Mach cones seems to be created. Relation 19 suggested that the slope should be 90 degrees.

### iii. The intermediate - hyperbolic case

Lastly, for this case the below system should hold true:

$$\frac{N_x^{og}}{N_y^{og}} = 1 - \frac{V^2}{c_s^2} = 0$$

$$\frac{(E_x^{og} - E_x^{rf})}{(E_y^{og} - E_y^{rf})} = \left(1 - \frac{V^2 H^2}{6l^2 c_s^2}\right) = 0$$

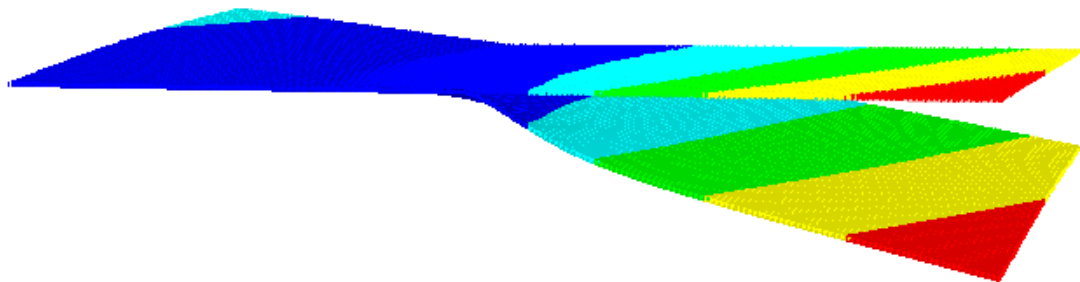
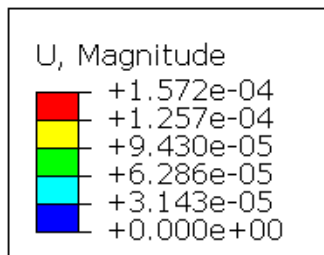
$$4 \frac{(G_{xy}^{og} - G_{xy}^{rf})}{(E_y^{og} - E_y^{rf})} = \left(2 - \frac{V^2 H^2}{6l^2 c_s^2}\right) = 1$$

This system has a a solution the following combination:

Prestress	$N_x^{og} = 0$	$N_y^{og} \neq 0$	
Original Mat.	$E_x^{og} = 10000$	$E_y^{og} = 10010$	$G_{xy}^{og} = 2510$
Reinforc. Mat.	$E_x^{rf} = 10000$	$E_y^{rf} = 10$	$G_{xy}^{rf} = 10$

55

The results are the following:



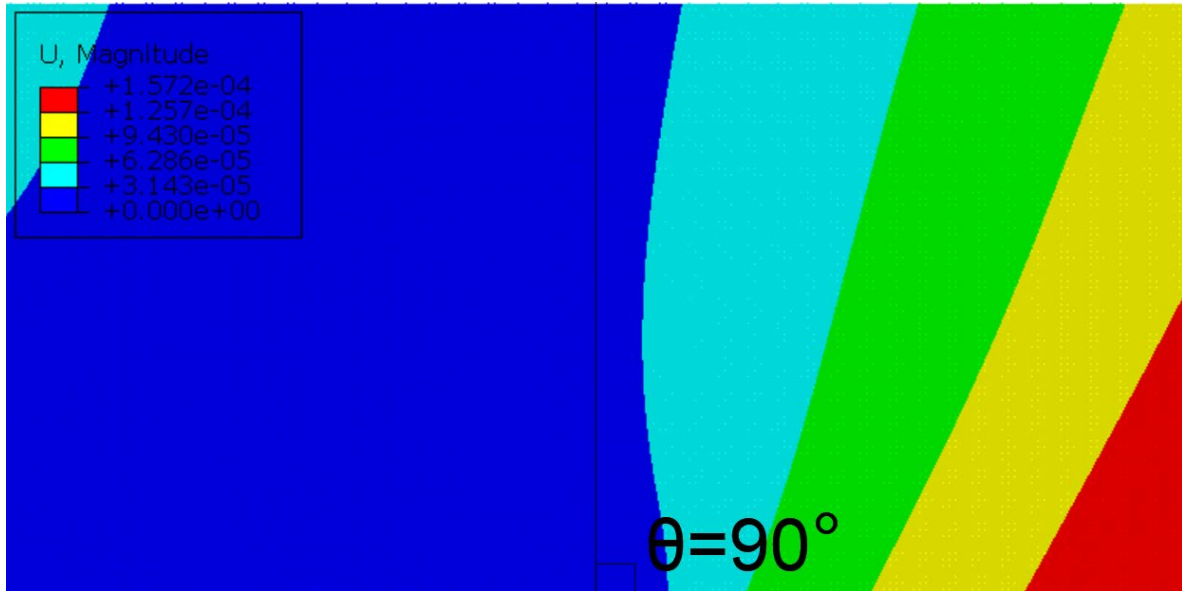


Fig. 102. The out-of-plane displacement for 3<sup>rd</sup> case.

For the combination of moduli (55), the modulus of elasticity of the connectors was set to  $0.5 \cdot 10^9$ . Mach cones seems to be created. Relation 19 suggested the slope should be 90 degrees.

## 8. Epilogue

Flexoelectricity, an extremely promising physical aspect that applies to any dielectric is responsible for the generation of electrical polarization in a material while mechanically stressed and proposes a wide variety of applications. These could be energy harvesting, active vibration control, health structure monitoring, and others, all of them applications to be seen a lot in the future. Flexoelectricity allows the construction of smart devices in buildings such as sensors and actuators. Earthquake isolation could also be benefited. There are the so-called FPS (Friction Pendulum System) isolators and even in some large structures like bridges the isolation enables some connections to break during an earthquake, so, when the lateral load is small the structure can stay still, but for higher loads, the connections allow the displacements to increase and so the actions are reduced (something like active vibration control). Flexoelectricity could improve those systems.

The reverse flexoelectric effect, producing strain gradient from electric polarization implies that, flexoelectricity should be taken into consideration in the formulation of the total energy density, and contribute to the constitutive laws. With this in mind, it is feasible to derive the governing equation of many problems such as the anti-plane flexoelectric problem. Anti-plane problems are extremely frequent in structural analysis, concerning reinforced concrete or metal structures, earthquake engineering and composite materials. In this simplified formulation, the polarization can be calculated.

### A. The research

In this research the flexoelectric effect in the anti-plane dynamic problem of the mode III crack was studied. The static problem however is included in the more general dynamic problem. For the formulation of the governing equation the total energy density was used. This way two equations (3 including the Maxwell's equation) were derived. One concerning the out-of-plane displacement of the anti-plane problem, and one which allows the calculation of the out-of-plane polarization.

The formulation of the equation referring to the displacement (which is similar to the governing equation of a normal anti-plane couple stress elasticity problem), allows the distinction of the problem in three regions, the elliptic, the intermediate and the hyperbolic. For the hyperbolic region the displacement can be calculated using a method of the characteristics and a Mach cone – like displacement can be suggested. The known displacement allows the calculation of the polarization. As it was proven the maximum polarization is visible on the crack tip, and at the end of the cohesion zone. Those two points are possible locations of electrical yielding (abrupt change of the polarization vector).

Flexoelectricity in a dynamic problem like the mode III crack can be combined with the propagation of waves, both mechanical because of the displacement and optical because of the polarization. The flexoelectric material is dispersive and thus the dispersion of the produced waves was also studied. It is known that electromagnetic waves are emitted in an earthquake. Earthquakes are due to the cracks at the flexoelectric earth's mantle. Therefore, a seismic action produces waves.

Lastly, as a similarity of the anti-plane flexoelectric problem and the prestressed Kirchhoff plate was observed, an analogue was used for numerical solution (FEM) of an anti-plane flexoelectric problem of a mode III crack. More specifically, inspired by the Analogue Equation Method, originally referred to the Boundary Elements, a methodology using two analog plates, instead an original one, enables the numerical calculation of the hyperbolic problem.

For the hyperbolic anti-plane problem, the displacement was proved numerically to form Mach cones. Those cones were created with respect of a pre-defined angle, for which the moduli of elasticity and the prestress action contributed.

Conclusively, solving an anti-plane problem, whether it is defined for flexoelectric or for the theory of couple stress elasticity, is analogue to solving a prestressed Kirchhoff plate. This analogue that was suggested in the bibliography, also seems to apply in the hyperbolic anti-plane problem, that reduces to a couple of parabolic plates.

## **B. Vision**

The flexoelectric anti-plane problem was shown to be extremely prominent. Experimental studies have yet to come. The connection of flexoelectricity with the propagation of waves is also promising. Rayleigh or Stoneley waves could be investigated with flexoelectricity. Yet, except for the mode III crack, there are other anti-plane problems that can be investigated with flexoelectricity like the bar pull-out which is an anti-plane problem and could be studied further.

Regarding the phenomenon of flexoelectricity my vision includes smart buildings, using this effect for various applications. Smart isolations (active vibration control) could be used to cope with seismic loading, or accidental loads. The reverse flexoelectric effect could be used to improve the mechanical capabilities of the materials during those loading conditions. From an energy concerning perspective, a building could harvest some electrical work produced due to oscillatory loading like the wind.

One noticeable application of flexoelectricity, and more specifically the anti-plane problem of a mode III crack, is to act as a sensor that signals when a crack appears and so a repair is needed. Cracks are usual in civil engineering structures, like in a concrete section, near a hole in a concrete or a steel element and near the arc welding of a steel section. Flexoelectricity could provide a signal to notify the incident of failure.

The above, however, need a further study of the phenomenon and optimization. This is my aspiration for the future, as this phenomenon has proved worthy of studying. Experimental research should be used to calibrate the theories. The study of problems similar to the anti-plane problem is desired, and can have important applications in the fields of structural, micromechanical, mechanical, or electromechanical engineering.

## 9. Appendices

### A. The governing equations of the anti-plane flexoelectric problem

For a centrosymmetric cubic crystal structure, the energy density containing terms of strains energy and polarizations can be written as follows:

$$U = \frac{1}{2} \left[ aP_3^2 + (b_{44} + b_{77})(P_{3,1}^2 + P_{3,2}^2) + 2e_{44} \left( (\varepsilon_{13} + \varepsilon_{31})P_{3,1} + (\varepsilon_{23} + \varepsilon_{32})P_{3,2} \right) \right. \\ \left. + 2f_{12} \left( (\varepsilon_{13,1} + \varepsilon_{31,1})P_3 + (\varepsilon_{23,2} + \varepsilon_{32,2})P_3 \right) + 2\mu(\varepsilon_{13}\varepsilon_{31} + \varepsilon_{23}\varepsilon_{32}) \right] \quad \text{A.1}$$

This formula was proposed by [Giannakopoulos and Zisis \(2019\)](#) and modified a bit and was also used in their later studies ([Giannakopoulos and Zisis \(2020 a, b\)](#)). This formula is a little peculiar. It contains terms of polarizations and polarization gradient, strain and strain gradient. Some of them, however, are missing and this is because of the anti-plane problem theory, which demands some displacements to be zero (and also some polarizations can be considered equal to zero because of the electric anti-plane problem).

$$u_x = u_1 \equiv 0$$

$$u_y = u_2 \equiv 0$$

$$u_z \equiv w(x, y) = u_3 \equiv w(x_1, x_2) \neq 0$$

And because only one displacement exists and this is independent from its corresponding direction, the strains are all zero except some shear strains.

$$\varepsilon_{11} = \frac{1}{2} \left( \frac{\partial u_1}{\partial x_1} + \frac{\partial u_1}{\partial x_1} \right) = 0$$

$$\varepsilon_{22} = \frac{1}{2} \left( \frac{\partial u_2}{\partial x_2} + \frac{\partial u_2}{\partial x_2} \right) = 0$$

$$\varepsilon_{33} = \frac{1}{2} \left( \frac{\partial u_3}{\partial x_3} + \frac{\partial u_3}{\partial x_3} \right) = \frac{\partial w(x_1, x_2)}{\partial x_3} = 0$$

$$\varepsilon_{12} = \varepsilon_{21} = \frac{1}{2} \left( \frac{\partial u_1}{\partial x_2} + \frac{\partial u_2}{\partial x_1} \right) = 0$$

$$\varepsilon_{13} = \varepsilon_{31} = \frac{1}{2} \left( \frac{\partial u_1}{\partial x_3} + \frac{\partial u_3}{\partial x_1} \right) = \frac{1}{2} \frac{\partial w(x_1, x_2)}{\partial x_1}$$



$$\varepsilon_{23} = \varepsilon_{32} = \frac{1}{2} \left( \frac{\partial u_2}{\partial x_3} + \frac{\partial u_3}{\partial x_2} \right) = \frac{1}{2} \frac{\partial w(x_1, x_2)}{\partial x_2}$$

Those are the strains that exist in the above relations. Also, their gradients are non-zero (with the exception of the strain gradient  $\varepsilon_{13,2} = \varepsilon_{31,2} = \varepsilon_{32,3} = \varepsilon_{23,3} = 0$ ) because as the strain is a function of the two in-plane coordinates, so are their gradients.

From now on, those strains will be referred as shown below:

$$\varepsilon_{13} = \varepsilon_{31} = \frac{1}{2} u_{3,1}$$

$$\varepsilon_{23} = \varepsilon_{32} = \frac{1}{2} u_{3,2}$$

$$\varepsilon_{13,1} = \varepsilon_{31,1} = \frac{1}{2} u_{3,11}$$

$$\varepsilon_{23,2} = \varepsilon_{32,2} = \frac{1}{2} u_{3,22}$$

The cross-section shear strain gradient  $\varepsilon_{13,2} = \varepsilon_{31,2} = \frac{1}{2} u_{3,12}$  and  $\varepsilon_{23,1} = \varepsilon_{32,1} = \frac{1}{2} u_{3,21}$ , were not neglected because of the anti-plane problem theory, as they are not zero. However, in the formula of the energy density they are coupled with polarizations that do not exist because of the anti-plane formulation.

Similar to the anti-plane displacement the polarization can be also considered:

$$P_1 = P_2 = 0$$

$$P_3 = P(x, y)$$

This means that also the only non-zero polarization gradients are the  $P_{3,1}$  and  $P_{3,2}$ .

From this point, the use of Toupin's Variational Principle, described in [Mindlin \(1968\)](#) will be the tool to extract the governing equations that describes the problem. Toupin's Variational Principle is similar to the principle of virtual work, with the exception of the electricity. With the addition of electricity, the integrals should be specified carefully. As electricity is concerned, the boundary of the body is not the end of the space, (as it can be considered, when only mechanical works are in place) but just a surface that separates the space into parts.

The total space, can be symbolized as  $V^*$  and is consisted of the space  $V$  that contains the body and  $V'$  that does not. The surface that separates  $V$  from  $V^*$  is the surface  $S$ .

$$\delta \int_{V^*} -H dV + \int_V (f_i \delta u_i + E^0_i \delta P_i) dV + \int_S t_i \delta u_i dt = 0 \quad \text{A.2}$$

- $H$ : is the total electric enthalpy density, which can contain terms of total energy density of deformations or polarization.  $H = U - \frac{1}{2} \varepsilon_0 (\Phi_{,i}^2) + \Phi_{,i} P_i$ .

In the above relation  $\varepsilon_0$  is the dielectric constant at vacuum and  $-\Phi_{,i}$  is the Maxwell self-field. Because of the anti-plane problem  $P_1 = P_2 = 0$ ,  $\Phi_{,3} = 0$ , the total electric enthalpy density is reduced to the following:  $U - \frac{1}{2} \varepsilon_0 (\Phi^2_{,1} + \Phi^2_{,2})$

This integral is applied to the total space, as it refers to the enthalpy.

- $f_i \delta u_i$ : is the potential work density caused by body forces
- $E^0_i \delta P_i$ : is the potential electric density caused by an initial in body electric field.
- $t_i \delta u_i$ : is the mechanical surface action.

The general idea using Toupin's Variational Principle is to reduce the above relation to one integral referring to the space and one referring to the boundary. The variations of the principal's variables lead to Euler conditions and the boundary conditions.

**Mindlin (1968)** expanded this theorem to include the kinetic energy, by adding the term of the kinetic energy to the above principle:

$$\delta \int_{t_0}^{t_1} dt \int_{V^*} T - H dV + \int_{t_0}^{t_1} dt \left\{ \int_V (f_i \delta u_i + E^0_i \delta P_i) dV + \int_S t_i \delta u_i dt \right\} = 0 \quad \text{A.3}$$

$T$ : is the kinetic energy,  $T = \frac{1}{2} \rho \dot{u}_3 \dot{u}_3$

$$\delta \int_{t_0}^{t_1} dt \int_{V^*} T - H dV + \int_{t_0}^{t_1} dt \left\{ \int_V (f_i \delta u_i + E^0_i \delta P_i) dV + \int_S t_i \delta u_i dt \right\} = 0$$

$$\delta \int_{t_0}^{t_1} \int_{V^*} T dV dt - \delta \int_{t_0}^{t_1} \int_{V^*} H dV dt + \int_{t_0}^{t_1} dt \left\{ \int_V (f_i \delta u_i + E^0_i \delta P_i) dV + \int_S t_i \delta u_i dt \right\} = 0$$

The first integral, that contains the kinetic energy, can easily be calculated through the Hamilton's principle, because  $\int_{t_1}^{t_2} \delta \left( \frac{1}{2} \rho \dot{u}_i u_i \right) \Big|_{V^*} dt$  can be considered equal to zero:

$$\begin{aligned}
\delta \int_{t_1}^{t_2} dt \int_{V^*} \left( \frac{1}{2} \rho \dot{u}_i \dot{u}_i \right) dV &= \delta \int_{t_1}^{t_2} dt \left\{ \left( \frac{1}{2} \rho \dot{u}_i u_i \right) \Big|_{V^*} - \int_{V^*} \left( \frac{1}{2} \rho \ddot{u}_i u_i \right) dV \right\} = \\
&= \delta \int_{t_1}^{t_2} \left( \frac{1}{2} \rho \dot{u}_i u_i \right) \Big|_{V^*} dt - \delta \int_{t_1}^{t_2} dt \int_{V^*} \left( \frac{1}{2} \rho \ddot{u}_i u_i \right) dV \\
&= \int_{t_1}^{t_2} \delta \left( \frac{1}{2} \rho \dot{u}_i u_i \right) \Big|_{V^*} dt - \int_{t_1}^{t_2} dt \int_{V^*} (\rho \ddot{u}_i \delta u_i) dV \\
&= - \int_{t_1}^{t_2} dt \int_{V^*} (\rho \ddot{u}_i \delta u_i) dV
\end{aligned}$$

And for the anti-plane flexoelectric problem  $\ddot{u}_1 = \ddot{u}_2 = 0$

$$\delta \int_{t_1}^{t_2} dt \int_{V^*} \left( \frac{1}{2} \rho \dot{u}_i \dot{u}_i \right) dV = - \int_{t_1}^{t_2} dt \int_{V^*} (\rho \ddot{u}_3 \delta u_3) dV \quad \text{A.4}$$

The second integral is a little more complex. For the anti-plane problem  $U - \frac{1}{2} \varepsilon_0 (\Phi^2_{,1} + \Phi^2_{,2})$ , and as the variation is concerned:

$$\delta H = \delta U - \delta \left\{ \frac{1}{2} \varepsilon_0 (\Phi^2_{,1} + \Phi^2_{,2}) \right\} \quad \text{A.5}$$

Starting with the variational of the total energy density, by using the rule of chain,

$$\begin{aligned}
\delta U &= \frac{\partial U}{\partial \varepsilon_{13}} \delta \varepsilon_{13} + \frac{\partial U}{\partial \varepsilon_{13}} \delta \varepsilon_{13} + \frac{\partial U}{\partial \varepsilon_{23}} \delta \varepsilon_{23} + \frac{\partial U}{\partial \varepsilon_{23}} \delta \varepsilon_{23} \\
&+ \frac{\partial U}{\partial \varepsilon_{13,1}} \delta \varepsilon_{13,1} + \frac{\partial U}{\partial \varepsilon_{23,2}} \delta \varepsilon_{23,2} + \frac{\partial U}{\partial \varepsilon_{31,1}} \delta \varepsilon_{31,1} + \frac{\partial U}{\partial \varepsilon_{32,2}} \delta \varepsilon_{32,2} \\
&+ \frac{\partial U}{\partial P_3} \delta P_3 + \frac{\partial U}{\partial P_{3,1}} \delta P_{3,1} + \frac{\partial U}{\partial P_{3,2}} \delta P_{3,2}
\end{aligned}$$

$$\begin{aligned}
\delta U &= \sigma_{13}\delta\varepsilon_{13} + \sigma_{31}\delta\varepsilon_{13} + \sigma_{23}\delta\varepsilon_{23} + \sigma_{32}\delta\varepsilon_{23} \\
&+ \tau_{113}\delta\varepsilon_{13,1} + \tau_{223}\delta\varepsilon_{23,2} + \tau_{131}\delta\varepsilon_{31,1} + \tau_{232}\delta\varepsilon_{32,2} \\
&- \bar{E}_3\delta P_3 + E_{13}\delta P_{3,1} + E_{23}\delta P_{3,2}
\end{aligned}$$

$$\delta U = \delta U_{sym. str.} + \delta U_{dip. str.} + \delta U_{pol.} + \delta U_{pol. grad.} \quad \text{A.6}$$

The above rule of chain demanded that the total energy density is a function of strains, strain gradients, polarizations and polarization gradients. The energy density that was initially proposed by [Mindlin \(1968\)](#) and later got modified by [Giannakopoulos and Zisis \(2019, 2020 a, b\)](#) obeys this condition.

The stresses and the electrical load can be calculated as follows:

#### *Symmetric Stresses*

$$\sigma_{13} = \frac{\partial U}{\partial \varepsilon_{13}} = 2\mu\varepsilon_{13} + e_{44}P_{3,1}$$

$$\sigma_{31} = \frac{\partial U}{\partial \varepsilon_{13}} = 2\mu\varepsilon_{13} + e_{44}P_{3,1}$$

$$\sigma_{23} = \frac{\partial U}{\partial \varepsilon_{23}} = 2\mu\varepsilon_{23} + e_{44}P_{3,2}$$

$$\sigma_{32} = \frac{\partial U}{\partial \varepsilon_{23}} = 2\mu\varepsilon_{23} + e_{44}P_{3,2}$$

#### *Dipolar stresses*

$$\tau_{113} = \frac{\partial U}{\partial \varepsilon_{13,1}} = f_{12}P_3$$

$$\tau_{223} = \frac{\partial U}{\partial \varepsilon_{23,2}} = f_{12}P_3$$

$$\tau_{131} = \frac{\partial U}{\partial \varepsilon_{31,1}} = f_{12}P_3$$

$$\tau_{232} = \frac{\partial U}{\partial \varepsilon_{32,2}} = f_{12}P_3$$

*Effective local electric force*

$$\bar{E}_3 = -\frac{\partial U}{\partial P_3} = -\alpha P_3 - f_{12} \left( (\varepsilon_{13,1} + \varepsilon_{31,1}) + (\varepsilon_{23,2} + \varepsilon_{32,2}) \right)$$

*Polarization gradient*

$$E_{13} = \frac{\partial U}{\partial P_{3,1}} = (b_{44} + b_{77})P_{3,1} + e_{44}(\varepsilon_{13} + \varepsilon_{31})$$

$$E_{23} = \frac{\partial U}{\partial P_{3,2}} = (b_{44} + b_{77})P_{3,2} + e_{44}(\varepsilon_{23} + \varepsilon_{32})$$

Note that because some strains are equal (the strain matrix is symmetrical), the differentiation in terms of the one strain, is non-zero for both strains. For example, because  $\varepsilon_{13} = \varepsilon_{31}$ :

$$\frac{\partial(\varepsilon_{13} + \varepsilon_{31})}{\partial \varepsilon_{13}} = \frac{\partial(\varepsilon_{13})}{\partial \varepsilon_{13}} + \frac{\partial(\varepsilon_{31})}{\partial \varepsilon_{13}} = \frac{\partial(\varepsilon_{13})}{\partial \varepsilon_{13}} + \frac{\partial(\varepsilon_{13})}{\partial \varepsilon_{13}} = 1 + 1 = 2$$

And also:

$$\frac{\partial(\varepsilon_{13}\varepsilon_{31} + \varepsilon_{23}\varepsilon_{32})}{\partial \varepsilon_{13}} = \frac{\partial(\varepsilon_{13}\varepsilon_{31})}{\partial \varepsilon_{13}} + \frac{\partial(\varepsilon_{23}\varepsilon_{32})}{\partial \varepsilon_{13}} = \frac{\partial(\varepsilon_{13}^2)}{\partial \varepsilon_{13}} + 0 = 2\varepsilon_{13} = 2\varepsilon_{31}$$

The same applies also in the strain gradients. Each one of the above is contributing to the potential energy density which is used in the Variational Principle.

### Energy from symmetric stresses

$$\delta U_{\text{sym. str.}} = \sigma_{13}\delta\varepsilon_{13} + \sigma_{31}\delta\varepsilon_{31} + \sigma_{23}\delta\varepsilon_{23} + \sigma_{32}\delta\varepsilon_{32}$$

$$\delta U_{\text{sym. str.}} = 2\sigma_{13}\delta\varepsilon_{13} + 2\sigma_{23}\delta\varepsilon_{23}$$

$$\delta U_{\text{sym. str.}} = \sigma_{13}\delta u_{3,1} + \sigma_{23}\delta u_{3,2}$$

$$\delta U_{\text{sym. str.}} = (\sigma_{13}\delta u_3)_{,1} - \sigma_{13,1}\delta u_3 + (\sigma_{23}\delta u_3)_{,2} - \sigma_{23,2}\delta u_3$$

$$\delta U_{\text{sym. str.}} = \{(\mu u_{3,1} + e_{44}P_{3,1})\delta u_3\}_{,1} - (\mu u_{3,11} + e_{44}P_{3,11})\delta u_3 \\ + \left( (\mu u_{3,2} + e_{44}P_{3,2})\delta u_3 \right)_{,2} - (\mu u_{3,22} + e_{44}P_{3,22})\delta u_3$$

$$\delta U_{\text{sym. str.}} = \{(\mu u_{3,1} + e_{44}P_{3,1})\delta u_3\}_{,1} + \{(\mu u_{3,2} + e_{44}P_{3,2})\delta u_3\}_{,2} \\ - \{(\mu u_{3,11} + e_{44}P_{3,11}) + (\mu u_{3,22} + e_{44}P_{3,22})\}\delta u_3$$

The term of the gradient will consist a boundary condition while the term with  $\delta u_3$  will directly modify the equation.

And by simplifying more:

$$\delta U_{sym. str.} = \{(\mu u_{3,i} + e_{44} P_{3,i}) \delta u_3\}_{,i} - \{(\mu \nabla^2 u_3 + e_{44} \nabla^2 P_3)\} \delta u_3 \quad \text{A.7}$$

### Energy from dipolar stresses

$$\begin{aligned} \delta U_{dip. str.} &= \tau_{113} \delta \varepsilon_{13,1} + \tau_{131} \delta \varepsilon_{31,1} + \tau_{223} \delta \varepsilon_{23,2} + \tau_{232} \delta \varepsilon_{32,2} \\ \delta U_{dip. str.} &= 2\tau_{113} \delta \varepsilon_{13,1} + 2\tau_{223} \delta \varepsilon_{23,2} \\ \delta U_{dip. str.} &= \tau_{113} \delta u_{3,11} + \tau_{223} \delta u_{3,22} \\ \delta U_{dip. str.} &= f_{12} P_3 \delta u_{3,11} + f_{12} P_3 \delta u_{3,22} \\ \delta U_{dip. str.} &= (f_{12} P_3 \delta u_{3,1})_{,1} - f_{12} P_{3,1} \delta u_{3,1} + (f_{12} P_3 \delta u_{3,2})_{,2} - f_{12} P_{3,2} \delta u_{3,2} \\ \delta U_{dip. str.} &= (f_{12} P_3 \delta u_3)_{,11} - 2(f_{12} P_{3,1} \delta u_{3,1})_{,1} + f_{12} P_{3,11} \delta u_3 \\ &\quad + (f_{12} P_3 \delta u_3)_{,22} - 2(f_{12} P_{3,2} \delta u_{3,2})_{,2} + f_{12} P_{3,22} \delta u_3 \\ \delta U_{dip. str.} &= \nabla^2 (f_{12} P_3 \delta u_3) - 2(f_{12} P_{3,i} \delta u_{3,i})_{,i} + f_{12} \nabla^2 P_3 \delta u_3 \quad \text{A.8} \end{aligned}$$

The first two terms will take part in a surface integral that will describe the boundary conditions, and the last term will be considered in the equations.

### Energy from the Polarization

$$\begin{aligned} \delta U_{pol} &= -\bar{E}_3 \delta P_3 \\ \delta U_{pol} &= \alpha P_3 \delta P_3 + f_{12} \left( \left( (\varepsilon_{13,1} + \varepsilon_{31,1}) + (\varepsilon_{23,2} + \varepsilon_{32,2}) \right) \right) \delta P_3 \\ \delta U_{pol} &= \alpha P_3 \delta P_3 + f_{12} (u_{3,11} + u_{3,22}) \delta P_3 \\ \delta U_{pol} &= \{\alpha P_3 + f_{12} \nabla^2 u_3\} \delta P_3 \quad \text{A.9} \end{aligned}$$

And lastly, **Energy from the polarization gradient**

$$\delta U_{pol. grad} = E_{13}\delta P_{3,1} + E_{23}\delta P_{3,2}$$

$$\begin{aligned} \delta U_{pol.g} = & \left\{ (b_{44} + b_{77})P_{3,1} + e_{44} \left( \frac{1}{2}u_{3,1} + \frac{1}{2}u_{3,1} \right) \right\} \delta P_{3,1} \\ & + \left\{ (b_{44} + b_{77})P_{3,2} + e_{44} \left( \frac{1}{2}u_{3,2} + \frac{1}{2}u_{3,2} \right) \right\} \delta P_{3,2} \end{aligned}$$

$$\begin{aligned} \delta U_{pol.g} = & \left[ \left\{ (b_{44} + b_{77})P_{3,1} + e_{44}u_{3,1} \right\} \delta P_{3,1} \right]_1 - \left\{ (b_{44} + b_{77})P_{3,11} + e_{44}u_{3,11} \right\} \delta P_3 \\ & + \left[ \left\{ (b_{44} + b_{77})P_{3,2} + e_{44}u_{3,2} \right\} \delta P_{3,2} \right]_2 - \left\{ (b_{44} + b_{77})P_{3,22} + e_{44}u_{3,22} \right\} \delta P_3 \end{aligned}$$

$$\delta U_{pol.g} = \left[ \left\{ (b_{44} + b_{77})P_{3,i} + e_{44}u_{3,i} \right\} \delta P_3 \right]_i - \left\{ (b_{44} + b_{77})\nabla^2 P_3 + e_{44}\nabla^2 u_3 \right\} \delta P_3 \quad \text{A.10}$$

Also, the variation:  $\delta \left\{ \varepsilon_0 \frac{1}{2} \varepsilon_0 (\Phi^2_{,1} + \Phi^2_{,2}) \right\}$

$$\delta \left\{ \varepsilon_0 \frac{1}{2} (\Phi^2_{,1} + \Phi^2_{,2}) \right\} = \varepsilon_0 \Phi_{,1} \delta \Phi_{,1} + \varepsilon_0 \Phi_{,2} \delta \Phi_{,2}$$

$$\delta \left\{ \varepsilon_0 \frac{1}{2} (\Phi^2_{,1} + \Phi^2_{,2}) \right\} = \left\{ \varepsilon_0 \Phi_{,1} \delta \Phi \right\}_{,1} - \varepsilon_0 \Phi_{,11} \delta \Phi + \left\{ \varepsilon_0 \Phi_{,2} \delta \Phi \right\}_{,2} - \varepsilon_0 \Phi_{,22} \delta \Phi$$

$$\delta \left\{ \varepsilon_0 \frac{1}{2} (\Phi^2_{,1} + \Phi^2_{,2}) \right\} = \left\{ \varepsilon_0 \Phi_{,i} \delta \Phi \right\}_{,i} - \varepsilon_0 \nabla^2 \Phi \delta \Phi \quad \text{A.11}$$

In those relations, of course,  $\nabla^2 = \frac{\partial^2}{\partial x_1^2} + \frac{\partial^2}{\partial x_2^2}$  and when the index  $i$  exists twice in the same expression, it symbolizes the Einstein summation for two values, e.g.  $\left\{ \varepsilon_0 \Phi_{,i} \delta \Phi \right\}_{,i} = \left\{ \varepsilon_0 \Phi_{,1} \delta \Phi \right\}_{,1} + \left\{ \varepsilon_0 \Phi_{,2} \delta \Phi \right\}_{,2}$

By importing those relations (A.6, A.7, A.8, A.9, A.10, A.11) into relation A.5:

$$\delta H = \delta U - \delta \left\{ \frac{1}{2} \varepsilon_0 (\Phi^2_{,1} + \Phi^2_{,2}) \right\}$$

$$\begin{aligned} \delta H = & \{(\mu u_{3,i} + e_{44} P_{3,i}) \delta u_3\}_{,i} - \{(\mu \nabla^2 u_3 + e_{44} \nabla^2 P_3)\} \delta u_3 + \nabla^2 (f_{12} P_3 \delta u_3) \\ & - 2(f_{12} P_{3,i} \delta u_{3,i})_{,i} + f_{12} \nabla^2 P_3 \delta u_3 + \{\alpha P_3 + f_{12} \nabla^2 u_3\} \delta P_3 \\ & + \{[(b_{44} + b_{77}) P_{3,i} + e_{44} u_{3,i}] \delta P_3\}_{,i} \\ & - \{(b_{44} + b_{77}) \nabla^2 P_3 + e_{44} \nabla^2 u_3\} \delta P_3 + \{\varepsilon_0 \Phi_{,i} \delta \Phi\}_{,i} - \varepsilon_0 \nabla^2 \Phi \delta \Phi \end{aligned}$$

$$\begin{aligned} \delta H = & \nabla^2 (f_{12} P_3 \delta u_3) + \{(\mu u_{3,i} + e_{44} P_{3,i}) \delta u_3\}_{,i} - 2(f_{12} P_{3,i} \delta u_{3,i})_{,i} & \text{A.12} \\ & + \{[(b_{44} + b_{77}) P_{3,i} + e_{44} u_{3,i}] \delta P_3\}_{,i} + \{\varepsilon_0 \Phi_{,i} \delta \Phi\}_{,i} \\ & - (\mu \nabla^2 u_3 + e_{44} \nabla^2 P_3) \delta u_3 + 2f_{12} \nabla^2 P_3 \delta u_3 + (\alpha P_3 + f_{12} \nabla^2 u_3) \delta P_3 \\ & - \{(b_{44} + b_{77}) \nabla^2 P_3 + e_{44} \nabla^2 u_3\} \delta P_3 - \varepsilon_0 \nabla^2 \Phi \delta \Phi \end{aligned}$$

And the integral:

$$\begin{aligned} & \delta \int_{t_0}^{t_1} dt \int_{V^*} T - H \, dV \\ & = - \int_{t_1}^{t_2} dt \int_{V^*} (\rho \ddot{u}_3 \delta u_3) \, dV \\ & - \int_{t_0}^{t_1} dt \int_{V^*} \left\{ \nabla^2 (f_{12} P_3 \delta u_3) + \{(\mu u_{3,i} + e_{44} P_{3,i}) \delta u_3\}_{,i} \right. \\ & - 2(f_{12} P_{3,i} \delta u_{3,i})_{,i} + \{[(b_{44} + b_{77}) P_{3,i} + e_{44} u_{3,i}] \delta P_3\}_{,i} + \{\varepsilon_0 \Phi_{,i} \delta \Phi\}_{,i} \\ & - (\mu \nabla^2 u_3 + e_{44} \nabla^2 P_3) \delta u_3 + f_{12} \nabla^2 P_3 \delta u_3 + (\alpha P_3 + f_{12} \nabla^2 u_3) \delta P_3 \\ & \left. - \{(b_{44} + b_{77}) \nabla^2 P_3 + e_{44} \nabla^2 u_3\} \delta P_3 - \varepsilon_0 \nabla^2 \Phi \delta \Phi \right\} \, dV \end{aligned}$$



$$\begin{aligned}
\delta \int_{t_0}^{t_1} dt \int_{V^*} T - H dV &= \int_{t_0}^{t_1} dt \int_{V^*} \{\nabla^2(f_{12}P_3\delta u_3)\} dV \\
&+ \int_{t_0}^{t_1} dt \int_{V^*} \left\{ -\{(\mu u_{3,i} + e_{44}P_{3,i})\delta u_3\}_{,i} + (f_{12}P_{3,i}\delta u_{3,i})_{,i} \right. \\
&- \left. [\{(b_{44} + b_{77})P_{3,i} + e_{44}u_{3,i}\}\delta P_3]_{,i} - \{\varepsilon_0\Phi_{,i}\delta\Phi\}_{,i} \right\} dV \\
&+ \int_{t_0}^{t_1} dt \int_{V^*} \left\{ -\rho\ddot{u}_3\delta u_3 + (\mu\nabla^2u_3 + e_{44}\nabla^2P_3)\delta u_3 - f_{12}\nabla^2P_3\delta u_3 \right. \\
&- \left. \{\alpha P_3 + f_{12}\nabla^2u_3\}\delta P_3 + \{(b_{44} + b_{77})\nabla^2P_3 + e_{44}\nabla^2u_3\}\delta P_3 + \varepsilon_0\nabla^2\Phi\delta\Phi \right\} dV
\end{aligned} \tag{A.13}$$

Now, the divergence theorem can be used and the first part of the integrals, which contains terms of the derivative of the variational, can be converted to a surface integral and be used for the boundary conditions:

$$\int_{V^*} \{\nabla^2(f_{12}P_3\delta u_3)\} dV = \int_S (f_{12}P_3\delta u_3)_{,i} n_i dS \tag{A.14}$$

And also:

$$\begin{aligned}
\int_{V^*} \left\{ -\{(\mu u_{3,i} + e_{44}P_{3,i})\delta u_3\}_{,i} + (f_{12}P_{3,i}\delta u_{3,i})_{,i} - [\{(b_{44} + b_{77})P_{3,i} + e_{44}u_{3,i}\}\delta P_3]_{,i} - \{\varepsilon_0\Phi_{,i}\delta\Phi\}_{,i} \right\} dV \\
= \\
\int_S \left\{ -(\mu u_{3,i} + e_{44}P_{3,i})n_i\delta u_3 + f_{12}P_{3,i}\delta u_{3,i}n_i - \{(b_{44} + b_{77})P_{3,i} + e_{44}u_{3,i}\}\delta P_3n_i - \varepsilon_0[\Phi_{,i}]\delta\Phi n_i \right\} dS
\end{aligned} \tag{A.15}$$

At this point, it should be noted that because this integral is referring to space  $V^*$  which is the total space, a distinction should be made. According to Gauss theorem of divergence, the volume integral of a space surrounded by a specific boundary can be turned into a surface integral referring to that boundary. This means that the integral should have been in space  $V$  ( $V^* = V + V'$ ). The integral in the space  $V$  can easily be processed via the Divergence Theorem. Also, regarding the Integral referring to space  $V'$ , the divergence theorem can also be applied as the boundary surface remains the same, but with opposite sign, as the direction of the unit vector becomes opposite:

$$\begin{aligned}\int_{V^*} (\dots)_i dV &= \int_V (\dots)_i dV + \int_{V'} (\dots)_i dV \\ &= \int_S (\dots)^{from\ side\ towards\ V} n_i dS - \int_S (\dots)^{from\ side\ towards\ V'} n_i dS\end{aligned}$$

The body, in which the strains and the polarization is being applied, belongs to space  $V$  and thus the integral  $\int_{V'} (\dots)_i dV$ , which refers to space  $V'$  should be zero. This is something that cannot hold true for Maxwell's self-field, and thus the second (negative) integral exists. Its difference should be zero by considering a continuity, but if no continuity is in place, then the result of this difference should be a jump condition:

$$\begin{aligned}\int_{V^*} \left\{ -\{(\mu u_{3,i} + e_{44} P_{3,i}) \delta u_3\}_{,i} + (f_{12} P_{3,i} \delta u_{3,i})_{,i} - \{[(b_{44} + b_{77}) P_{3,i} + e_{44} u_{3,i}] \delta P_3\}_{,i} \right\} dV \\ = \\ \int_V \left\{ -\{(\mu u_{3,i} + e_{44} P_{3,i}) \delta u_3\}_{,i} + (f_{12} P_{3,i} \delta u_{3,i})_{,i} - \{[(b_{44} + b_{77}) P_{3,i} + e_{44} u_{3,i}] \delta P_3\}_{,i} \right\} + 0\end{aligned}$$

While:

$$\begin{aligned}\int_{V^*} \left\{ -\{\varepsilon_0 \Phi_{,i} \delta \Phi\}_{,i} \right\} dV &= -\varepsilon_0 \int_{V^*} \left\{ \{\Phi_{,i} \delta \Phi\}_{,i} \right\} dV \\ &= -\varepsilon_0 \left\{ \int_V \left\{ \{\Phi_{,i} \delta \Phi\}_{,i} \right\} dV + \int_{V'} \left\{ \{\Phi_{,i} \delta \Phi\}_{,i} \right\} dV \right\} \\ &= -\varepsilon_0 \left\{ \int_S \left\{ (\Phi_{,i} \delta \Phi)^{from\ side\ towards\ V} n_i \right\} dV - \int_S \left\{ (\Phi_{,i} \delta \Phi)^{from\ side\ towards\ V'} n_i \right\} dV \right\} \\ &= -\varepsilon_0 \left\{ \int_S \left\{ [(\Phi_{,i} \delta \Phi)^{from\ side\ towards\ V} - (\Phi_{,i} \delta \Phi)^{from\ side\ towards\ V'}] n_i \right\} dV \right\} \\ &= -\varepsilon_0 \left\{ \int_S \left\{ [\Phi_{,i} \delta \Phi] n_i \right\} dV \right\} \\ &= \int_S \left\{ -\varepsilon_0 [\Phi_{,i}] n_i \delta \Phi \right\} dV\end{aligned}$$

By importing relation [A.14](#) and relations [A.15](#) into relation [A.13](#):

$$\begin{aligned}
& \delta \int_{t_0}^{t_1} dt \int_{V^*} T - H \, dV \\
&= \int_{t_0}^{t_1} dt \int_S (f_{12} P_3 \delta u_3)_{,i} n_i \, dS \\
&+ \int_{t_0}^{t_1} dt \int_S \{ -(\mu u_{3,i} + e_{44} P_{3,i}) n_i \delta u_3 + f_{12} P_{3,i} \delta u_{3,i} n_i \\
&- \{ (b_{44} + b_{77}) P_{3,i} + e_{44} u_{3,i} \} \delta P_3 n_i - \varepsilon_0 [\Phi_{,i}] \delta \Phi n_i \} \, dS \\
&+ \int_{t_0}^{t_1} dt \int_{V^*} \{ -\rho \ddot{u}_3 \delta u_3 + (\mu \nabla^2 u_3 + e_{44} \nabla^2 P_3) \delta u_3 - f_{12} \nabla^2 P_3 \delta u_3 \\
&- \{ \alpha P_3 + f_{12} \nabla^2 u_3 \} \delta P_3 + \{ (b_{44} + b_{77}) \nabla^2 P_3 + e_{44} \nabla^2 u_3 \} \delta P_3 \\
&+ \varepsilon_0 \nabla^2 \Phi \delta \Phi \} \, dV
\end{aligned} \tag{A.16}$$

With those calculations the first integral of Toupin's Variational Principle is complete. For the second integral,  $\int_V (f_i \delta u_i + E^0_i \delta P_i) \, dV$ , since both mechanical and electrical action are applied to the body and not to the outside, easily this integral can be manipulated to the following:

$$\int_V (f_i \delta u_i + E^0_i \delta P_i) \, dV = \int_{V^*} (f_i \delta u_i + E^0_i \delta P_i) \, dV$$

And for the anti-plane flexoelectric problem the above relation can be written as follows because the in-plane potential displacement and polarization can be ignored ( $u_1 = u_2 = 0 \rightarrow \delta u_1 = \delta u_2 = 0$ ,  $(P_1 = P_2 = 0 \rightarrow \delta P_1 = \delta P_2 = 0)$ )

$$\int_V (f_i \delta u_i + E^0_i \delta P_i) \, dV = \int_{V^*} (f_3 \delta u_3 + E^0_3 \delta P_3) \, dV \tag{A.17}$$

And finally, by importing both A.16 and A.17, into Toupin's Variational Principle as proposed by Mindlin (1968), A.3:

$$\delta \int_{t_0}^{t_1} dt \int_{V^*} T - H \, dV + \int_{t_0}^{t_1} dt \left\{ \int_V (f_i \delta u_i + E^0_i \delta P_i) \, dV + \int_S t_i \delta u_i \, dt \right\} = 0$$

↔

$$\begin{aligned}
& \int_S (f_{12}P_3 \delta u_3)_i n_i ds \\
& + \int_S \{ -(\mu u_{3,i} + e_{44}P_{3,i})n_i \delta u_3 + f_{12}P_{3,i} \delta u_{3,i} n_i \\
& - \{ (b_{44} + b_{77})P_{3,i} + e_{44}u_{3,i} \} \delta P_3 n_i - \varepsilon_0 [\Phi_{,i}] \delta \Phi n_i \} dS \\
& + \int_{V^*} \{ -\rho \ddot{u}_3 \delta u_3 + (\mu \nabla^2 u_3 + e_{44} \nabla^2 P_3) \delta u_3 - f_{12} \nabla^2 P_3 \delta u_3 \\
& - \{ \alpha P_3 + f_{12} \nabla^2 u_3 \} \delta P_3 + \{ (b_{44} + b_{77}) \nabla^2 P_3 + e_{44} \nabla^2 u_3 \} \delta P_3 \\
& + \varepsilon_0 \nabla^2 \Phi \delta \Phi \} dV + \int_{V^*} (f_3 \delta u_3 + E^0_3 \delta P_3) dV + \int_S t_3 \delta u_3 dt = 0 \\
& \leftrightarrow \\
& \int_{V^*} \left\{ -\rho \ddot{u}_3 \delta u_3 + (\mu \nabla^2 u_3 + e_{44} \nabla^2 P_3) \delta u_3 - f_{12} \nabla^2 P_3 \delta u_3 - \{ \alpha P_3 + f_{12} \nabla^2 u_3 \} \delta P_3 \right. \\
& \quad + \{ (b_{44} + b_{77}) \nabla^2 P_3 + e_{44} \nabla^2 u_3 \} \delta P_3 + \varepsilon_0 \nabla^2 \Phi \delta \Phi \\
& \quad \left. + \int_{V^*} (f_3 \delta u_3 + E^0_3 \delta P_3) \right\} dV \\
& \leftrightarrow \\
& + \int_S \{ -(\mu u_{3,i} + e_{44}P_{3,i})n_i \delta u_3 + f_{12}P_{3,i} \delta u_{3,i} n_i - \{ (b_{44} + b_{77})P_{3,i} + e_{44}u_{3,i} \} \delta P_3 n_i \\
& \quad - \varepsilon_0 [\Phi_{,i}] \delta \Phi n_i + t_3 \delta u_3 \} dS = 0
\end{aligned} \tag{A.18}$$

The first integral refers to the in-body condition, while the second describes the boundary condition.

The in-body condition, that consists of three variationals, provides three equations because the variationals can take any value possible independently, as described by [Giannakopoulos and Zisis \(2019, 2021 a, b\)](#). The first equation can be obtained through the factor of  $\delta u_3$  and describes the Conservation of linear momentum, the second one that is produced by the factor of the potential polarization  $\delta P_3$ , describes the conservation of the electric field and the last one, that is produced from the potential of Maxwell's self-field  $\delta \Phi$  describes the Maxwell equation. Those equations are also called Euler conditions.

### The conservation of linear momentum ( $\delta u_3$ )

$$\begin{aligned}
-\rho \ddot{u}_3 + \mu \nabla^2 u_3 + e_{44} \nabla^2 P_3 - f_{12} \nabla^2 P_3 + f_3 &= 0 \\
\mu \nabla^2 u_3 + (e_{44} - f_{12}) \nabla^2 P_3 + f_3 &= \rho \ddot{u}_3
\end{aligned} \tag{A.19}$$

### The conservation of electric field ( $\delta P_3$ )

$$-\alpha P_3 - f_{12} \nabla^2 u_3 + (b_{44} + b_{77}) \nabla^2 P_3 + e_{44} \nabla^2 u_3 + E^0_3 = 0$$

$$-\alpha P_3 + \frac{(e_{44} - f_{12})}{2} \nabla^2 u_3 + (b_{44} + b_{77}) \nabla^2 P_3 + E^0_3 = 0 \quad \text{A.20}$$

### Maxwell equations ( $\delta\Phi$ )

$$\nabla^2 \Phi = 0 \quad \text{A.21}$$

Note that the term  $\nabla^2 = \frac{\partial^2}{\partial x_1^2} + \frac{\partial^2}{\partial x_2^2}$ .

Also, with a similar way the boundary conditions can be extruded, from the second integral:

$$-(\mu u_{3,i} + e_{44} P_{3,i}) n_i + t_3 = 0$$

$$\{(b_{44} + b_{77}) P_{3,i} + e_{44} u_{3,i}\} n_i = 0$$

$$-\varepsilon_0 [\Phi_{,i}] n_i = 0$$

$$f_{12} P_{3,i} n_i = 0$$

i

By considering the gradient to the direction perpendicular the the surface, the derivative in respect of the unit vector can be written as beneath.

$$\frac{\partial}{\partial n_i} = \frac{\partial}{\partial n} = n_i \frac{\partial}{\partial x_i} = n_1 \frac{\partial}{\partial x_1} + n_2 \frac{\partial}{\partial x_2}$$

↔

ii

$$(\dots)_{,n} = n_i (\dots)_{,i}$$

This way, the boundary conditions i can be rewritten with the use of ii as follows:

$$-(\mu u_{3,n} + e_{44} P_{3,n}) + t_3 = 0 \quad \text{A.22}$$

$$(b_{44} + b_{77})P_{3,n} + e_{44}u_{3,n} = 0$$

$$-\varepsilon_0[\Phi_{,n}] = 0$$

$$f_{12}P_{3,n} = 0$$

And of course, because the problem is dynamic, there should also be some initial conditions.

The construction of the governing equation can happen by solving the system of the conservation equations. First by considering the initial body force  $f_3$  equal to zero and then by solving equation A.19 in terms of polarization's second gradient  $\nabla^2 P_3$

$$\mu\nabla^2 u_3 + (e_{44} - f_{12})\nabla^2 P_3 = \rho\ddot{u}_3$$

$$\nabla^2 P_3 = \frac{\rho\ddot{u}_3 - \mu\nabla^2 u_3}{(e_{44} - f_{12})} \quad \text{A.23}$$

Importing A.23 into equation A.20, while also considering the initial out-of-plane electrical field equal to zero:

$$-\alpha P_3 + (b_{44} + b_{77})\nabla^2 P_3 + (e_{44} - f_{12})\nabla^2 u_3 = 0$$

$$-\alpha P_3 + (b_{44} + b_{77})\frac{\rho\ddot{u}_3 - \mu\nabla^2 u_3}{(e_{44} - f_{12})} + (e_{44} - f_{12})\nabla^2 u_3 = 0$$

And then differentiating twice each variable (multiplying all terms with  $\nabla^2 = \frac{\partial^2}{\partial x_1^2} + \frac{\partial^2}{\partial x_2^2}$ ), and then substituting into relation A.23 once again:

$$-\alpha \frac{\rho\ddot{u}_3 - \mu\nabla^2 u_3}{(e_{44} - f_{12})} + (b_{44} + b_{77})\frac{\rho\nabla^2 \ddot{u}_3 - \mu\nabla^4 u_3}{(e_{44} - f_{12})} + (e_{44} - f_{12})\nabla^4 u_3 = 0$$

This relation is similar to the one proposed by Giannakopoulos and Zisis (2019, 2021 a, b) and can be written simpler as follows:

$$\begin{aligned}
& -\alpha \frac{\rho \ddot{u}_3}{e_{44} - f_{12}} + \alpha \frac{\mu \nabla^2 u_3}{e_{44} - f_{12}} + \frac{b_{44} + b_{77}}{e_{44} - f_{12}} \rho \nabla^2 \ddot{u}_3 - \frac{b_{44} + b_{77}}{e_{44} - f_{12}} \mu \nabla^4 u_3 + e_{44} - f_{12} \nabla^4 u_3 = 0 \\
& \alpha \mu \nabla^2 u_3 - (b_{44} + b_{77}) \mu \nabla^4 u_3 + (e_{44} - f_{12})^2 \nabla^4 u_3 = \alpha \rho \ddot{u}_3 - (b_{44} + b_{77}) \rho \nabla^2 \ddot{u}_3 \\
& \mu \nabla^2 u_3 - \left\{ \frac{(b_{44} + b_{77}) \mu}{\alpha} - \frac{(e_{44} - f_{12})^2}{\alpha} \right\} \nabla^4 u_3 = \rho \ddot{u}_3 - \frac{(b_{44} + b_{77})}{\alpha} \rho \nabla^2 \ddot{u}_3 \tag{A.24}
\end{aligned}$$

The term  $\frac{b_{44} + b_{77}}{\alpha} - \frac{(e_{44} - f_{12})^2}{\alpha \mu}$  represents the microstructural length  $l$  from which the below relation holds:

$$\frac{l^2}{2} = \frac{b_{44} + b_{77}}{\alpha} - \frac{(e_{44} - f_{12})^2}{\alpha \mu} \tag{A.25}$$

Also, the term  $\frac{(b_{44} + b_{77})}{\alpha}$  represents the micro-inertial length  $H$ , in respect to the following equation:

$$\frac{H^2}{12} = \frac{(b_{44} + b_{77})}{\alpha} \tag{A.26}$$

Those two lengths should always be greater than zero, (in addition to the other parameters from which they consist of). In particular, the below limits to the parameters should hold:

$$\begin{aligned}
& \mu > 0 \\
& A > 0 \\
& f_{12} > 0 \\
& e_{44} > 0 \\
& b_{44} + b_{77} > 0 \\
& \mu(b_{44} + b_{77}) - e_{44}^2 > 0 \\
& f_{44} > 0
\end{aligned}$$

Note that the parameter  $f_{44}$ , is not contained in any relation.

Finally, importing the two length parameters A.25, A.26 into relation A.24 results to the governing equation that refers solely to the displacement, by having taken in consideration also the reverse flexoelectric effect.:

$$\mu \nabla^2 u_3 - \mu \frac{l^2}{2} \nabla^4 u_3 = \rho \ddot{u}_3 - \frac{H^2}{12} \rho \nabla^2 \ddot{u}_3 \quad \text{A.27}$$

The second equation, that describes the produced polarization in terms of displacement in the anti-plane flexoelectric problem, comes from the conservation of the linear momentum [A.19](#), this time, being solved in respect to the displacement,

$$\nabla^2 u_3 = \frac{\rho \ddot{u}_3}{\mu} - \frac{(e_{44} - f_{12})}{\mu} \nabla^2 P_3 \quad \text{A.28}$$

and then importing into the conservation of the electric field [A.20](#):

$$\begin{aligned} -\alpha P_3 + \frac{(e_{44} - f_{12})}{2} \left\{ \frac{\rho \ddot{u}_3}{\mu} - \frac{(e_{44} - f_{12})}{\mu} \nabla^2 P_3 \right\} + (b_{44} + b_{77}) \nabla^2 P_3 &= 0 \\ P_3 - \left\{ \frac{(b_{44} + b_{77})}{\alpha} - \frac{(e_{44} - f_{12})^2}{\mu \alpha} \right\} \nabla^2 P_3 &= \frac{(e_{44} - f_{12})}{\mu \alpha} \rho \ddot{u}_3 \end{aligned}$$

And then by the two length parameters:

$$P_3 - \frac{l^2}{2} \nabla^2 P_3 = \frac{(e_{44} - f_{12})}{\mu \alpha} \rho \ddot{u}_3 \quad \text{A.29}$$

The anti-plane flexoelectric problem is described by [A.27](#), [A.29](#), [A.21](#), subjected to the boundary conditions [A.22](#).



### B. The transformation of the anti-plane flexoelectric equation (remove the time)

Both equations A.27, A.29 are dynamic equations, as they contain terms of acceleration. This is something that easily can be dealt with, by considering a second system of coordinates  $(\xi, \eta)$ . This system should be independent from the velocity and thus it should be moving with the same velocity that defines the problem dynamic.

The easiest example, is the propagation of a mode III crack, that moves with a constant velocity  $V$ . This is also, one of the most common dynamic anti-plane problems.

This transformation, that was proposed by Giannakopoulos and Zisis (2019, 2020 a, b), suggests the new system of coordinates to be consisted of the  $(\xi, \eta)$  coordinates, which connect to the global coordinates  $(x, y)$ , through the below formula:

$$\begin{aligned}\xi &= x + Vt \\ \eta &= y\end{aligned}\tag{B.1}$$

The differentiations are also modified:

$$\begin{aligned}\nabla^2 &= \frac{\partial^2}{\partial x^2} + \frac{\partial^2}{\partial y^2} = \frac{\partial^2}{\partial \xi^2} + \frac{\partial^2}{\partial \eta^2} \\ \nabla^4 &= \nabla^2 \nabla^2 = \frac{\partial^4}{\partial x^4} + 2 \frac{\partial^4}{\partial x^2 \partial y^2} + \frac{\partial^4}{\partial y^4} = \frac{\partial^4}{\partial \xi^4} + 2 \frac{\partial^4}{\partial \xi^2 \partial \eta^2} + \frac{\partial^4}{\partial \eta^4} \\ \frac{\partial^2}{\partial t^2} &= V^2 \frac{\partial^2}{\partial \xi^2}\end{aligned}\tag{B.2}$$

and because of the chain rule, after importing those (B.2) to A.27:

$$\mu \frac{\partial^2 u_3}{\partial \xi^2} + \mu \frac{\partial^2 u_3}{\partial \eta^2} - \mu \frac{l^2 \partial^4 u_3}{2 \partial \xi^4} - 2\mu \frac{l^2 \partial^4 u_3}{2 \partial \xi^2 \partial \eta^2} - \mu \frac{l^2 \partial^4 u_3}{2 \partial \eta^4} = \rho V^2 \frac{\partial^2 u}{\partial \xi^2} - V^2 \frac{\rho H^2 \partial^4 u}{12 \partial \xi^4} - V^2 \frac{\rho H^2 \partial^4 u}{12 \partial \xi^2 \partial \eta^2}$$

↔

$$(\mu - \rho V^2) \frac{\partial^2 u_3}{\partial \xi^2} + \mu \frac{\partial^2 u_3}{\partial \eta^2} + \left( V^2 \frac{\rho H^2}{12} - \mu \frac{l^2}{2} \right) \frac{\partial^4 u_3}{\partial \xi^4} + \left( V^2 \frac{\rho H^2}{12} - 2\mu \frac{l^2}{2} \right) \frac{\partial^4 u_3}{\partial \xi^2 \partial \eta^2} - \mu \frac{l^2 \partial^4 u_3}{2 \partial \eta^4} = 0$$

↔

$$\left( 1 - \frac{\rho V^2}{\mu} \right) \frac{\partial^2 u_3}{\partial \xi^2} + \frac{\partial^2 u_3}{\partial \eta^2} + \left( \frac{\rho V^2 H^2}{\mu} - \frac{l^2}{2} \right) \frac{\partial^4 u_3}{\partial \xi^4} + \left( \frac{\rho V^2 H^2}{\mu} - 2 \frac{l^2}{2} \right) \frac{\partial^4 u_3}{\partial \xi^2 \partial \eta^2} - \mu \frac{l^2 \partial^4 u_3}{2 \partial \eta^4} = 0$$

Also, by substituting  $c_s = \sqrt{\mu/\rho}$ , the wave shear velocity,

$$\left(1 - \frac{V^2}{c_s^2}\right) \frac{\partial^2 u_3}{\partial \xi^2} + \frac{\partial^2 u_3}{\partial \eta^2} - \frac{l^2}{2} \left(1 - \frac{V^2 H^2}{6l^2 c_s^2}\right) \frac{\partial^4 u_3}{\partial \xi^4} - \frac{l^2}{2} \left(2 - \frac{V^2 H^2}{6l^2 c_s^2}\right) \frac{\partial^4 u_3}{\partial \xi^2 \partial \eta^2} - \frac{l^2}{2} \frac{\partial^4 u_3}{\partial \eta^4} = 0 \quad \text{B.3}$$

While the second equation A.29 transforms as follows:

$$P_3 - \frac{l^2}{2} \left( \frac{\partial^2 P_3}{\partial \xi^2} + \frac{\partial^2 P_3}{\partial \eta^2} \right) = V^2 \frac{\rho(e_{44} - f_{12})}{a\mu} \frac{\partial^2 u}{\partial \xi^2} \quad \text{B.4}$$

Note that, this transformation demanded the velocity to be constant (steady state case). The general case however, demands a transformation like the following instead of B.1:

$$\xi = x + \int_{t_0}^t V(x, y, \tau) d\tau$$

$$\eta = y$$

but by the use of numerical integration (Simpson's rule, Gauss' 1<sup>st</sup> order (rule of the middle value)), any velocity can be modified with this way.

### C. The couple stress elasticity theory

The theory of Couple stress elasticity, described by [Gourgiotis and Georgiadis \(2007\)](#) follows an alternative perspective, through the balance laws of continuum mechanics and specifically, the conservation of momentum. The conservation of momentum can be written in the below form as two integrals, one defined in the volume of the body of interest and one in the boundary of the body. This time, all things are mechanical with no electricity involved and so a more detailed perspective of space is not needed (as in the flexoelectric problem with volume  $V^*$ ).

The equation of the linear momentum is:

$$\int_s T_i^{(n)} ds + \int_V F_i dV = 0 \quad \text{C.1}$$

And the equation of rotational momentum is:

$$\int_s x_j T_k^{(n)} e_{ijk} + M_i^{(n)} ds + \int_V x_j F_k e_{ijk} + C_i dV = 0 \quad \text{C.2}$$

In the above relations  $T_i$  is the surface force-traction,  $M_i$  is the moment per unit area (moment traction),  $F_i$  is the body force and lastly  $C_i$  is the body moment.

The specific characteristic of the couple stress elasticity, is that both the stress tensor and the couple stress tensor (made from the moment traction), are not necessarily symmetrical. Those tensors are relevant to the traction, when the surface is defined.

$$T_i^{(n)} = \sigma_{ij} \tau n_j \quad \text{C.3}$$

$$M_i^{(n)} = \mu_{ij} \tau n_j \quad \text{C.4}$$

By importing [C.3](#), [C.4](#) into relations [C.1](#) and [C.2](#), the divergence theorem can be used, to transform the surface integrals to volume integrals.

$$\begin{aligned} \int_s T_i^{(n)} ds &= \int_s \sigma_{ij} \tau n_j ds \\ &= \int_V \sigma_{ji,j} dV \end{aligned}$$

$$\begin{aligned} \int_s x_j T_k^{(n)} e_{ijk} + M_i^{(n)} ds &= \int_s x_j \sigma_{km}^\tau n_m e_{ijk} + \mu_{ij}^\tau n_j ds \\ &= \int_V \sigma_{jk} e_{ijk} + x_j \sigma_{mk,m} e_{ijk} + \mu_{ji,j} dV \end{aligned}$$

Equation C.1 transforms to:

$$\int_V \sigma_{ji,j} + F_i dV = 0$$

$$\sigma_{ji,j} + F_i = 0 \quad \text{C.5}$$

While equation C.2 is transformed to the following:

$$\int_V \sigma_{jk} e_{ijk} + x_j \sigma_{mk,m} e_{ijk} + \mu_{ji,j} + x_j F_k e_{ijk} + C_i dV = 0$$

And by importing relation C.5 into the above:

$$\int_V \sigma_{jk} e_{ijk} - x_j F_i e_{ijk} + \mu_{ji,j} + x_j F_k e_{ijk} + C_i dV = 0$$

$$\sigma_{jk} e_{ijk} + \mu_{ji,j} + C_i = 0 \quad \text{C.6}$$

Note that both  $\sigma_{ij}$  and  $\mu_{ij}$  are asymmetric tensors, in contrast to the classic elasticity. However, it is possible for a decomposition of stresses to occur. The stresses could be decomposed into a symmetric and an anti-symmetric part, and the couple stresses into a spherical and a deviatoric part.

$$\sigma_{ij} = \frac{\sigma_{ij} + \sigma_{ji}}{2} + \frac{\sigma_{ij} - \sigma_{ji}}{2} = \tau_{ij} + \alpha_{ij} \quad \text{C.7}$$

$$\mu_{ij} = m_{ij} + \frac{1}{3} \delta_{ij} \mu_{kk} \quad \text{C.8}$$

This way C.6 can be written as follows:

$$\begin{aligned} \sigma_{jk} e_{ijk} + \mu_{ji,j} + C_i &= 0 \\ \tau_{jk} e_{ijk} + \alpha_{jk} e_{ijk} + \mu_{ji,j} + C_i &= 0 \\ \tau_{jk} e_{ijk} e_{mli} + \alpha_{jk} e_{ijk} e_{mli} + \mu_{ji,j} e_{mli} + C_i e_{mli} &= 0 \\ \tau_{jk} e_{ijk} e_{iml} + \alpha_{jk} e_{ijk} e_{iml} + \mu_{ji,j} e_{mli} + C_i e_{mli} &= 0 \\ \tau_{jk} (\delta_{jm} \delta_{kl} - \delta_{jl} \delta_{km}) + \alpha_{jk} (\delta_{jm} \delta_{kl} - \delta_{jl} \delta_{km}) + \mu_{ji,j} e_{mli} + C_i e_{mli} &= 0 \\ (\tau_{ml} - \tau_{lm}) + (\alpha_{ml} - \alpha_{lm}) + \mu_{ji,j} e_{mli} + C_i e_{mli} &= 0 \\ (\tau_{ml} - \tau_{ml}) + (\alpha_{ml} + \alpha_{ml}) + \mu_{ji,j} e_{mli} + C_i e_{mli} &= 0 \\ \alpha_{ml} + \frac{1}{2} \mu_{ji,j} e_{mli} + \frac{1}{2} C_i e_{mli} &= 0 \end{aligned} \quad \text{C.9}$$

With the same procedure C.5 transforms to the following:

$$\begin{aligned} \sigma_{ji,j} + F_i &= 0 \\ \tau_{ij,j} - \alpha_{ij,j} + F_i &= 0 \end{aligned} \quad \text{C.10}$$

Lastly, the substitution of C.9 into C.10 leads to the single equation that describes the equilibrium in the couple stress elasticity problem:

$$\begin{aligned} \tau_{ij,j} - \alpha_{ij,j} + F_i &= 0 \\ \tau_{ml,l} - \alpha_{ml,l} + F_m &= 0 \\ \tau_{ml,l} + \left( \frac{1}{2} \mu_{ji,j} e_{mli} + \frac{1}{2} C_i e_{mli} \right)_{,l} + F_m &= 0 \\ \tau_{ml,l} + \frac{1}{2} \mu_{ji,jl} e_{mli} + \frac{1}{2} C_{i,l} e_{mli} + F_m &= 0 \end{aligned} \quad \text{C.11}$$

And because:

$$\mu_{ji,jl}e_{mli} = m_{ji,jl}e_{mli} - \frac{1}{3} \frac{\delta_{ij}\mu_{kk}}{x_j x_l} e_{mli} = m_{ji,jl}e_{mli} \quad \text{C.12}$$

The balance law, equation C.13, gets the following form:

$$\tau_{ml,l} + \frac{1}{2} m_{ji,jl} e_{mli} + \frac{1}{2} C_{i,l} e_{mli} + F_m = 0 \quad \text{C.13}$$

The free index is the index  $m$  and C.13 is equivalent to three equations. By ignoring the body actions:

$$\begin{aligned} \tau_{11,1} + \tau_{12,2} + \tau_{13,3} + \frac{1}{2} m_{13,12} - \frac{1}{2} m_{12,13} + \frac{1}{2} m_{23,22} - \frac{1}{2} m_{22,23} + \frac{1}{2} m_{33,32} - \frac{1}{2} m_{32,33} &= 0 \\ \tau_{21,1} + \tau_{22,2} + \tau_{23,3} + \frac{1}{2} m_{11,13} - \frac{1}{2} m_{13,11} + \frac{1}{2} m_{21,23} - \frac{1}{2} m_{23,21} + \frac{1}{2} m_{31,33} - \frac{1}{2} m_{33,31} &= 0 \\ \tau_{31,1} + \tau_{32,2} + \tau_{33,3} + \frac{1}{2} m_{12,11} - \frac{1}{2} m_{11,12} + \frac{1}{2} m_{22,21} - \frac{1}{2} m_{21,22} + \frac{1}{2} m_{32,31} - \frac{1}{2} m_{31,32} &= 0 \end{aligned}$$

Note, that relation C.12 is a result of the following calculations, considering that  $e_{mli}$  is not zero for the following combinations and also considering that  $\mu_{kk}$  is smooth enough:

$e_{mli}$	
$e_{mli} = 1$	$e_{mli} = -1$
{1,2,3}	{1,3,2}
{2,3,1}	{2,1,3}
{3,1,2}	{3,2,1}

$$\frac{\delta_{ij}\mu_{kk}}{x_j x_l} e_{mli} = \frac{\mu_{kk}}{x_j x_l} \delta_{ij} e_{mli} = \mu_{kk,jl} e_{mlj} = \begin{cases} \mu_{kk,32} - \mu_{kk,23} \\ \mu_{kk,13} - \mu_{kk,31} \\ \mu_{kk,21} - \mu_{kk,12} \end{cases}$$

The strains can be defined geometrically, as the theory can be considered linear (couple stress elasticity does not consider the contribution of second order derivatives in the strain formulation, but the contribution of strain gradient).

*The strains*

$$\varepsilon_{ij} = \frac{1}{2}(u_{i,j} + u_{j,i}) \quad \text{C.14}$$

*The Spins*

$$\omega_{ij} = \frac{1}{2}(u_{i,j} - u_{j,i}) \quad \text{C.15}$$

*The rotational vector*

$$\omega_i = \frac{1}{2}e_{ijk}u_{k,j} \quad \text{C.16}$$

*The strain Gradients*

$$\kappa_{ij} = \omega_{j,i} = \frac{1}{2}e_{jkm}u_{m,ki} \quad \text{C.17}$$

The strain gradient matrix seems to be asymmetrical and also, its trace seems to be zero. The compatibility equations can be the Saint Venant's compatibility equations.

By assuming a linear isotropic material, the potential-energy density can take the following form:

$$U \equiv U(\varepsilon_{ij}, \kappa_{ij}) = \frac{1}{2}\lambda\varepsilon_{ii}\varepsilon_{jj} + \mu\varepsilon_{ij}\varepsilon_{ij} + 2\eta\kappa_{ij}\kappa_{ij} + 2\eta'\kappa_{ij}\kappa_{ji} \quad \text{C.18}$$

The constitutive laws are produced via differentiations:

*Stresses (total stresses)*

$$\tau_{ij} = \frac{\partial U}{\partial \varepsilon_{ij}} = \frac{1}{2}\lambda\varepsilon_{ii}\delta_{ij} + \frac{1}{2}\lambda\varepsilon_{jj}\delta_{ij} + 2\mu\varepsilon_{ij} = \lambda\varepsilon_{kk}\delta_{ij} + 2\mu\varepsilon_{ij} \quad \text{C.19}$$

*Couple stresses (deviatoric part)*

$$m_{ij} = \frac{\partial U}{\partial \kappa_{ij}} = 4\eta\kappa_{ij} + 2\eta'\kappa_{ji} + 2\eta'(\kappa_{ij}\delta_{ij})\delta_{ji} = 4\eta\kappa_{ij} + 4\eta'\kappa_{ji} \quad \text{C.20}$$

Note that through this method only the symmetrical stresses can be calculated, as the differentiation was done in terms of the strains and the spins were neglected in those formulations. The strains are symmetrical and thus this constitutive law refers only to symmetrical stresses. The strain gradients are produced from the spins, which are deviatoric, and through differentiations, the strain gradients  $\kappa_{ij}$  deviatoric should remain. Thus, the couple stresses that are found from the total energy density are the deviatoric part. The spherical part, however, is not needed, since it is not present in relation C.13 (the balance law).

By importing C.19 and C.20 into relation C.13, the equation that is produced describes the couple stress elasticity problem.

#### iv. The anti-plane formulation in terms of couple stress elasticity

Considering an anti-plane formulation, the above relations are simplified greatly. Since:

$$\begin{aligned} u_x = u_1 &\equiv 0 \\ u_y = u_2 &\equiv 0 \\ u_z = u_3 = w(x, y) &= w(x_1, x_2) \neq 0 \end{aligned}$$

From C.14, the below results can be extracted:

$$\varepsilon_{ij} = \begin{bmatrix} 0 & 0 & \frac{1}{2}u_{3,1} \\ 0 & 0 & \frac{1}{2}u_{3,2} \\ \frac{1}{2}u_{3,1} & \frac{1}{2}u_{3,2} & 0 \end{bmatrix}$$

From C.15, the spin matrix gets the following form:

$$\omega_{ij} = \begin{bmatrix} 0 & 0 & \frac{1}{2}u_{3,1} \\ 0 & 0 & \frac{1}{2}u_{3,2} \\ -\frac{1}{2}u_{3,1} & -\frac{1}{2}u_{3,2} & 0 \end{bmatrix}$$

The spin matrix has three independent components that can be written in a vector form.



$$\omega_i = \begin{cases} \frac{1}{2} u_{3,2} \\ -\frac{1}{2} u_{3,1} \\ 0 \end{cases}$$

By applying in C.17 the corresponding rotational vector:

$$\kappa_{ij} = \begin{cases} \frac{1}{2} u_{3,21} & -\frac{1}{2} u_{3,11} & 0 \\ \frac{1}{2} u_{3,22} & -\frac{1}{2} u_{3,12} & 0 \\ 0 & 0 & 0 \end{cases}$$

This way the constitutive laws C.19 and C.20 are described by the following matrix relations:

$$\tau_{ij} = \begin{bmatrix} 0 & 0 & \mu u_{3,1} \\ 0 & 0 & \mu u_{3,1} \\ \mu u_{3,1} & \mu u_{3,1} & 0 \end{bmatrix} \quad \text{C.21}$$

$$m_{ij} = \begin{bmatrix} 2(\eta + \eta') u_{3,21} & -2\eta u_{3,11} + 2\eta' u_{3,22} & 0 \\ 2\eta u_{3,22} - 2\eta' u_{3,11} & -2(\eta + \eta') u_{3,12} & 0 \\ 0 & 0 & 0 \end{bmatrix} \quad \text{C.22}$$

At this point, the balance law should be used (C.13). By deleting the component that is equal to zero and neglecting the body actions, the below relations are produced:

$$\text{for } m = 1$$

C.23

$$\tau_{11,1} + \tau_{12,2} + \tau_{13,3} + \frac{1}{2} m_{13,12} - \frac{1}{2} m_{12,13} + \frac{1}{2} m_{23,22} - \frac{1}{2} m_{22,23} + \frac{1}{2} m_{33,32} - \frac{1}{2} m_{32,33} = 0$$

$$\tau_{13,3} - \frac{1}{2} m_{12,13} - \frac{1}{2} m_{22,23} = 0$$

for  $m = 2$ 

C.24

$$\tau_{21,1} + \tau_{22,2} + \tau_{23,3} + \frac{1}{2}m_{11,13} - \frac{1}{2}m_{13,11} + \frac{1}{2}m_{21,23} - \frac{1}{2}m_{23,21} + \frac{1}{2}m_{31,33} - \frac{1}{2}m_{33,31} = 0$$

$$\tau_{23,3} + \frac{1}{2}m_{11,13} + \frac{1}{2}m_{21,23} = 0$$

for  $m = 3$ 

C.25

$$\tau_{31,1} + \tau_{32,2} + \tau_{33,3} + \frac{1}{2}m_{12,11} - \frac{1}{2}m_{11,12} + \frac{1}{2}m_{22,21} - \frac{1}{2}m_{21,22} + \frac{1}{2}m_{32,31} - \frac{1}{2}m_{31,32} = 0$$

$$\tau_{31,1} + \tau_{32,2} + \frac{1}{2}m_{12,11} - \frac{1}{2}m_{11,12} + \frac{1}{2}m_{22,21} - \frac{1}{2}m_{21,22} = 0$$

Obviously, the first two equations C.23 and C.24 are self-satisfied, as the derivatives in the anti-plane problem in respect of the out-of-plane direction are zero.

Importing C.21 and C.22 into relation C.25:

$$\tau_{31,1} + \tau_{32,2} + \frac{1}{2}m_{12,11} - \frac{1}{2}m_{11,12} + \frac{1}{2}m_{22,21} - \frac{1}{2}m_{21,22} = 0$$

↔

$$(\mu u_{3,1})_{,1} + (\mu u_{3,2})_{,2} + \frac{1}{2}(-2\eta u_{3,11} + 2\eta' u_{3,22})_{,11} - \frac{1}{2}(2(\eta + \eta') u_{3,21})_{,12}$$

$$+ \frac{1}{2}(-2(\eta + \eta') u_{3,12})_{,21} - \frac{1}{2}(2\eta u_{3,22} - 2\eta' u_{3,11})_{,22} = 0$$

↔

$$\mu u_{3,11} + \mu u_{3,22} - \eta u_{3,1111} + \eta' u_{3,1122} - 2(\eta + \eta') u_{3,1122} - \eta u_{3,2222} + \eta' u_{3,1122} = 0$$

↔

$$\mu \nabla^2 u_3 - \eta u_{3,1111} + \eta' u_{3,1122} - 2\eta u_{3,1122} - 2\eta' u_{3,1122} - \eta u_{3,2222} + \eta' u_{3,1122} = 0$$

↔

$$\leftrightarrow$$

$$\mu \nabla^2 u_3 - \eta (u_{3,1111} + 2 u_{3,1122} + u_{3,2222}) = 0$$

$$\leftrightarrow$$

$$\mu \nabla^2 u_3 - \eta \nabla^2 (\nabla^2 u_3) = 0$$

And by considering the microstructural length:

$$l = \sqrt{2 \frac{\eta}{\mu}} \quad \text{C.26}$$

(This means that  $\eta = \mu \frac{l^2}{2}$ ).

the governing equation of the anti-plane static problem according to the theory of couple stress elasticity is best defined by relation C.27:

$$\mu \nabla^2 u_3 - \mu \frac{l^2}{2} \nabla^4 u_3 = 0 \quad \text{C.27}$$

In the above equation there are obviously body actions, which may be forces per unit area, or moment gradient per unit area. In any case, however, they can be added in the same way. By considering the body action  $X_3$  equal to:

$$X_3 = -\frac{1}{2} C_{i,l} e_{3li} - F_3 \quad \text{C.28}$$

And by adding C.28 into C.27 (in left hand-side):

$$\mu \nabla^2 u_3 - \mu \frac{l^2}{2} \nabla^4 u_3 = X_3 \quad \text{C.29}$$

**v. The anti-plane dynamic couple stress elasticity problem.**

The dynamic problem can be added in the above formulation, through the addition of kinetic energy, and the use of Hamilton's principle. The principle of virtual work can have the following form (note that, the full part of the principle needs the space integral):

$$\int_{t_1}^{t_2} \int_V \delta T + \delta U + \delta A \, dV \, dt = \int_{t_1}^{t_2} \int_V \delta W_{nc} \, dV \, dt \quad \text{C.30}$$

- $T$  is the kinetic energy. In this problem, because of couple stress elasticity the kinetic energy can be written as follows:

$$T = \frac{1}{2} \rho \dot{u}_3 \dot{u}_3 + \frac{\rho H^2}{6} (\dot{\omega}_1 \dot{\omega}_1 + \dot{\omega}_2 \dot{\omega}_2) \quad \text{C.31}$$

Because of the theory of couple stress elasticity, which contains components of strain gradient made from the spin tensor, the spins should be included in the expression of the kinetic energy.

In the above relation  $H$  is the micro-inertial length and  $(\dot{\dots})$  symbolizes the time derivative. Obviously, the potential kinetic energy is the following:

$$\delta T = \rho \dot{u}_3 \delta \dot{u}_3 + \frac{\rho H^2}{3} (\dot{\omega}_1 \delta \dot{\omega}_1 + \dot{\omega}_2 \delta \dot{\omega}_2)$$

And through the use of Hamilton's principle:

$$\begin{aligned} \int_{t_1}^{t_2} \delta T \, dt &= \int_{t_1}^{t_2} \rho \dot{u}_3 \delta \dot{u}_3 + \frac{\rho H^2}{3} (\dot{\omega}_1 \delta \dot{\omega}_1 + \dot{\omega}_2 \delta \dot{\omega}_2) \, dt \\ &= \left[ \dot{u}_3 \delta \dot{u}_3 + \frac{\rho H^2}{3} (\dot{\omega}_1 \delta \dot{\omega}_1 + \dot{\omega}_2 \delta \dot{\omega}_2) \right]_{t_1}^{t_2} - \int_{t_1}^{t_2} \rho \ddot{u}_3 \delta u_3 + \frac{\rho H^2}{3} (\ddot{\omega}_1 \delta \omega_1 + \ddot{\omega}_2 \delta \omega_2) \, dt \\ &= 0 - \int_{t_1}^{t_2} \rho \ddot{u}_3 \delta u_3 + \frac{\rho H^2}{3} (\ddot{\omega}_1 \delta \omega_1 + \ddot{\omega}_2 \delta \omega_2) \, dt \\ &= - \int_{t_1}^{t_2} \rho \ddot{u}_3 \delta u_3 + \frac{\rho H^2}{12} (\ddot{u}_{3,2} \delta u_{3,2} + \ddot{u}_{3,1} \delta u_{3,1}) \, dt \end{aligned}$$

As the space integral is concerned, this formulation can be splitted in a space integral and a boundary integral, following the divergence theorem:

$$\begin{aligned}
\int_V \int_{t_1}^{t_2} \delta T dt dV &= \int_V - \int_{t_1}^{t_2} \rho \ddot{u}_3 \delta u_3 + \frac{\rho H^2}{12} (\ddot{u}_{3,2} \delta u_{3,2} + \ddot{u}_{3,1} \delta u_{3,1}) dt dV = \\
&= - \int_V \int_{t_1}^{t_2} \rho \ddot{u}_3 \delta u_3 - \frac{\rho H^2}{12} (\ddot{u}_{3,22} \delta u_3 + \ddot{u}_{3,11} \delta u_3) \\
&\quad + \frac{\rho H^2}{12} [(\ddot{u}_{3,2} \delta u_3)_{,2} + (\ddot{u}_{3,1} \delta u_3)_{,1}] dt dV \\
&= \int_{t_1}^{t_2} \left[ - \int_V \left\{ \rho \ddot{u}_3 \delta u_3 - \frac{\rho H^2}{12} (\ddot{u}_{3,22} \delta u_3 + \ddot{u}_{3,11} \delta u_3) \right\} dV - \frac{\rho H^2}{12} \int_s (\ddot{u}_{3,2} n_2 \delta u_3 + \ddot{u}_{3,1} n_1 \delta u_3) dS \right] dt \quad \text{C.32}
\end{aligned}$$

By neglecting the kinetic energy, the governing equation is C.29. While taking it into account, it produces one additional term, which is described by the volume integral and one additional boundary condition, which is described by the surface integral.

The term that should be added, in relation C.29 because of the dynamics of the problem, is contained in the volume integral in relation C.32, and specifically is the factor of the potential displacement.

$$Ad. Kinet. Term = -\rho \ddot{u}_3 + \frac{\rho H^2}{12} (\nabla^2 \ddot{u}_3) \quad \text{C.33}$$

Adding relation C.33 in the governing equation C.29 produces the governing equation of the anti-plane dynamic couple stress elasticity problem.

$$\mu \nabla^2 u_3 - \mu \frac{l^2}{2} \nabla^4 u_3 = X_3 + \rho \ddot{u}_3 - \frac{\rho H^2}{12} (\nabla^2 \ddot{u}_3)$$

And by neglecting the body actions,

$$\mu \nabla^2 u_3 - \mu \frac{l^2}{2} \nabla^4 u_3 = \rho \ddot{u}_3 - \frac{\rho H^2}{12} (\nabla^2 \ddot{u}_3) \quad \text{C.34}$$

Note that relations C.34 is the same as relation A.27 and thus the transformation that is described in Appendix B holds.

The same equation would have been produced also by using the principle of virtual works all along. For this scenario:

- $U$  is the total energy density, that can be described by relations C.18. This energy contains displacement first and second gradients and thus needs once more the divergence theorem to expose the potential displacement  $\delta u_3$ . Also, some boundary condition would have been produced from this procedure.
- $A$  is any other work that may occur because of conservative forces. In this, dampers can be included. In the previous procedure this energy is produced from the external body actions.
- $W_{nc}$ : The work of non-conservative action can be included in this energy. In the previous procedure, the work of the body actions is the summation of the energy of the conservative and non-conservative actions.

The last two parts can be neglected, in order for the calculations to get simpler.

### D. The transformation on the hyperbolic problem based on the characteristics

Giannakopoulos and Zisis (2021 a, b) propose for the hyperbolic region, a transformation, that helps the calculation of the displacement and also the polarization, on the hyperbolic case, based on characteristic.

This transformation, that follows a spiral group theory, uses a new system of coordinates, of one variable and this one should be wave-like.

The transformation consists of two parts. The first is applied on the coordinates. One new coordinate  $\bar{\eta}$  is used instead of  $(\xi, \eta)$ . This transformation can be described by the following relation.

$$\bar{\eta} = \frac{\xi}{l} \pm \frac{\eta}{l} \sqrt{\frac{V^2 H^2}{6l^2 c_s^2} - 1} \quad \text{D.1}$$

Also, the derivatives are formulated as follows:

$$\begin{aligned} \frac{\partial(\dots)}{\partial \xi} &= \frac{\partial(\dots)}{\partial \bar{\eta}} \frac{\partial \bar{\eta}}{\partial \xi} = \frac{1}{l} \frac{\partial(\dots)}{\partial \bar{\eta}} \\ \frac{\partial^2(\dots)}{\partial \xi^2} &= \frac{\partial(\partial(\dots)/\partial \xi)}{\partial \xi} = \frac{1}{l} \frac{\partial(\partial(\dots)/\partial \bar{\eta})}{\partial \bar{\eta}} = \frac{1}{l^2} \frac{\partial(\partial(\dots)/\partial \bar{\eta})}{\partial \bar{\eta}} = \frac{1}{l^2} \frac{\partial^2(\dots)}{\partial \bar{\eta}^2} \\ \frac{\partial^4(\dots)}{\partial \xi^4} &= \frac{1}{l^4} \frac{\partial^4(\dots)}{\partial \bar{\eta}^4} \end{aligned}$$

$$\frac{\partial(\dots)}{\partial \eta} = \frac{\partial(\dots)}{\partial \bar{\eta}} \frac{\partial \bar{\eta}}{\partial \eta} = \pm \frac{1}{l} \left( \sqrt{\frac{V^2 H^2}{6l^2 c_s^2} - 1} \right) \frac{\partial(\dots)}{\partial \bar{\eta}} \quad \text{D.2}$$

$$\frac{\partial^2(\dots)}{\partial \eta^2} = \frac{1}{l^2} \left( \frac{V^2 H^2}{6l^2 c_s^2} - 1 \right) \frac{\partial^2(\dots)}{\partial \bar{\eta}^2}$$

$$\frac{\partial^4(\dots)}{\partial \eta^4} = \frac{1}{l^4} \left( \frac{V^2 H^2}{6l^2 c_s^2} - 1 \right)^2 \frac{\partial^4(\dots)}{\partial \bar{\eta}^4}$$

$$\frac{\partial^4(\dots)}{\partial \eta^2 \partial \xi^2} = \frac{1}{l^4} \left( \frac{V^2 H^2}{6l^2 c_s^2} - 1 \right) \frac{\partial^4(\dots)}{\partial \bar{\eta}^4}$$

Importing the derivatives D.2 to equation B.3

$$\frac{1}{l^2} \left(1 - \frac{V^2}{c_s^2}\right) \frac{\partial^2 u_3}{\partial \bar{\eta}^2} + \frac{1}{l^2} \left(\frac{V^2 H^2}{6l^2 c_s^2} - 1\right) \frac{\partial^2 u_3}{\partial \bar{\eta}^2} - \frac{l^2}{2} \frac{1}{l^4} \left(1 - \frac{V^2 H^2}{6l^2 c_s^2}\right) \frac{\partial^4 u_3}{\partial \bar{\eta}^4} - \frac{l^2}{2} \frac{1}{l^4} \left(\frac{V^2 H^2}{6l^2 c_s^2} - 1\right) \left(2 - \frac{V^2 H^2}{6l^2 c_s^2}\right) \frac{\partial^4 u_3}{\partial \bar{\eta}^4} - \frac{l^2}{2} \frac{1}{l^4} \left(\frac{V^2 H^2}{6l^2 c_s^2} - 1\right)^2 \frac{\partial^4(\dots)}{\partial \bar{\eta}^4} = 0$$

↔

$$\left\{ \frac{1}{l^2} \left(1 - \frac{V^2}{c_s^2}\right) + \frac{1}{l^2} \left(\frac{V^2 H^2}{6l^2 c_s^2} - 1\right) \right\} \frac{\partial^2 u_3}{\partial \bar{\eta}^2} + \frac{1}{2l^2} \left\{ -1 + \frac{V^2 H^2}{6l^2 c_s^2} - 3 \frac{V^2 H^2}{6l^2 c_s^2} + \left(\frac{V^2 H^2}{6l^2 c_s^2}\right)^2 + 2 - \left(\frac{V^2 H^2}{6l^2 c_s^2}\right)^2 + 2 \frac{V^2 H^2}{6l^2 c_s^2} - 1 \right\} \frac{\partial^4(\dots)}{\partial \bar{\eta}^4} = 0$$

$$\left(\frac{V^2 H^2}{6l^2 c_s^2} - \frac{V^2}{c_s^2}\right) \frac{\partial^2 u_3}{\partial \bar{\eta}^2} = 0 \quad \text{D.3}$$

The second part of the transformation requires the substitution of the out-of-plane displacement with its logarithm. This transformation is described by the following relation:

$$\bar{h}(\bar{\eta}) = \ln u_3 \quad \text{D.4}$$

This way:

$$\begin{aligned} \frac{\partial^2 u_3}{\partial \bar{\eta}^2} &= \frac{\partial^2 e^{\bar{h}}}{\partial \bar{\eta}^2} = \frac{\partial}{\partial \bar{\eta}} \left( \frac{\partial e^{\bar{h}}}{\partial \bar{\eta}} \right) = \frac{\partial}{\partial \bar{\eta}} \left( e^{\bar{h}} \frac{\partial \bar{h}}{\partial \bar{\eta}} \right) = \frac{\partial e^{\bar{h}}}{\partial \bar{\eta}} \frac{\partial \bar{h}}{\partial \bar{\eta}} + e^{\bar{h}} \frac{\partial}{\partial \bar{\eta}} \left( \frac{\partial \bar{h}}{\partial \bar{\eta}} \right) \\ &= e^{\bar{h}} \left( \frac{\partial \bar{h}}{\partial \bar{\eta}} \right)^2 + e^{\bar{h}} \frac{\partial^2 \bar{h}}{\partial \bar{\eta}^2} \end{aligned} \quad \text{D.5}$$

Importing the second transformation D.5 into relation D.3, the governing equation of the out-of-plane displacement, in the hyperbolic problem becomes the following (D.6):

$$\left(\frac{V^2 H^2}{6l^2 c_s^2} - \frac{V^2}{c_s^2}\right) \left[ \left(\frac{\partial \bar{h}}{\partial \bar{\eta}}\right)^2 + \frac{\partial^2 \bar{h}}{\partial \bar{\eta}^2} \right] = 0 \quad \text{D.6}$$

Also, the polarization equation, B.4, transforms as well:



$$\begin{aligned}
 P_3 - \frac{l^2}{2} \frac{1}{l^2} \frac{\partial^2 P_3}{\partial \bar{\eta}^2} - \frac{l^2}{2} \frac{1}{l^2} \left( \frac{V^2 H^2}{6l^2 c_s^2} - 1 \right) \frac{\partial^2 P_3}{\partial \bar{\eta}^2} &= V^2 \frac{1}{l^2} \frac{\rho(e_{44} - f_{12})}{a\mu} \frac{\partial^2 u}{\partial \bar{\eta}^2} \\
 P_3 - \frac{1}{2} \frac{\partial^2 P_3}{\partial \bar{\eta}^2} - \frac{1}{2} \left( \frac{V^2 H^2}{6l^2 c_s^2} - 1 \right) \frac{\partial^2 P_3}{\partial \bar{\eta}^2} &= V^2 \frac{1}{l^2} \frac{\rho(e_{44} - f_{12})}{a\mu} \frac{\partial^2 u}{\partial \bar{\eta}^2} \\
 P_3 - \frac{V^2 H^2}{12l^2 c_s^2} \frac{\partial^2 P_3}{\partial \bar{\eta}^2} &= \frac{V^2}{l^2} \frac{\rho(e_{44} - f_{12})}{a\mu} \frac{\partial^2 u}{\partial \bar{\eta}^2}
 \end{aligned}
 \tag{D.7}$$

Relation D.7 has the below form:

$$P_3 - A \frac{\partial^2 P_3}{\partial \bar{\eta}^2} = B \frac{\partial^2 u}{\partial \bar{\eta}^2}
 \tag{D.8}$$

Where:

$$A = \frac{V^2 H^2}{12l^2 c_s^2}
 \tag{D.9}$$

$$B = \frac{V^2}{l^2} \frac{\rho(e_{44} - f_{12})}{a\mu}
 \tag{D.10}$$

### E. The Integration with the discontinuities

Chapter 4, uses some advanced mathematical results, which should be proved. Those concern the integrals in which the Dirac's delta function is included, its gradient and also the Heaviside function. Some necessary points of theory, that justify those calculations exist on [Ronald N. Bracewell \(1999\)](#).

#### i. The integral $\int g(x) * H(x - c) dx$

This integral can be easily calculated by using integration by parts. By considering the anti-derivative of the function " $g(x)$ ":

$$\theta(x) = \int g(x) dx$$

can be written as beneath:

$$\begin{aligned} \int g(x) * H(x - c) dx &= \int \theta'(x) * H(x - c) dx \\ &= \theta(x) * H(x - c) - \int \theta(x) * \delta(x - c) dx \\ &= \theta(x) * H(x - c) - \theta(c) * H(x - c) \\ &= \int g(x) dx * H(x - c) - \int g(x) dx \Big|_{x=c} * H(x - c) \end{aligned} \tag{E.1}$$

The integral  $\int \theta(x) * \delta(x - c) dx$  is equal to  $\theta(c) * H(x - c)$ . However, this is something to be proved later.

#### ii. The integral $\int g(x) * \delta(x - c) dx$

From bibliography, [Ronald N. Bracewell \(1999\)](#) the below formula relative with the integrals of relations that include the Dirac's delta function, can be considered true:

$$\int_{-\infty}^{\infty} g(x) * \delta(x) dx = g(0) \tag{E.2}$$

Also, it is known that the antiderivative, which can be depicted as an integral (indefinite integral), can be written as a defined integral, in the right space.

$$\int f(x) dx = \int_{-\infty}^x f(x_0) dx_0$$

Using the Macaulay brackets of zero order or the Heaviside function, it is possible to rewrite the above integral as it goes to infinite. As the integral of a constant function equals to zero, is also zero, then by defining the function that resides inside the integral to be zero for “ $x_0$ ” greater than the “ $x$ ”, the above integral can be written until infinite. In this case the function “ $f(x_0)$ ” should be replaced with the function “ $f(x_0) * H(x - x_0)$ ”. This way the following can be considered:

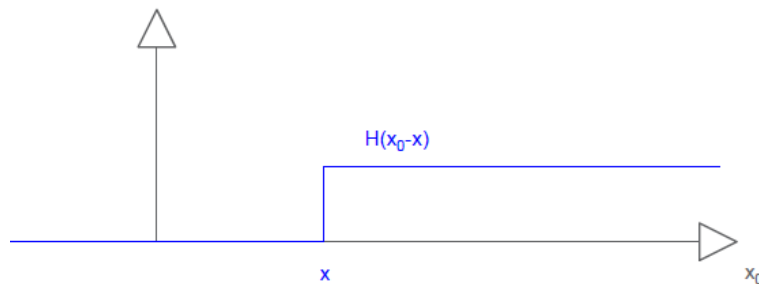


Fig. 103. The Heaviside function.

It is very important to notice that in the current situation the variable  $x_0$  represented the coordinate and the variable  $x$  represents a value in that axis. The space, in which that function  $f$  should be zero, is the same with the space, where the Heaviside function is equal to 1 and the space where the function  $f$  should be non-zero is where the above Heaviside is zero. Thus, it is noticeable that  $f(x_0) * \{1 - H(x_0 - x)\} = f(x_0) * H(x - x_0)$

$$\int f(x) dx = \int_{-\infty}^x f(x_0) dx_0 = \int_{-\infty}^{\infty} f(x_0) * H(x - x_0) dx_0$$

As the purpose is to calculate the integral “ $\int g(x)\delta(x - c) dx$ ” a substitution is required. More specifically, a substitution of “ $f(x) = g(x)\delta(x - c)$ ”:

$$\int g(x) * \delta(x - c) dx = \int_{-\infty}^x g(x_0) * \delta(x_0 - c) dx_0$$

$$\begin{aligned}
&= \int_{-\infty}^{\infty} g(x_0) * \delta(x_0 - c) * H(x - x_0) dx_0 \\
&= \int_{-\infty}^{\infty} \{g(x_0) * H(x - x_0)\} * \delta(x_0 - c) dx_0
\end{aligned}$$

Now, by changing the variable “ $x_0 = \eta + c$ ”:

$$\begin{aligned}
\int g(x) * \delta(x - c) dx &= \int_{-\infty}^{\infty} \{g(\eta + c) * H(x - \eta - c)\} * \delta(\eta + c - c) d\eta \\
&= \int_{-\infty}^{\infty} \{g(\eta + c) * H(x - \eta - c)\} * \delta(\eta) d\eta \\
&= g(\eta + c) * H(x - \eta - c) |_{\eta=0} \\
&= g(c) * H(x - c)
\end{aligned}$$

E.3

### iii. The integral $\int g(x) * \delta'(x - c) dx$

This integral has a form suitable for integration by parts:

$$\begin{aligned}
\int g(x) * \delta'(x - c) dx &= g(x) * \delta(x - c) - \int \frac{\partial g(x)}{\partial x} * \delta(x - c) dx \\
&= g(x) * \delta(x - c) - \left. \frac{\partial g(x)}{\partial x} \right|_{x=c} * H(x - c)
\end{aligned}$$

Where obviously  $\delta'(x - c) = \partial \delta(x - c) / \partial x$ .

This means when  $g(\eta) = e^{-\eta/\sqrt{A}} * f(\eta)$ , the following can be considered:

$$\begin{aligned}
\int e^{-\eta/\sqrt{A}} * f(\eta) * \delta'(x - a) dx &= e^{-\eta/\sqrt{A}} * f(\eta) * \delta(\eta - a) \\
&+ \frac{e^{-\eta/\sqrt{A}} * f(\eta)}{\sqrt{A}} \Big|_{\eta=a} * H(\eta - a) \\
&- e^{-\eta/\sqrt{A}} * f'(\eta) \Big|_{\eta=a} * H(\eta - a)
\end{aligned} \tag{E.4}$$

In the case of the linear profile, the gradient of the function:

$$f'(\eta) = \frac{\partial f(\eta)}{\partial \eta} \Big|_{\eta=a} = \frac{u_{max}}{b - a} \tag{E.5}$$

For this linear case, the last term of the integral is also calculated. The second however is neglected as it was asked, the vertical displacement in the crack tip to be zero. The same happens also for the other integral with “b” instead of “a” and also the integral with the plus in the exponent.

The spike term, which is the term that includes the delta function can be given two interpretations. The first one, which can be done in both linear and 3<sup>rd</sup> order displacement, is to leave it there and in some point the one spike from the integral with the minus in the exponent will cancel out the spike of integral with a plus in the exponent.

However, in some cases (e.g. the “screw dislocation”) this will not be enough as the spikes doesn’t cancel out. This is why a second interpretation is needed.

#### iv. The spike

In some point the term “ $\theta(\eta) * \delta(\eta - a)$ ” appears while “ $\theta(a) = 0$ ” (e.g., “ $\theta(\eta) = e^{\frac{\eta-a}{\sqrt{A}}} - e^{-\frac{\eta-a}{\sqrt{A}}}$ ”). This expression is pretty awkward because there is a pathological situation of multiplying zero with infinite. Is this infinite, zero, or something in between? To answer this, the continuity of the polarization should be demanded.

If the function “ $\theta(x)$ ” is continuous near “ $x = a$ ” then:

$$\lim_{x \rightarrow a} \theta(x) = \theta(0) = 0$$

This requirement can be easily satisfied as the function “ $\theta(x)$ ” is the function that joins the maximum and the minimum displacement. (e.g., Linear or 3<sup>rd</sup> order polynomial).

Also, as the Dirac's delta function is concerned, which is discontinuous, the limit can also be estimated. When " $x \rightarrow a^-$ " the " $x$ " is different than " $a$ " and thus the limit is equal to zero. The same happens from the other side.

$$\lim_{x \rightarrow a^-} \delta(x - a) = 0$$

$$\lim_{x \rightarrow a^+} \delta(x - a) = 0$$

$$\lim_{x \rightarrow a} \delta(x - a) = 0$$

Obviously, the Dirac's delta function is discontinuous as:

$$0 = \lim_{x \rightarrow a} \delta(x - a) \neq \delta(0) = \infty$$

The limit of the function " $\theta(\eta) * \delta(\eta - a)$ " is however in any case equal to zero.

$$\lim_{x \rightarrow a} \{\theta(\eta) * \delta(\eta - a)\} = 0$$

If, for any reason, the result needs to be continuous, then the following suggestion is true in an area near " $a$ ":

$$\left( e^{\frac{\eta-a}{\sqrt{A}}} - e^{-\frac{\eta-a}{\sqrt{A}}} \right) * \delta(\eta - a) = 0 \quad \text{E.6}$$

And then this suggestion is expanded everywhere, because far from " $a$ " the Dirac's delta function is zero.

## F. The joining functions

### i. The polynomial function of 3<sup>rd</sup> order

One easy way to find a polynomial function is to insert the value of the gradient of the function on points a and b, in which the function should have a minimum and a maximum and thus those gradients should be zero.

$$f(a) = 0$$

$$f(b) = u_{max}$$

$$\left. \frac{\partial f(x)}{\partial x} \right|_{x=a} = 0$$

$$\left. \frac{\partial f(x)}{\partial x} \right|_{x=b} = 0$$

Those boundary conditions allow a consideration of a function with four unknown variables.

$$f(x) = t * x^3 + m * x^2 + c * x + d$$

This function has the following gradient:

$$\frac{\partial f(x)}{\partial x} = 3 * t * x^2 + 2 * m * x + c$$

By importing the above function and its gradient to the boundary conditions, proposed in the beginning, the following system is produced:

$$\left\{ \begin{array}{l} t * a^3 + m * a^2 + c * a + d = 0 \\ t * b^3 + m * b^2 + c * b + d = u_{max} \\ 3 * t * a^2 + 2 * m * a + c = 0 \\ 3 * t * b^2 + 2 * m * b + c = 0 \end{array} \right.$$

Or in matrix form:

$$\begin{bmatrix} a^3 & a^2 & a & 1 \\ b^3 & b^2 & b & 1 \\ 3a^2 & 2a & 1 & 0 \\ 3a^2 & 2a & 1 & 0 \end{bmatrix} * \begin{Bmatrix} t \\ m \\ c \\ d \end{Bmatrix} = \begin{Bmatrix} 0 \\ u_{max} \\ 0 \\ 0 \end{Bmatrix}$$

This system can easily be solved via a symbolic language.

$$\begin{Bmatrix} t \\ m \\ c \\ d \end{Bmatrix} = \frac{u_{max}}{a^3 - 3 * a^2 * b + 3 * a * b^2 - b^3} * \begin{Bmatrix} 2 \\ -3 * (a + b) \\ 6 * a * b \\ a^2 * (a - 3b) \end{Bmatrix}$$

Obviously, the dimension of  $a$  and  $b$ , is the same as the dimension of the coordinate  $x$ .

As a result, a third order function that obeys the demanded boundary conditions is the following:

$$f(x) = u_{max} * \frac{2 * x^3 - 3 * (a + b) * x^2 + 6 * a * b * x + a^2 * (a - 3b)}{a^3 - 3 * a^2 * b + 3 * a * b^2 - b^3} \quad \text{F.1}$$

## ii. The polynomial function of 5<sup>th</sup> order

The 3<sup>rd</sup> degree function, gives from one hand good results. From the other hand the form of the displacement has some errors. One easy way to fix this error, to make the displacement more trapezoid, (to make the function looks more like the linear case), is to increase the order of the function.

By importing two more “boundary conditions” which look more alike the condition of symmetry or anti-symmetry, it is possible to create a function of 5<sup>th</sup> degree, with 6 unknown values.

The conditions that should be imported are the conditions in the middle of the length between points  $a$  and  $b$ . In this point,  $((a + b)/2)$  the value of the displacement should be  $u_{max}/2$  while the gradient of the function should be as the linear gradient equal to  $u_{max}/(b - a)$ .

The 5<sup>th</sup> degree polynomial function has the below form:

$$f(x) = g * x^5 + h * x^4 + t * x^3 + m * x^2 + c * x + d \quad \text{F.2}$$



Which has two additional unknown variables. The boundary conditions are the following:

$$f(a) = 0$$

$$f\left(\frac{a+b}{2}\right) = \frac{u_{max}}{2}$$

$$f(b) = u_{max}$$

$$\left.\frac{\partial f(x)}{\partial x}\right|_{x=a} = 0$$

$$\left.\frac{\partial f(x)}{\partial x}\right|_{x=\frac{a+b}{2}} = \frac{u_{max}}{b-a}$$

$$\left.\frac{\partial f(x)}{\partial x}\right|_{x=b} = 0$$

And the system that needs to be solved is the following

$$\begin{bmatrix} a^5 & a^4 & a^3 & a^2 & a & 1 \\ b^5 & b^4 & b^3 & b^2 & b & 1 \\ \left(\frac{a+b}{2}\right)^5 & \left(\frac{a+b}{2}\right)^4 & \left(\frac{a+b}{2}\right)^3 & \left(\frac{a+b}{2}\right)^2 & \left(\frac{a+b}{2}\right) & 1 \\ 5 * a^4 & 4 * a^3 & 3 * a^2 & 2 * a & 1 & 0 \\ 5 * b^4 & 4 * b^3 & 3 * b^2 & 2 * a & 1 & 0 \\ 5 * \left(\frac{a+b}{2}\right)^4 & 4 * \left(\frac{a+b}{2}\right)^3 & 3 * \left(\frac{a+b}{2}\right)^2 & 2 * \left(\frac{a+b}{2}\right) & 1 & 0 \end{bmatrix} * \begin{pmatrix} g \\ h \\ t \\ m \\ c \\ d \end{pmatrix} = \begin{pmatrix} 0 \\ \frac{u_{max}}{2} \\ u_{max} \\ 0 \\ \frac{u_{max}}{b-a} \\ 0 \end{pmatrix}$$

$$\begin{pmatrix} g \\ h \\ t \\ m \\ c \\ d \end{pmatrix} = \frac{u_{max}}{(a-b)^5} * \begin{pmatrix} 20 * (a+b) \\ 18 * \left(a^2 + \frac{22}{9} * a * b + b^2\right) \\ 7 * (a+b) * \left(a^2 + \frac{26}{7} * a * b + b^2\right) \\ 14 * a * b * \left(a^2 + \frac{6}{7} * a * b + b^2\right) \\ 14 * a^2 * (a^3 - 5 * a^2 * b + 3 * a * b^2 - 7 * b^3) \end{pmatrix} \quad \text{F.3}$$

Importing F.3 to F.2, the polynomial function of 5<sup>th</sup> order that obeys the criteria for the joining function is produced.

## G. The calculations that describe the induced polarization

### i. Linear Function

A Polynomial function that can describe the displacement, could be a linear function and as it was calculated above, the right formula of the joining function is the following:

$$\begin{aligned}
 f(\eta) &= \frac{u_{max}}{b-a} * (\eta - a) \\
 \frac{\partial f(\eta)}{\partial \eta} &= \frac{u_{max}}{b-a} \\
 \frac{\partial^2 f(\eta)}{\partial \eta^2} &= 0
 \end{aligned}
 \tag{G.1}$$

This function is none other than the function that describes the displacement between point  $a$  and  $b$  in relation 22, as this function creates a trapezoidal distribution of displacements.

For this function the first integral that resides in relation **x** of chapter 4 can be simplified to the following relation:

$$\begin{aligned}
 \int e^{\frac{-\eta}{\sqrt{A}}} * \frac{\partial^2 u(\eta)}{\partial \eta^2} d\eta &= \int e^{\frac{-\eta}{\sqrt{A}}} * \frac{\partial^2 f(\eta)}{\partial \eta^2} * [H(\eta - \alpha) - H(\eta - b)] d\eta \\
 &+ \int e^{\frac{-\eta}{\sqrt{A}}} * 2 * \frac{\partial f(\eta)}{\partial \eta} * [\delta(\eta - \alpha) - \delta(\eta - b)] d\eta \\
 &+ \int e^{\frac{-\eta}{\sqrt{A}}} * f(\eta) * [\delta'(\eta - \alpha) - \delta'(\eta - b)] d\eta \\
 &+ \int e^{\frac{-\eta}{\sqrt{A}}} * u_{max} * \delta'(\eta - b) d\eta
 \end{aligned}$$

The first term vanishes as the second derivative is always zero. By applying the calculation, as described before in **Appendix E** and **chapter 4**, the following calculations take place:

$$\int e^{\frac{-\eta}{\sqrt{A}}} * \frac{\partial^2 u(\eta)}{\partial \eta^2} d\eta = \int e^{\frac{-\eta}{\sqrt{A}}} * 2 * \frac{\partial f(\eta)}{\partial \eta} * [\delta(\eta - \alpha) - \delta(\eta - b)] d\eta$$

$$\begin{aligned}
& + \int e^{\frac{-\eta}{\sqrt{A}}} * f(\eta) * [\delta'(\eta - a) - \delta'(\eta - b)] d\eta \\
& + \int e^{\frac{-\eta}{\sqrt{A}}} * u_{max} * \delta'(\eta - b) d\eta \\
\int e^{\frac{-\eta}{\sqrt{A}}} * \frac{\partial^2 u(\eta)}{\partial \eta^2} d\eta & = 2 * \frac{\partial f(\eta)}{\partial \eta} * e^{\frac{-\eta}{\sqrt{A}}} \Big|_{\eta=a} * H(\eta - a) - 2 * \frac{\partial f(\eta)}{\partial \eta} * e^{\frac{-\eta}{\sqrt{A}}} \Big|_{\eta=b} * H(\eta - b) \\
& + e^{\frac{-\eta}{\sqrt{A}}} * f(\eta) * \delta(\eta - a) + \left\{ \frac{e^{\frac{-\eta}{\sqrt{A}}} * f(\eta)}{\sqrt{A}} - e^{\frac{-\eta}{\sqrt{A}}} * \frac{\partial f(\eta)}{\partial \eta} \right\} \Big|_{\eta=a} * H(\eta - a) \\
& - e^{\frac{-\eta}{\sqrt{A}}} * f(\eta) * \delta(\eta - b) - \left\{ \frac{e^{\frac{-\eta}{\sqrt{A}}} * f(\eta)}{\sqrt{A}} - e^{\frac{-\eta}{\sqrt{A}}} * \frac{\partial f(\eta)}{\partial \eta} \right\} \Big|_{\eta=b} * H(\eta - b) \\
& + e^{\frac{-\eta}{\sqrt{A}}} * u_{max} * \delta(\eta - b) + \frac{e^{\frac{-\eta}{\sqrt{A}}} * u_{max}}{\sqrt{A}} \Big|_{\eta=b} * H(\eta - b)
\end{aligned}$$

Because  $f(\eta) = 0$  and  $f(\eta) = u_{max}$ , some simplifications can occur. By substitution of these, the following relations are created:

$$\begin{aligned}
\int e^{\frac{-\eta}{\sqrt{A}}} * \frac{\partial^2 u(\eta)}{\partial \eta^2} d\eta & = \frac{u_{max}}{b - a} * e^{\frac{-a}{\sqrt{A}}} * H(\eta - a) - \frac{u_{max}}{b - a} * e^{\frac{-b}{\sqrt{A}}} * H(\eta - b) \\
& + e^{\frac{-\eta}{\sqrt{A}}} * f(\eta) * \delta(\eta - a) + e^{\frac{-\eta}{\sqrt{A}}} * \{u_{max} - f(\eta)\} * \delta(\eta - b)
\end{aligned}$$

$$\begin{aligned}
\int e^{\frac{-\eta}{\sqrt{A}}} * \frac{\partial^2 u(\eta)}{\partial \eta^2} d\eta & = \frac{u_{max}}{b - a} * \left\{ e^{\frac{-a}{\sqrt{A}}} * H(\eta - a) - e^{\frac{-b}{\sqrt{A}}} * H(\eta - b) \right\} \\
& + e^{\frac{-\eta}{\sqrt{A}}} * f(\eta) * \delta(\eta - a) + e^{\frac{-\eta}{\sqrt{A}}} * \{u_{max} - f(\eta)\} * \delta(\eta - b)
\end{aligned}$$

G.2

Similarly, the second integral takes the beneath form:

$$\begin{aligned}
\int e^{\frac{\eta}{\sqrt{A}}} * \frac{\partial^2 u(\eta)}{\partial \eta^2} d\eta &= \int e^{\frac{\eta}{\sqrt{A}}} * 2 * \frac{\partial f(\eta)}{\partial \eta} * [\delta(\eta - a) - \delta(\eta - b)] d\eta \\
&+ \int e^{\frac{\eta}{\sqrt{A}}} * f(\eta) * [\delta'(\eta - a) - \delta'(\eta - b)] d\eta \\
&+ \int e^{\frac{\eta}{\sqrt{A}}} * u_{max} * \delta'(\eta - b) d\eta
\end{aligned}$$

By using the boundary values of the joining function:

$$\begin{aligned}
\int e^{\frac{\eta}{\sqrt{A}}} * \frac{\partial^2 u(\eta)}{\partial \eta^2} d\eta &= 2 * \frac{\partial f(\eta)}{\partial \eta} * e^{\frac{\eta}{\sqrt{A}}} \Big|_{\eta=a} * H(\eta - a) - 2 * \frac{\partial f(\eta)}{\partial \eta} * e^{\frac{\eta}{\sqrt{A}}} \Big|_{\eta=b} * H(\eta - b) \\
&+ e^{\frac{\eta}{\sqrt{A}}} * f(\eta) * \delta(\eta - a) - \left\{ \frac{e^{\frac{\eta}{\sqrt{A}}} * f(\eta)}{\sqrt{A}} + e^{\frac{\eta}{\sqrt{A}}} * \frac{\partial f(\eta)}{\partial \eta} \Big|_{\eta=a} \right\} * H(\eta - a) \\
&- e^{\frac{\eta}{\sqrt{A}}} * f(\eta) * \delta(\eta - b) + \left\{ \frac{e^{\frac{\eta}{\sqrt{A}}} * f(\eta)}{\sqrt{A}} + e^{\frac{\eta}{\sqrt{A}}} * \frac{\partial f(\eta)}{\partial \eta} \Big|_{\eta=b} \right\} \\
&\quad * H(\eta - b) \\
&+ e^{\frac{\eta}{\sqrt{A}}} * u_{max} * \delta(\eta - b) - \frac{e^{\frac{\eta}{\sqrt{A}}} * u_{max}}{\sqrt{A}} \Big|_{\eta=b} * H(\eta - b)
\end{aligned}$$

And by substituting:

$$\begin{aligned}
\int e^{\frac{\eta}{\sqrt{A}}} * \frac{\partial^2 u(\eta)}{\partial \eta^2} d\eta &= \frac{u_{max}}{b - a} * e^{\frac{a}{\sqrt{A}}} * H(\eta - a) - \frac{u_{max}}{b - a} * e^{\frac{b}{\sqrt{A}}} * H(\eta - b) \\
&+ e^{\frac{\eta}{\sqrt{A}}} * f(\eta) * \delta(\eta - a) + e^{\frac{\eta}{\sqrt{A}}} * \{u_{max} - f(\eta)\} * \delta(\eta - b) \\
\int e^{\frac{\eta}{\sqrt{A}}} * \frac{\partial^2 u(\eta)}{\partial \eta^2} d\eta &= \frac{u_{max}}{b - a} * \left\{ e^{\frac{a}{\sqrt{A}}} * H(\eta - a) - e^{\frac{b}{\sqrt{A}}} * H(\eta - b) \right\} \\
&+ e^{\frac{\eta}{\sqrt{A}}} * f(\eta) * \delta(\eta - a) + e^{\frac{\eta}{\sqrt{A}}} * \{u_{max} - f(\eta)\} * \delta(\eta - b)
\end{aligned}$$

G.3

By substituting those two integrals, relations G.2 and G.3 to the relation x (chapter 4) the polarization can be given by the beneath relation:

$$\begin{aligned}
 P_3(\eta) &= c_1 * e^{+\frac{\eta}{\sqrt{A}}} + c_2 * e^{-\frac{\eta}{\sqrt{A}}} \\
 &+ \frac{B}{2 * \sqrt{A}} * \left[ -e^{+\frac{\eta}{\sqrt{A}}} * \int e^{-\frac{\eta}{\sqrt{A}}} * \frac{d^2 u_3}{d\eta^2} d\eta + e^{-\frac{\eta}{\sqrt{A}}} * \int e^{+\frac{\eta}{\sqrt{A}}} * \frac{d^2 u_3}{d\eta^2} d\eta \right] \\
 P_3(\eta) &= c_1 * e^{+\frac{\eta}{\sqrt{A}}} + c_2 * e^{-\frac{\eta}{\sqrt{A}}} + \frac{B}{2 * \sqrt{A}} * \frac{u_{max}}{b-a} * \left[ -e^{+\frac{\eta}{\sqrt{A}}} * \left\{ e^{\frac{-a}{\sqrt{A}}} * H(\eta - a) - e^{\frac{-b}{\sqrt{A}}} * H(\eta - b) \right\} \right. \\
 &\quad \left. + e^{-\frac{\eta}{\sqrt{A}}} * \left\{ e^{\frac{a}{\sqrt{A}}} * H(\eta - a) - e^{\frac{b}{\sqrt{A}}} * H(\eta - b) \right\} \right] \\
 &+ \frac{B}{2 * \sqrt{A}} * \left[ -e^{+\frac{\eta}{\sqrt{A}}} * \left\{ e^{\frac{-\eta}{\sqrt{A}}} * f(\eta) * \delta(\eta - a) + e^{\frac{-\eta}{\sqrt{A}}} * \{u_{max} - f(\eta)\} * \delta(\eta - b) \right\} \right] \\
 &+ \frac{B}{2 * \sqrt{A}} * \left[ +e^{-\frac{\eta}{\sqrt{A}}} * \left\{ e^{\frac{\eta}{\sqrt{A}}} * f(\eta) * \delta(\eta - a) + e^{\frac{\eta}{\sqrt{A}}} * \{u_{max} - f(\eta)\} * \delta(\eta - b) \right\} \right] \\
 P_3(\eta) &= c_1 * e^{+\frac{\eta}{\sqrt{A}}} + c_2 * e^{-\frac{\eta}{\sqrt{A}}} + \frac{B}{2 * \sqrt{A}} * \frac{u_{max}}{b-a} * \left[ -e^{+\frac{\eta}{\sqrt{A}}} * \left\{ e^{\frac{-a}{\sqrt{A}}} * H(\eta - a) - e^{\frac{-b}{\sqrt{A}}} * H(\eta - b) \right\} \right. \\
 &\quad \left. + e^{-\frac{\eta}{\sqrt{A}}} * \left\{ e^{\frac{a}{\sqrt{A}}} * H(\eta - a) - e^{\frac{b}{\sqrt{A}}} * H(\eta - b) \right\} \right] \\
 &+ \frac{B}{2 * \sqrt{A}} * [-f(\eta) * \delta(\eta - a) - \{u_{max} - f(\eta)\} * \delta(\eta - b)] \\
 &+ \frac{B}{2 * \sqrt{A}} * [f(\eta) * \delta(\eta - a) + \{u_{max} - f(\eta)\} * \delta(\eta - b) *]
 \end{aligned}$$

$$P_3(\eta) = c_1 * e^{+\frac{\eta}{\sqrt{A}}} + c_2 * e^{-\frac{\eta}{\sqrt{A}}} + \frac{B}{2 * \sqrt{A}} * \frac{u_{max}}{b-a} * \left[ -e^{+\frac{\eta-a}{\sqrt{A}}} * H(\eta-a) + e^{+\frac{\eta-b}{\sqrt{A}}} * H(\eta-b) \right. \\ \left. + e^{-\frac{\eta-a}{\sqrt{A}}} * H(\eta-a) - e^{-\frac{\eta-b}{\sqrt{A}}} * H(\eta-b) \right] \quad \text{G.4}$$

As it was also mentioned in [Appendix F](#), those two spike terms (red) cancel out themselves.

### ii. 3<sup>rd</sup> degree function

Another case of a function that can fit, in the cohesive zone, between the maximum and the minimum value is a polynomial function of third order. That function that was determined in [Appendix F](#) has an analogue procedure with the linear function.

$$f(\eta) = \frac{u_{max}}{a^3 - 3ab^2 + 3ab^2 - b^3} \{2\eta^3 - 3(a+b)\eta^2\} + 6ab\eta + (a-3b)a^2 \quad \text{G.5}$$

$$\frac{\partial^2 f(\eta)}{\partial \eta^2} = \frac{u_{max}}{a^3 - 3ab^2 + 3ab^2 - b^3} * \{12\eta - 6(a+b)\}$$

In this case however, the first term of each integral that needs to be calculated, is non zero as the second derivative is also non zero. However, by definition, the gradient of this function at point  $a$  and  $b$  is zero, so the second term in each integral vanishes instead.

$$\int e^{-\frac{\eta}{\sqrt{A}}} * \frac{\partial^2 u(\eta)}{\partial \eta^2} d\eta = \int e^{-\frac{\eta}{\sqrt{A}}} * \frac{\partial^2 f(\eta)}{\partial \eta^2} * [H(\eta-a) - H(\eta-b)] d\eta \\ + \int e^{-\frac{\eta}{\sqrt{A}}} * 2 * \frac{\partial f(\eta)}{\partial \eta} * [\delta(\eta-a) - \delta(\eta-b)] d\eta \\ + \int e^{-\frac{\eta}{\sqrt{A}}} * f(\eta) * [\delta'(\eta-a) - \delta'(\eta-b)] d\eta \\ + \int e^{-\frac{\eta}{\sqrt{A}}} * u_{max} * \delta'(\eta-b) d\eta$$

The calculation of the first term needs the calculation of the respectively antiderivative beforehand.

The first antiderivative, that refers to the integral in which the exponential contains the minus sign can be calculated as beneath.

$$\begin{aligned}
 g(\eta) &= \int e^{\frac{-\eta}{\sqrt{A}}} * \frac{\partial^2 f(\eta)}{\partial \eta^2} d\eta \\
 &= \int e^{\frac{-\eta}{\sqrt{A}}} * \frac{u_{max}}{\dots} * \{12\eta - 6(a + b)\} d\eta \\
 &= \int \frac{u_{max}}{\dots} * 12\eta * e^{\frac{-\eta}{\sqrt{A}}} d\eta - \int \frac{u_{max}}{\dots} * 6(a + b) * e^{\frac{-\eta}{\sqrt{A}}} * d\eta \\
 &= \frac{u_{max}}{\dots} * \left\{ -12 * \eta * \sqrt{A} * e^{\frac{-\eta}{\sqrt{A}}} - 12 * A * e^{\frac{-\eta}{\sqrt{A}}} + 6 * \sqrt{A} * (a + b) * e^{\frac{-\eta}{\sqrt{A}}} \right\} \\
 &= \frac{u_{max}}{\dots} * e^{\frac{-\eta}{\sqrt{A}}} * \{ -12 * \eta * \sqrt{A} - 12 * A + 6 * \sqrt{A} * (a + b) \}
 \end{aligned}$$

And thus, the first integral is the following:

$$\begin{aligned}
 \int e^{\frac{-\eta}{\sqrt{A}}} * \frac{\partial^2 u(\eta)}{\partial \eta^2} d\eta &= \int e^{\frac{-\eta}{\sqrt{A}}} * \frac{\partial^2 f(\eta)}{\partial \eta^2} * [H(\eta - \alpha) - H(\eta - b)] d\eta \\
 &+ \int e^{\frac{-\eta}{\sqrt{A}}} * 2 * \frac{\partial f(\eta)}{\partial \eta} * [\delta(\eta - \alpha) - \delta(\eta - b)] d\eta \\
 &+ \int e^{\frac{-\eta}{\sqrt{A}}} * f(\eta) * [\delta'(\eta - \alpha) - \delta'(\eta - b)] d\eta \\
 &+ \int e^{\frac{-\eta}{\sqrt{A}}} * u_{max} * \delta'(\eta - b) d\eta
 \end{aligned}$$

$$\begin{aligned}
\int e^{\frac{-\eta}{\sqrt{A}}} * \frac{\partial^2 u(\eta)}{\partial \eta^2} d\eta &= g(\eta) * H(\eta - a) - g(a) * H(\eta - a) - g(\eta) * H(\eta - b) + g(b) * H(\eta - b) \\
&+ 2 * \frac{\partial f(\eta)}{\partial \eta} * e^{\frac{-\eta}{\sqrt{A}}} \Big|_{\eta=a} * H(\eta - a) - 2 * \frac{\partial f(\eta)}{\partial \eta} * e^{\frac{-\eta}{\sqrt{A}}} \Big|_{\eta=b} * H(\eta - b) \\
&+ e^{\frac{-\eta}{\sqrt{A}}} * f(\eta) * \delta(\eta - a) + \left\{ \frac{e^{\frac{-\eta}{\sqrt{A}}} * f(\eta)}{\sqrt{A}} - e^{\frac{-\eta}{\sqrt{A}}} * \frac{\partial f(\eta)}{\partial \eta} \right\} \Big|_{\eta=a} * H(\eta - a) \\
&- e^{\frac{-\eta}{\sqrt{A}}} * f(\eta) * \delta(\eta - b) - \left\{ \frac{e^{\frac{-\eta}{\sqrt{A}}} * f(\eta)}{\sqrt{A}} - e^{\frac{-\eta}{\sqrt{A}}} * \frac{\partial f(\eta)}{\partial \eta} \right\} \Big|_{\eta=b} * H(\eta - b) \\
&+ e^{\frac{-\eta}{\sqrt{A}}} * u_{max} * \delta(\eta - b) + \frac{e^{\frac{-\eta}{\sqrt{A}}} * u_{max}}{\sqrt{A}} \Big|_{\eta=b} * H(\eta - b)
\end{aligned}$$

However, because  $\frac{\partial f(\eta)}{\partial \eta} \Big|_{\eta=b} = \frac{\partial f(\eta)}{\partial \eta} \Big|_{\eta=a} = 0$ ,  $f(\eta) = 0$  and  $u_{max} - f(\eta) = 0$

$$\begin{aligned}
\int e^{\frac{-\eta}{\sqrt{A}}} * \frac{\partial^2 u(\eta)}{\partial \eta^2} d\eta &= g(\eta) * H(\eta - a) - g(a) * H(\eta - a) - g(\eta) * H(\eta - b) + g(b) * H(\eta - b) \\
&+ \frac{\partial f(\eta)}{\partial \eta} * e^{\frac{-\eta}{\sqrt{A}}} \Big|_{\eta=a} * H(\eta - a) - \frac{\partial f(\eta)}{\partial \eta} * e^{\frac{-\eta}{\sqrt{A}}} \Big|_{\eta=b} * H(\eta - b) \\
&+ \left\{ \frac{e^{\frac{-\eta}{\sqrt{A}}} * f(\eta)}{\sqrt{A}} \right\} \Big|_{\eta=a} * H(\eta - a) \\
&+ \frac{e^{\frac{-\eta}{\sqrt{A}}}}{\sqrt{A}} \{u_{max} - f(\eta)\} \Big|_{\eta=b} * H(\eta - b) \\
&+ e^{\frac{-\eta}{\sqrt{A}}} * f(\eta) * \delta(\eta - a) + e^{\frac{-\eta}{\sqrt{A}}} * \{u_{max} - f(\eta)\} * \delta(\eta - b)
\end{aligned}$$



$$\begin{aligned}
\int e^{\frac{-\eta}{\sqrt{A}}} * \frac{\partial^2 u(\eta)}{\partial \eta^2} d\eta &= g(\eta) * H(\eta - a) - g(a) * H(\eta - a) \\
&- g(\eta) * H(\eta - b) + g(b) * H(\eta - b) \\
&+ e^{\frac{-\eta}{\sqrt{A}}} * f(\eta) * \delta(\eta - a) + e^{\frac{-\eta}{\sqrt{A}}} * \{u_{max} - f(\eta)\} * \delta(\eta - b)
\end{aligned}$$

And by substituting the antiderivative:

$$\begin{aligned}
\int e^{\frac{-\eta}{\sqrt{A}}} * \frac{\partial^2 u(\eta)}{\partial \eta^2} d\eta &= e^{\frac{-\eta}{\sqrt{A}}} * \frac{u_{max}}{\dots} * \{-12 * \eta * \sqrt{A} - 12 * A + 6 * \sqrt{A} * (a + b)\} H(\eta - a) \\
&- e^{\frac{-a}{\sqrt{A}}} * \frac{u_{max}}{\dots} * \{-12 * a * \sqrt{A} - 12 * A + 6 * \sqrt{A} * (a + b)\} H(\eta - a) \\
&- e^{\frac{-\eta}{\sqrt{A}}} * \frac{u_{max}}{\dots} * \{-12 * \eta * \sqrt{A} - 12 * A + 6 * \sqrt{A} * (a + b)\} H(\eta - b) \\
&+ e^{\frac{-b}{\sqrt{A}}} * \frac{u_{max}}{\dots} * \{-12 * b * \sqrt{A} - 12 * A + 6 * \sqrt{A} * (a + b)\} H(\eta - b) \\
&+ e^{\frac{-\eta}{\sqrt{A}}} * f(\eta) * \delta(\eta - a) + e^{\frac{-\eta}{\sqrt{A}}} * \{u_{max} - f(\eta)\} * \delta(\eta - b)
\end{aligned}$$

Lastly, by multiplying the above integral with the term  $-e^{\frac{\eta}{\sqrt{A}}}$  some simplifications can occur

$$\begin{aligned}
-e^{\frac{\eta}{\sqrt{A}}} * \int e^{\frac{-\eta}{\sqrt{A}}} * \frac{\partial^2 u(\eta)}{\partial \eta^2} d\eta &= -\frac{u_{max}}{\dots} * \{-12 * \eta * \sqrt{A} - 12 * A + 6 * \sqrt{A} * (a + b)\} H(\eta - a) \\
&+ e^{\frac{\eta-a}{\sqrt{A}}} * \frac{u_{max}}{\dots} * \{-12 * a * \sqrt{A} - 12 * A + 6 * \sqrt{A} * (a + b)\} H(\eta - a) \\
&+ \frac{u_{max}}{\dots} * \{-12 * \eta * \sqrt{A} - 12 * A + 6 * \sqrt{A} * (a + b)\} H(\eta - b) \\
&- e^{\frac{\eta-b}{\sqrt{A}}} * \frac{u_{max}}{\dots} * \{-12 * b * \sqrt{A} - 12 * A + 6 * \sqrt{A} * (a + b)\} H(\eta - b)
\end{aligned}$$

$$-f(\eta) * \delta(\eta - a) - \{u_{max} - f(\eta)\} * \delta(\eta - b)$$

$$-e^{\frac{\eta}{\sqrt{A}}} * \int e^{\frac{-\eta}{\sqrt{A}}} * \frac{\partial^2 u(\eta)}{\partial \eta^2} d\eta = \frac{u_{max}}{\dots} *$$

$$\left[ -\{-12 * \eta * \sqrt{A} - 12 * A + 6 * \sqrt{A} * (a + b)\} \{H(\eta - a) - H(\eta - b)\} \right.$$

$$+ e^{\frac{\eta-a}{\sqrt{A}}} * \{-12 * a * \sqrt{A} - 12 * A + 6 * \sqrt{A} * (a + b)\} H(\eta - a)$$

$$\left. - e^{\frac{\eta-b}{\sqrt{A}}} * \{-12 * b * \sqrt{A} - 12 * A + 6 * \sqrt{A} * (a + b)\} H(\eta - b) \right]$$

$$-f(\eta) * \delta(\eta - a) - \{u_{max} - f(\eta)\} * \delta(\eta - b)$$

## G.6

Similarly, the second antiderivative (in the exponential the sign is the plus) can be calculated as follows:

$$\zeta(\eta) = \int e^{\frac{\eta}{\sqrt{A}}} * \frac{\partial^2 f(\eta)}{\partial \eta^2} d\eta$$

$$= \int e^{\frac{\eta}{\sqrt{A}}} * \frac{u_{max}}{\dots} * \{12\eta - 6(a + b)\} d\eta$$

$$= \int \frac{u_{max}}{\dots} * 12\eta * e^{\frac{\eta}{\sqrt{A}}} d\eta - \int \frac{u_{max}}{\dots} * 6(a + b) * e^{\frac{\eta}{\sqrt{A}}} * d\eta$$

$$= \frac{u_{max}}{\dots} * \left\{ 12 * \eta * \sqrt{A} * e^{\frac{\eta}{\sqrt{A}}} - 12 * A * e^{\frac{\eta}{\sqrt{A}}} - 6 * \sqrt{A} * (a + b) * e^{\frac{-\eta}{\sqrt{A}}} \right\}$$

$$= \frac{u_{max}}{\dots} * e^{\frac{\eta}{\sqrt{A}}} * \{12 * \eta * \sqrt{A} - 12 * A - 6 * \sqrt{A} * (a + b)\}$$

And by substituting the second integral the second antiderivative can be calculated as beneath:

$$\begin{aligned}
\int e^{\frac{\eta}{\sqrt{A}}} * \frac{\partial^2 u(\eta)}{\partial \eta^2} d\eta &= \int e^{\frac{\eta}{\sqrt{A}}} * \frac{\partial^2 f(\eta)}{\partial \eta^2} * [H(\eta - a) - H(\eta - b)] d\eta \\
&+ \int e^{\frac{\eta}{\sqrt{A}}} * 2 * \frac{\partial f(\eta)}{\partial \eta} * [\delta(\eta - a) - \delta(\eta - b)] d\eta \\
&+ \int e^{\frac{\eta}{\sqrt{A}}} * f(\eta) * [\delta'(\eta - a) - \delta'(\eta - b)] d\eta \\
&+ \int e^{\frac{\eta}{\sqrt{A}}} * u_{max} * \delta'(\eta - b) d\eta
\end{aligned}$$

$$\begin{aligned}
\int e^{\frac{\eta}{\sqrt{A}}} * \frac{\partial^2 u(\eta)}{\partial \eta^2} d\eta &= \zeta(\eta) * H(\eta - a) - \zeta(a) * H(\eta - a) \\
&- \zeta(\eta) * H(\eta - b) + \zeta(b) * H(\eta - b) \\
&+ e^{\frac{\eta}{\sqrt{A}}} * f(\eta) * \delta(\eta - a) + e^{\frac{\eta}{\sqrt{A}}} * \{u_{max} - f(\eta)\} * \delta(\eta - b)
\end{aligned}$$

$$\begin{aligned}
\int e^{\frac{\eta}{\sqrt{A}}} * \frac{\partial^2 u(\eta)}{\partial \eta^2} d\eta &= e^{\frac{\eta}{\sqrt{A}}} * \frac{u_{max}}{\dots} * \{12 * \eta * \sqrt{A} - 12 * A - 6 * \sqrt{A} * (a + b)\} H(\eta - a) \\
&- e^{\frac{a}{\sqrt{A}}} * \frac{u_{max}}{\dots} * \{12 * a * \sqrt{A} - 12 * A - 6 * \sqrt{A} * (a + b)\} H(\eta - a) \\
&- e^{\frac{\eta}{\sqrt{A}}} * \frac{u_{max}}{\dots} * \{12 * \eta * \sqrt{A} - 12 * A - 6 * \sqrt{A} * (a + b)\} H(\eta - b) \\
&+ e^{\frac{b}{\sqrt{A}}} * \frac{u_{max}}{\dots} * \{12 * b * \sqrt{A} - 12 * A - 6 * \sqrt{A} * (a + b)\} H(\eta - b) \\
&+ e^{\frac{\eta}{\sqrt{A}}} * f(\eta) * \delta(\eta - a) + e^{\frac{\eta}{\sqrt{A}}} * \{u_{max} - f(\eta)\} * \delta(\eta - b)
\end{aligned}$$

Lastly by applying the multiplication with the term  $-e\frac{-\eta}{\sqrt{A}}$ , the below simplification can occur:

$$\begin{aligned}
e\frac{-\eta}{\sqrt{A}} * \int e\frac{\eta}{\sqrt{A}} * \frac{\partial^2 u(\eta)}{\partial \eta^2} d\eta &= \frac{u_{max}}{\dots} * \{12 * \eta * \sqrt{A} - 12 * A - 6 * \sqrt{A} * (a + b)\} H(\eta - a) \\
-e\frac{\eta-a}{\sqrt{A}} * \frac{u_{max}}{\dots} * \{12 * a * \sqrt{A} - 12 * A - 6 * \sqrt{A} * (a + b)\} H(\eta - a) & \\
-\frac{u_{max}}{\dots} * \{12 * \eta * \sqrt{A} - 12 * A - 6 * \sqrt{A} * (a + b)\} H(\eta - b) & \\
+e\frac{\eta-b}{\sqrt{A}} * \frac{u_{max}}{\dots} * \{12 * b * \sqrt{A} - 12 * A - 6 * \sqrt{A} * (a + b)\} H(\eta - b) & \\
+f(\eta) * \delta(\eta - a) + \{u_{max} - f(\eta)\} * \delta(\eta - b) &
\end{aligned}$$

$$\begin{aligned}
+e\frac{-\eta}{\sqrt{A}} * \int e\frac{\eta}{\sqrt{A}} * \frac{\partial^2 u(\eta)}{\partial \eta^2} d\eta &= \frac{u_{max}}{\dots} * \\
& \left[ +\{12 * \eta * \sqrt{A} - 12 * A - 6 * \sqrt{A} * (a + b)\} \{H(\eta - a) - H(\eta - b)\} \right. \\
& \quad -e\frac{\eta-a}{\sqrt{A}} * \{12 * a * \sqrt{A} - 12 * A - 6 * \sqrt{A} * (a + b)\} H(\eta - a) \\
& \quad \left. +e\frac{\eta-b}{\sqrt{A}} * \{12 * b * \sqrt{A} - 12 * A - 6 * \sqrt{A} * (a + b)\} H(\eta - b) \right] \\
& +f(\eta) * \delta(\eta - a) + \{u_{max} - f(\eta)\} * \delta(\eta - b)
\end{aligned}$$

By importing equations G.6 and G.7, onto equation x of chapter 4, the polarization, assuming a vertical displacement of a polynomial function of 3<sup>rd</sup> grade, can be given by the below formula:

$$P_3(\eta) = c_1 * e^{+\frac{\eta}{\sqrt{A}}} + c_2 * e^{-\frac{\eta}{\sqrt{A}}} + \frac{B}{2 * \sqrt{A}} * \left[ -e^{+\frac{\eta}{\sqrt{A}}} * \int e^{-\frac{\eta}{\sqrt{A}}} * \frac{d^2 u_3}{d\eta^2} d\eta + e^{-\frac{\eta}{\sqrt{A}}} * \int e^{+\frac{\eta}{\sqrt{A}}} * \frac{d^2 u_3}{d\eta^2} d\eta \right]$$

$$P_3(\eta) = c_1 * e^{+\frac{\eta}{\sqrt{A}}} + c_2 * e^{-\frac{\eta}{\sqrt{A}}} + \frac{B}{2 * \sqrt{A}} * \frac{u_{max}}{\dots} *$$

$$\left[ \{ +12 * \eta * \sqrt{A} + 12 * A - 6 * \sqrt{A} * (a + b) \} \{ H(\eta - a) - H(\eta - b) \} \right]$$

$$+ e^{\frac{\eta-a}{\sqrt{A}}} * \{ -12 * a * \sqrt{A} - 12 * A + 6 * \sqrt{A} * (a + b) \} H(\eta - a)$$

$$- e^{\frac{\eta-b}{\sqrt{A}}} * \{ -12 * b * \sqrt{A} - 12 * A + 6 * \sqrt{A} * (a + b) \} H(\eta - b) +$$

$$\left[ \{ 12 * \eta * \sqrt{A} * -12 * A - 6 * \sqrt{A} * (a + b) \} \{ H(\eta - a) - H(\eta - b) \} \right]$$

$$- e^{-\frac{\eta-a}{\sqrt{A}}} * \{ 12 * a * \sqrt{A} - 12 * A - 6 * \sqrt{A} * (a + b) \} H(\eta - a)$$

$$+ e^{\frac{\eta-b}{\sqrt{A}}} * \{ 12 * b * \sqrt{A} - 12 * A - 6 * \sqrt{A} * (a + b) \} H(\eta - b) \left[ \right]$$

$$- f(\eta) * \delta(\eta - a) - \{ u_{max} - f(\eta) \} * \delta(\eta - b)$$

$$+ f(\eta) * \delta(\eta - a) + \{ u_{max} - f(\eta) \} * \delta(\eta - b)$$

$$\begin{aligned}
P_3(\eta) = & c_1 e^{+\frac{\eta}{\sqrt{A}}} + c_2 e^{-\frac{\eta}{\sqrt{A}}} + \frac{B}{2 * \sqrt{A}} * \frac{u_{max}}{\dots} * \left[ \{+24\eta\sqrt{A} - 12\sqrt{A}(a + b)\} \{H(\eta - a) - H(\eta - b)\} \right. \\
& + H(\eta - a) \left\{ e^{\frac{\eta-a}{\sqrt{A}}} \{-12a\sqrt{A} - 12A + 6\sqrt{A}(a + b)\} - e^{-\frac{\eta-a}{\sqrt{A}}} \{12a\sqrt{A} - 12A - 6\sqrt{A}(a + b)\} \right\} \\
& \left. - H(\eta - b) \left\{ e^{\frac{\eta-b}{\sqrt{A}}} \{-12b\sqrt{A} - 12A + 6\sqrt{A}(a + b)\} - e^{-\frac{\eta-b}{\sqrt{A}}} \{12b\sqrt{A} - 12A - 6\sqrt{A}(a + b)\} \right\} \right]
\end{aligned}$$

G.8

## 10. Bibliography

- ABAQUS, 2012. User's Manual. version 6.12. Hibbit, Karlsson and Sorensen Inc..
- Adali, S., 1982. Stability of a rectangular plate under nonconservative and conservative forces. *International Journal of Solids and Structures*, 18(12), pp. 1043-1052.
- Babouskos, N. & Katsikadelis, J. T., 2009. flutter instability of damped plates under combined conservative and nonconservative loads. *Arch Appl Mech*, Volume 79, p. 541–556.
- Bracewell, R. N., 1999. *The Fourier Transform and its Application*. s.l.:McGraw, Hill, Science Engineering Math.
- Courant, R. & Lax, A., 1955. Remarks on Cauchy's problem for hyperbolic partial differential equations with constant coefficients in several independent variables. *Comm. Pure Appl. Math.*, Volume 8, pp. 497-502.
- Deng, Q. et al., 2020. The impact of flexoelectricity on materials,. *J. Appl. Phys*, Volume 128, p. 080902.
- Diprima, R. C. & Boyce, W. E., 1997. *Elementary Differential Equations and Boundary Value Problems*. 6th ed. s.l.:John Wiley & Sons.
- Gavardinas, I., Giannakopoulos, A. E. & Zisis, T., 2018. A von Karman plate analogue for solving anti-plane problems in couple stress and dipolar gradient elasticity. *International Journal of Solids and Structures*, Volume 148–149, pp. 169-180.
- Giannakopoulos, A. E., Knisovitis, C., Georgousis, G. & Kontou, E., 2021. Fracture experiments and flexoelectric response of PVDF. *Mat Design Process Comm.*, 3(2), p. e150.
- Giannakopoulos, A. E. & Zisis, T., 2019. Uniformly moving screw dislocation in flexoelectric materials. *European Journal of Mechanics - A/Solids*, Volume 78, p. 103843.
- Giannakopoulos, A. E. & Zisis, T., 2021. Steady-state antiplane crack considering the flexoelectrics effect: surface waves and flexoelectric metamaterials. *Arch Appl Mech*, Volume 91, pp. 713-738.
- Giannakopoulos, A. E. & Zisis, T., 2021. Uniformly moving antiplane crack in flexoelectric materials. *European Journal of Mechanics - A/Solids*, Volume 85, p. 104136.
- Gourgiotis, P. & Georgiadis, H., 2007. Distributed dislocation approach for cracks in couple-stress elasticity: shear modes. *Int J Fract*, Volume 147, p. 83–102.
- Häsler, E., Stein, L. & Harbauer, G., 277-282. Implantable physiological power supply with PVDF film. *Ferroelectrics*, 60(1), p. 1984.
- Katsikadelis, J. T., 1994. *The analog equation method – a powerful BEM-based solution technique for solving linear and nonlinear engineering problems*. Southampton, UK, Computational Mechanics Publications, pp. 169-189.
- Kim, G.-W., Kim, J. & Kim, J.-H., 2014. Flexible piezoelectric vibration energy harvester using a trunk-shaped beam structure inspired by an electric fish fin. *Int. J. Precis. Eng. Manuf.*, Volume 15, p. 1967–1971.
- Knisovitis, C., 2019. *Flexoelectric structural elements*. Athens: National Technical University of Athens, School of Civil Engineering.

- Lax, A., 1956. On Cauchy's problem for partial differential equations with multiple characteristics. *Comm. Pure Appl. Math.*, Volume 9, pp. 135-169.
- Maranganti, R., Sharma, N. & Sharma, P., 2006. Electromechanical coupling in nonpiezoelectric materials due to nanoscale nonlocal size effects: Green's function solutions and embedded inclusions. *Physical Review B*, 74(1), p. 014110.
- Maranganti, R. & Sharma, P., 2009. Atomistic determination of flexoelectric properties of crystalline dielectrics. *Phys. Rev. B*, 80(5).
- Mindlin, R., 1965. Second gradient of strain and surface-tension in linear elasticity. *International Journal of Solids and Structures*, 1(4), pp. 417-438.
- Mindlin, R., 1968. Polarization gradient in elastic dielectrics. *International Journal of Solids and Structures*, 4(6), pp. 637-642.
- Seung-Bok, C. & Gi-Woo, K., 2017. Measurement of flexoelectric response in polyvinylidene fluoride films for piezoelectric vibration energy harvesters. *Journal of Physics D: Applied Physics*, 50(7), p. 075502.
- Shi, G. & Bezzine, G., 1988. A General Boundary Integral Formulation for the Anisotropic Plate Bending Problems. *Journal of Composite Materials*, 22(8), pp. 694-716.
- Timoshenko, S. & Woinowsky-Krieger, S., 1959. *Theory of plates*. 2nd ed. s.l.:McGraw-Hill book Company.
- Wang, B., Yang, S. & Sharma, P., 2019. Flexoelectricity as a universal mechanism for energy harvesting from crumpling of thin sheets. *American Physical Society, Phys. Rev. B*, 100(3).
- Yang, W., Deng, Q., Liang, X. & Shen, S., 2018. Lamb wave propagation with flexoelectricity and strain gradient elasticity considered. *Smart Materials and Structures*, 27(8).
- Yang, W., Liang, X., Deng, Q. & Shen, S., 2020. Rayleigh wave propagation in a homogeneous centrosymmetric flexoelectric half-space. *Ultrasonics*, Volume 103, p. 106105.
- Zisis, T., 2018. Anti-plane loading of microstructured materials in the context of couple stress theory of elasticity: half-planes and layers. *Arch Appl Mech*, Volume 88, p. 97-110.